

LSCS-UFSAR

CHAPTER 4.0 - REACTOR

TABLE OF CONTENTS

	<u>Page</u>
4.0 <u>REACTOR</u>	4.1-1
4.1 <u>SUMMARY DESCRIPTION</u>	4.1-1
4.1.1 Reactor Vessel	4.1-1
4.1.2 Reactor Internal Components	4.1-1
4.1.2.1 Reactor Core	4.1-1
4.1.2.1.1 General	4.1-1
4.1.2.1.2 Core Configuration	4.1-3
4.1.2.1.3 Fuel Assembly Description	4.1-4
4.1.2.1.3.1 Fuel Rod	4.1-4
4.1.2.1.3.2 Fuel Bundle	4.1-4
4.1.2.1.4 Assembly Support and Control Rod Location	4.1-5
4.1.2.2 Shroud	4.1-5
4.1.2.3 Shroud Head and Steam Separators	4.1-6
4.1.2.4 Steam Dryer Assembly	4.1-6
4.1.3 Reactivity Control Systems	4.1-7
4.1.3.1 Operation	4.1-7
4.1.3.2 Description of Rods	4.1-7
4.1.3.3 Supplementary Reactivity Control	4.1-8
4.1.4 Analysis Techniques	4.1-8
4.1.4.1 Reactor Internal Components	4.1-8
4.1.4.1.1 MASS (Mechanical Analysis of Space Structure)	4.1-9
4.1.4.1.1.1 Program Description	4.1-9
4.1.4.1.1.2 Program Version and Computer	4.1-9
4.1.4.1.1.3 History of Use	4.1-9
4.1.4.1.1.4 Extent of Application	4.1-9
4.1.4.1.2 SNAP (MULTISHELL)	4.1-9
4.1.4.1.2.1 Program Description	4.1-9
4.1.4.1.2.2 Program Version and Computer	4.1-10
4.1.4.1.2.3 History of Use	4.1-10
4.1.4.1.2.4 Extent of Application	4.1-10
4.1.4.1.3 GASP	4.1-10
4.1.4.1.3.1 Program Description	4.1-10
4.1.4.1.3.2 Program Version and Computer	4.1-10
4.1.4.1.3.3 History of Use	4.1-11
4.1.4.1.3.4 Extent of Application	4.1-11
4.1.4.1.4 NOHEAT	4.1-11

Table of Contents (Cont'd)

4.1.4.1.4.1	Program Description	4.1-11
4.1.4.1.4.2	Program Version and Computer	4.1-11
4.1.4.1.4.3	History of Use	4.1-11
4.1.4.1.4.4	Extent of Application	4.1-12
4.1.4.1.5	FINITE	4.1-12
4.1.4.1.5.1	Program Description	4.1-12
4.1.4.1.5.2	Program Version and Computer	4.1-12
4.1.4.1.5.3	History of Use	4.1-12
4.1.4.1.5.4	Extent of Application	4.1-12
4.1.4.1.6	SAMIS	4.1-12
4.1.4.1.6.1	Program Description	4.1-12
4.1.4.1.6.2	Program Version and Computer	4.1-13
4.1.4.1.6.3	History of Use	4.1-13
4.1.4.1.6.4	Extent of Application	4.1-13
4.1.4.1.7	General Matrix Manipulation Program(GEMOP)	4.1-14
4.1.4.1.7.1	Program Description	4.1-14
4.1.4.1.7.2	Program Version and Computer	4.1-14
4.1.4.1.7.3	History of Use	4.1-14
4.1.4.1.7.4	Extent of Application	4.1-14
4.1.4.1.8	SHELL 5	4.1-14
4.1.4.1.8.1	Program Description	4.1-14
4.1.4.1.8.2	Program Version and Computer	4.1-15
4.1.4.1.8.3	History of Use	4.1-15
4.1.4.1.8.4	Extent of Application	4.1-15
4.1.4.1.9	HEATER	4.1-15
4.1.4.1.9.1	Program Description	4.1-15
4.1.4.1.9.2	Program Version and Computer	4.1-15
4.1.4.1.9.3	History of Use	4.1-16
4.1.4.1.9.4	Extent of Application	4.1-16
4.1.4.1.10	FAP-71 (Fatigue Analysis Program)	4.1-16
4.1.4.1.10.1	Program Description	4.1-16
4.1.4.1.10.2	Program Version and Computer	4.1-16
4.1.4.1.10.3	History of Use	4.1-16
4.1.4.1.10.4	Extent of Application	4.1-16
4.1.4.1.11	CREEP/PLASTICITY	4.1-17
4.1.4.1.11.1	Program Description	4.1-17
4.1.4.1.11.2	Program Version and Computer	4.1-17
4.1.4.1.11.3	History of Use	4.1-17
4.1.4.1.11.4	Extent of Application	4.1-17
4.1.4.2	Fuel Rod Thermal Analysis	4.1-17
4.1.4.3	Reactor Systems Dynamics	4.1-18
4.1.4.4	Nuclear Engineering Analysis	4.1-18
4.1.4.5	Neutron Fluence Calculations	4.1-18
4.1.4.6	Thermal Hydraulic Calculations	4.1-19

LSCS-UFSAR

Table of Contents (Cont'd)

4.1.5	References	4.1-19
4.2	<u>FUEL SYSTEM</u>	4.2-1
4.2.1	Design Bases	4.2-1
4.2.1.1	Safety Design Bases	4.2-1
4.2.1.2	Power Generation Design Basis	4.2-3
4.2.1.2.1	Material Selection	4.2-3
4.2.1.2.2	Effects of Irradiation and Fuel Swelling	4.2-3
4.2.1.2.3	Fuel Densification	4.2-4
4.2.1.2.3.1	GE Fuel	4.2-4
4.2.1.2.3.2	FANP Fuel	4.2-5
4.2.1.2.4	Incipient UO ₂ Center Melting	4.2-5
4.2.1.2.4.1	GE Fuel	4.2-5
4.2.1.2.4.2	FANP Fuel	4.2-5
4.2.1.2.5	Maximum Allowable Stresses	4.2-6
4.2.1.2.5.1	GE Fuel	4.2-6
4.2.1.2.5.2	FANP Fuel	4.2-7
4.2.1.2.6	Capacity for Fission Gas Inventory	4.2-7
4.2.1.2.7	Maximum Internal Gas Pressure	4.2-7
4.2.1.2.7.1	GE Fuel	4.2-7
4.2.1.2.7.2	FANP Fuel	4.2-8
4.2.1.2.8	Internal Pressure and Cladding Stresses During Normal Conditions	4.2-8
4.2.1.2.9	Cycling and Fatigue Limits	4.2-8
4.2.1.2.9.1	GE Analysis	4.2-8
4.2.1.2.9.2	FANP Analysis	4.2-9
4.2.1.2.10	Deflections	4.2-9
4.2.1.2.10.1	GE Evaluation	4.2-9
4.2.1.2.10.2	FANP Evaluation	4.2-9
4.2.1.2.11	Flow-Induced Fuel Rod Vibrations	4.2-10
4.2.1.2.12	Fretting Corrosion	4.2-10
4.2.1.2.13	Seismic Loadings	4.2-10
4.2.1.2.14	Chemical Properties of Cladding and Fuel Material	4.2-11
4.2.1.2.15	Design Ratios	4.2-11
4.2.1.2.15.1	Limiting Parameter Values	4.2-11
4.2.1.2.15.1.1	Normal and Upset Design Conditions	4.2-11
4.2.1.2.15.1.2	Emergency and Faulted Design Conditions	4.2-12
4.2.1.2.15.2	Actual Parameter Values	4.2-12
4.2.1.2.16	Fuel Assembly Limits	4.2-13
4.2.1.2.16.1	Fuel Rods	4.2-13
4.2.1.2.16.2	Fuel Spacer	4.2-13
4.2.1.2.16.3	Water Rods	4.2-14

LSCS-UFSAR

Table of Contents (Cont'd)

4.2.1.2.16.4	Channel	4.2-14
4.2.1.2.16.5	Tie Plates	4.2-15
4.2.1.2.17	Reactivity Control Assembly and Burnable Poison Rods	4.2-15
4.2.1.2.17.1	Safety Design Bases for Reactivity Control	4.2-15
4.2.1.2.17.1.1	Specific Design Characteristics	4.2-16
4.2.1.2.18	Surveillance Program	4.2-17
4.2.2	Description and Design Drawings	4.2-18
4.2.2.1	Core Cell	4.2-18
4.2.2.2	Fuel Assembly	4.2-18
4.2.2.3	Fuel Bundle	4.2-18
4.2.2.4	Fuel Rod	4.2-19
4.2.2.5	Fuel Pellets	4.2-21
4.2.2.6	Fuel Channel	4.2-22
4.2.2.7	Reactivity Control Assembly and Burnable Poison Rods	4.2-23
4.2.2.7.1	Control Rods	4.2-23
4.2.2.7.1.1	General Electric Control Rods	4.2-22
4.2.2.7.1.2	ASEA-ATOM Control Rods	4.2-24
4.2.2.7.2	Velocity Limiter	4.2-25
4.2.2.7.3	Burnable Poison Rods	4.2-25
4.2.3	Design Limits and Evaluation	4.2-26
4.2.3.1	Fuel Damage Analysis	4.2-26
4.2.3.2	Fuel Damage Experience	4.2-27
4.2.3.3	Potential for a Water-Logging Rupture	4.2-28
4.2.3.4	Potential for Hydriding	4.2-29
4.2.3.5	Dimensional Stability	4.2-29
4.2.3.6	Fuel Densification	4.2-30
4.2.3.7	Fuel Cladding Temperatures	4.2-30
4.2.3.8	Peaking Factors	4.2-31
4.2.3.8.1	Local Peaking Factors	4.2-31
4.2.3.8.2	Axial and Gross Peaking Factors	4.2-31
4.2.3.9	Temperature Transients with Water- logged Fuel Element	4.2-31
4.2.3.10	Potential Damaging Temperature Effects During Transients	4.2-32
4.2.3.11	Energy Release During Fuel Element Burnout	4.2-32
4.2.3.12	Energy Release for Rupture of Water- logged Fuel Elements	4.2-34
4.2.3.13	Fuel Rod Behavior Effects from Coolant Flow Blockage	4.2-34
4.2.3.14	Channel Evaluation	4.2-35

LSCS-UFSAR

Table of Contents (Cont'd)

4.2.3.15	Fuel Reliability	4.2-36
4.2.3.16	Fuel Operating and Developmental Experience	4.2-37
4.2.3.17	Fuel Assembly	4.2-37
4.2.3.17.1	Loads Assessment of Fuel Assembly Components	4.2-38
4.2.3.18	Spacer Grid and Channel Boxes	4.2-38
4.2.3.19	Burnable Poison Rods	4.2-38
4.2.3.20	Control Rods	4.2-38
4.2.3.20.1	Materials Adequacy Throughout Design Lifetime	4.2-38
4.2.3.20.2	Dimensional and Tolerance Analysis	4.2-38
4.2.3.20.3	Thermal Analysis of the Tendency to Warp	4.2-39
4.2.3.20.4	Forces for Expulsion	4.2-39
4.2.3.20.5	Functional Failure of Critical Components	4.2-39
4.2.3.20.6	Precluding Excessive Rates of Reactivity Addition	4.2-39
4.2.3.20.7	Effect of Fuel Rod Failure on Control Rod Channel Clearances	4.2-39
4.2.3.20.8	Mechanical Damage	4.2-39
4.2.3.20.8.1	First Mode of Failure	4.2-40
4.2.3.20.8.2	Second Mode of Failure	4.2-40
4.2.3.20.9	Analysis of Guide Tube Design	4.2-40
4.2.3.20.10	Evaluation of Control Rod Velocity Limiter	4.2-41
4.2.3.21	Rod Bowing	4.2-41
4.2.3.21.1	GE Evaluation	4.2-41
4.2.3.21.2	FANP Evaluation	4.2-42
4.2.3.22	Fission Gas Release	4.2-42
4.2.3.23	Ballooning and Rupture	4.2-43
4.2.3.23.1	GE Evaluation	4.2-43
4.2.3.23.2	FANP Evaluation	4.2-44
4.2.4	Testing and Inspection Plan	4.2-44
4.2.4.1	Testing and Inspection (Enrichment and Burnable Poison Concentrations)	4.2-45
4.2.4.1.1	Enrichment Control Program	4.2-45
4.2.4.1.2	Gadolinia Inspections	4.2-46
4.2.4.1.3	Reactor Control Rods	4.2-47
4.2.4.2	Surveillance Inspection and Testing of Irradiated Fuel Rods	4.2-47

LSCS-UFSAR

Table of Contents (Cont'd)

4.2.4.3	Operating Experience with Gadolinia-Containing Fuel	4.2-48
4.2.5	References	4.2-49
4.3	<u>NUCLEAR DESIGN</u>	4.3-1
4.3.1	Design Bases	4.3-1
4.3.1.1	Safety Design Bases	4.3-1
4.3.1.2	Power Generation Design Bases	4.3-2
4.3.2	Description	4.3-2
4.3.2.1	Nuclear Design Description	4.3-2
4.3.2.1.1	Fuel Nuclear Properties	4.3-3
4.3.2.2	Power Distributions	4.3-4
4.3.2.2.1	Local Power Distribution	4.3-5
4.3.2.2.2	Radial Power Distribution	4.3-5
4.3.2.2.3	Axial Power Distribution	4.3-5
4.3.2.2.4	Power Distribution Calculations	4.3-6
4.3.2.2.5	Power Distribution Measurements	4.3-6
4.3.2.2.6	Power Distribution Accuracy	4.3-6
4.3.2.2.7	Power Distribution Anomalies	4.3-6
4.3.2.3	Reactivity Coefficients	4.3-7
4.3.2.3.1	Void Reactivity Coefficients	4.3-7
4.3.2.3.2	Moderator Temperature Coefficient	4.3-7
4.3.2.3.3	Doppler Reactivity Coefficient	4.3-8
4.3.2.3.4	Power Coefficient	4.3-9
4.3.2.4	Control Requirements	4.3-9
4.3.2.4.1	Shutdown Reactivity	4.3-9
4.3.2.4.2	Reactivity Variations	4.3-10
4.3.2.5	Control Rod Patterns and Reactivity Worths	4.3-11
4.3.2.5.1	Control Rod Withdrawal Sequences	4.3-11
4.3.2.5.1.1	Control Rod Withdrawal Sequences in the Startup Range	4.3-12
4.3.2.5.1.2	Control Rod Withdrawal Sequences in the RWM Power Range	4.3-13
4.3.2.5.1.3	Maximum Control Rod Worth Pattern with a Single Error in the RWM Power Range	4.3-14
4.3.2.5.2	Control Rod Worth Calculations	4.3-14
4.3.2.5.2.1	Control Rod Worth in the Startup Range and RWM Power Range	4.3-14
4.3.2.5.2.2	Control Rod Worth in the Reactor Power Range > 10% Rated Power	4.3-15
4.3.2.5.3	Scram Reactivity	4.3-15

Table of Contents (Cont'd)

4.3.2.6	Criticality of Reactor During Refueling	4.3-16
4.3.2.6.1	Criticality of Reactor	4.3-16
4.3.2.6.2	Criticality of Fuel Assemblies	4.3-16
4.3.2.7	Stability	4.3-16
4.3.2.7.1	Xenon Transients	4.3-16
4.3.2.7.2	Thermal Hydraulic Stability	4.3-17
4.3.2.8	Vessel Irradiation	4.3-17
4.3.3	Analytical Methods	4.3-17
4.3.4	References	4.3-18
4.4	<u>THERMAL AND HYDRAULIC DESIGN</u>	4.4-1
4.4.1	Design Bases	4.4-1
4.4.1.1	Safety Design Bases	4.4-1
4.4.1.2	Power Generation Design Bases	4.4-1
4.4.1.3	Requirements for Steady-State Conditions	4.4-1
4.4.1.4	Requirements for Transient Conditions	4.4-2
4.4.1.5	Summary of Design Bases	4.4-2
4.4.1.5.1	Fuel Cladding Integrity	4.4-3
4.4.1.5.2	Fuel Assembly Integrity	4.4-3
4.4.1.5.3	Fuel-Cladding Gap Characteristics	4.4-3
4.4.2	Description of Thermal Hydraulic Design of Reactor Core	4.4-3
4.4.2.1	Summary Comparison	4.4-3
4.4.2.2	Critical Power Ratio	4.4-3
4.4.2.2.1	Boiling Correlations	4.4-4
4.4.2.2.1.1	GE Fuel	4.4-4
4.4.2.2.1.2	FANP Fuel	4.4-4
4.4.2.3	Maximum Average Planar Linear Heat Generation Rate (MAPLHGR)	4.4-5
4.4.2.3.1	Design Power Distribution	4.4-6
4.4.2.4	Void Fraction Distribution	4.4-7
4.4.2.5	Core Coolant Flow Distribution	4.4-7
4.4.2.6	Core Pressure Drop and Hydraulic Loads	4.4-8
4.4.2.6.1	Friction Pressure Drop	4.4-8
4.4.2.6.2	Local Pressure Drop	4.4-9
4.4.2.6.3	Elevation Pressure Drop	4.4-9
4.4.2.6.4	Acceleration Pressure Drop	4.4-10

Table of Contents (Cont'd)

4.4.2.7	Correlation and Physical Data	4.4-11
4.4.2.7.1	Pressure Drop Correlations	4.4-11
4.4.2.7.2	Void Fraction Correlation	4.4-11
4.4.2.7.3	Heat Transfer Correlation	4.4-12
4.4.2.8	Thermal Effects of Operational Transients	4.4-12
4.4.2.9	Uncertainties in Estimates	4.4-12
4.4.2.9.1	Transition Boiling Uncertainties	4.4-12
4.4.2.9.2	Variation of Fuel Damage Limit	4.4-13
4.4.2.9.3	Effects of Misoriented Fuel Bundle	4.4-13
4.4.2.10	Flux Tilt Considerations	4.4-13
4.4.3	Description of the Thermal and Hydraulic Design of the Reactor Coolant System	4.4-13
4.4.3.1	Plant Configuration Data	4.4-13
4.4.3.2	Operating Restrictions on Pumps	4.4-14
4.4.3.3	Power-Flow Operating Map	4.4-14
4.4.3.4	Temperature-Power Operating Map (PWR)	4.4-14
4.4.3.5	Load-Following Characteristics	4.4-14
4.4.3.6	Thermal and Hydraulic Characteristics Summary Table	4.4-14
4.4.4	Evaluation	4.4-14
4.4.4.1	Critical Heat Flux	4.4-14
4.4.4.2	Core Hydraulics	4.4-14
4.4.4.3	Influence of Power Distribution	4.4-14
4.4.4.4	Core Thermal Response	4.4-15
4.4.4.5	Analytical Methods	4.4-15
4.4.4.5.1	Reactor Model	4.4-15
4.4.4.5.2	System Flow Balances	4.4-16
4.4.4.5.3	System Heat Balances	4.4-17
4.4.4.5.4	Uncertainties in Design Analyses	4.4-18
4.4.4.6	Reactor Stability Analysis	4.4-18
4.4.4.6.1	Introduction	4.4-18
4.4.4.6.2	Description	4.4-19
4.4.4.6.3	Solution Description for Thermal-Hydraulic Stability	4.4-19
4.4.4.6.4	Stability Criteria	4.4-20
4.4.4.6.5	Expected Oscillation Modes	4.4-21
4.4.4.6.6	Analysis Approach	4.4-22
4.4.4.6.7	Mathematical Model	4.4-23
4.4.4.6.8	Initial Core Analysis Results	4.4-24
4.4.5	Testing and Verification	4.4-25
4.4.6	Instrumentation Requirements	4.4-25
4.4.6.1	Loose Parts Monitoring System (Deleted)	4.4-25
4.4.7	References	4.4-27

Table of Contents (Cont'd)

4.5	<u>REACTOR MATERIALS</u>	4.5-1
4.5.1	Control Rod System Structural Materials	4.5-1
4.5.1.1	Material Specifications	4.5-1
4.5.1.2	Special Materials	4.5-2
4.5.1.3	Processes, Inspections and Tests	4.5-2
4.5.1.4	Control of Delta Ferrite Content	4.5-3
4.5.1.5	Protection of Materials During Fabrication, Shipping and Storage	4.5-3
4.5.2	Reactor Internals Materials	4.5-4
4.5.2.1	Material Specifications	4.5-4
4.5.2.2	Controls on Welding	4.5-6
4.5.2.3	Nondestructive Examination of Wrought Seamless Tubular Products	4.5-6
4.5.2.4	Fabrication and Processing of Austenitic Stainless Steel	4.5-6
4.5.2.5	Regulatory Guide Conformance Assessment	4.5-6
4.6	<u>FUNCTIONAL DESIGN OF REACTIVITY CONTROL SYSTEMS</u>	4.6-1
4.6.1	Information for Control Rod Drive Systems (CRDS)	4.6-1
4.6.1.1	Control Rod Drive System Design	4.6-1
4.6.1.1.1	Design Bases	4.6-1
4.6.1.1.1.1	General Design Bases	4.6-1
4.6.1.1.1.1.1	Safety Design Bases	4.6-1
4.6.1.1.1.1.2	Power Generation Design Basis	4.6-2
4.6.1.1.2	Description	4.6-2
4.6.1.1.2.1	Control Rod Drive Mechanisms	4.6-2
4.6.1.1.2.2	Drive Components	4.6-3
4.6.1.1.2.2.1	Drive Piston	4.6-3
4.6.1.1.2.2.2	Index Tube	4.6-4
4.6.1.1.2.2.3	Collet Assembly	4.6-4
4.6.1.1.2.2.4	Piston Tube	4.6-4
4.6.1.1.2.2.5	Stop Piston	4.6-5
4.6.1.1.2.2.6	Flange and Cylinder Assembly	4.6-5
4.6.1.1.2.2.7	Lock Plug	4.6-6
4.6.1.1.2.3	Materials of Construction	4.6-6
4.6.1.1.2.3.1	Index Tube	4.6-6
4.6.1.1.2.3.2	Coupling Spud	4.6-7
4.6.1.1.2.3.3	Collet Fingers	4.6-7
4.6.1.1.2.3.4	Seals and Bushings	4.6-7
4.6.1.1.2.3.5	Summary	4.6-7

LSCS-UFSAR

Table of Contents (Cont'd)

4.6.1.1.2.4	Control Rod Drive Hydraulic System	4.6-8
4.6.1.1.2.4.1	Hydraulic Requirements	4.6-8
4.6.1.1.2.4.2	System Description	4.6-9
4.6.1.1.2.4.2.1	Supply Pump	4.6-9
4.6.1.1.2.4.2.2	Accumulator Charging Pressure	4.6-10
4.6.1.1.2.4.2.3	Drive Water Pressure	4.6-10
4.6.1.1.2.4.2.4	Cooling Water Header	4.6-11
4.6.1.1.2.4.2.5	Return Line	4.6-11
4.6.1.1.2.4.2.6	Scram Discharge Volume	4.6-11
4.6.1.1.2.4.3	Hydraulic Control Units	4.6-12
4.6.1.1.2.4.3.1	Insert Drive Valve	4.6-12
4.6.1.1.2.4.3.2	Insert Exhaust Valve	4.6-13
4.6.1.1.2.4.3.3	Withdraw Drive Valve	4.6-13
4.6.1.1.2.4.3.4	Withdraw Exhaust Valve	4.6-13
4.6.1.1.2.4.3.5	Speed Control Valves	4.6-13
4.6.1.1.2.4.3.6	Scram Pilot Valves	4.6-13
4.6.1.1.2.4.3.7	Scram Inlet Valve	4.6-13
4.6.1.1.2.4.3.8	Scram Exhaust Valve	4.6-14
4.6.1.1.2.4.3.9	Scram Accumulator	4.6-14
4.6.1.1.2.4.3.10	Alternate Rod Insertion Scram Valves	4.6-14
4.6.1.1.2.5	Control Rod Drive System Operation	4.6-15
4.6.1.1.2.5.1	Rod Insertion	4.6-15
4.6.1.1.2.5.2	Rod Withdrawal	4.6-15
4.6.1.1.2.5.3	Scram	4.6-16
4.6.1.1.2.6	Instrumentation	4.6-17
4.6.1.2	Control Rod Drive Housing Supports	4.6-17
4.6.1.2.1	Safety Objective	4.6-17
4.6.1.2.2	Safety Design Bases	4.6-17
4.6.1.2.3	Description	4.6-17
4.6.2	Evaluations of the CRDS	4.6-19
4.6.2.1	Failure Mode and Effects Analysis	4.6-19
4.6.2.2	Protection from Common Mode Failures	4.6-19
4.6.2.3	Safety Evaluation	4.6-19
4.6.2.3.1	Control Rod Drives	4.6-19
4.6.2.3.1.1	Evaluation of Scram Time	4.6-19
4.6.2.3.1.2	Analysis of Malfunction Relating to Rod Withdrawal	4.6-20
4.6.2.3.1.2.1	Drive Housing Fails at Attachment Weld	4.6-20
4.6.2.3.1.2.2	Rupture of Hydraulic Line(s) to Drive Housing Flange	4.6-21
4.6.2.3.1.2.2.1	Pressure-Under Line Break	4.6-21
4.6.2.3.1.2.2.2	Pressure-Over Line Break	4.6-22
4.6.2.3.1.2.2.3	Simultaneous Breakage of Pressure- Over and Pressure-Under Lines	4.6-22

LSCS-UFSAR

Table of Contents (Cont'd)

4.6.2.3.1.2.3	All Drive Flange Bolts Fail in Tension	4.6-22
4.6.2.3.1.2.4	Weld Joining Flange to Housings Fails in Tension	4.6-23
4.6.2.3.1.2.5	Housing Wall Ruptures	4.6-24
4.6.2.3.1.2.6	Flange Plug Blows Out	4.6-25
4.6.2.3.1.2.7	Drive Pressure Control Valve Closure (Reactor Pressure, 0 psig)	4.6-26
4.6.2.3.1.2.8	Ball Check Valve Fails to Close Passage to Vessel Ports	4.6-26
4.6.2.3.1.2.9	Hydraulic Control Unit (HCU) Valve Failures	4.6-26
4.6.2.3.1.2.10	Collet Fingers Fail to Latch	4.6-27
4.6.2.3.1.2.11	Withdrawal Speed Control Valve Failure	4.6-27
4.6.2.3.2	Scram Reliability of CRDS	4.6-27
4.6.2.3.2.1	Reliability Analysis	4.6-28
4.6.2.3.2.2	Control Rod Support and Operation	4.6-28
4.6.2.3.3	Control Rod Drive Housing Supports	4.6-28
4.6.2.3.3.1	Safety Evaluation	4.6-28
4.6.3	Testing and Verification of the CRDS	4.6-29
4.6.3.1	Control Rods	4.6-29
4.6.3.1.1	Testing and Inspection	4.6-29
4.6.3.2	Control Rod Drives	4.6-29
4.6.3.2.1	Testing and Inspection	4.6-29
4.6.3.2.1.1	Development Tests	4.6-29
4.6.3.2.1.2	Factory Quality Control Tests	4.6-30
4.6.3.2.1.3	Operational Tests	4.6-31
4.6.3.2.1.4	Acceptance Tests	4.6-31
4.6.3.2.1.5	Surveillance Tests	4.6-32
4.6.3.3	Control Rod Drive Housing Supports	4.6-34
4.6.3.3.1	Testing and Inspection	4.6-34
4.6.4	Information for Combined Performance of Reactivity Systems	4.6-34
4.6.4.1	Vulnerability to Common Mode Failures	4.6-34
4.6.4.2	Accidents Taking Credit for Two or More Reactivity Control Systems	4.6-34
4.6.5	Evaluation of Combined Performance	4.6-34
4.6.6	References	4.6-35

LSCS-UFSAR

CHAPTER 4.0 - REACTOR

LIST OF TABLES

<u>NUMBER</u>	<u>TITLE</u>
4.2-1	Typical Limiting LHGR's for Gadolinia-Urania Fuel Rods (kW/ft) (Deleted)
4.2-2a	GE Stress Intensity Limits
4.2-2b	FANP Stress Intensity Limits
4.2-3	Conditions of Design Resulting from In-Reactor Process Conditions Combined with Earthquake Loading
4.2-4(a)	Data for the 8X8R Fuel Design
4.2-4(b)	Data for the GE 8x8NB(GE 9B) Fuel Design
4.2-4(c)	Data for the FANP ATRIUM-9B Fuel Design
4.2-4(d)	Data for the FANP ATRIUM-10 Fuel Design
4.2-5	Post-Shipment Fuel Inspection Fuel Inspection Objectives
4.3-1	Maximum Incremental Rod Worths Using BPWS for Each of the Given Rod Groups
4.3-2	Neutron Fluxes Related to Vessel Irradiation
4.3-3	24 Group Multigroup Neutron Flux at the Core Equivalent Radius
4.4-1	Thermal and Hydraulic Design Characteristics of the Reactor Core
4.4-2	Void Distribution
4.4-2a	Axial Power Distribution Used to Generate Void and Quality Distributions (Typical)
4.4-3	Flow Quality Distribution (Typical)
4.4-4	Core Flow Distribution (Typical)
4.4-5	Typical Range of Test Data
4.4-6	Description of Uncertainties (Deleted)
4.4-7	Reactor Coolant System Geometrical Data
4.4-8	Lengths and Sizes of Safety Injection Lines
4.4-9	Bypass Flow Paths

LSCS-UFSAR

CHAPTER 4.0 - REACTOR

LIST OF FIGURES AND DRAWINGS

FIGURES

<u>NUMBER</u>	<u>TITLE</u>
4.1-1	Core Arrangement
4.1-2	Core Cell - GE 8X8R Fuel Type
4.1-2a	Core Cell - GE 8X8NB Fuel Type
4.1-2b	Core Cell – FANP ATRIUM-9B Fuel
4.1-2c	Core Cell FANP ATRIUM-10 Fuel
4.1-2d	GE14 Lattice Arrangement
4.1-3	Fuel Assembly – (GE 8X8R Shown)
4.1-3a	Fuel Assembly GE 8X8NB Fuel
4.1-3b	Fuel Assembly FANP ATRIUM 9B Fuel
4.1-3c	Fuel Assembly FANP ATRIUM-9B Fuel
4.1-3d	Fuel Assembly FANP ATRIUM-10 Fuel
4.1-3e	GE14 Fuel Bundle (Typical)
4.1-4a	General Electric Original Equipment Control Rod Assembly
4.1-4b	General Electric Typical Duralife 215 Control Rod Assembly
4.1-4c	General Electric Typical Marathon Control Rod Assembly
4.1-5	Steam Separator
4.1-6	Steam Dryer
4.1-7	Steam Dryer Panel
4.2-1	Schematic of Four Bundle Cell Arrangement
4.2-2	Bypass Flow Paths
4.2-3	Fuel Bundle - 8X8R and BP8X8R Fuel Types
4.2-3a	Fuel Bundle - GE 8X8EB Fuel Type
4.2-3b	Fuel Bundle - GE 8X8NB Fuel Type
4.2-3c	Fuel Bundle FANP ATRIUM 9B Type
4.2-3d	Fuel Bundle FANP ATRIUM-10 Type
4.2-3e	GE14 Fuel Bundle (Typical)
4.2-4	[Deleted]
4.2-5	Control Rod Velocity Limiter
4.2-5a	Fabricast Velocity Limiter
4.2-6	Typical Cladding Temperature vs. Heat Flux - BOL - 8X8R Fuel Type
4.2-7	Typical Cladding Temperature vs. Heat Flux - Late Life- 8X8R Fuel Type
4.2-8	Typical Energy Release as a Function of Time
4.3-1	Initial Core Loading Map (Deleted)
4.3-1a	Unit 1 Cycle 5 Core Loading Map (Deleted)
4.3-1b	Unit 2 Cycle 5 Core Loading Map (Deleted)
4.3-2	K_{∞} as a Function of Exposure at Various Void Fractions, High Enrichment, Dominant Fuel Type (Typical)

LSCS-UFSAR

FIGURES (Cont'd)

<u>NUMBER</u>	<u>TITLE</u>
4.3-3	Atom Fraction as a Function of Exposure, High Enrichment, Dominant Fuel Type, 40% Voids (Typical)
4.3-4	Fission Fraction as a Function of Exposure, High Enrichment, Dominant Fuel Type, 40% Voids (Typical)
4.3-5	Neutron Generation Time vs. Exposure at 40% Voids (Typical)
4.3-6	Delayed Neutron Fraction vs. Exposure at 40% Voids (Typical)
4.3-7	Variation of Maximum Rod Power as a Function of Exposure for High Enrichment, 40% Voids (Deleted)
4.3-8	Variation of Maximum Rod Power as a Function of Exposure (Deleted)
4.3-9	Variation of Bundle Average Maximum R-Factor as a Function of Bundle Average Exposure for Uncontrolled High Enriched Bundle (Deleted)
4.3-10	Radial Power Factors (Deleted)
4.3-11	Typical Beginning of Cycle and End of Cycle Core Average Axial Power - 764 Core, BWR/4 and BWR/5
4.3-12	Moderator Void Reactivity Coefficient at EOC-1 Initial Cycle (GE)
4.3-13	Doppler Reactivity Coefficient as a Function of Fuel Exposure and Average Fuel Temperature at an Average Void Content of 40% High Enrichment Initial Cycle (GE)
4.3-14	Cold Shutdown Example of a Margin Curve
4.3-15	Control Rod Assignments for Groups 1 through 4 (Sequence A)
4.3-16	Control Rod Assignments for Groups 5 Through 10 (Sequence A)
4.3-17	Control Rod Assignments for Groups 1 Through 4 (Sequence B)
4.3-18	Control Rod Assignments for Groups 5 Through 10 (Sequence B)
4.3-19	Hot Operating EOC-1 Scram Reactivity
4.3-20	Xenon Reactivity Buildup and Burnout After Shutdown
4.3-21	Radial Power Distribution
4.3-22	Axial Power Distribution
4.4-1	Damping Coefficient vs. Decay Ratio (Second Order Systems)
4.4-2	Hydrodynamic and Core Stability Model
4.4-3	Model Block Diagram with Valve Flow Control
4.4-4	Comparison of Tests Results with Reactor Core Analysis (Deleted)
4.4-5	Core Reactivity Stability (End of Cycle) (Deleted)

LSCS-UFSAR

FIGURES (Cont'd)

<u>NUMBER</u>	<u>TITLE</u>
4.4-6	10 psi Pressure Regulator Setpoint Step at 51.5% Rated Power (Natural Circulation)
4.4-7	10 Cent Rod Reactivity Step at 51.5% Rated Power (Natural Circulation)
4.4-8	6-inch Water Level Setpoint Step at 51.5% Rated Power (Natural Circulation)
4.4-9	10 psi Pressure Regulator Setpoint Step at 105% Rated Power and 100% Rated Flow
4.4-10	10 Cent Rod Reactivity Step at 105% Rated Power and 100% Rated Flow
4.4-11	10% Load Demand Step at 105% Rated Power and 100% Rated Flow
4.4-12	6-inch Water Setpoint Step at 105% Rated Power and 100% Rated Flow
4.4-13	10 psi Pressure Regulator Setpoint Step at 68% Power and 50% Rated Flow
4.4-14	10 Cent Rod Reactivity Step at 68% Rated Power and 50% Rated Flow
4.4-15	10% Load Demand Step at 68% Rated Power and 50% Rated Flow
4.4-16	6-inch Water Level Setpoint Step at 68% Rated Power and 50% Rated Flow
4.6-1	Control Rod to Control Rod Drive Coupling
4.6-2	Control Rod Drive Unit
4.6-3	Control Rod Drive Unit (Schematic)
4.6-4	Control Rod Drive Unit (Cutaway)
4.6-5	Control Rod Drive Hydraulic System Process Diagram
4.6-6	Process Data, Control Rod Drive Hydraulic System
4.6-7	Control Rod Drive Hydraulic Control Unit
4.6-8	Control Rod Drive Housing Support

LSCS-UFSAR

DRAWINGS CITED IN THIS CHAPTER*

DRAWING*

SUBJECT

M-97	P&ID Reactor Water Cleanup System, Unit 1
M-100	P&ID Control Rod Drive Hydraulic Piping, Unit 1
M-143	P&ID Reactor Water Cleanup System, Unit 2
M-146	P&ID Control Rod Drive Hydraulic Piping, Unit 2

* The listed drawings are included as “General References” only; i.e., refer to the drawings to obtain additional detail or to obtain background information. These drawings are not part of the UFSAR. They are controlled by the Controlled Documents Program.

CHAPTER 4.0 - REACTOR

4.1 SUMMARY DESCRIPTION

The reactor assembly consists of the reactor vessel and its internal components of the core, shroud, steam separator and dryer assemblies, and jet pumps. Also included in the reactor assembly are the control rods, control rod drive housings, and the control rod drives. Figure 3.9-2 shows the arrangement of reactor assembly components. A summary of the important design and performance characteristics is given in FSAR Section 1.3. Loading conditions for reactor assembly components are specified in Section 3.9.

4.1.1 Reactor Vessel

The reactor vessel design and description are covered in Section 5.3.

4.1.2 Reactor Internal Components

The major reactor internal components are the core (fuel, channels, control blades, and instrumentation), the core support structure (including the core shroud, top guide, and core plate), the shroud head and steam separator assembly, the steam dryer assembly, and the jet pumps. These reactor internals are stainless steel, Zircaloy or other corrosion-resistant alloys. All major internal components of the vessel can be remotely removed except the jet pump diffusers, the jet pump risers, the shroud, the core spray lines, ECCS spargers, and the feedwater sparger. The removal of the steam dryers, shroud head and steam separators, fuel assemblies, incore assemblies, control rods, orificed fuel supports, and control rod guide tubes can be accomplished on a routine basis.

4.1.2.1 Reactor Core

4.1.2.1.1 General

The design of the boiling water reactor core and fuel is based on the proper combination of many design variables and extensive operating experience. These factors contribute to the achievement of high reliability.

A number of important features of the boiling water reactor core design are summarized in the following items:

- a. The BWR core mechanical design is based on application of design basis analysis, operating experience, and experimental test results.

LSCS-UFSAR

- b. The basic thermal and mechanical criteria applied in the design have been proven by irradiation of statistically significant quantities of fuel. The maximum linear heat generation rate is specified so that design criteria are met.
- c. The design power distribution used to size the core represents a worst expected state of operation.
- d. The General Electric thermal analysis basis, GETAB, is applied for GE reloads to assure that more than 99.9% of the fuel rods in the core are expected to avoid boiling transition for the most severe abnormal operational transient described in Chapter 15.0. The FANP “SPCB Critical Power Correlation” and “ANFB Critical Power Correlation” (References 17, 18, and 23) are used to assure that more than 99.9% of the fuel rods avoid boiling transition for the most severe abnormal operational transient described in Chapter 15. The probability of boiling transition occurring during normal reactor operation is insignificantly small.
- e. Because of the large negative moderator density coefficient of reactivity, the BWR is inherently self-limiting for safety. Other advantages are the uses of coolant flow for load following, the inherent self-flattening of the radial power distribution, the ease of control, the spatial xenon stability, and the ability to override xenon in order to follow load.

Boiling water reactors do not have power instabilities due to xenon. This has been demonstrated by special tests which have been conducted on operating BWR's in an attempt to force the reactor into xenon instability. No xenon instabilities have ever been observed in the test results. All of these indicators have confirmed that xenon transients are highly damped in a BWR due to the large negative power coefficient of reactivity (Reference 1).

Important features of the reactor core arrangement are as follows:

- a. There are five types of control blades currently being used, all of which are bottom-entry cruciform control rods. The original General Electric (D-100) control blades (referred to as original equipment) consist of boron carbide powder in stainless steel tubes surrounded by a stainless steel sheath. The original equipment control blades have been irradiated for more than 8 years in the Dresden-1 reactor and have accumulated thousands of hours of service without a significant failure in operating BWR's.

LSCS-UFSAR

The second and third types are Westinghouse CR82 and CR82M-1 control blades. They have wings which are built from a solid bar of stainless steel which contains both boron carbide powder and Hafnium.

The fourth type is the General Electric Duralife 215 design. This design is similar to the Original Equipment design but utilizes hafnium in the loading pattern to allow a longer neutronic blade lifetime.

Finally, the fifth type is the General Electric Marathon design. This design differs from the Original Equipment and Duralife 215 designs in that the Marathon design does not utilize a sheath. The Marathon utilizes square outer tubes with round inner diameters. These tubes are welded together and filled with B₄C and hafnium. The Marathon design also differs from the Original Equipment and Duralife design in that the tie rod is segmented to assist in keeping the weight close to the Original Equipment design.

- b. The fixed incore ion chambers provide continuous power range neutron flux monitoring. A probe tube in each incore assembly provides for a traversing ion chamber for calibration and axial detail. Source and intermediate range monitors are located incore and are axially retractable. The incore location of the startup and source range instruments provides coverage of the large reactor core and provides an acceptable signal-to-noise ratio and neutron-to-gamma ratio. All incore instrument leads enter from the bottom and continuous neutron flux monitoring is provided during refueling. Incore instrumentation is further discussed in Chapter 7.0.
- c. As shown by experience obtained at Dresden-1 and other plants, an operator, utilizing the incore flux monitor system, can maintain the desired power distribution within a large core by proper control rod sequencing.
- d. The Zircaloy channels provide a fixed flow path for the boiling coolant, serve as a guiding surface for the control rods, and protect the fuel during handling operations.
- e. The mechanical reactivity control permits criticality checks during refueling and provides maximum plant safety. The core is designed to be subcritical at any time in its operating history with any one control rod fully withdrawn.
- f. The selected control rod pitch represents a practical value of individual control rod reactivity worth. It allows ample clearance below the pressure vessel between control rod drive mechanisms for ease of maintenance and removal.

4.1.2.1.2 Core Configuration

The reactor core is arranged as an upright circular cylinder containing a large number of fuel cells located within the reactor vessel. The coolant flows upward through the core. The core arrangement (plan view) and the lattice configuration for GE8X8R and GE8X8NB type fuels are shown in Figures 4.1-1, 4.1-2, and 4.1-2a, and for GE14 fuel types in Figure 4.1-2d. The lattice configurations for other GE fuel types can be found in Reference 16. Reload nuclear fuel fabricated by FANP was introduced into the reactor cores for LaSalle Unit 2 Cycle 8 and LaSalle Unit 1 Cycle 9. As noted in Figures 4.1-2b and 4.1-2c, the FANP fuel assemblies differ slightly from the earlier GE fuel designs. See References 25, 26, 29, 30 and 31 design descriptions and detailed lattice configurations for FANP fuel. Reload nuclear fuel fabricated by Global Nuclear Fuel (GNF, formerly GE) was re-introduced into the LaSalle Unit 1 Cycle 11 reactor core. The lattice configuration is described in Reference 16.

4.1.2.1.3 Fuel Assembly Description

As can be seen from the referenced figures, the boiling water reactor core is composed of essentially two components: fuel assemblies (Figures 4.1-3 through 4.1-3e), and control rods (Figure 4.1-4). The GE fuel assemblies in LaSalle are depicted in Figures 4.1-3a, and 4.1-3e. The FANP fuel assemblies (for FANP ATRIUM-9B and ATRIUM-10) in LaSalle are depicted in Figures 4.1-3b through Figure 4.1-3d. The control rod mechanical configurations are shown in Figure 4.1-4. The typical type fuel (GE type) illustrated in Figure 4.1-3a and the control rod mechanical configurations in Figure 4.1-4 are basically the same as those used in Dresden-1 and in all subsequent boiling water reactors. Reference 16 describes the design details of the GE fuel assemblies and Reference 25, 26, 29, 30 and 31 describe the design details of the FANP fuel assemblies.

FANP reload fuel is designed to be compatible with the coresident GE fuel in all operational modes of the reactor core.

4.1.2.1.3.1 Fuel Rod

A fuel rod consists of UO_2 pellets and a Zircaloy cladding tube. A fuel rod is made by stacking pellets into a Zircaloy cladding tube which is evacuated and backfilled with helium, and sealed by welding Zircaloy end plugs in each end of the tube.

The rod is designed to withstand the applied loads, both external and internal. The fuel pellet is sized to provide sufficient volume within the fuel tube to accommodate differential expansion between fuel and cladding. Fuel rod design bases are discussed in more detail in Subsection 4.2.1.

4.1.2.1.3.2 Fuel Bundle

Each fuel bundle contains fuel rods and water rods or water channels/boxes which are spaced and supported in a square (8 x 8, 9 x 9 or 10 x 10) array by a lower and upper tie plate. The fuel bundle has two important design features:

- a. The bundle design places minimum external forces on a fuel rod; each fuel rod is free to expand in the axial direction.
- b. The unique structural design permits the removal and replacement, if required, of individual fuel rods.

The fuel assemblies of which the core is comprised are designed to meet all the criteria for core performance and to provide ease of handling. Selected fuel rods in each assembly differ from the others in uranium enrichment. This arrangement produces more uniform power production across the fuel assembly, and thus allows

a significant reduction in the amount of heat transfer surface required to satisfy the design thermal limitations.

4.1.2.1.4 Assembly Support and Control Rod Location

Peripheral fuel assemblies which are not adjacent to a control blade are supported by the core plate. Otherwise, individual fuel assemblies in the core rest on fuel support pieces mounted on top of the control rod guide tubes. Each guide tube, with its fuel support piece, bears the weight of four assemblies and is supported by a control rod drive housing which transmits weight to the stub tube and to the bottom head of the reactor vessel. The core plate provides lateral support and guidance at the top of each control rod guide tube.

The top guide, mounted inside the core shroud, provides lateral support and guidance for each fuel assembly. The reactivity of the core is controlled by cruciform control rods containing boron carbide and/or hafnium metal. The control rods occupy alternate spaces between fuel assemblies. Each independent drive enters the core from the bottom, and can accurately position its associated control rod during normal operation and yet exert approximately ten times the force of gravity to insert the control rod during the scram mode of operation. Bottom entry allows optimum power shaping in the core, ease of refueling, and convenient drive maintenance.

4.1.2.2 Shroud

The shroud is a cylindrical, stainless steel structure which surrounds the core and provides a barrier to separate the upward flow through the core from the downward flow in the annulus and also provides a floodable volume in the unlikely event of an accident which could drain the reactor pressure vessel. A flange at the top of the shroud mates with a flange on the shroud head and steam separators. The upper cylindrical wall of the shroud and the shroud head form the core discharge plenum. The jet pump discharge diffusers penetrate the shroud support below the core elevation to introduce the coolant to the inlet plenum. To prevent direct flow from the inlet to the outlet nozzles of the recirculation loops, the shroud support is welded to the vessel wall. The shroud support is designed to support and locate the jet pumps, core support structure, and the peripheral fuel assemblies.

Mounted inside the upper shroud cylinder in the space between the top of the core and the upper shroud flange are the core spray spargers with spray nozzles for injection of cooling water. The core spray spargers and nozzles do not interfere with the installation or removal of fuel from the core.

4.1.2.3 Shroud Head and Steam Separators

The shroud head consists of a flange and dome onto which is welded an array of standpipes, with a steam separator located at the top of each standpipe. The shroud head mounts on the flange at the top of the cylinder and forms the cover of the core discharge plenum region. The joint between the shroud head and shroud flange does not require a gasket or other replacement sealing technique. The fixed axial flow-type steam separators have no moving parts and are made of stainless steel.

In each separator, the steam-water mixture rising from the standpipe impinges on vanes which give the mixture a spin to establish a vortex wherein the centrifugal forces separate the steam from the water. Steam leaves the separator at the top and passes into the wet steam plenum below the dryer. The separated water exits from the lower end of the separator and enters the pool that surrounds the standpipes to enter the downcomer annulus. An internal steam separator schematic is shown in Figure 4.1-5.

For ease of removal, the shroud head is bolted to the shroud top flange by long shroud head bolts that extend above the separators for easy access during refueling. The shroud head is guided into position on the shroud via guide rods on the inside of the vessel and locating pins located on the shroud head. The objective of the shroud head bolt design is to provide direct access to the bolts during reactor refueling operations with minimum-depth, underwater tool manipulation during the removal and installation of the assemblies.

4.1.2.4 Steam Dryer Assembly

The steam dryer assembly is mounted in the reactor vessel above the shroud head and forms the top and sides of the wet steam plenum. Vertical guide rods on the inside of the vessel provide alignment for the dryer assembly during installation. The dryer assembly is supported by pads extending from the vessel wall and is locked into position during operation by the reactor vessel top head. Steam from the separators flows upward into the dryer assembly. The steam leaving the top of the dryer assembly flows into vessel steam outlet nozzles which are located alongside the steam dryer assembly. Moisture is removed by the dryer vanes and flows first through a system of troughs and pipes to the pool surrounding the separators and then into the downcomer annulus between the core shroud and reactor vessel wall. The schematics of a typical steam dryer panel are shown in Figures 4.1-6 and 4.1-7.

4.1.3 Reactivity Control Systems

4.1.3.1 Operation

The control rods perform dual functions of power distribution shaping and reactivity control. Power distribution in the core is controlled during operation of the reactor by manipulation of selected patterns of rods. The rods, which enter from the bottom of the near-cylindrical reactor core, are positioned in such a manner to counterbalance steam voids in the top of the core and effect significant power flattening. These groups of control elements, used for power flattening, experience a somewhat higher duty cycle and neutron exposure than the other rods in the control system.

The reactivity control function requires that all rods be available for either reactor "scram" (prompt shutdown) or reactivity regulation. Because of this, the control elements are mechanically designed to withstand the dynamic forces resulting from a scram. They are connected to bottom-mounted, hydraulically actuated drive mechanisms which allow either axial positioning for reactivity regulation or rapid scram insertion. The design of the rod-to-drive connection permits each blade to be attached or detached from its drive without disturbing the remainder of the control system. The bottom-mounted drives permit the entire control system to be left intact and operable for tests with the reactor vessel open.

4.1.3.2 Description of Rods

The original equipment (D-100) and Duralife 215 control blade designs are cruciform-shaped control rods and contain 76 vertical stainless steel tubes (19 tubes in each wing of the cruciform) filled with vibration-compacted boron-carbide powder and/or hafnium metal. The tubes are seal welded with end plugs on either end. In the tubes containing boron-carbide powder, stainless steel balls are used to separate the tubes into individual compartments. The stainless steel balls are held in position by slight crimp in the tube. The individual tubes act as pressure vessels to contain the helium gas released by the boron-neutron capture reaction. The tubes are held in a cruciform array by a stainless steel sheath extending the full length of the tubes. The Duralife 215 design incorporates a hafnium plate near the top of the blade to lengthen the blade neutronic lifetime.

The Marathon design is similar but uses vertical outer tubes with round inner diameters. These tubes are welded together and filled with B₄C and hafnium. The design does not utilize a sheath around the tubes. The Westinghouse CR82 and CR82M-1 designs are similar but use horizontal holes drilled into the wing that are filled with absorber. In the original equipment (D-100) design and the Duralife 215 design a steel stiffener is located approximately at the midspan of each cruciform wing.

LSCS-UFSAR

The control rod can be positioned at 6-inch steps and have a nominal withdrawal and insertion speed of 3 in/sec.

A top handle aligns the tubes and provides structural rigidity at the top of the control rod (GE models shown in Figure 4.1.4(a-c)). Rollers housed in the handle provide guidance for control rod insertion and withdrawal. The Westinghouse design uses pads rather than handle rollers.

A bottom casting is also used to provide structural rigidity and contains positioning rollers and a cone-shaped velocity limiter. The handle and lower casting are welded into a single structure by means of a small cruciform post located in the center of the control rod.

LSCS-UFSAR

The velocity limiter is a device which is an integral part of the control rod and protects against the low probability of a rod drop accident. It is designed to limit the free fall velocity and reactivity insertion rate of a control rod so that minimum fuel damage would occur. It is a one-way device, in that control rod scram time is not significantly affected.

Control rods are cooled by the core bypass flow (Figure 4.2-2). The core bypass flow is made up of recirculation flow from several leakage flow paths.

4.1.3.3 Supplementary Reactivity Control

The control requirements of the initial core are designed to be considerably in excess of the equilibrium core requirements because of the long initial operating cycle. To meet the reactivity control requirements of the initial core load, or any core load with excess reactivity, gadolinia (Gd_2O_3) is selectively placed in several fuel rods of each fuel assembly (except for the 92 natural uranium assemblies used in the initial cycle for both units and 48 low enriched ATRIUM-10 bundles first loaded in LaSalle Unit 2 Cycle 10).

4.1.4 Analysis Techniques

4.1.4.1 Reactor Internal Components

Computer codes for the analysis of the internal components are listed as follows:

- a. MASS, (see also 4.1.4.1.1)
- b. SNAP (MULTISHELL),
- c. GASP,
- d. NOHEAT,
- e. FINITE,
- f. SAMIS,
- g. GEMOP,
- h. SHELL 5
- i. HEATER,
- j. FAP-71,

- k. CREEP-PLAST, and
- l. SAP4G07
- m. ANSYS

Detailed descriptions of these programs are given in the following subsections.

4.1.4.1.1 MASS (Mechanical Analysis of Space Structure)

4.1.4.1.1.1 Program Description

The program, proprietary to the General Electric Company, is an outgrowth of the PAPA (Plate and Panel Analysis) program originally developed by L. Beitch in the early 1960's. The program is based on the principle of the finite element method. Governing matrix equations are formed in terms of joint displacement using a "stiffness-influence-coefficient" concept originally proposed by L. Beitch (Reference 2). The program offers curved beam, plate, and shell elements. It can handle mechanical and thermal loads in a static analysis and predict natural frequencies and mode shapes in a dynamic analysis.

4.1.4.1.1.2 Program Version and Computer

The current version maintained by the original developer, L. Beitch, of the General Electric Aircraft Engine Division in Evandale, Ohio is used. The program operates on the Honeywell 6000 computer.

4.1.4.1.1.3 History of Use

Since its development in the early 1960's, the program has been successfully applied to a wide variety of jet engine structural problems, many of which involve extremely complex geometries. The use of the program in the Nuclear Energy Operation also started shortly after its development.

4.1.4.1.1.4 Extent of Application

Besides the Jet Engine Division and Nuclear Energy Operations, the Missile and Space Division, the Appliance Division, and the Turbine Division of General Electric have also applied the program to a wide range of engineering problems. The Nuclear Energy Operation uses it mainly for piping and jet pump analyses.

4.1.4.1.2 SNAP (MULTISHELL)

4.1.4.1.2.1 Program Description

The SNAP program, which is also called MULTISHELL, is the General Electric code which determines the loads, deformations, and stresses of axisymmetric shells of revolution (cylinders, cones, disc, toroids, and rings) for axisymmetric thermal boundary and surface load conditions.

Thin shell theory is inherent in the solution of E. Peissner's differential equations for each shell's influence coefficients. Surface loading capability includes pressure, average temperature, and linear through-wall gradients; the latter two may be linearly varied over the shell meridian. The theoretical limitations of this program are the same as those of classical theory.

4.1.4.1.2.2 Program Version and Computer

The current version maintained by the General Electric Jet Engine Division at Evandale, Ohio is being used on the Honeywell 6000 computer in the Nuclear Energy Operation.

4.1.4.1.2.3 History of Use

The initial version of the Shell Analysis Program was completed by the Jet Engine Division in 1961. Since then, a considerable amount of modification and addition has been made to accommodate its broadening area of application. Its application in GE has a history longer than 10 years.

4.1.4.1.2.4 Extent of Application

The program has been used to analyze jet engine, space vehicle, and nuclear reactor components. Because of its efficiency and economy, in addition to reliability, it has been one of the main shell analysis programs in General Electric.

4.1.4.1.3 GASP

4.1.4.1.3.1 Program Description

GASP is a finite element program for the stress analysis of axisymmetric or plane two-dimensional geometries. The element representations can be either quadrilateral or triangular. Axisymmetric or plane structural loads can be input at nodal points. Displacements, temperatures, pressure loads, and axial inertia can be accommodated. Effective plastic stress and strain distributions can be calculated using a bilinear stress-strain relationship by means of an iterative convergence procedure.

4.1.4.1.3.2 Program Version and Computer

LSCS-UFSAR

The GE version, originally obtained from the developer, Professor E. L. Wilson, operates on the Honeywell 6000 computer.

4.1.4.1.3.3 History of Use

The program was developed by E. L. Wilson in 1965 (Reference 3). The present version in GE has been in operation since 1967.

4.1.4.1.3.4 Extent of Application

The application of GASP in GE is mainly for elastic analysis of axisymmetric and plane structures under thermal and pressure loads. The GE version has been extensively tested and used by engineers in the company.

4.1.4.1.4 NOHEAT

4.1.4.1.4.1 Program Description

The NOHEAT program is a two-dimensional and axisymmetric transient nonlinear temperature analysis program. An unconditionally stable numerical integration scheme is combined with iteration procedure to compute temperature distribution within the body subjected to arbitrary time- and temperature-dependent boundary conditions.

The program utilizes the finite element method. Included in the analysis are the three basic forms of heat transfer: conduction, radiation, and convection, as well as internal heat generation. In addition, cooling pipe boundary conditions are also treated. The output includes temperature of all the nodal points for the time instants required by the user. The program can handle multitransient temperature input.

4.1.4.1.4.2 Program Version and Computer

The current version of the program is an improvement of the program originally developed by I. Farhoomand and Professor E. L. Wilson of the University of California at Berkeley (Reference 4). The program operates on the Honeywell 6000 computer.

4.1.4.1.4.3 History of Use

The program was developed in 1971 and installed in the General Electric Honeywell computer by one of its original developers, I. Farhoomand, in 1972. A number of heat transfer problems related to the reactor pedestal have been satisfactorily solved using the program.

4.1.4.1.4.4 Extent of Application

The program using finite element formulation is compatible with the finite element stress-analysis computer program GASP. Such compatibility simplified the connection of the two analyses and minimizes human error.

4.1.4.1.5 FINITE

4.1.4.1.5.1 Program Description

FINITE is a general-purpose finite element computer program for elastic stress analysis of two-dimensional structural problems including (1) plane stress, (2) plane strain, and (3) axisymmetric structures. It has provision for thermal, mechanical, and body force loads. The materials of the structure may be homogeneous or inhomogeneous and isotropic or orthotropic. The development of the FINITE program is based on the GASP program (Subsection 4.1.4.1.3).

4.1.4.1.5.2 Program Version and Computer

The present version of the program at GE was obtained from the developer, J. E. McConnelee of GE/Gas Turbine Department in 1969 (Reference 5). This version is used on the Honeywell 6000 computer.

4.1.4.1.5.3 History of Use

Since completion in 1969, the program has been widely used in the Gas Turbine and the Jet Engine Departments of the General Electric Company for the analysis of turbine components.

4.1.4.1.5.4 Extent of Application

The program is used at GE in the analysis of axisymmetric or nearly axisymmetric BWR internals.

4.1.4.1.6 SAMIS

4.1.4.1.6.1 Program Description

The SAMIS program is well designed to solve problems involving matrix algebra with particular emphasis on structural applications. The user has control over the flow of the calculations through the use of "pseudo instructions." Execution of the program is performed in two phases - the generation phase and the manipulative phase. Input data defining the idealization of a structure is read, and stiffness, stress, and load coefficient matrices are generated for elements available to the

LSCS-UFSAR

user. The program has two fundamental and widely used finite elements incorporated. A triangular flat plate element, called a Facet, is available for idealization of plate and shell structures and a straight beam element is available for idealization of frames and trusses and plate/shell structure stiffener representation.

The element formulation and analyses are based on the finite element matrix displacement method. The triangular plate and beam elements are capable of resisting stretching, shearing, bending, and twisting stresses. In the second phase of execution, the generated or input matrices are manipulated according to the rules of matrix algebra as directed by the user.

The program is written in modular form making it easy to add new modules without major reprogramming of subroutines. This facilitates adding to the structural element library other elements to extend idealization capability. Those structural problems consisting of elements that cannot be adequately idealized by triangular plate or beam elements may have their stiffness coefficients submitted directly as input matrices.

4.1.4.1.6.2 Program Version and Computer

The SAMIS version, now operating on the Honeywell 6000 computer of GE, was obtained from the developer, Philco Corporation, Western Development Laboratory (WDL) via the General Electric Space Division. A considerable amount of modification was made on the input and output of the original version to suit the analysis need of this division of GE. Both spectrum and time-history analyses can be performed using the GE version.

4.1.4.1.6.3 History of Use

The SAMIS program was developed by the Philco Corporation, Western Development Laboratories (WDL) under contract to and in association with the Jet Propulsion Laboratory in 1966. The program was first used in the General Electric Company in 1967 and in this division of GE in 1970.

4.1.4.1.6.4 Extent of Application

The current GE version of SAMIS has been extensively used in the analysis of reactor components' response to seismic loadings since 1970. Results of test problems were found to agree closely with theoretical results of the same problem (References 6, 7, and 8).

4.1.4.1.7 General Matrix Manipulation Program (GEMOP)

4.1.4.1.7.1 Program Description

General Matrix Manipulation Program is a general matrix manipulation program capable of performing the majority of standard matrix operations. There presently are 41 operation commands in the program. A maximum of nine full 60 x 60 matrices and six 60-element vectors may be stored incore at any one time. Also available for scratch and storage are up to a maximum of three tapes. This latest version of the program includes subroutines for calculating earthquake, or other forcing functions, and response of a lumped mass structure, either by time history or spectral response methods. The most used features are the eigenvalue and eigenvector subroutines, and the response subroutine. The response is calculated for a system subjected to any piecewise linear forcing function.

4.1.4.1.7.2 Program Version and Computer

The current version of the program being used in GE was obtained from the originator, the General Electric Knolls Atomic Power Laboratory, in June 1969. It was converted from CDC to GE computers. The program is now installed on the Honeywell 6000 computers which is essentially a modification of the original GE computer.

4.1.4.1.7.3 History of Use

The program was originally written in the General Electric Knolls Atomic Power Laboratory for the solution of vibration problems. In 1969, it was converted and modified by General Electric to use on its GE/Honeywell computer for the solution of seismic problems.

4.1.4.1.7.4 Extent of Application

Since its installation in the GE/Nuclear Energy Operation in 1969, the General Matrix Manipulation Program has been constantly used to solve seismic problems involving small lumped-mass systems of less than 80 degrees of freedom. Because of its limitation on problem size, the program is being replaced by SAMIS.

4.1.4.1.8 SHELL 5

4.1.4.1.8.1 Program Description

Shell 5 is a finite shell element program used to analyze smoothly curved thin shell structures with any distribution of elastic material properties, boundary constraints, and mechanical thermal and displacement loading conditions. The

basic element is triangular whose membrane displacement fields are linear polynomial functions and whose bending displacement field is a cubic polynomial function (Reference 9). Five degrees of freedom (three displacements and two bending rotations) are obtained at each nodal point. Output displacements and stresses are in a local (tangent) surface coordinate system.

Due to the approximation of element membrane displacements by linear functions, the inplane rotation about the surface normal is neglected. Therefore, the only rotations considered are due to bending of the shell cross section, and application of the method is not recommended for shell intersection (or discontinuous surface) problems where inplane rotation can be significant.

4.1.4.1.8.2 Program Version and Computer

A copy of the source deck of Shell 5 is maintained in GE. Shell 5 operates on the UNIVAC 1108 computer.

4.1.4.1.8.3 History of Use

Shell 5 is a program developed by Gulf General Atomic Incorporated (Reference 10) in 1969. The program has been in production status at Gulf General Atomic, General Electric, and at other major computer operating systems since 1970.

4.1.4.1.8.4 Extent of Application

Shell 5 has been used at General Electric to analyze reactor shroud support and torus. Satisfactory results were obtained.

4.1.4.1.9 HEATER

4.1.4.1.9.1 Program Description

HEATER is a computer program used in the hydraulic design of feedwater spargers and their associated delivery header and piping. The program utilizes test data obtained by GE using full-scale mockups of feedwater spargers combined with a series of models which represent the complex mixing processes obtained in the upper plenum, downcomer, and lower plenum. Mass and energy balances throughout the nuclear steam supply system are modeled in detail (Reference 11).

4.1.4.1.9.2 Program Version and Computer

This program was developed at GE in FORTRAN IV for the Honeywell 6000 computer.

4.1.4.1.9.3 History of Use

The program was developed by various individuals in GE beginning in 1970. The present version of the program has been in operation since January 1972.

4.1.4.1.9.4 Extent of Application

The program is used in the hydraulic design of the feedwater spargers for each BWR plant, in the evaluation of design modifications, and the evaluation of unusual operational conditions.

4.1.4.1.10 FAP-71 (Fatigue Analysis Program)

4.1.4.1.10.1 Program Description

The FAP-71 computer code, or Fatigue Analysis Program, is a stress analysis tool used to aid in performing ASME-III Nuclear Vessel Code structural design calculations. Specifically, FAP-71 is used in determining the primary plus secondary stress range and number of allowable fatigue cycles at points of interest. For structural locations at which the 3S (P+Q) ASME Code limit is exceeded, the program can perform either (or both) of two elastic-plastic fatigue life evaluations: 1) one method reported in ASME Paper 68-PVP-3, and 2) the present method documented in Paragraph NB-3228.3 of the 1971 edition of the ASME Section III Nuclear Vessel Code. The program can accommodate up to 25 transient stress states of as many as 20 structural locations.

4.1.4.1.10.2 Program Version and Computer

The present version of FAP-71 was completed by L. Young of GE in 1971 (Reference 12). The program currently is on the GE Honeywell 6000 computer.

4.1.4.1.10.3 History of Use

Since its completion in 1971, the program has been applied to several design analyses of GE BWR vessels.

4.1.4.1.10.4 Extent of Application

The program is used in conjunction with several shell analysis programs in determining the fatigue life of BWR mechanical components subject to thermal transients.

4.1.4.1.11 CREEP/PLASTICITY

4.1.4.1.11.1 Program Description

A finite element program used for the analysis of two-dimensional (plane and axisymmetric) problems under conditions of creep and plasticity. The creep formulation is based on the memory theory of creep in which the constitutive relations are cast in the form of hereditary integrals. The material creep properties are built into the program and they represent annealed 304 stainless steel. Any other creep properties can be included if required.

The plasticity treatment is based on kinematic hardening and von Mises yield criterion. The hardening modulus can be constant or a function of strain.

4.1.4.1.11.2 Program Version and Computer

The program can be used for elastic-plastic analysis with or without the presence of creep. It can also be used for creep analysis without the presence of instantaneous plasticity. A detailed description of theory is given in Reference 14. The program is operative on Univac-1108.

4.1.4.1.11.3 History of Use

This program was developed by Y. R. Rashid (Reference 14) in 1971. It underwent extensive program testing before it was put on production status.

4.1.4.1.11.4 Extent of Application

The program is used at GE in the channel cross section mechanical analysis.

4.1.4.1.12

The SAP4G07 computer code is used to evaluate modifications to the Jet Pumps. The SAP4G07 finite element code utilizes similar analytic approaches and provides consistently conservative results when compared to the MASS computer code (UFSAR 4.1.4.1.1). The MASS code is outdated and was replaced with the SAP4G07 code. SAP4G07 is a Level II verified program for jet pump applications. The SAP4G07 finite element computer code has been in general use for jet pump structural and modal analysis since the early 1980s.

Since the early 2000s, the ANSYS software has also been used for finite element stress analysis of jet pump modifications. ANSYS is widely used in numerous industries.

4.1.4.2 Fuel Rod Thermal Analysis

Fuel and thermal design analyses are performed for GE fuel using the GESTR-MECHANICAL Program as described in Reference 15

Fuel and thermal design analyses are performed for FANP fuel using the RODEX2 and RODEX2A codes described in References 21 and 22.

4.1.4.3 Reactor Systems Dynamics

The analysis techniques and computer codes used in reactor systems dynamics are described in References 13 and 27. Subsection 4.4.4.6 also provides a complete stability analysis for the reactor coolant system.

4.1.4.4 Nuclear Engineering Analysis

The analysis techniques are fully described and referenced in Subsection 4.3.3. The codes used in the analysis are:

<u>Computer Code</u>	<u>Function</u>
Lattice Physics Model	Calculates averaged few-group cross sections, bundle reactivities, and relative fuel rod powers within the fuel bundle.
BWR Reactor Simulator	Calculates three-dimensional nodal power distributions, exposures, and thermal hydraulic characteristics as burnup progresses.

4.1.4.5 Neutron Fluence Calculations

Multigroup neutron flux calculations outside of the core were carried out using a one-dimensional Sn transport code (SN1D) with general anisotropic scattering, order 8 and P expansion of P3. The transport calculations incorporate, as an initial starting point, the neutron fission distributions prepared from the core physics data as a fixed distributed source. Anisotropic scattering was considered for all regions outside of the core. The cross sections were prepared with a 1/E flux weighting and P matrices for anisotropic scattering, but did not include resonance self-shielding factors. Fast neutron fluxes greater than 1 MeV for locations other than the core midplane region were calculated

using a point kernel approach. The point kernel approach sums the contribution of many subdivisions in the core to the point of concern. The attenuation between the core and point of concern was evaluated using a modified Albert Welton point kernel. With this analysis method, an additional normalization was used to force a fit between the point kernel techniques and the transport analysis methods.

More recently, the NRC issued Regulatory Guide (RG) 1.190, which provides state of the art calculation and measurement procedures that are acceptable to the NRC for determining Reactor Pressure Vessel (RPV) neutron fluence. LSCS RPV fluence has been evaluated using a method in accordance with the recommendations of RG 1.190. Future evaluations of RPV fluence will be completed using a method in accordance with the recommendations of RG 1.190 (as noted in Reference 28).

4.1.4.6 Thermal Hydraulic Calculations

A parallel flow path computer program is used to perform the steady-state BWR reactor core thermal-hydraulic analysis. Program input includes the core geometry, operating power, pressure, coolant flow rate and inlet enthalpy, and power distribution within the core. Output from the program includes core pressure drop, coolant flow distribution, critical power ratio, and axial variations of quality, density, and enthalpy for each channel type. The program is capable of analyzing a core consisting of a mixture of fuel types (e.g., 8 x 8, 9 x 9 or 10 x 10 reload and old fuel, with or without water rods or water boxes).

4.1.5 References

1. R. L. Crowther, "Xenon Considerations in Design of Boiling Water Reactors," APED-5640, June 1968.
2. L. Beitch, "Shell Structures Solved Numerically by Using a Network of Partial Panels," AIAA Journal, Vol. 5, No. 3, March 1967.
3. E. L. Wilson, "A Digital Computer Program for the Finite Element Analysis of Solids with Non-Linear Materials Properties," Aerojet General Technical Memo No. 23, Aerojet General, July 1965.
4. I. Farhoomand and E. L. Wilson, "Non-Linear Heat Transfer Analysis of Axisymmetric Solids," SESM Report SESM 71-6, University of California, Berkeley, California 1971.
5. J. E. McConnelee, "Finite-Users Manual," General Electric TIS Report DF 69SL206, March 1969.
6. R. J. Melosh et al., "Structural Analysis and Matrix Interpretive System (SAMIS) Program Report Rev. 1," Tech. Memo 33-307, Jet Propulsion Laboratory, Pasadena, California, December 15, 1966.

LSCS-UFSAR

7. R. J. Melosh and H. N. Christiansen, "Structural Analysis and Matrix Interpretive System (SAMIS) Program: Technical Report," Tech. Memo 33-311, Jet Propulsion Laboratory, Pasadena, California, November 1, 1966.
8. T. E. Lang, "Structural Analysis and Matrix Interpretive System (SAMIS) User Report," Tech. Memo 33-305, Jet Propulsion Laboratory, Pasadena, California, March 1, 1967.

LSCS-UFSAR

9. R. W. Clough and C. P. Johnson, "A Finite Element Approximation for the Analysis of Thin Shells," International Journal Solid Structures, Vol. 4, 1968.
10. "A Computer Program for the Structural Analysis of Arbitrary Three-Dimensional Thin Shells," Report No. GA-9952, Gulf General Atomic.
11. A. B. Burgess, "User Guide and Engineering Description of HEATER Computer Program," March 1974.
12. L. J. Young, "FAP-71 (Fatigue Analysis Program) Computer Code," GE/NED Design Analysis Unit R. A. Report No. 49, January 1972.
13. "Stability and Dynamic Performance of the General Electric Boiling Water Reactor," NEDO-21506, January 1977.
14. Y. R. Rashid, "Theory Report for CREEP-PLAST Computer Program," GEAP-10546, AEC Research and Development Report, January 1972.
15. "General Electric Standard Application for Reactor Fuel (GESTAR II)," NEDE-24011-P-A, (Latest approved revision).
16. NEDE-31152P, "GE Fuel Bundle Designs," (Latest Revision).
17. Advanced Nuclear Fuels Critical Power Methodology for Boiling water Reactors/Advanced Nuclear Fuels Corporation Critical Power Methodology for Boiling Water Reactors: Methodology for Analysis of Assembly Channel Bowing Effects/NRC Correspondence, XN-NF-524 (P)(A) Revision 2, and Supplement 1 Revision 2, Supplement 2, Advanced Nuclear Fuels Corporation, November 1990.
18. ANFB Critical Power Correlation, ANF-1125 (P)(A) and Supplements 1 and 2, Advanced Nuclear Fuels Corporation, April 1990; ANFB Critical Power Correlation Application for Co-Resident Fuel, EMF-1125(P)(A), Supplement 1, Appendix C, Siemens Power Corporation, August 1997; and ANFB Critical Power Correlation Determination of Atrium-9B Additive Constant Uncertainties, ANF-1125(P)(A) Supplement 1, Appendix E, Siemens Power Corporation, September 1998.
19. Generic Mechanical Design Criteria for BWR Fuel Designs, ANF-89-98(P)(A), Revision 1, Siemens Power Corporation, April 1991.
20. LaSalle Administrative Technical Requirements

LSCS-UFSAR

21. RODEX2 Fuel Rod Thermal-Mechanical Response Evaluation Model, XN-NF-81-58(P)(A) and Supplements 1 and 2 Revision 2, Exxon Nuclear Company, Richland, WA 99352, May 1986.
22. RODEX2A (BWR) Fuel Rod Thermal-Mechanical Evaluation Model, XN-NF-85-74(P)(A), Exxon Nuclear Company, August 1986.
23. SPCB Critical Power Correlation, EMF-2209(P)(A) Revision 2, Siemens Power Corporation, September 2003.
24. Boiling Water Reactor Licensing Methodology Summary, EMF-94-217(P), Revision 1, Siemens Power Corporation, Nuclear Division, October 1995.
25. Fuel Design Report of LaSalle 2, Cycle 8 ATRIUM™-9B Fuel Assemblies, EMF-96-122(P), Revision 1, Siemens Power Corporation, Nuclear Division, September 1996.
26. Mechanical and Thermal-Hydraulic Design Report for LaSalle Units 1 and 2 ATRIUM™-10 Fuel Assemblies, EMF-2589(P), Revision 0, Framatome ANP Richland, Inc., July 2001.
27. BWR Stability Analysis: Assessment of STAIF with Input from MICROBURN-B2, EMF-CC-074(P) Volume 4 Revision 0, Siemens Power Corporation, August 2000.
28. Safety Evaluation related to Amendment 160 to FOL No. NPF-11 and Amendment 146 to FOL No. NPF-18, dated 8/13/2003.
29. "Mechanical Design Report for LaSalle Unit 1 Reload LSA1-12 ATRIUM™-10 Fuel Assemblies," EMF-3226(P), Revision 0, Framatome ANP, October 2005.
30. "LaSalle Units 1 and 2 Thermal-Hydraulic Design Report for ATRIUM™-10 Fuel Assemblies," EMF-3212(P), Revision 0, Framatome ANP, October 2005.
31. "Mechanical Design Report for LaSalle Unit 2 Reload LSA2-12 ATRIUM™-10 Fuel Assemblies", ANP-2562P, Revision 0, AREVA NP, September 2006.

4.2 FUEL SYSTEM

4.2.1 Design Bases

This section and its subsections were written to describe the design basis consideration used in the design of the GE initial core and reload fuel. For historical purposes, these sections remain in the UFSAR as long as such fuel remains in the reactor or stored in the spent fuel pool.

Detailed descriptions of the design basis considerations used in the design of the FANP reload fuel can be found in Reference 46 and 49. If a FANP reference contains the equivalent information as what is being presented for GE, that reference is provided.

4.2.1.1 Safety Design Bases

The fuel assembly is designed to ensure, in conjunction with the core nuclear characteristics (Section 4.3), the core thermal and hydraulic characteristics (Section 4.4), the plant equipment characteristics and the instrumentation and protection system, that fuel damage does not result in the release of radioactive materials in excess of the guideline values of 10 CFR 20, 50, and 100.

The mechanical design process emphasizes that:

- a. the fuel assembly provides substantial fission product retention capability during all potential operational modes, and
- b. the fuel assembly provides sufficient structural integrity to prevent operational impairment of any reactor safety equipment.

Assurance of the design basis considerations is provided by the following fuel assembly capabilities:

- a. Pressure and temperature capabilities

The fuel assembly and its components are capable of withstanding the predicted thermal, pressure, and mechanical interaction loadings occurring during startup testing, normal operation, and abnormal operation without impairment of operational capability.

LSCS-UFSAR

b. Handling capability

The fuel assembly and each component thereof is capable of withstanding loading predicted to occur during handling without impairment of operational capability.

c. Earthquake loading capability (OBE)

The fuel assembly and each component thereof is capable of sustaining incore loading predicted to occur from an operating basis earthquake (OBE), when occurring during normal operating conditions without impairment of operational capability.

d. Earthquake loading capability (SSE)

The fuel assembly and each component thereof is capable of sustaining incore loading predicted to occur from a safe shutdown earthquake (SSE) when occurring during normal operation without:

1. exceeding deflection limits which allow control rod insertion, and
2. fragmentation or severance of any bundle component.

e. Accident capability

The capability of the fuel assembly to withstand the control rod drop accident, the pipe breaks inside and outside containment accidents, the fuel handling accident, and one recirculation pump seizure accident, is determined by analysis of the specific event.

The ability of the fuel assembly to provide the preceding capabilities is evaluated by one or more of the following:

- a. design ratios developed by utilizing continually evolving, state-of-the-art numerical analysis techniques (Subsection 4.2.1.2.15);
- b. analytical procedures based on classical methods (Subsection 4.2.1.2.5); and
- c. experience and testing (Subsection 4.2.3.2).

For the initial reloads of the FANP ATRIUM-9B and ATRIUM-10 fuel, the control rod drop accident, the pipe breaks inside and outside containment accidents, and the fuel handling accident were all evaluated for the fuel assembly's capability to withstand their effects. The recirculation pump seizure event was not analyzed by FANP for their ATRIUM-9B or ATRIUM-10 fuel; it was dispositioned as bounded by the LOCA accident. The control rod drop accident is evaluated each cycle for both FANP and GE reloads.

4.2.1.2 Power Generation Design Basis

The fuel assembly is designed to ensure, in conjunction with the core nuclear characteristics, the core thermal and hydraulic characteristics, the plant equipment characteristics and the instrumentation and protection system, that fuel damage limits will not be exceeded during either planned operation or abnormal operational transients caused by any single equipment malfunction or single operator error.

4.2.1.2.1 Material Selection

The basic materials used in fuel assemblies are Zircaloy, natural zirconium, Type 304 stainless steel, Inconel-X, and ceramic uranium dioxide and gadolinia. These materials have been shown from earlier reactor experience to be compatible with BWR conditions and to retain their design function capability during reactor operation. Additional information on material properties is referenced in Reference 41.

4.2.1.2.2 Effects of Irradiation and Fuel Swelling

Irradiation affects both fuel and cladding material properties. The effects include increased cladding strength and reduced cladding ductility. In addition, irradiation in a thermal reactor environment results in the buildup of both gaseous and solid fission products within the UO_2 fuel pellet which tend to increase the pellet diameter, i.e., fuel irradiation swelling. Pellet internal porosity and pellet-to-cladding gap have been specified such that the thermal expansion and irradiation swelling are accommodated throughout life. The irradiation swelling model is based on data reported in References 2 and 3 and on an evaluation of high exposure data reported in Reference 4.

Observations and calculations based on this refined model for relative UO_2 fuel/cladding expansion indicate that the as-fabricated UO_2 pellet porosity is adequate (without pellet dishing) to accommodate the fission-product-induced UO_2 swelling out to expected exposures.

The primary purpose of the gap between the UO_2 fuel pellet and Zircaloy cladding is to accommodate differential diametral expansion of fuel pellet and cladding and, thus, preclude the occurrence of excessive gross diametral cladding strain. A short time after reactor startup, the fuel cracks radially and redistributes out to the

cladding. Experience has shown, however, the gap volume remains available in the form of radial cracks to accommodate gross diametral fuel expansion.

The value of thermal conductance used in BWR fuel design is derived from postirradiation data on exposed fuel with an initial pellet-to-cladding gap which is significantly larger than that employed in the General Electric fuel design.

Axial ratcheting of fuel cladding is not considered in BWR fuel rod design. Prototypical fuel rods have been operated in the Halden test reactor with axial elongation transducers. No significant axial ratcheting has been observed (Reference 5).

Fission product buildup also tends to cause a slight reduction in fuel melting temperature. The melting point of UO_2 is considered to decrease with irradiation based on data from Reference 6.

In the temperature range of interest (500°C), the fuel thermal conductivity is not considered to be significantly affected by irradiation as reported in Reference 7.

A small fraction of the gaseous fission products is released from the fuel pellets to produce an increase in fuel rod internal gas pressure as discussed further in Subsection 4.2.1.2.7. In general, such irradiation effects on fuel performance have been characterized by available data and are considered in determining the design features and performance. Thus, the irradiation effects on fuel performance are inherently considered when determining whether or not the stress intensity limits and temperature limits are satisfied.

In Reference 49, FANP states that the BWR evaluation models for densification and swelling are included in the NRC approved fuel performance codes, References 50 and 51.

4.2.1.2.3 Fuel Densification

4.2.1.2.3.1 GE Fuel

Fuel performance calculations that account for some specific effects of fuel densification have been performed with an approved version of the General Electric analytical model, GESTR-Mechanical. The approved analytical model incorporates time-dependent fuel densification, time-dependent gap closure and cladding creepdown for the calculation of gap conductance. Other fuel performance predictions, such as cladding response, are also calculated. Cladding collapse has not been observed in boiling water reactor fuel rods, but its theoretical occurrence is calculated with a Code, SAFE-COLAPS, contained in Reference 26 and approved by the NRC (Reference 35). All of the fuel cladding used at LSCS has been shown not to collapse during the life of the fuel.

4.2.1.2.3.2 FANP Fuel

Fuel densification and swelling are limited by design criteria specified for fuel temperature, cladding strain, cladding collapse, and internal pressure criteria (Reference 49).

Creep collapse of the cladding and the subsequent potential for fuel failure is avoided in the FANP fuel system design by eliminating the formation of axial gaps. The maximum cladding circumferential creep and ovalization consistent with the time of maximum densification is computed during a creep collapse evaluation to demonstrate that no axial gaps are present. The evaluation must show that the pellet column is compact at the burnup of maximum densification (approximately 6000 MWd/MTU). The internal plenum spring provides an axial load on the fuel stack that is sufficient to assist in the closure of any gaps caused by handling, shipping, and densification. Evaluation of cladding creep stability in the unsupported condition is performed considering the compressive load on the cladding due to the difference between primary system pressure and the fuel rod internal pressure. FANP fuel is designed to minimize the potential for the formation of axial gaps in the fuel and to minimize clad creepdown which would prevent the closure of axial gaps or allow creep collapse (Reference 49).

4.2.1.2.4 Incipient UO₂ Center Melting

4.2.1.2.4.1 GE Fuel

The fuel rod is evaluated to ensure that fuel rod failure due to fuel melting is not expected to occur during normal steady-state operation. Incipient center melting is expected to occur in fresh GE UO₂ fuel rods at the linear heat generation rate (LHGR) described in Reference 41. The LHGR values for incipient center melt decrease slightly with burnup. The effect of gadolinia concentration and fuel exposure on the LHGR at calculated incipient center melting is also described in Reference 41.

4.2.1.2.4.2 FANP Fuel

Fuel failure from the overheating of the fuel pellets is not allowed. The centerline temperature of the fuel pellets must remain below melting during normal operation and anticipated operational occurrences. The melting point of the fuel includes adjustments for burnup and gadolinia content. FANP establishes steady state and transient design LHGR limits for each fuel type which protect against centerline melting. These LHGR limits are appropriate for normal operation and anticipated operational occurrences throughout the design lifetime of the fuel (Reference 49).

4.2.1.2.5 Maximum Allowable Stresses

The strength theory, terminology, and stress categories presented in the ASME Boiler and Pressure Vessel Code, Section III, are used as a guide in the mechanical design and stress analysis of the reactor fuel rods. The mechanical design is based on the maximum shear stress theory for combined stresses. The equivalent stress intensities used are defined as the difference between the most positive and least positive principal stresses in a triaxial field. Thus, stress intensities are directly comparable to strength values found from tensile tests. Table 4.2-2a and b present a summary of the basic stress intensity limits that are applied for Zircaloy-2 cladding for both GE fuel and FANP ATRIUM-9B and ATRIUM-10 fuel.

4.2.1.2.5.1 GE Fuel

In this analysis of BWR Zircaloy-clad UO₂ pellet fuel, continuous functional variations of mechanical properties with exposure are not employed since the irradiation effects become saturated at very low exposure. At beginning of life, the cladding mechanical properties employed are the unirradiated values. At subsequent times in life, the cladding mechanical properties employed are the saturated irradiated values. The only exception to this is that unirradiated mechanical properties are employed above the temperatures for which irradiation effects on cladding mechanical properties are assumed to be annealed out. It is significant that the values of clad yield strength and ultimate tensile strength employed represent the approximate lower bound of data on cladding fabricated by General Electric, i.e., approximately two standard deviations below the mean value.

In this analysis the calculated stress and the yield strength or ultimate strength are combined into a dimensionless quantity called the design ratio. This quantity is the ratio of calculated stress intensity to the design stress limit for a particular stress category. The design stress limit for a particular stress category is defined as a fraction of either the yield strength or ultimate strength, whichever is lower. Thus, the design ratio is a measure of the fraction of the allowable stress represented by the calculated stress.

Analyses are performed to show that the stress intensity limits given in Table 4.2-2a and b are not exceeded during continuous operation with linear heat generation rates up to the design operating limit, or during transient operation above the design operating limit. Stresses due to external coolant pressure, internal gas pressure, thermal effects, spacer contact, flow-induced vibration, and manufacturing tolerances are considered. Cladding mechanical properties used in stress analyses are based on test data of fuel rod cladding for the applicable temperature.

Fuel rods are evaluated to assure that the fuel will not fail due to stresses or strains exceeding the fuel rod mechanical capability. The analysis performed is described in Reference 41.

4.2.1.2.5.2 FANP Fuel

FANP requires compliance with both Standard Review Plan criteria for pellet/cladding interaction for steady state and transient conditions over the lifetime of the fuel. The first one is that transient – induced deformations must be less than 1% uniform cladding strain. The second is that fuel melting cannot occur. Compliance with the fuel melting criteria is discussed in Section 4.2.1.2.4.2.

The design basis for the fuel cladding stress limits is that the fuel system will not be damaged due to fuel cladding stresses. Conservative limits are derived from the ASME Boiler Code, Section III, Article-2000; and the specified 0.2% offset yield strength and ultimate strength for Zircaloy (Reference 49).

4.2.1.2.6 Capacity for Fission Gas Inventory

The available fission gas retention volume is determined based upon the following assumptions:

- a. Nominal as-built plenum length and cladding inside diameter.
- b. Maximum expected fuel-cladding differential expansion.
- c. No credit for fuel-cladding annulus (gap).
- d. The "net" volume is corrected for the volume of the components contained within the fuel rod plenum.

4.2.1.2.7 Maximum Internal Gas Pressure

Fuel rod internal pressure is due to the helium which is backfilled during rod fabrication, the volatile content of the UO_2 , and the fraction of gaseous fission products which are released from the UO_2 . Nominal tolerances are assumed in defining the hot plenum volume used to compute fuel rod internal gas pressure.

4.2.1.2.7.1 GE Fuel

The fuel rod internal pressure is calculated using the perfect gas law ($P = NRT/V$). A quantity of 1.35 milligram-moles of fission gas is produced per MWd of power production. In fuel rod pressure and stress calculations, 4.0% of the fission gas produced is calculated to be released from any UO_2 volume at a temperature less than 3000° F and 100% from any UO_2 above 3000° F. This fission gas release model has been demonstrated by experiment to be conservative over the complete range of design temperature and exposure conditions (Reference 4). The calculated maximum fission gas release fraction in the highest design power density rod is less than 25%. This calculation is conservative because it assumes the worst peaking

factors applied constantly to this rod. The percentage of total fuel rod radioactivity released to the rod plenum is much less than 25% because of radioactive decay during diffusion from the UO_2 .

Creepdown and creep collapse of the plenum are not considered because significant creep in the plenum region is not expected. The fuel rod is designed to be free-standing throughout its lifetime. The temperature and neutron flux in the plenum region are considerably lower than in the fueled region, thus the margin to creep collapse is substantially greater in the plenum. Direct measurements of irradiated fuel rods have given no indication of significant creepdown of the plenum.

The fuel rod is evaluated to assure that the effects of rod internal pressure during normal steady state operation will not result in fuel failure. The analysis is further described in Reference 41.

4.2.1.2.7.2 FANP Fuel

To prevent unstable thermal behavior and to maintain the integrity of the cladding, FANP limits the maximum internal rod pressure relative to system pressure to avoid significant hydride reorientation during cooldown conditions or depressurization conditions. When the fuel rod internal pressure exceeds system pressure, the pellet-cladding gap has to remain closed if it is already closed or it should not tend to open for steady or increasing power conditions. Outward circumferential creep which may cause an increase in pellet-to-cladding gap must be prevented since it would lead to higher fuel temperature and higher fission gas release. The maximum internal pressure is also limited to protect embrittlement of the cladding caused by hydride reorientation during cooldown and depressurization conditions (Reference 49).

4.2.1.2.8 Internal Pressure and Cladding Stresses During Normal Conditions

The internal pressure is applied coincident with the applicable coolant pressure to compute the resulting cladding stresses, which, combined with cladding stresses from other sources, must satisfy the stress limits described in Subsection 4.2.1.2.5.

4.2.1.2.9 Cycling and Fatigue Limits

4.2.1.2.9.1 GE Analysis

The fatigue analysis utilizes the linear cumulative damage rule (Miner's hypothesis) as documented in "Fatigue Design Basis for Zircaloy Components" (Reference 12). The fatigue analysis is based on the estimated number of temperature, pressure, and power cycles. The fuel assembly and fuel rod cladding are evaluated to ensure that strains due to cyclic loadings will not exceed the fatigue capability.

4.2.1.2.9.2 FANP Analysis

Cycle loading associated with relatively large changes in power can cause cumulative damage which may eventually lead to fatigue failure. Therefore, FANP requires that the cladding not exceed a cumulative fatigue usage factor of 0.67. The O'Donnell and Langer fatigue curves are used in the analysis. These fatigue curves have been adjusted to incorporate the recommended '2 or 20' safety factor. This safety factor reduces the stress amplitude by factor of 2 or reduces the number of cycles by a factor of 20, whichever is more conservative. The fatigue curves provide the maximum allowed number of cyclic loading for each stress amplitude. The fatigue usage factor is the number of expected cycles divided by the number of allowed cycles. The total cladding usage factor is the sum of the individual usage factors for each duty cycle (Reference 49).

4.2.1.2.10 Deflections

4.2.1.2.10.1 GE Evaluation

The operational fuel rod deflections considered are the deflections due to:

- a. manufacturing tolerances,
- b. flow-induced vibration,
- c. thermal effects, and
- d. axial load.

There are two criteria that limit the magnitude of these deflections. One criterion is that the cladding stress limits must be satisfied; the other is that the fuel rod-to-rod and rod-to-channel clearances must be sufficient to allow free passage of coolant water to all heat transfer surfaces. Thermal-hydraulic testing has demonstrated that allowing a statistical minimum clearance of 0.060 inch rod-to-rod and 0.030 inch rod-to-channel at two standard deviations away from the nominal clearance is sufficient to ensure a very low probability of local rod overheating due to boiling transition. The fuel rod is evaluated to ensure that fuel rod bowing does not result in fuel failure due to boiling transition.

4.2.1.2.10.2 FANP Evaluation

Differential expansion between the fuel rods, and lateral thermal and flux gradients can lead to lateral creep bow of the rods in the spans between spacer grids. This lateral creep bow alters the pitch between the rods and may affect the peaking and local heat transfer. The FANP design basis for fuel rod bowing is that lateral displacement of the fuel rods shall not be of sufficient magnitude to impact thermal margins. Extensive post-irradiation examinations have confirmed that such rod

bow has not reduced spacing between adjacent rods by more than 50%. The potential effect of this bow on thermal margins is negligible. Rod bow at extended burnup does not affect thermal margins due to the lower power achieved at high exposure (Reference 49).

4.2.1.2.11 Flow-Induced Fuel Rod Vibrations

Flow-induced fuel rod vibrations depend primarily on flow velocity and fuel rod geometry. The stress levels resulting from the vibrations are negligibly low and well below the endurance limit of all affected components. This phenomenon is further described in GE References 13 and 41.

Reference 47 discusses the FANP calculations for flow induced vibrations. Vibrational stresses due to flow induced vibrations are calculated with the Paidoussis analysis which assumes:

- 1) The structural stiffness of the rod is due to cladding only.
- 2) The sections of the fuel rod between spacers and/or tie plate supports are modelled structurally as a simple beam with pinned ends.
- 3) Flow velocity, viscosity, and virtual mass for the amplitude calculations are evaluated as suggested by Paidoussis.

4.2.1.2.12 Fretting Corrosion

Fretting wear has been considered in establishing the fuel mechanical design basis. Specific GE fuel designs described in Reference 41 have been incorporated to eliminate fretting wear. Tests of these designs have been conducted both out-of-reactor as well as in-reactor prior to application in a complete reactor core basis. All tests and post-irradiation examinations have indicated that fretting corrosion does not occur. Post-irradiation examination of many fuel rods indicates only minor fretting wear. Excessive wear at spacer contact points has never been observed with the current spacer configuration. Additional information on testing relative to fretting wear is contained in Reference 41. FANP discusses fretting wear in Reference 49.

4.2.1.2.13 Seismic Loadings

The fuel is analyzed for loading in the reactor resulting from seismic accelerations. The fuel seismic design basis is the design basis presented in References 15, 17 and 41 for GE fuel. The fuel seismic design basis for FANP fuel is presented in Reference 49. Reference 48 verifies that the FANP seismic criteria were met for a particular reload.

4.2.1.2.14 Chemical Properties of Cladding and Fuel Material

The fuel material, fuel rod, pellets, and cladding are discussed generally in Subsections 4.2.2.2 through 4.2.2.5. Testing and inspection of fuel is covered in Subsection 4.2.4. Reference 41 reports the specific fuel parameters of the fuel used for LSCS. Reference 19 presents the BWR fuel experience through September 1974. Reference 42 represents later BWR fuel experience. References 46, 48, and 49 report specific fuel parameters for FANP fuel.

4.2.1.2.15 Design Ratios

Design ratios are defined by the following relationship: $D.R. = A/L$ where D.R. is the design ratio, L is the limiting parameter value, and A is the actual parameter value. Design ratios of less than one are demonstrated for component parameters influenced by loading conditions which may affect the structural or dimensional integrity of the fuel assembly or any component thereof.

4.2.1.2.15.1 Limiting Parameter Values

The following information is based on GE methodology. For a discussion on FANP methodologies see Reference 46, 47, 48, 49 and 55.

4.2.1.2.15.1.1 Normal and Upset Design Conditions

Limiting parameter values for each component are determined in the following manner as defined by Table 4.2-3:

- a. For stress resulting from mean value or steady-state loading, the limiting value is determined by consideration of the material 0.2% offset yield strength or the equivalent strain, as established at operating temperature.
- b. For stress resulting from load cycling, limiting parameter values are determined from fatigue limits.
- c. For stress resulting from loading of significant duration, the limiting parameter is determined from consideration of stress rupture as defined by the Larson-Miller parameter. If metal temperatures are below the level of applicability of stress rupture for the material or if the yield strength is more limiting then the limiting value of stress is determined from consideration of the material 0.2% offset yield strength or the equivalent strain, as established at operating temperatures.

LSCS-UFSAR

- d. Where stress rupture and fatigue cycling are both significant, the following limiting condition is applied:

$$\left(\sum_{I=1 \text{ to } n} \frac{\text{actual time at stress}}{\text{allowable time at stress}} + \sum_{I=1 \text{ to } m} \frac{\text{actual number of cycles}}{\text{allowable cycles at stress}} \right) \leq 1$$

- e. Critical instability loads shall be derived from test data when available or from analytical methods when applicable test data are not available.
- f. Deflection limits are those values of component deformation which could cause an undesirable event such as impairment of control rod movement or an excessive leakage flow rate.

4.2.1.2.15.1.2 Emergency and Faulted Design Conditions

Limiting parameter values are determined in the following manner as defined by Table 4.2-3:

- a. Stress limits are determined from consideration of the ultimate tensile strength or equivalent strain of the material, as established at operating temperatures.
- b. Critical instability loads are determined from test data when available or from analytical methods when applicable test data is not available.
- c. Deflection limits are those values of deformation that if occurring could lead to a more serious consequence such as prevention of control rod insertion.

4.2.1.2.15.2 Actual Parameter Values

The following information is based on GE methodology. For a discussion on FANP methodologies see References 46, 47, 48, 49 and 55.

Actual parameter values are determined from the following considerations:

- a. Effective stresses are determined at each point of interest using the theory of constant elastic strain energy of distortion:

$$2 \sigma_e^2 = (\sigma_x - \sigma_y)^2 + (\sigma_y - \sigma_z)^2 + (\sigma_z - \sigma_x)^2 + 6(\tau_{xy}^2 + \tau_{yz}^2 + \tau_{zx}^2).$$

Stress concentration may be applied only to the alternating stress component.

- b. Design values of instability loads are scaled up to allow for uncertainty in manner of load application, variation in modulus of elasticity, and difference between the actual case and the theoretical one.
- c. Calculated values of deflection for comparison with deflection limits may be based on the resulting permanent set after load removal if load removal occurs before damage may result.

4.2.1.2.16 Fuel Assembly Limits

The design limits applicable to each component are discussed in the following paragraphs. In order to provide a fuller understanding of how the limits will be applied, a functional description of each component and a discussion of the loadings on each component are provided.

The general configuration of the fuel assembly and the detailed configurations of the assembly components are the result of the evolutionary change in customer, performance, manufacturing and serviceability requirements and the experience obtained since the initial design conception. In general, the experience obtained in prior fuel designs is relied upon very heavily to qualify particular component configurations for production fuel application. More sophisticated analytical techniques are continually being developed and applied to fuel design.

4.2.1.2.16.1 Fuel Rods

A discussion of the mechanical analysis of the fuel rod and the appropriate stress intensity limits was provided in Subsection 4.2.1.2.5. In addition, a fuel rod fatigue analysis is performed as described in Subsection 4.2.1.2.9.

As explained in Subsection 4.2.3.21, significant fuel rod bowing due to binding at the spacers is not expected to occur. Other contributors to rod bowing during normal operation and transients are manufacturing tolerances and thermal gradients. These factors are considered in the design.

4.2.1.2.16.2 Fuel Spacer

The primary function of the fuel spacer is to provide lateral support and spacing of the fuel rods, with consideration of thermal-hydraulic performance, fretting wear, strength, neutron economy, and producibility.

The mechanical loadings on the spacer structure during normal operation and transients result from the rod positioning spacer spring forces and from local

loadings at the water rod-spacer positioning device. During a seismic event, the spacer transmits the lateral acceleration loadings from the fuel rods into the channel, while maintaining the spatial relationship between the rods.

As noted above, the spacer represents an optimization of a number of considerations. Thermal-hydraulic development effort has gone into designing the particular configuration of the spacer parts. The resultant configurations give enhanced hydraulic performance. Extensive flow testing has been performed employing prototypical spacers to define single-phase and two-phase flow characteristics. Details of the mechanical design of the spacers used at LSCS can be found in Reference 41 for GE fuel and References 46, 47, 48 and 55 for FANP fuel.

4.2.1.2.16.3 Water Rods or Water Channel

The main mechanical function of the water rod(s) (or water channel) is to maintain the axial position of the fuel spacers. For the ATRIUM-10 Fuel, the water channel also provides the structural connection between the upper and lower tie plates.

Differential thermal expansion between fuel rods and the water rods (or water channel) can introduce axial loadings into the water rod (or water channel) through the frictional forces between the fuel rods and the spacers. This differential growth is considered in the design process as discussed in Reference 41 for GE fuel and References 46 and 55 for FANP fuel.

The water rods or water channel provide flow through the center portion of the fuel assembly, thereby providing additional moderation within the bundle interior. This improves uranium utilization and operational flexibility.

4.2.1.2.16.4 Channel

Assurance that the channels maintain their dimensional integrity, strength, and spatial position throughout their lifetime is provided in the following ways:

- a. Dimensional integrity, as related to relaxation of residual forming stresses, is provided through the channel specifications and by qualification of the manufacturing process to these specifications. The operational experience with channels produced using the current process has demonstrated satisfactory relaxation characteristics (Reference 17).
- b. The performance of the channels currently in operation has shown no tendency for gross inservice deformations, although long-term creep deformation and channel bulge have been identified as a potential life-limiting phenomenon (References 17 and 45).
- c. Channel material strength is assured through the material specification of yield and ultimate strength. Quality

measurements are made to show compliance with this specification. Irradiation substantially increases the material strength.

- d. Mechanical integrity of the channel (that is, assurance that the channel will maintain its spatial position and integrity) is provided by designing the channel to the limits stated in Subsection 4.2.2.6 and item e following. The design limits used are based on the unirradiated strength of the material, thereby providing substantial material strength margin throughout most of the life of the channel.
- e. During normal and transient operation, the channel is subjected to differential pressure loadings. The pressure loadings are evaluated to ensure the channel will not experience excessive deflection and subsequent channel wear.

4.2.1.2.16.5 Tie Plates

The upper and lower tie plates serve the functions of supporting the weight of the fuel and positioning the rod ends during all phases of operation and handling. The loading on the lower tie plate during operation and transients comprise the fuel weight, the weight of the channel, and the forces from the expansion springs at the top of the fuel rods. The loading of the upper tie plate is the expansion springs' force. The expansion springs permit differential expansion between the fuel rods without introducing high axial forces into the rods.

Most of this loading arises from the weight of the fuel rods and the channel, which are not cyclic loadings. During accidents the tie plates are subjected to the normal operational loads plus the blowdown and seismic loadings. During handling, the tie plates are subjected to acceleration and impact loading. The stress design limit for the tie plates for all phases of operation and normal handling is discussed in Reference 41 for GE fuel. Reference 48 contains information regarding the upper and lower tie plate loads for FANP ATRIUM-9B and ATRIUM-10 fuel.

The ATRIUM-10 fuel design includes FANP's FUELGUARD debris resistant lower tie plate. This design was chosen for two reasons: 1) to address the main cause of BWR fuel failures over the past few years – debris induced fuel rod fretting; and 2) to reduce overall assembly pressure drop to better assure adequate core flow is available for reactor power maneuvering.

The FUELGUARD lower tie plate design consists of a parallel array of blades with curved portions in the middle. The blades are arranged so that there is no line of sight through the grid thus preventing the passage of long narrow objects and objects larger than the pitch of the blades. The blades for the FUELGUARD on the ATRIUM-10 are brazed in position.

The GE14 fuel design is assembled with a debris filter Lower Tie Plate (LTP) as standard equipment. The debris filter LTP increases the single phase pressure drop by approximately 0.3 psi over the non-debris filter LTP. The debris filter LTP has an underlying grid that screens out the debris and mitigates the debris related fuel rod failures by reducing the size of debris that can enter the fuel assembly. More detailed description of the debris filter LTP can be found in Reference 58.

4.2.1.2.17 Reactivity Control Assembly and Burnable Poison Rods

4.2.1.2.17.1 Safety Design Bases for Reactivity Control

The limiting criteria for shutdown reactivity margins are given in Subsection 4.3.1.1 as items a and f. The cold-clean shutdown margin is shown in Figure 4.3-14 for the initial cycle of Units 1 and 2. The presence of the burnable poison Gd_2O_3 is apparent in the curve shape as k_{eff} rises concurrent with poison depletion. The negative reactivity worth of the gadolinia-containing fuel rods decreases in a nearly linear manner so that it closely matches the depletion of fissile material. The curve

shown in Figure 4.3-14 is typical for most cycles, although differences will exist from cycle to cycle.

The reactivity control mechanical design includes control rods and gadolinia burnable poison in selected fuel rods within fuel assemblies and meets the following safety design bases.

- a. The control rods have sufficient mechanical strength to prevent displacement of their reactivity control material.
- b. The control rods have sufficient strength and are so designed as to prevent deformation that could inhibit their motion.
- c. Each control rod has a device to limit its free-fall velocity sufficiently to avoid damage to the nuclear system process barrier by the rapid reactivity increase resulting from a free-fall of one control rod from its fully inserted position to the position where the drive was withdrawn.

4.2.1.2.17.1.1 Specific Design Characteristics

The acceptability of the control rod and control rod drive under scram loading condition is demonstrated by functional testing instead of analysis or adherence to formally defined stress limits. The results of such testing are given in Reference 10.

The basis of the mechanical design of the control rod blade clearances is that there is no interference which will restrict the passage of the control rod blade.

Mechanical insertion requirements during normal operation are selected to provide adequate operability and load following capability, and are able to control the reactivity addition resulting from burnout of peak shutdown xenon at 100% power.

Scram insertion requirements are chosen to provide sufficient shutdown margin to meet all safety criteria for plant operational transients (Chapter 15.0).

The selection of materials for use in the control rod design is based upon their in-reactor properties. The irradiated properties of Type 304 austenitic stainless steel, 316 stainless steel and CF3 which comprise the major portion of the assembly, B₄C powder, hafnium Inconel-X, and stellite are well known and are taken into account in establishing the mechanical design of the control rod components. The basic cruciform control rod design and materials have been operating successfully in all GE reactors. No problems associated with component materials have been observed.

The radiation effects on B₄C powder include the release of gaseous products, and the B₄C cladding is designed to sustain the resulting internal pressure buildup. The corrosion rate and the physical properties, e.g., density, modulus of elasticity,

dimensional aspects, etc., of austenitic stainless steel, 316 stainless steel, CF3 and Inconel-X are essentially unaffected by the irradiation experienced in the BWR reactor core. The effects upon the mechanical properties, i.e., yield strength, ultimate tensile strength, percent elongation, and ductility on the Type 304 stainless steel cladding also are well known and are considered in mechanical design.

Visual examinations of control rods which have been subjected to high exposure rates have disclosed no significant material degradation (Reference 11).

Rod positioning increments (notch lengths) are selected to provide adequate power shaping capability. The combination of rod speed and notch length must also meet the limiting reactivity addition rate criteria.

For all LaSalle cores, supplementary reactivity control must be provided in such a way that the high initial k_{eff} can be compensated throughout the active core. Gadolinia containing fuel rods are used in normal fuel assemblies to attain this objective. Some assemblies contain more gadolinia than others to improve flattening both in the radial and axial directions.

The gadolinia is uniformly distributed in the UO_2 pellet and forms a solid solution. The presence of the high cross section gadolinium isotopes results in a relatively low heat generation rate in those rods (this heat generation rate is also adjusted by the position of the gadolinia rods within the fuel assembly). During a fuel cycle, the gadolinia essentially burns out thus enabling a progressive increase in rod power and a concurrent increase in net assembly power. At later stages of fuel exposure the power of the gadolinia-urania fuel rods decreases.

Precise quality control measures are utilized during the manufacture of gadolinia bearing UO_2 pellets and also during the assembly of these fuel pellets into fuel rods. Special procedures assure accurate placement and quantity control for placement of gadolinia rods.

4.2.1.2.18 Surveillance Program

See Subsection 4.6.3.2 for information regarding the control rod surveillance program.

The surveillance tests for the control rod drive system include an acceptance test, preinstallation test, operational test prior to startup, and tests during startup. Specific surveillance tests are performed following a refueling outage when core alterations are made, to demonstrate that the core can be made subcritical with a margin of $0.0038 \Delta k$ at any time in the subsequent fuel cycle with the strongest operable control rod fully withdrawn and all other operable control rods fully inserted.

4.2.2 Description and Design Drawings

4.2.2.1 Core Cell

A core cell consists of a control rod and the four fuel assemblies which immediately surround it (Figure 4.2-1). Each core cell is associated with a four-lobed fuel support piece. Around the outer edge of the core, certain fuel assemblies are not immediately adjacent to a control rod and are supported by individual peripheral fuel support pieces.

The top guide is an "egg-crate" structure of stainless steel bars which form a four-bundle cell. The four fuel assemblies are lowered into this cell and, when seated, springs mounted at the tops of the channels force the channels into the corners of the cell such that the sides of the channels contact the grid beams (Figure 4.2-1).

4.2.2.2 Fuel Assembly

A fuel assembly consists of fuel bundle and the channel which surrounds it (Figure 4.1-3). The fuel assemblies are arranged in the reactor core to approximate a right circular cylinder inside the core shroud. Each fuel assembly is supported by a fuel support piece and the top guide. A summary of nuclear fuel data for the GNF (formerly GE) 8x8R, 8x8NB and GE14 fuel designs are presented in Tables 4.2-4a, 4.2-4b and 4.2-4e, respectively. A summary of nuclear fuel data for the FANP ATRIUM-9B and ATRIUM-10 fuel designs are presented in Tables 4.2-4c and 4.2-4d, respectively. Other pertinent data are presented in References 41, 44, 46, 48 and 49.

4.2.2.3 Fuel Bundle

The 8x8R and BP8x8R (Figure 4.2-3) fuel bundles contain 62 fuel rods and two water rods which are spaced and supported in a square (8 x 8) array by the lower and upper tie plates. The GE8x8EB fuel design (Figure 4.2-3a) provides for the use of up to four water rods. However, the GE 8X8EB fuel bundles at LaSalle have two water rods. The GE8X8NB fuel design (Figure 4.2-3b) contains 60 fuel rods and one large centrally located water rod.

The GE14 fuel design (Figure 4.2-3e) is based on a 10x10 array that contains 78 full length rods, 14 part length rods and 2 large water rods that effectively replaced 8 fuel rods. The 14 part length rods terminate just past the top of the fifth spacer. Eight full length rods are used as tie rods. The rods are spaced and supported by the upper and debris filter lower tie plates and eight spacers over the length of the fuel rods. This assembly is encased in an interactive thick corner/thin wall fuel channel. Finger springs control the coolant leakage flow between the debris filter lower tie plate and the channel.

LSCS-UFSAR

Additional assembly and component description for the GE14 fuel design are provided in Reference 58.

The ATRIUM-9B reload fuel assembly design (Figure 4.2-3c) is a 9 x 9 array with 72 enriched uranium fuel rods. The interior is an inert water channel. The ATRIUM-10 reload fuel assembly design (Figure 4.2-3d) is a 10X10 array with 83 full-length fuel rods, 8 part-length fuel rods, and one centrally located water channel. The lower tie plate has a nosepiece which has the function of supporting the fuel assembly in the reactor. The upper tie plate has a handle for transferring the fuel bundle from one location to another. The identifying assembly number is engraved on the top of the handle and a boss projects from one side of the handle to aid in assuring proper fuel assembly orientation. Both upper and lower tie plates position the rod ends for operation and handling. The tie plates also support the weight of the fuel during operation and handling in the 8x8R, 8x8NB, and ATRIUM-9B fuel designs. For the ATRIUM-10 fuel design, the weight of the fuel is supported by the water channel. Finger springs are also employed with the LSCS design. The finger springs are located between the lower tie plate and the channel for the purpose of controlling the bypass flow through that flowpath (Figure 4.2-2, Flow Path 8).

Additional details of the finger springs are provided in Section 9 of References 14 and 49. Zircaloy fuel rod spacers equipped with Inconel springs maintain rod-to-rod spacing.

FANP Fuel

For the FANP ATRIUM-9B fuel, eight of the fueled rods are tie rods. Some of the rods contain gadolinia as a burnable absorber. Fuel rod pitch is maintained by seven spacers. The spacers are a welded zircaloy-4 structure with Inconel 718 springs. The centrally located water channel captures the spacers to maintain the proper axial spacing.

The assembly contains one water channel to improve uranium utilization and operational flexibility. It provides unvoided water to the inner portion of the assembly, thereby, providing additional moderation. The relatively large amounts unvoided water in the interior of the assembly increases the hot-cold reactivity swing. This feature allows greater operational flexibility by allowing longer cycles while maintaining appropriate shutdown margin.

For fuel rod removal, the upper tie plate must be depressed against the compression springs a short distance in order to allow the locking sleeves to be rotated 90°. After rotating the locking sleeves, the upper tie plate is then free to be removed for fuel rod extraction or replacement.

The lower tie plate consists of a machined stainless steel casting with a grid plate for lower end cap engagement and a lower nozzle to distribute coolant to the assembly.

The upper tie plate is a cast and machined grid plate with attached bail handle to provide for fuel assembly handling and orientation. A unique serial identification number is engraved on the bail handle of each tie plate. This number can be read under water to allow identification of the assemblies in the core.

The identification of fuel type and enrichment may be marked on the end of each fuel rod upper end cap.

Additional assembly and component descriptions for the ATRIUM-9B fuel are provided in References 46 and 48.

The ATRIUM-10 fuel assembly consists of many of the same design features as the ATRIUM-9B presented above. Specifically, the ATRIUM-10 consists of a lower tie plate with a debris filter (FUELGUARD), an upper tie plate, 91 fuel rods, 8 spacer grids, a central water channel (or box) and miscellaneous assembly hardware. Of the 91 fuel rods, 8 are part-length fuel rods. The structural members of the fuel assembly include the tie plates, spacer grids, water channel, and connecting hardware. The structural connection between the lower tie plate and upper tie

plate is provided by the water channel. Seven spacers occupy the normal axial locations, while an eighth spacer is located a few inches above the lower tie plate. In a manner similar to an FANP PWR design, the lowermost spacer restrains the fuel rods just above the lower tie plate.

Additional assembly and component descriptions for the ATRIUM-10 fuel are provided in References 55 and 56.

4.2.2.4 Fuel Rod

Each fuel rod consists of high density ($\geq 95\%$ of theoretical density) UO_2 fuel pellets stacked in a Zircaloy cladding tube which is evacuated, backfilled with helium, and sealed by Zircaloy end plugs welded in each end. Beginning with the fresh fuel in LaSalle Unit 1 Cycle 2, all fuel rods are zirconium-barrier fuel with the exception of the fuel rods in 48 ATRIUM-10 fuel bundles first loaded in LaSalle Unit 2 Cycle 10. The zirconium-barrier fuel has a zircaloy fuel cladding with a metallurgically bonded layer of zirconium on the inner surface. Adequate free volume is provided within

each fuel rod in the form of pellet-to-cladding gap and a plenum region at the top of the fuel rod to accommodate thermal and irradiation expansion of the UO_2 and the internal pressures resulting from the helium fill gas, impurities, and gaseous fission products liberated over the design life of the fuel. A plenum spring, or retainer, is provided in the plenum space to prevent movement of the fuel column inside the fuel rod during fuel shipping and handling (Figure 4.1-3). For GE fuel bundles, a hydrogen getter is also provided in the plenum space as assurance against the inadvertent admission of moisture or hydrogenous impurities into a fuel rod. Additional information concerning the getter is provided in Section 8 of Reference 14 and in Reference 41.

Prior to the introduction of ATRIUM-10 fuel design at LaSalle, three types of rods were used in GE and ATRIUM-9B fuel bundles: standard rods, tie rods, and nonfueled water rods (Figures 4.2-3 through 4.2-3e). The eight tie rods in each bundle have upper end plugs which extend through the upper tie plate casting. The eight tie rods are structural members of the fuel assembly. They serve to connect the upper and lower tie plates. The tie rods contain fuel and have upper and lower end caps designed for connection to the tie plates. These rods are threaded into the lower tie plate and latch into the upper tie plate to hold the assembly together. The tie rods carry the assembly weight during handling and provide the coil spring reaction support. These tie rods support the weight of the assembly only during fuel handling operations when the assembly hangs by the handle; during operation, the fuel rods are supported by the lower tie plate. Fifty-four rods in the 8x8R and BP8x8R bundles are standard fuel rods. The GE8x8EB bundle has fifty-four standard fuel rods, eight tie rods, and two water rods. The GE8X8NB fuel design contains fifty-two standard fuel rods, eight tie rods, and one centrally located water rod.

The GE14 fuel design, inserted in LaSalle after the ATRIUM-10 design, contains 70 full length standard rods, 14 part length fuel rods, 8 tie rods and 2 large non fueled water rods.

The ATRIUM-9B has 64 standard fuel rods, 8 tie rods, and one centrally located square water channel. The end plugs of the standard rods have shanks which fit into bosses in the tie plates. An expansion spring is located over the upper end plug shank of each rod in the assembly to keep the rods seated in the lower tie plate while allowing independent axial expansion by sliding within the holes of the upper tie plate. For FANP 9X9 fuel, all fuel rods except for the tie rods have coil compression springs located between the top of the fuel rods and the bottom surface of the upper tie plate. These compression springs provide a force to aid in seating the fuel rods in the lower tie plate and react against the upper tie plate. The springs accommodate variations in rod lengths arising from manufacturing tolerances and permit axially non-uniform thermal and irradiation induced growth of the fuel rods (Reference 49).

LSCS-UFSAR

Two rods in each 8x8R and BP8x8R fuel bundle are hollow water tubes, one of which (the spacer-positioning water rod) positions seven Zircaloy fuel rod spacers axially in the bundle. The GE8x8EB fuel bundle may have more water rods, and the GE8X8NB has one large centrally located water rod. The spacer rods are hollow Zircaloy tubes. The spacer-positioning water rod is equipped with the square bottom end plug. The spacer-positioning water rod is assembled to the spacers by sliding the rod through the spacer cells with the welded tabs oriented in the direction of the corner of the spacer cell. The rod is then rotated so that the tabs fit above and below the elements of the spacer structure, thereby positioning the spacer in the required axial position. The rod is prevented from rotating and

unlocking the spacers by the engagement of its (square) lower end plug with the tie plate hole. Several holes are punched around the circumference of each of the water rods near each end to allow coolant water to flow through the rod.

In the GE14 design, two rods in the bundle are hollow water tubes, one of which positions eight high performance Zr-2 fuel rod spacers axially in the bundle. These two water rods are hollow Zircaloy tubes that encompass eight fuel rod positions. The spacer positioning water rod has tabs welded on it above and below each spacer position. This water rod acts as the spacer capture rod for the fuel assembly. The tabs prevent excessive movement of the fuel spacers in either the upward or downward directions. Several holes are punched around the circumference of each of the water rods near each end to allow coolant water to flow through the rod.

For the ATRIUM-9B fuel, one essentially square water channel is located in the central region of the fuel assembly replacing nine fuel rods in a 3 x 3 array. The water-filled channel has inlet and outlet holes located at the lower and upper end caps. These holes are dimensioned to maintain unvoided water during steady-state operation inside the water channel. The end fittings are made of zircaloy-4. The channel is made from two "U" shaped strips cut and formed from the same sheet of zircaloy-4.

The wall thickness is 0.0285 inches and provides adequate strength. The lower end cap of the water channel is threaded and it connects to the lower tie plate. The upper end cap penetrates the upper tie plate and provides a sliding joint to allow for differential growth.

The water channel has zircaloy stops welded on the outside of the channel at axial locations corresponding to the spacer locations. There is a small gap between the stops and each spacer to allow differential thermal expansion between the channel and the fuel rods (Reference 49).

The ATRIUM-10 fuel bundle design is similar in design to the ATRIUM-9B. The most significant difference is in the load-bearing member of the fuel bundle. The ATRIUM-10 does not utilize tie-rods. Instead the central water channel bears the load of the assembly. The attachment of the upper tie plate is accomplished using a simple bayonet-type locking mechanism. All moveable parts in the bayonet attachment are captured such that no parts can come loose during tie plate removal or reactor operation. The reduced number of components results in part from having a single upper tie plate locking mechanism. To keep the upper tie plate in place, there is one, large compression spring on the water channel rather than the multitude of compression springs on individually fuel rods commonly associated with other designs. Also, no tie rod nuts or locking tabs are required as the water channel carries the weight of the fuel assembly during movement rather than tie rods as in most other BWR fuel designs. Additional component information for the ATRIUM-10 fuel design is provided in References 55 and 56.

4.2.2.5 Fuel Pellets

The fuel pellets consist of high density ceramic uranium dioxide manufactured by compacting and sintering uranium dioxide powder into right cylindrical pellets. The GE pellets have flat ends and chamfered edges while ATRIUM-9B and ATRIUM-10 pellets are dished and have an outward land taper. Ceramic uranium dioxide is chemically inert to the cladding at operating temperatures and is resistant to attack by water.

Several U-235 enrichments are used in the fuel assemblies. Fuel element design and manufacturing procedures have been developed to prevent errors in enrichment location within a fuel assembly. The LSCS fuel bundle incorporates the use of small amounts of gadolinium as a burnable poison in selected fuel rods.

The GE 8x8R, GE 8x8NB, ATRIUM-9B and ATRIUM-10 fuel design features are summarized in Tables 4.2-4 through 4.2-4(e). Characteristics of other fuel types used at LSCS are given in References 41, 44, 46, 49, and 58.

4.2.2.6 Fuel Channel

Separate licensing topical reports (References 17, 41, 45 and 58) provide complete descriptions and analytical results for channels supplied by General Electric Company and used in conjunction with the fuel described herein. The use of the GE14 fuel design at LaSalle introduces the first use of a non-uniform wall thickness channel. The GE14 channel is an interactive channel with a thick corner-thin wall design (120 mil corners and 75 mil wall thickness). This channel is described in more detail in Reference 58. Reference 57 contains the specific design details for the fuel channels supplied by FANP. However, the following functional description is included in this report for completeness.

LSCS-UFSAR

The BWR Zircaloy fuel channel performs the following functions:

- (1) Forms the fuel bundle flow path outer periphery for bundle coolant flow.
- (2) Provides surfaces for control rod guidance in the reactor core.
- (3) Provides structural stiffness to the fuel bundle during lateral loadings applied from fuel rods through the fuel spacers.
- (4) Minimizes, in conjunction with the finger springs and bundle lower tieplate, coolant bypass flow at the channel/lower tieplate interface.
- (5) Transmits fuel assembly seismic loadings to the top guide and fuel support of the core internal structures.
- (6) Provides a heat sink during loss-of-coolant accident (LOCA).
- (7) Provides a stagnation envelope for in-core fuel sipping.

The channel is open at the bottom and makes a sliding seal fit on the lower tieplate surface. The upper end of the fuel assemblies in a four-bundle cell are positioned in the corners of the cell against the top guide beams by the channel fastener springs. At the top of the channel, two diagonally opposite corners have welded tabs, one of which supports the weight of the channel from a threaded raised post and the upper tieplate. One of these raised posts has a threaded hole. The channel is attached using the threaded channel fastener assembly, which also includes the fuel assembly positioning spring. Channel-to-channel spacing is provided for by means of spacer buttons located on the upper portion of the channel adjacent to the control rod passage area.

In the mid 1970s, channel box wear and cracking was observed, first in a foreign plant and later in a few domestic boiling water reactors. The wear was located adjacent to incore neutron monitor and startup source locations. It was postulated and later confirmed by out-of-reactor testing, that the wear was caused by vibration of the incore tubes due primarily to a high-velocity jet of water flowing through the bypass flow holes in the lower core plate. To eliminate significant vibration of instrument and source tubes and the resultant wear on channel loop corners, LaSalle incorporated modifications similar to those described in Reference 36. These modifications involve the elimination of the bypass holes in the lower core plate and addition of two holes in the lower tie plate of each assembly to provide an alternate flow path. This design modification has been determined to have

negligible adverse effects on the mechanical, thermal, and nuclear performance of the channel boxes. Channel box wear has been observed to have been significantly reduced in operating boiling water reactors following the design modification.

Proper orientation of fuel assemblies in the reactor core is readily verified by visual observation and is assured by verification procedures during core loading. Five separate visual indications of proper fuel assembly orientation exist:

- a. The channel fastener assemblies, including the spring and guard used to maintain clearances between channels, are located at one corner of each fuel assembly adjacent to the center of the control rod.
- b. The identification boss on the fuel assembly handle points toward the adjacent control rod.
- c. The channel spacing buttons are adjacent to the control rod passage area.
- d. The assembly identification numbers which are located on the fuel assembly handles are all readable from the direction of the center of the cell.
- e. There is cell-to-cell symmetry.

Experience has demonstrated that these design features are clearly visible so that any misoriented fuel assembly would be readily distinguished during core loading verification.

Appropriate description and design drawings of reactivity control assemblies are included in Subsection 4.6.1.1.2.

4.2.2.7 Reactivity Control Assembly and Burnable Poison Rods

4.2.2.7.1 Control Rods

The control rods perform the dual function of power shaping and reactivity control. Four types of control rods are used at LSCS. Three designs are supplied by General Electric, and the fourth type supplied by ASEA-ATOM (ABB). Power distribution in the core is controlled during operation of the reactor by manipulating selected patterns of control rods. Control rod displacement tends to counterbalance steam void effects at the top of the core and results in significant axial power flattening.

4.2.2.7.1.1 General Electric Control Rods

Figures 4.1-4(a,b,c) show drawings of the General Electric Control Rods.

The General Electric original equipment and Duralife 215 control rod designs consist of a sheathed cruciform array of stainless steel tubes filled with boron-carbide powder. The Marathan design consists of square outer tubes with round inner diameters welded together and filled with B₄C capsules and hafnium rods. The control rods are 9.74 inches in total span and are separated uniformly throughout the core on a 12-inch pitch. Each control rod is surrounded by four fuel assemblies.

The main structural member of Original Equipment and Duralife 215 control rod designs is made of Type 304 stainless steel and consists of a top handle, a bottom casting with a velocity limiter and control rod drive coupling, a vertical cruciform center post, and four U-shaped absorber tube sheaths. The top handle, bottom casting, and center post are welded into a single skeletal structure. The U-shaped sheaths are resistance-welded to the center post, handle, and castings to form a rigid housing to contain the boron-carbide-filled absorber rods.

The Marathon design utilizes a 316 stainless steel handle, tie rod, transition piece, fins and locking plug. As of 1999, the velocity limiter utilized on General Electric Designs (fabricast) is made of a CF3 casting. The absorber tubes are made of 304 Rad Resist Stainless steel and welded together for rigidity.

Rollers at the top and bottom of the control rod guide the control rod as it is inserted and withdrawn from the core. The control rods are cooled by the core bypass flow. The U-shaped sheaths are perforated to allow the coolant to circulate freely about the absorber tubes. Operating experience has shown that control rods constructed as described above are not susceptible to dimensional distortions.

The boron-carbide (B₄C) powder in the absorber tubes is compacted to about 70% of its theoretical density. The boron-carbide contains a minimum of 76.5% by weight natural boron. The boron-10 minimum content of the boron is 18% by weight. Absorber tubes are made of Type 304 (or 304 rad resist) stainless steel. Each absorber tube is 0.188 inch in outside diameter and has a 0.025-inch wall thickness. Absorber tubes are sealed by a plug welded into each end. The boron-carbide is longitudinally separated into individual compartments by stainless steel balls at approximately 16-inch intervals. The steel balls are held in place by a slight crimp of the tube. Should boron-carbide tend to compact in service, the steel balls distribute the resulting voids over the length of the adsorber tube.

4.2.2.7.1.2 ASEA-ATOM (ABB) Control Rods

The second type of Control Rod utilized at LSCS is the ASEA-ATOM (ABB) CR82B. The ASEA-ATOM control rod functions the same as the General Electric control rod, however the design of the ASEA-ATOM control rod is slightly different. Each of the four ASEA-ATOM control blade wings has 520 horizontal holes (0.20 inch diameter) drilled directly into the blade wing (thus eliminating the perforated U-shaped absorber tube sheaths used in the General Electric Control Rod design).

LSCS-UFSAR

The first 6 inches of the blade (beneath the top handle) consist of 22 holes containing hafnium rodlets. The remaining 498 holes contain boron-carbide powder compacted to above 70% of its theoretical density. The boron-carbide contains between 76.5-81% by weight natural boron. The boron-10 content in the ASEA-ATOM control rods is 19.9 +/- 0.3 atom %. The horizontal holes are covered with a stainless steel bar at the outer edge of the blade wing and are connected through a narrow slit. This allows gas pressure equalization between holes and prevents significant displacement of

the B₄C powder.

4.2.2.7.2 Velocity Limiter

The control rod velocity limiter (Figures 4.2-5 and 4.2-5a) is an integral part of the bottom assembly of each control rod. This engineered safeguard protects against a high reactivity insertion rate by limiting the control rod velocity in the event of a control-rod-drop. It is a one-way device in that the control rod scram velocity is not significantly affected but the control rod dropout velocity is reduced to a permissible limit.

The velocity limiter is in the form of two nearly mated conical elements that act as a large clearance piston inside the control rod guide tube. The lower conical element is separated from the upper conical element by four radial spacers 90 degrees apart and is at a 15-degree angle relative to the upper conical element, with the peripheral separation less than the central separation.

The hydraulic drag forces on a control rod are proportional to approximately the square of the rod velocity and are negligible at normal rod withdrawal or rod insertion speeds. However, during the scram stroke, the rod reaches high velocity and the drag forces must be overcome by the drive mechanism.

To limit control rod velocity during dropout but not during scram, the velocity limiter is provided with a streamlined profile in the scram (upward) direction. Thus, when the control rod is scrammed, water flows over the smooth surface of the upper conical element into the annulus between the guide tube and the limiter. In the dropout direction, however, water is trapped by the lower conical element and discharged through the annulus between the two conical sections. Because this water is jetted in a partially reversed direction into water flowing upward in the annulus, a severe turbulence is created, thereby slowing the descent of the control rod assembly to less than 3.11 ft/sec for current control blade designs.

4.2.2.7.3 Burnable Poison Rods

To meet the reactivity control requirements of any core load with excess reactivity, gadolinia-urania fuel rods are placed in each fuel assembly except for the natural uranium assemblies used in the initial cycle for both units and 48 low enriched ATRIUM-10 bundles first loaded in LaSalle Unit 2 Cycle 10. Some assemblies contain more gadolinia than others to improve transverse power flattening. Also, some assemblies contain axially distributed gadolinium to improve axial power flattening. GD₂O₃ is uniformly distributed in the UO₂ pellet and forms a solid solution.

4.2.3 Design Limits and Evaluation

A discussion of the fuel thermal-mechanical design limits and evaluation results for the BP8x8R, GE8x8EB, GE8X8NB, and GE14 fuel designs is given in Section 2 of Reference 41. A similar discussion of the limits and results for the 8x8R fuel design is given in Appendix C of this reference. A similar discussion of the thermal mechanical design limits and evaluation results for the FANP fuel can be found in Reference 46 through 49, 55, and 56. The information contained in the following Subsections is provided as a historical reference.

4.2.3.1 Fuel Damage Analysis

Fuel damage is defined as a perforation of the fuel rod cladding which would permit the release of fission products to the reactor coolant.

The mechanisms which could cause fuel damage in reactor operational transients are: (a) severe overheating of the fuel rod cladding caused by inadequate cooling, and (b) rupture of the fuel rod cladding due to strain caused by relative expansion of the UO₂ pellet. Cladding failure due to overpressure from vaporization of UO₂ following a rapid reactivity transient is not considered to be an operational transient.

A value of 1% plastic strain of the Zircaloy cladding has traditionally been defined as the limit below which fuel damage due to overstraining of the fuel cladding is not expected to occur. The 1% plastic strain value is based on General Electric data on the strain capability of irradiated Zircaloy cladding segments from fuel rods operated in several BWR's (Reference 4). None of the data obtained falls below the 1% plastic strain value. However, a statistical distribution fit to the available data indicates the 1% plastic strain value to be approximately the 95% point in the total population. This distribution implies, therefore, a small (< 5%) probability that some cladding segments may have plastic elongation less than 1% at failure.

For fresh UO₂ fuel the calculated linear heat generation rate (LHGR) corresponding to 1% diametral plastic strain of the cladding is approximately 25 kW/ft. Later in life, the calculated LHGR corresponding to 1% diametral plastic strain decreases to approximately 24 kW/ft at 20,000 MWd/tU and approximately 22 kW/ft at 40,000 MWd/tU. However, due to a depletion of fissionable material, the high-exposure fuel has less nuclear capability and will operate at correspondingly lower powers, so that a wide margin is maintained throughout life between the operating LHGR and the LHGR calculated to cause 1% cladding diametral strain.

The addition of small amounts of gadolinia to UO₂ results in a reduction in the fuel thermal conductivity and melting temperature. The result is a reduction in the LHGR's calculated to cause 1% plastic diametral strain for gadolinia-urania fuel rods. However, to compensate for this the gadolinia-urania fuel rods are designed to provide margins similar to standard UO₂ rods.

4.2.3.2 Fuel Damage Experience

The early GE BWR fuel experience has been extensively described in previous reports. In general, the Zircaloy cladding performance in the very early plants was good; however, some fuel failure mechanisms were encountered and corrected. They are not significantly affecting current fuel performance. Details of this experience are provided in References 4, 19, 20 and 40. Later BWR fuel experience is given in Reference 41.

One of the early causes of fuel failures was internal hydriding of the Zircaloy cladding due to internal attack by hydrogen. The source of hydrogen was primarily small amounts of moisture introduced into the fuel rod. A detailed analysis of the potential sources of hydrogen or moisture shows that the only source large enough to explain primary hydride failure was the UO_2 pellet itself. Major process steps such as increased fuel rod drying temperatures and dry grinding of pellets were incorporated in the manufacture of UO_2 pellets to ensure that no significant moisture could be present in the as-fabricated fuel rod. In addition, the fuel rod design was changed to incorporate a hydrogen gettering system to further assure that neither moisture nor any sporadic hydrogen is ever available to cause hydride failure of the cladding.

Another fuel failure mechanism encountered in operating BWR fuel is crud induced localized corrosion (CILC). CILC, however, has not been experienced at LaSalle.

The one class of fuel failure mechanisms which has restricted operation on LaSalle Units 1 and 2 is known as "pellet-cladding interaction" (PCI). The failures are caused by the direct interaction between the irradiated uranium fuel, including its inventory of fission products, and the zircaloy fuel sheath, or cladding. The incidence of such failures is closely linked to the power history of the fuel rod and to the severity and duration of power changes. Consequently, in order to reduce the probability of fuel failures due to the PCI phenomenon, operational constraints were placed on the reactors.

These constraints were placed on local nodal power increases (ramp rates). Although these constraints have been very successful in reducing the incidence of fuel failures, they were costly in terms of operational flexibility. Consequently, there was strong incentive to provide a type of fuel resistant to PCI. There have been a number of fuel design improvements that were made to minimize PCI failures. These improvements include:

- (a) the pellet geometry has been modified to include chamfered pellet ends and a shorter length in order to reduce the magnitude of inservice pellet distortions contributing to local cladding strains. For FANP Fuel, the pellet geometry includes a land taper, dish and short length for enriched and gadolinia pellets. These features have been shown to reduce PCI.

LSCS-UFSAR

- (b) the cladding heat treatment temperature has been increased in order to reduce the statistical variability in cladding mechanical properties;
- (c) change from 7 x 7 to 8 x 8 to 9 x 9 to 10x10 lattice design to reduce fuel thermal duty; and
- (d) introduction of zirconium-barrier fuel.

Improvements (a), (b) and (c) were made prior to 1975. These, however, did not totally eliminate the PCI problem and it was necessary for plants to continue operation within the ramp rate guidelines. Extensive testing at Quad Cities Unit 2 showed that the introduction of zirconium-barrier fuel eliminated the need for use of the ramp rate guidelines on those fuel assemblies.

The initial cycle fuel for LaSalle Units 1 and 2 did not incorporate the zirconium-barrier fuel. Consequently, operation was maintained within the PCIOMR guidelines for all fuel assemblies. However, reload fuel for subsequent cycles will be zirconium-barrier fuel with the exception of 48 low enriched ATRIUM-10 bundles first loaded in LaSalle Unit 2 Cycle 10. Operation of the zirconium-barrier fuel will be restrained only by the Technical Specifications. However, industry experience will continue to be utilized in order to implement appropriate administrative operating policies that may be more conservative than Technical Specifications. Operation of the non-barrier ATRIUM-10 fuel will be restrained by the guidelines provided by the fuel manufacturer (FANP).

Operation with failed fuel rods has demonstrated that the fission product release rate from defective fuel rods can be controlled by regulating power level. The rate of increase in released activity apparently associated with progressive deterioration of failed rods has been deduced from chronological plots of the off-gas activity measurements in operating plants. These data indicate that the activity release level can be lowered by lowering the local power density in the vicinity of the fuel rod failure. This measured data also indicates that catastrophic failure of the fuel assembly does not occur upon continued operation and that the presence of a failed rod in a fuel assembly does not result in propagation of failure to neighboring rods. Shutdown can be scheduled, as required, to repair or replace fuel assemblies that have large defects.

Evaluation of the fission product release rate for failed fuel rods shows a wide variation in the activity release levels. Correlation of the release rates to defect type, size and specific power level indicates that fission product release rates are functions of power density and that progressive deterioration is a function of time. Available failure data are insufficient to quantify the detailed correlation between these variables.

4.2.3.3 Potential For a Water-Logging Rupture

For water-logging to occur, the fuel cladding must have a small pinhole. Pinholes are eliminated during production by 100% leak check of assemblies. The leak

detector system consists of a high vacuum system capable of attaining pressures less than 5×10^{-3} torr, and a mass spectrometer capable of detecting leaks smaller than the design limit (1×10^{-8} std. cc/sec). The fuel bundle or fuel rod is placed in the vacuum chamber and evacuated to less than 1×10^{-4} torr. After the vacuum is attained, the mass spectrometer tuned to the helium mass range is switched into the system. The output meter of the mass spectrometer will indicate the presence of any helium gas in the chamber. The design basis for the fuel precludes the potential for a water-logging rupture throughout the fuel cycle.

4.2.3.4 Potential For Hydridding

The design basis for fuel in regard to the cladding hydridding mechanism is to assure, through a combination of engineering specifications and strict manufacturing controls, that production fuel will not contain excessive quantities of moisture or hydrogenous impurities. Analysis of BWR fuel performance on fuel manufactured since July 1972 has indicated that this failure mechanism has been eliminated in BWR fuel through the adoption of the changes in the fuel rod design and manufacturing processes described in Subsection 4.2.3.2 and in Reference 41.

FANP addressed internal hydridding in Reference 49. The absorption of hydrogen by the cladding can result in cladding failure due to reduced ductility and formation of hydride platelets. Careful moisture control during fuel fabrication reduces the potential for hydrogen absorption on the inside of the cladding. The fabrication limit for total hydrogen in the fuel pellets is less than 2.0 ppm (References 46 and 49).

4.2.3.5 Dimensional Stability

The fuel assembly and fuel components are designed to assure dimensional stability in service. The fuel cladding and channel specifications include provisions to preclude dimensional changes due to residual stresses. In addition, the fuel assembly has been designed to accommodate dimensional changes that occur in service due to thermal differential expansion and irradiation effects. For example, the fuel rods are free to expand lengthwise independent of each other, and the channel is free to expand relative to the fuel bundle.

The differential thermal expansion between the tie plates and spacer grid is calculated to introduce a bending stress of less than 400 psi at the end of the fuel tube. Additional information regarding this calculation is presented in Section 4 of Reference 1.

LSCS-UFSAR

During shipment the fuel bundle is in a horizontal position with flexible packing separators installed between the fuel rod so that the weight of the fuel rods is supported by the shipping container rather than the spacer grids. Siemens fuel rods are supported by the fuel assembly spacers during shipment. Siemens has performed testing to verify that this is acceptable for the Atrium-9B fuel assembly. Fuel bundle shipping procedures are qualified by a test performed on each new design, and each individual bundle is inspected relative to important dimensional characteristics following shipment to verify that no dimensional deviations have occurred.

The two major handling loads of concern are (1) the loads due to maximum upward acceleration of the fuel assembly while grappled, and (2) the loads due to impact of the fuel assembly into the fuel support while grappled. Analyses of these loading conditions have been performed and the resulting fuel assembly component stresses are within design limits. Additional information on fuel handling and shipping loads for GE fuel is presented in Section 5 of Reference 1 and in Reference 41.

FANP addresses fuel assembly handling loads in Reference 49. The FANP assembly design must withstand all normal axial loads from shipping and fuel handling operations without permanent deformation. FANP uses either a stress analysis or testing to demonstrate compliance. The analysis or test uses an axial load of 2.5 times the static fuel assembly weight. At this load, the fuel assembly structural components must not show any yielding. Because of the design, failure from axial loads will occur at the tie rod end caps rather than in the cladding or tie plates. The fuel rod plenum has a design criteria associated with handling requirements. The spring must maintain a force against the stack weight to prevent column movement during handling (Reference 49).

4.2.3.6 Fuel Densification

The amount of incore fuel densification in BWR Zircaloy clad UO_2 pellet fuel has been observed to be small and is not considered to have any significant effects on fuel performance. Detailed consideration of the occurrence and potential effects of incore fuel densification in General Electric BWR's is reported in Reference 5 and its supplements. See Section 4.2.1.2.3.2 for a similar discussion for FANP Fuel.

4.2.3.7 Fuel Cladding Temperatures

Fuel cladding temperatures for 8x8R type fuel are shown in Figure 4.2-6 as a function of surface heat flux for beginning of life conditions. A core distribution of segment powers is developed. The value of Zircaloy-2 thermal conductivity used in these calculations is approximately 9.0 Btu/hr-ft² F.

Calculated fuel cladding temperatures for 8x8R type fuel for late-in-life conditions are shown on Figure 4.2-7 as a function of heat flux. The solid lines on Figure 4.2-7 represent the expected fuel cladding temperatures. The temperatures employed in mechanical design evaluations are calculated using a conservative design allowance for the degradation in fuel rod surface heat transfer coefficient due to the accumulation of system corrosion products on the surface of the rod (crud) and cladding corrosion (zirconium oxide formation). The expected fuel cladding temperatures are calculated employing a more realistic allowance for the effects of crud and oxide on the fuel rod surface heat transfer coefficient. The calculated peak cladding temperatures are used in the thermal and mechanical design analyses addressed in Reference 41. The fuel cladding temperatures for other fuel types can be found in Reference 41.

FANP also prevents the fuel rod cladding from overheating by minimizing the probability of exceeding thermal margin limits on limiting fuel rods during normal operation and anticipated operational occurrences (Reference 49).

4.2.3.8 Peaking Factors

The typical power distribution is divided into several components: the radial peaking factor, local peaking, and axial peaking. The maximum radial peaking factor is defined as the total power produced in the most limiting fuel assembly divided by the core average fuel assembly power. The maximum local peaking factor is defined as the maximum fuel rod heat flux in a fuel assembly divided by the fuel assembly average fuel rod heat flux. The maximum axial peaking factor is defined as the maximum heat flux along the length of a given fuel rod divided by the average heat flux of that rod. The initial reactor core design employs typical power peaking factors shown in Table 4.4-1. Peaking factors for reload cores are such that margins to limits for LHGR, MCPR, and APLHGR remain within the COLR limits.

4.2.3.8.1 Local Peaking Factors

The enrichment distribution in each fuel assembly is selected to reduce the relative local peak-to-average fuel rod power ratio within each assembly. The local peaking factor used for the initial design is provided in Table 4.4-1.

4.2.3.8.2 Axial and Gross Peaking Factors

The axial and gross peaking factors used for the initial core design are provided in Table 4.41. Axial and gross peaking factors for reload cores are such that margins to limits for LHGR, MCPR, and APLHGR remain within the COLR limits.

4.2.3.9 Temperature Transients with Waterlogged Fuel Element

As indicated in Subsection 4.2.3.3, the potential for water-logging is considered in the fuel design. For waterlogging to occur, the fuel cladding must have a small pinhole. Pinholes are eliminated during production by 100% leak check of assemblies. The leak detector system employed is described in Subsection 4.2.3.3. Since waterlogging is not expected and since it has not been observed in commercial power BWR fuel, no specific analysis of the consequences is performed.

In the unlikely event that a waterlogged fuel element does exist in a BWR core, it should not have a significant potential for cladding burst (due to internal pressure) during a transient power increase unless the transient started from a cold or very low power condition. Normal reactor heatup rates are sufficiently slow ($\leq 100^\circ \text{ F/hr}$ increase in coolant temperature) such that water vapor formed inside a waterlogged fuel rod would be expected to evacuate the rod through the same passage it entered,

allowing internal and external pressures to equilibrate as the coolant temperature and pressure rise to the rated conditions.

Once the internal and external pressures are at equilibrium, at rated coolant pressure and temperature, transient power increases should, in general, have the effect of only slightly reducing the internal fuel rod plenum volume due to differential thermal expansion between fuel and cladding, thus effecting a small, short-term increase in internal fuel rod pressure. The potential short-term increase in pressure due to this effect would, in general, be small, (e.g., a power increase from the cold condition to peak rated power would increase internal pressure less than 15% in the peak power fuel rod fuel rod). For the range of anticipated transients, the cladding primary membrane stress resulting from the temporary increase in internal pressure above the coolant pressure would not be expected to exceed the cladding stress design limits of Subsection 4.2.1.2.5.

4.2.3.10 Potential Damaging Temperature Effects During Transients

There are no predicted significant temperature effects during a power transient resulting from a single operator error or single equipment malfunction which result in fuel rod, control rod, or structural damage. The calculated fuel rod cladding strain for this class of transients is significantly below the calculated damage limit. The predicted additional bowing deflection for this class of transients is small compared to the steady-state rod-to-channel clearance.

4.2.3.11 Energy Release During Fuel Element Burnout

The metal-water chemical reaction between zirconium and water is given by:



where $\Delta\text{H} = 140$ cal/g-mole. The reaction rate is conservatively given by the familiar Baker-Just rate equation:

$$W^2 = 33.3 \times 10^6 \tau \exp\left(\frac{-45,500}{RT}\right) \quad (4.2 - 2)$$

where ΔW is milligrams of zirconium reacted per cm^2 of surface area, τ is time (seconds), R is the gas constant, (cal/mol- $^\circ$ K), and T is the temperature of zirconium ($^\circ$ K). This rate equation has been shown to be conservatively high by a factor of 2 (Reference 21). The above equation can be differentiated to give the rate at which the thickness of the cladding is oxidized. This becomes:

$$\text{th} = \frac{A_1}{\Delta X} \exp\left(-\frac{A_2}{T}\right) \quad (4.2 - 3)$$

where:

th = rate at which the cladding thickness is oxidizing,

LSCS-UFSAR

- ΔX = oxidized cladding thickness,
- A_1, A_2 = appropriate constants, and
- T = reaction temperature.

The reaction rate is inversely proportional to the oxide buildup; therefore, at a given cladding temperature the reaction rate is self-limiting as the oxide builds up. The total energy release from this chemical reaction over a time period is given by:

$$Q_T = \int^t N_{rods} (-\Delta H) CL \rho \Delta X dt \quad (4.2 - 4)$$

where:

- N_{rods} = number of rods experiencing boiling transition (at temperature T),
- $-\Delta H$ = heat of reaction,
- C = cladding circumferences,
- L = axial length rod experiencing boiling transition, and
- ρ = density of zirconium.

This equation can be integrated and compared to the normal bundle energy release if the following conservative assumptions are made:

- a. At an axial plane all the rods experience boiling transition and are at the same temperature. This is highly conservative since, if boiling transition occurs, it will normally occur on the high power rod(s).
- b. Boiling transition is assumed to occur uniformly around the circumference of a rod. This generally occurs only at one spot.
- c. The rods are assumed to reach some temperature T instantaneously and stay at this temperature for an indefinite amount of time.

This integration has been performed per axial foot of bundle and the total energy release as a function of time has been compared to the total energy release of a high power bundle (6 MW) over an equal amount of time. The results are shown in Figure 4.2-8. For example, if the temperature of all rods along a 1-foot section of the bundle were instantly increased to 1500° F, the total amount of energy that has

been released at 0.1 seconds is 0.4% of the total energy that has been released by the bundle (6 MW x 0.1 second). Note that the fractional energy release decreases rapidly with time even though a constant temperature is maintained. This is because the reaction is self-limiting as was discussed above with the Baker-Just equation.

The amount of energy released is dependent on the temperature transient, and the surface area that has experienced heatup. This, of course, is dependent on the initiating transient. For example, if boiling transition were to occur during steady-state operating conditions, the cladding surface temperature would range from 1000° F to 1500° F depending on the heat fluxes and heat transfer coefficient. Even assuming all rods experience boiling transition instantaneously, the magnitude of the energy release is insignificant. Significant boiling transition is not possible at normal operating conditions because of the thermal margins at which the fuel is operated. This is also true for abnormal transients. It can, therefore, be concluded that the energy release and potential for a chemical reaction is not an important consideration during normal operation or abnormal transients.

4.2.3.12 Energy Release for Rupture of Waterlogged Fuel Elements

Experiments have been performed to show that waterlogged fuel elements can fail at a lower damage threshold than nonwaterlogged fuel during rapid reactivity excursion from the cold condition (References 22 and 23), (i.e., 60 cal/g as compared to > 300 cal/g). No analysis of cladding stress has been performed by GE for such conditions. One can postulate that if such a failure occurred, the resultant energy release and pressure pulse would be much less than for a nonwaterlogged fuel rod which exceeded its damage threshold since the energy level required for damage is apparently much lower in the waterlogged fuel element. Any fuel dispersion that might result in such a case would further reduce the severity of such a transient.

4.2.3.13 Fuel Rod Behavior Effects from Coolant Flow Blockage

In Reference 24, GE evaluated the consequences of a fuel bundle flow blockage incident. The percent of flow blocked to the bundle reduces the MCPR margin, and must be considered when evaluating the effects of a known lost part. A portion of reference 24 also discusses the consequences associated with 100% blockage of a fuel bundle; however, this event was never reviewed and approved by the NRC, nor has it ever been made a licensing requirement.

Reference 16 provides an updated discussion, applicable to GE9, FANP ATRIUM-9B fuel, and FANP ATRIUM-10 fuel, of the effects of flow blockages on MCPR margin. This relationship is used to determine the impact of known lost parts. This document also discusses the potential for fuel fretting for parts small enough to migrate into the bundle. Fuel fretting may lead to fuel failures, which would be detected by the offgas system. If a blocked bundle becomes suddenly unblocked, the increase in reactivity is less than the delayed neutron fraction, and therefore a prompt critical excursion is avoided.

4.2.3.14 Channel Evaluation

An evaluation of fuel channel loading due to internally applied pressure has been performed. Tests have been conducted to verify the applicability of the "fixed-fixed beam" analytical model under uniform load.

To confirm the applicability of the analytical model, a channel section was pressurized and the resultant deflections were measured and compared with the deflections predicted by the analytical model. A 4-foot-long section of channel with welded end plates was used for the test. The channel section was pressurized at room temperature in steps up to a pressure which was equivalent to a calculated stress intensity of approximately three times the yield strength of the channel material. Measurements of channel deflection were made for each pressure step and at zero pressure following each step. The deflection of the channel walls was found to be linear with pressure in the pressure range tested. The measured deflection was within approximately 5% to 10% of the deflection predicted by the analytical model. There was no measurable permanent deformation of the channel walls until the calculated stress in the wall had reached approximately 1.2 times the measured yield strength of the test channel.

The good performance of the channels have been demonstrated by both in-reactor experience and tests. The preponderance of the experience has been with channels that are 5.278 inches inside width with 0.080-inch wall thickness. Channel sizes ranging from 4.290 inches inside width with 0.060-inch walls to 6.543 inches inside width with 0.100-inch walls, are included. The LSCS channel is 5.278 inches inside width with either 0.100-inch or 0.080-inch walls, depending on the specific reload. Additional information regarding channel analyses is presented in Section 2 of Reference 1 and in References 17, 45 and 57.

Channel Management

Channels are not being reused at LaSalle. This is one of the assumptions that is used for the MCPR safety limit calculations by FANP.

To preclude unacceptable fuel element channel box deflection, a channel verification program, as discussed below, is implemented at LaSalle.

The following general guidelines are followed to detect and control the potential of channel bowing.

- a. Records are kept of channel location and exposure for each operating cycle.
- b. Channels are not retained in the outer row of the core for more than two successive operating cycles.

- c. At the beginning of each fuel cycle, the combined outer row residence time for any two channels in any control rod cell should not exceed four peripheral cycles.

Prior to the beginning of a new operating cycle, control rod drive friction tests shall be performed for those core cells exceeding the above general guidelines or containing fuel channels with exposures greater than 30,000 MWd/T (associated fuel bundle exposures).

In lieu of friction testing, fuel channel measurements may be used to justify use of fuel channels exceeding 30,000 MWd/T exposure for a maximum of four additional operating cycles.

In the future, analytical channel lifetime prediction methods, benchmarked and backed by periodic measurements of a sample of the highest duty fuel channels, may be used to assure clearance between control rod blades and fuel channels without additional testing.

4.2.3.15 Fuel Reliability

The information in this section is historical GE data on fuel reliability experience. The fuel component characteristics which can influence fuel reliability include: (a) the fuel pellet thermal and mechanical properties, dimensions, density, and U-235 enrichment; (b) the Zircaloy cladding thermal and mechanical properties, dimensions, and defects; (c) the fuel rod internal void volume and impurities; (d) the fuel rod-to-rod and rod-to-channel spacing; and (e) the spring constants of the fuel rod spacer springs which maintain contact between the spacer and the fuel rods. Important fuel pellet, cladding, and associated hardware characteristics and dimensions for the 8x8R fuel design are provided in Table 4.2-4 and Figure 4.1-2. The characteristics of other fuel designs may be found in Reference 41, 47, 48, or 49.

The large volume of irradiation experience to date with GE BWR fuel indicates only a few mechanisms which have actually had a direct impact on fuel reliability; namely, cladding defects, excessive deposition of system corrosion products, cladding hydriding resulting from hydrogen impurity, and pellet-cladding interaction.

The cladding defects have been virtually eliminated through implementation of improved quality inspection equipment and more stringent quality control requirements during fuel fabrication. Excessive deposition of corrosion products has also been virtually eliminated through improved control of corrosion product impurities in the reactor feedwater and by manufacturing improvements. Cladding hydriding is the result of excessive amounts of hydrogenous impurities (moisture and/or hydrogenous material) inadvertently introduced into the rod

during the fuel fabrication process. Analysis of BWR fuel performance on fuel manufactured since July 1972 has indicated that this failure mechanism has been eliminated in BWR fuel through the adoption of the changes in the fuel rod design and manufacturing processes described in Subsection 4.2.3.2 and Reference 41.

Pellet-cladding interaction is the fuel failure mechanism which currently has the greatest effects on reactor operation at LaSalle. It has been identified as resulting from the combination of two basic effects: (a) the observed variability in local cladding strains due to pellet-cladding interaction which can result in the random occurrence of higher-than-average local strain value; and (b) the statistical variability in postirradiation ductility of the cladding which can result in the random occurrence of tubing segments with ductility lower than average. The fuel design improvements described in Subsection 4.2.3.2 have been shown to virtually eliminate PCI as a major cause of fuel failures. When zirconium-barrier fuel replaces all initial cycle fuel, the ramp rate guidelines may be virtually eliminated as a restraint on reactor operations. However, administrative restrictions may still be maintained.

The cladding liner material is an enhanced zirconium alloy. The purpose of the material enhancement to the liner is to reduce the potential for secondary hydriding following the intrusion of coolant into a fuel rod.

4.2.3.16 Fuel Operating and Developmental Experience

Production fuel rods employing gadolinia-urania fuel pellets have been in use since 1965. Fuel operating experience is documented in References 4, 19, 40 and 42.

4.2.3.17 Fuel Assembly

During shipment the fuel bundle is in a horizontal position with flexible packing separators installed between the fuel rods so that the weight of the fuel rods is supported by the shipping container rather than the spacer grids. FANP fuel rods are supported by the fuel assembly spacers during shipment. FANP has performed testing to verify that this is acceptable for the Atrium-9B and ATRIUM-10 fuel assemblies. Fuel bundle shipping procedures are qualified by a test performed on each new design, and each individual bundle is inspected relative to important dimensional characteristics following shipment to verify that no dimensional deviations have occurred.

The two major handling loads of concern are (1) the loads due to maximum upward acceleration of the fuel assembly while grappled, and (2) the loads due to impact of the fuel assembly into the fuel support while grappled. Analyses of these loading conditions have been performed and the resulting fuel assembly component stresses are within design limits. Additional information of fuel handling and shipping loads is presented in Section 5 of Reference 1 and in Reference 41.

FANP has also evaluated their fuel for fuel handling and shipping concerns. The assembly design must withstand all normal axial loads from shipping and fuel handling operations without permanent deformation. FANP uses either a stress analysis or testing to demonstrate compliance (Reference 46 and 55).

The rod plenum spring also has design criteria associated with handling requirements. The spring must maintain a force against the stack weight to prevent column movement during handling.

4.2.3.17.1 Loads Assessment of Fuel Assembly Components

The analytical methods and acceptance criteria applied to determine the fuel assembly response to externally applied forces are both deemed to be in accordance with the requirements of Appendix A to SRP 4.2. LaSalle County Station fuel assembly capability has been evaluated accordingly with acceptable results. Information on load assessment of fuel assembly components is provided in Table 3.9-4.

4.2.3.18 Spacer Grid and Channel Boxes

Refer to Subsection 4.2.3.14.

4.2.3.19 Burnable Poison Rods

The failure rate of the gadolinia-urania fuel rods is negligible, from previous operating experience over the years.

4.2.3.20 Control Rods

4.2.3.20.1 Materials Adequacy Throughout Design Lifetime

The adequacy of the materials throughout the design life was evaluated in the mechanical design of the control rods. The primary materials, B₄C powder, Hafnium, and Type 304 and Type 316L austenitic stainless steel, have been found suitable in meeting the demands of the BWR environment.

4.2.3.20.2 Dimensional and Tolerance Analysis

Layout studies are done to ensure that, given the worst combination of extreme detail part tolerances at assembly, no interference exists which will restrict the movement of control rods. In addition, preoperational verification is made on each control blade assembly to show that the acceptable levels of operational performance are met.

4.2.3.20.3 Thermal Analysis of the Tendency to Warp

All parts of the control rod assembly remain at approximately the same temperature during reactor operation, negating the problem of distortion or warpage. Differential thermal growth is allowed for in the mechanical design. A minimum axial gap is maintained between absorber rod tubes and the control rod frame assembly for this purpose. In addition, dissimilar metals are avoided.

4.2.3.20.4 Forces for Expulsion

An analysis was made to evaluate the maximum pressure forces which could tend to eject a control rod from the core. The results of this analysis are given in Subsection 4.6.2.3.1.2.2 under item "Rupture of Hydraulic Line(s) to Drive Housing Flange." In summary, if the collet were to remain open, which is unlikely, calculations indicate that the steady-state control rod withdrawal velocity would be 2 ft/sec for a pressure-under line break, the limiting case for rod withdrawal.

4.2.3.20.5 Functional Failure of Critical Components

The consequences of a functional failure of critical components have been evaluated and the results are covered in Subsection 4.6.2.3.2.

4.2.3.20.6 Precluding Excessive Rates of Reactivity Addition

In order to preclude excessive rates of reactivity addition, analysis has been performed both on the velocity limiter device and the effect of probable control rod failures (Subsection 4.6.2.3.2).

4.2.3.20.7 Effect of Fuel Rod Failure on Control Rod Channel Clearances

The control rod drive mechanical design ensures a sufficiently rapid and forceful insertion of control rods so that no channel misalignments or distortion could hinder reactor shutdown by impeding a significant number of rods from full insertion.

4.2.3.20.8 Mechanical Damage

Analysis has been performed for all areas of the control system showing that system mechanical damage does not affect the capability to continuously provide reactivity control.

The following discussion summarizes the analysis performed on the control rod guide tube.

LSCS-UFSAR

The guide tube can be subjected to any or all of the following loads:

- a. inward load due to pressure differential,
- b. lateral loads due to flow across the guide tube,
- c. dead weight, and
- d. seismic.

In all cases analysis was performed considering both a recirculation line break and a steamline break, events which result in the largest hydraulic loadings on a control rod guide tube.

Two primary modes of failure were considered in the guide tube analysis: exceeding allowable stress and excessive elastic deformation. It was found that the allowable stress limit will not be exceeded and that the elastic deformations of the guide tube never are great enough to cause the free movement of the control rod to be jeopardized.

4.2.3.20.8.1 First Mode of Failure

The first mode of failure is evaluated by the addition of all the stresses resulting from the maximum loads for the faulted condition. This results in the maximum theoretical stress value for that condition. Making a linear supposition of all calculated stresses and comparing this value to the allowable limit defined by the ASME Boiler and Pressure Vessel Code yields a factor of safety of approximately 3. For faulted conditions the factor of safety is approximately 4.2.

4.2.3.20.8.2 Second Mode of Failure

Evaluation of the second mode of failure is based on clearance reduction between the guide tube and the control rod. The minimum allowable clearance is about 0.1 inch. This assumes maximum ovality and minimum diameter of the guide tube and the maximum control rod dimension. The analysis showed that if the approximate 6000 psi for the faulted condition were entirely the result of differential pressure, the clearance between the control rod and the guide tube would reduce by a value of approximately 0.01 inch. This gives a design margin of 10 between the theoretically calculated maximum displacement and the minimum allowable clearance.

4.2.3.20.9 Analysis of Guide Tube Design

Two types of instability were considered in the analysis of guide tube design. The first was the classic instability associated with vertically loaded columns. The second was the diametral collapse when a circular tube experiences external to internal differential pressure.

The limiting axially applied load is approximately 77,500 pounds resulting in a material compressive stress of 17,450 psi (code allowable stress). Comparing the actual load to the yield stress level gives a design margin greater than 20 to 1. From these values it can be concluded that the guide tube is not an unstable column.

When a circular tube experiences external to internal differential pressure, two modes of failure are possible depending on whether the tube is long or short. In the analysis here the guide tube is taken to be an infinitely long tube with the maximum allowable ovality and minimum wall thickness. The conditions will result in the lowest critical pressure calculation for the guide tube (i.e., if the tube were short, the critical pressure calculation would give a higher number). The critical pressure is approximately 140 psi. However, if the maximum allowable stress is reached at a pressure lower than the critical pressure, then that pressure is limiting. This is the case for a BWR guide tube. The allowable stress of 17,450 psi will be reached at approximately 93 psi. Comparing the maximum possible pressure differential for a steamline break to the limiting pressure of 93 psi gives a design margin greater than 3 to 1. Therefore, the guide tube is not unstable with respect to differential pressure.

4.2.3.20.10 Evaluation of Control Rod Velocity Limiter

The control rod velocity limiter limits the free fall velocity of the control rod to a value that cannot result in nuclear system process barrier damage. This velocity is evaluated by the rod-drop accident analysis in Chapter 15.0.

4.2.3.21 Rod Bowing

4.2.3.21.1 GE Evaluation

Irradiation-induced bowing in fuel rods and assemblies is a phenomenon which is not, in itself, a failure mechanism. However, rod bowing must be addressed in the design analysis so as to establish operational tolerances. General Electric has indicated that boiling water reactor fuel operating experience, testing, and analysis indicate that there is no significant problem with rod bowing even at small rod-to-rod and rod-to-channel clearances. Specifically, General Electric noted that: (1) no gross bowing has been observed (excluding the rod bowing-related failures in an early design); (2) a very low frequency of minor bowing has been observed; (3) mechanical analysis indicates deflections within design bases; and (4) thermal-hydraulic testing has shown that small rod-to-rod and rod-to-channel clearances pose no significant problem. Based on those report observations and Reference 37, that address: (1) updates the General Electric rod bowing experience; (2) verifies the accuracy with which General Electric measures rod bowing; and (3) documents the overall General Electric rod bowing safety analyses, there is no reason to anticipate a problem with fuel rod or assembly bowing during operation of LaSalle.

4.2.3.21.2 FANP Evaluation

Differential expansion between the fuel rods, and lateral thermal and flux gradients can lead to lateral creep bow of the rods in the spans between spacer grids. This lateral creep bow alters the pitch between the rods and may affect the peaking and local heat transfer. The FANP design basis for fuel rod bowing is that lateral displacement of the fuel rods shall not be of sufficient magnitude to impact thermal margins. Extensive post-irradiation examinations have confirmed that such rod bow has not reduced spacing between adjacent rods by more than 50%. The potential effect of this bow on thermal margins is negligible. Rod bow at extended burnup does not affect thermal margins due to the lower powers achieved at high exposure (Reference 49).

4.2.3.22 Fission Gas Release

The information in this section is historical GE data on fuel reliability experience. In 1976, the NRC had questioned the validity of fission gas release calculations in most fuel performance codes, including GEGAP - III (Reference 34), for a burnup greater than 20,000 megawatt days per ton of uranium. The General Electric Company was informed of this concern (Ref. 28) and was provided with a method of correcting fission gas release calculations for burnups greater than 20,000 megawatt days per ton of uranium (Ref. 29). Subsequently, the General Electric Company provided (Ref. 30) a generic reanalysis of fuel performance calculations using GEGAP - III with the NRC's fission correction factor for BWR 2/3/4 plants with 7x7 and 8x8 fuel assemblies. Although the reanalysis was not specifically performed for the LaSalle fuel, a referenced 8x8 reanalysis performed for early refloodings plants bounded the LaSalle case. In the generic reanalysis, fuel rod internal pressure was shown to remain below system pressure for rod peak burnups below 40,000 megawatt days per ton of uranium. This conclusion remains unchanged for the prepressurized fuel design (Ref. 31). The generic reanalysis did, however, result in higher initial stored energy and rupture pressure in the loss-of-coolant accident conditions, the higher fission gas release results in a maximum increase of 85 degrees Fahrenheit in calculated peak cladding temperature at end-of-life (approximately 33,000 megawatt days per tons of uranium planar average exposure). This added temperature increment results in calculated peak cladding temperatures of less than 2100 degrees Fahrenheit for average burnups below 33,000 megawatt days per ton of uranium and thus would not violate the 2200 degrees Fahrenheit loss-of coolant accident peak cladding temperature limit required by 10 CFR 50.46.

A full reanalysis of the effects of fission gas release prior to exceeding a peak local burnup of 20,000 megawatt days per ton of uranium was required by the NRC for LaSalle. General Electric proposed that credit for approved emergency core cooling system evaluation model changes be used to offset any detrimental effects of fission gas release at high burnups (Ref. 32). The proposal was accepted by the NRC

provided the more recent generic analysis was applicable to LaSalle. Per reference 33 CEC Co stated the latter generic analysis is applicable to LaSalle. The issue of enhanced fission gas release at high burnup is satisfactorily resolved for LaSalle.

4.2.3.23 Ballooning and Rupture

4.2.3.23.1 GE Evaluation

The information in this section is historical GE data on fuel reliability experience. In another loss-of-coolant accident related area of concern, the NRC had been generically evaluating three fuel material models that are used in emergency core cooling system evaluations. These models predict cladding rupture temperature, cladding burst strain, and fuel assembly flow blockage.

In a letter from L. O. DelGeorge to A. Schwencer dated May 21, 1981, CEC Co endorsed the results of a generic sensitivity study performed by General Electric submitted to the NRC by letter dated May 15, 1981. As reported in this generic study, General Electric has assessed the boiling water reactor emergency core cooling system sensitivity to rupture temperature by using three rupture temperature models: (1) the General Electric CHASTE model, (2) the NUREG-0630 model, and (3) a proposed General Electric model termed the adjusted model. For the LaSalle type of 8 x 8 with 2 water rod fuel design (designated the "improved 8 x 8 design"), General Electric found that the use of the NUREG-0630 model resulted in an increased peak cladding temperature of up to 50 degrees Fahrenheit over that which was obtained with the CHASTE model. However, sensitivity studies performed on the adjusted model, which is a combination of the CHASTE and NUREG-0630 models and may be the better of the three models, found the maximum impact on peak cladding temperature to be ≤ 10 degrees Fahrenheit.

With regard to the boiling water reactor emergency core cooling system sensitivity to burst strain, the General Electric submittal assessed the impact of using a burst strain model that bounds the burst strain model given in NUREG-0630.

It is estimated from the impact (i.e., < 5 degrees Fahrenheit) of the reduced versus the CHASTE model comparison that if the comparison had been made against the unaltered NUREG-0630 strain model, the impact would have been < 115 degrees Fahrenheit. In light of the calculated 2009 degrees Fahrenheit loss-of-coolant accident peak cladding temperature for LaSalle, sufficient margin exists between the 2200 degrees Fahrenheit peak cladding temperature limit as required by 10 CFR 50.46 and the calculated 2009 degrees Fahrenheit LaSalle peak cladding temperature to accommodate an uncertainty of 115 degrees Fahrenheit in the peak cladding temperature.

4.2.3.23.2 FANP Evaluation

During a severe loss of coolant accident, the cladding swelling and burst strain can result in flow blockage. Therefore, the LOCA analysis must consider the cladding swelling and burst strain impacts on the flow. FANP uses the models in NUREG 0630 for cladding rupture. There is no explicit limit on the deformation. However, the calculations with the deformation models must satisfy the event criteria given in 10CFR 50.46. This swelling and rupture model is an integral part of the LOCA evaluation and is not part of the mechanical design analysis (Reference 49).

4.2.4 Testing and Inspection Plan

Rigid quality control requirements are enforced at every stage of fuel manufacturing to ensure that the design specifications are met. Written manufacturing procedures and quality control plans define the steps in the manufacturing process. The quality control plan is provided in Reference 43. Each fuel tube is subjected to dimensional inspection and ultrasonic inspection to reveal defects in the cladding wall. Destructive tests are performed on representative samples from each lot of tubing, including chemical analysis, tensile, and burst tests. Integrity of end plug welds is assured by standardization of weld processes based on radiographic and metallographic inspection of welds. Completed fuel rods are helium leak tested to detect the escape of helium through the tubes and end plugs or welded regions. The UO_2 powder characteristics and pellet densities, composition, and surface finish are controlled by regular sampling inspections. The UO_2 weights are recorded at every stage in manufacturing. Dimensional measurements and visual inspections of critical areas, such as fuel rod-to-rod clearances, are performed after assembly. Each separate pellet enrichment group has at times been characterized by a single stamp. Such a control has varied over time and varied among fuel vendors. Fuel rods are individually numbered prior to fuel loading: (a) to aid in identifying which pellet type is to be loaded in each fuel rod; (b) to aid in identifying which position in the fuel assembly each fuel rod is to be loaded; and (c) to facilitate total fuel material accountability for a given project.

Prior to introduction of FANP fuel, further identification of individual fuel rod gadolinia concentrations and uranium enrichments is accomplished by symbolization on the upper end plug shank for each differing rod. Each upper end plug is ensured proper placement on a fuel rod by reference to the specific fuel rod type. Each fuel rod is ensured of proper placement within a fuel bundle by inspection of the fuel rod serial number on the lower end plug or clad bar code. For FANP fuel beginning with FANP ATRIUM-10 fuel loaded into LaSalle 2 Cycle 10, fuel rod identity was tracked by use of a bar code on the cladding. This facilitates proper tracking at the fuel fabrication factory including proper loading into the fuel bundle skeleton through automated controls. Computer software ensures that the correct rods are loaded into the proper locations in the fuel bundle.

Fuel rod inspection includes metallographic and radiographic (not applicable to upset shape welded fuel rods) examination of fuel rods on a sample basis. Sample tests are performed for qualification of weld stations, weld parameters, and weld operators prior to application. Production samples are tested as a check on the process and process controls.

Fuel assembly inspections consist of complete dimensional checks of channels and fuel bundles prior to shipment. A sample of fuel bundles is given another visual and dimensional inspection of significant dimensions at the reactor site prior to use. Comparable tests and inspections are used by FANP.

Onsite receipt of fuel rods and other reactor internals is the responsibility of EGC. General Electric and Framatome ANP, Inc. do provide recommendations to the purchaser for receipt, inspection, and handling of these components. General Electric and Framatome ANP, Inc. also perform audits to ensure that these activities are performed in compliance with General Electric and Framatome ANP, Inc. requirements. Such audits, however, are performed solely to satisfy General Electric and Framatome ANP, Inc. interests relative to warranty fulfillment.

The sampling rate and method of the site fuel receiving inspection are outlined in Table 4.2-5. However, current LaSalle fuel inspection procedures meet the requirements outlined in the fuel vendor's Quality Plan, which may or may not be the same as the sampling rate shown in Table 4.2-5.

Verification of enrichment and burnable poison concentrations is described in Subsection 4.2.4.1.

4.2.4.1 Testing and Inspection (Enrichment and Burnable Poison Concentrations)

The shutdown reactivity requirement is verified during initial fuel loading and at any time that core loading is changed. Nuclear limitations for control rod drives and SLC are verified by periodically testing the individual system.

The following serves to identify the various test and inspections employed by the Fuel Vendor(s) in verifying the nuclear characteristics of the fuel and reactivity control systems. Comparable tests and inspections are used by FANP.

4.2.4.1.1 Enrichment Control Program

GE uses emission spectrometry for determining impurities and mass spectrometry for verifying the U-235 enrichment in samples of UO_2 powder. FANP verifies that samples of incoming UF_6 and the resultant UO_2 powder are within limits for impurities by emission spectroscopy. The U-235 content of a statistical sample of UF_6 is verified by gamma counting and by mass spectroscopy measurement.

A sample of the sintered pellets is also checked for impurities by emission spectroscopy. FANP performs chemical verification of impurities and O/U measurements on sintered pellets by emission spectroscopy, wet chemistry and

LSCS-UFSAR

inert gas fusion. GE verifies the O/U ratio of UO₂ pellets and gadolinia bearing pellets up to 6 w/o Gd₂O₃ concentration by gravimetric methods. The O/U ratio for gadolinia bearing pellets with concentration above 6 w/o Gd₂O₃ is confirmed using a spectrophotometric method. (GE uses emission spectrometry)

Each rod is gamma scanned to screen out any possible but unlikely misplaced pellet or enrichment deviations.

4.2.4.1.2 Gadolinia Inspections

The same rigid quality control requirements observed for standard UO₂ fuel are employed in manufacturing gadolinia-urania fuel. Gadolinia-bearing UO₂ fuel pellets of a given enrichment and gadolinia concentration are maintained in separate groups throughout the manufacturing process. For General Electric, the percent enrichment and gadolinia concentration characterizing a pellet group are identified by a stamp on the pellet. For Siemens, gadolinia pellets are uniquely identified with a symbol stamped on the pellet.

Fuel rods are individually numbered prior to loading of fuel pellets into the fuel rods: (1) to identify which pellet group is loaded in each fuel rod; (2) to identify which position in the fuel assembly each fuel rod is loaded; and (3) to facilitate total material accountability for a given project. The correct location of all fuel rods in the bundle is ensured through the use of a computer-controlled, automated bundle assembly machine.

The following quality control inspections are made:

- a. Gadolinia concentration in the gadolinia-urania powder blend is verified.
- b. Sintered pellet UO₂-Gd₂O₃ solid-solution homogeneity across a fuel pellet is verified by examination of ceramographic specimens.
- c. Gadolinia-urania pellet identification is verified.
- d. Gadolinia-urania fuel rod identification is checked.
- e. Each gadolinia - urania fuel rod is scanned to assure proper assembly.
- f. Gadolinia content is verified by X-ray fluorescence measurements of each pellet or scanning the assembled rod.

All assemblies and rods of a given project are inspected to ensure overall accountability of fuel quantity and placement for the project.

FANP uses similar practices and techniques for gadolinia inspection.

4.2.4.1.3 Reactor Control Rods

Inspections and tests are conducted at various points during the manufacture of control rod assemblies to ensure that design requirements are being met. All boron carbide lots are analyzed and certified by the supplier. Among the items tested are:

- a. chemical composition,
- b. boron weight percent,
- c. boron isotopic content, and
- d. particle size distribution.

Following receipt of the boron carbide and review of material certificates, additional samples from each lot are tested including those previously listed. Control is maintained on the B₄C powder through the remaining steps prior to loading into the absorber rod tubes.

Certified test results are obtained on other control rod components. The absorber rod tubing is subjected to extensive testing by the tubing supplier, including 100% ultrasonic examination. Metallographic examinations are conducted on several tubes randomly selected from each lot to verify cleanliness and absence of conditions resulting from improper fabrication, cleaning or heat treatment. Other checks are made on the subassemblies and final control rod assembly, including weld joints inspected and B₄C loading.

4.2.4.2 Surveillance Inspection and Testing of Irradiated Fuel Rods

General Electric has a cooperative program of surveillance of BWR fuel, both production and developmental, which operates beyond current production fuel experience as it becomes available for inspection. The schedule of inspection is, of course, contingent on the availability of the fuel as influenced by plant operation. This program is provided in Reference 41.

The lead experience fuel rods (with respect to exposure, linear heat generation rate, and the combination of both) are selectively inspected. Inspection techniques used include:

- a. leak detection tests, such as "sipping;"
- b. visual inspection with various aids such as binoculars, borescope, periscope, and/or underwater TV with a photographic record of observations as appropriate;

LSCS-UFSAR

- c. nondestructive testing of selected fuel rods by ultrasonic and eddy current test techniques; and
- d. dimensional measurements of selected fuel rods.

Unexpected conditions or abnormalities which may arise, such as distortions, cladding perforation, or surface disturbances are analyzed. Resolution of specific technical questions indicated by site examinations may require examination of selected fuel rods in the Radioactive Material Laboratory (RML) facilities.

The results of the program are used to evaluate the boiling water reactor fuel design methods and criteria used by General Electric.

The results of the surveillance program are generally reviewed with the Division of Reactor Licensing and documented in generic fuel experience licensing topical reports.

Historical fuel performance results prior to 1979 on highly precharacterized lead test assemblies are provided in several reports listed in Reference 38. The lead test assemblies are utilized as one means of providing some confirmation of design adequacy or early warning of negative features of the design. Details on lead test assembly programs are provided in Reference 39.

In addition to fuel bundle inspection, the fuel channels are under surveillance in continuing programs. These surveillance programs are designed not only for the evaluation of present day products, but are also providing data in the areas of alternate materials and design modeling.

4.2.4.3 Operating Experience with Gadolinia-Containing Fuel

Production fuel rods employing gadolinia-urania fuel pellets have been in use since 1965. During this time, a substantial number of gadolinia-urania rods have been successfully irradiated to appreciable exposures. Additional information on gadolinia-urania physical and irradiation characteristics, material properties, and operating experiences is provided in Reference 25.

Temperature coefficients are virtually unchanged because of gadolinia. The gadolinia-bearing pellets act as thermally gray or black adsorbers, and their effect on moderator coefficients in the lattice is not essentially different from that of the control which they replace. Doppler response is unaffected because the gadolinia has essentially no effect on the resonance group flux or on the U-238 content of the core.

The concentration of gadolinia has been selected so that the initial concentration of the high cross section isotopes, Gd-155 and -157, will be completely depleted by the end of the first cycle. The irradiation products of this process are other gadolinia

isotopes having low cross sections. Power in the gadolinium pins generally remains below 90% of the average bundle power. The control augmentation effect disappears on a predetermined schedule without changes in the chemical composition of the fuel or the physical makeup of the core.

The thermal margins described by the steady-state operating limits (LHGR, APLHGR and MCPR) are easily maintained in a gadolinia core because additional power shaping is possible through spatial variation of the burnable poison loading. The damage limits on gadolinia-urania fuel rods are designed with similar margins as maintained for the UO₂ rods.

4.2.5 References

1. NEDO-20948-P, "BWR/6 Fuel Design," December 1975.
2. WAPD-TM-283, "Effects of High Burnup on Zircaloy-clad, Bulk UO₂ Plate Fuel Element Samples," September 1962.
3. WAPD-TM-629, "Irradiation Behavior of Zircaloy-Clad Fuel Rods Containing Dished End UO₂ Pellets," July 1967.
4. H. E. Williamson and D. C. Ditmore, "Experience with BWR Fuel Through September 1971," NEDO-10505, May 1972.
5. D. C. Ditmore and R. B. Elkins, "Densification Considerations in BWR Fuel Design and Performance," NEDM-10735, December 1972.
6. J. A. Christensen, "Melting Point of Irradiated Uranium Dioxide," WACP-6065, February 1965.
7. "Thermal Conductivity of Uranium Dioxide," Technical Report series No. 59, IACA, Vienna, 1966.
8. Supplement 1 to the Technical Report on Densification of General Electric Reactor Fuels, December 1973.
9. This reference has been deleted.
10. J. P. Fritz, "Testing of Cruciform Control Rods for BWR/6" NEDO-10565, April 1972.
11. R. J. Benche, "Visual and Photographic Examination of Dresden-1 High Exposure Control Rod B-87" NEDO-10541, April 1972.

LSCS-UFSAR

12. W. F. O'Donnel and B. F. Langer, "Fatigue Design Basis for Zircaloy Components," Nuclear Science and Engineering, Vol. 20, pp. 1-12, 1964.
13. E. P. Quinn, "Vibration of Fuel Rods in Parallel Flow," GEAP-4059, July 1962.
14. NEDO-20360-1P, Revision 4, "General Electric Boiling Water Reactor Generic Reload Application for 8x8 Fuel," March 1976.
15. "Design Safety Standards for Boiling Water Reactors," compiled by Safety and Standards Unit, NEDE-10370, June 1971.
16. EMF-96-137(P), Revision 2, "LaSalle Lost Parts Analysis," Framatome ANP, January 2006.
17. "BWR Fuel Channel Mechanical Design and Deflection," NEDO-21354, September 1976.
18. This reference has been deleted.
19. R. B. Elkins, "Experience with BWR Fuel Through September 1974," NEDO-20922, June 1975.
20. H. E. Williamson and D. C. Ditmore, "Current State of Knowledge High Performance BWR Zircaloy-Clad UO₂ Fuel," NEDO-10173, May 1970.
21. "Thermal Response and Cladding Performance of an Internally Pressurized, Zircaloy Clad, Simulated BWR Fuel Bundle Cooled by Spray Under Loss-of-Coolant Conditions," GEAP-13112, April 1971.
22. L. A. Stephan, "The Response of Waterlogged UO₂ Fuel Rods to Power Burst," IDO-ITR-105, April 1969.
23. L. A. Stephan, "The Effects of Cladding Material and Heat Treatment on the Response of Waterlogged UO₂ Fuel Rods to Power Bursts," IN-ITR-111, January 1970.
24. "Consequences of a Postulated Flow Blockage Incident in a Boiling Water Reactor," NEDO-10174, Revision 1, October 1977.
25. G. A. Potts, "Urania-Gadolinia Nuclear Fuel Physical and Irradiation Characteristics and Material Properties," NEDE-20943 (proprietary), NEDO-20943 (nonproprietary), January 1977.

LSCS-UFSAR

26. "Creep Collapse Analysis of BWR Fuel Using Safe-Collapse Model," NEDE-20606 (Proprietary), NEDO-20606A (Non-Proprietary) August 1976.
27. This reference has been deleted.
28. D. F. Ross (NRC) Letter to G.G. Sherwood (GE) dated November 23, 1976.
29. NUREG-0418, "Fission Gas Release from Fuel at High Burnup," March, 1978.
30. G.G. Sherwood (GE) Letter to D.F. Ross (NRC) dated December 22, 1976.
31. General Electric report, NEDO - 23786-1, "Fuel Rod Pressurization - Amendment 1," May 1978.
32. Letters from R. E. Engel to T.A. Ippolito dated May 6, 1981 and May 23, 1981.
33. L. O Del George letter to A. Schwencer (NRC) dated September 21, 1981.
34. General Electric topical report NEDO-20181, "GEGAP-III: A Model for the Predictions of Pellet - Cladding Thermal Conductance in BWR Fuel Rods," November 1973
35. Letter from W.R. Butler (NRC) To I. Stuart (GE), dated April 4, 1975.
36. General Electric report, NEDO - 21156, "Supplemental Information for Plant Modification's to Eliminate Significant In-core Vibration," January, 1976.
37. General Electric topical report, NEDE - 24284, "Fuel Rod Bowing in General Electric Boiling Water Reactors," Dated August 1980.
38. NUREG 0633, "Fuel Performance Annual Report," December 1979.
39. General Electric report, NEDC 24609, "Boiling Water Reactor Fuel Rod Performance Evaluation Program," February 1979.
40. General Electric report NEDE, 21660-P, "Experience with BWR Fuel through December 1976," July 1977.

LSCS-UFSAR

41. General Electric report NEDE-24011-P-A, "General Electric Standard Application For Reactor Fuel (GESTAR II)", (latest approved revision).
42. Letter Number MFN-078-086/JSC-067-086, J. S. Channley (GE) to C. H. Berlinger (NRC), "1985 Fuel Experience Report," August 13, 1986.
43. "Nuclear Energy Business Group BWR Quality Assurance Program Description," NEDO-11209-04A, March 1978.
44. NEDE-31152, "GE Fuel Bundle Designs," (latest revision).
45. General Electric Report GE-NE-523-A191-1294, "Final Report of the Impact of Using GE9 80-Mil Fuel Channel for the LaSalle Units 1 and 2", latest revision and supplements.
46. Advanced Nuclear Fuels Corporation Generic Mechanical Design for Advanced Nuclear Fuels 9x9-IX and 9x9-9X Reload Fuel, ANF-89-014(A), Revision 1 and Supplements 1-2, Advanced Nuclear Fuels Corporation, Richland, WA, October 1991.
47. Generic Mechanical Design for Exxon Nuclear Jet Pump BWR Reload Fuel, XN-NF-85-67(A), Exxon Nuclear Fuels Corporation, September 1986.
48. FANP document, Cycle Specific Fuel Design Report.
49. Generic Mechanical Design Criteria for BWR Fuel Designs, ANF-89-098(P)(A), Revision 1, Supplement 1, Advanced Nuclear Fuels Corporation, May 1995.
50. RODEX2A (BWR) Fuel Rod Thermal-Mechanical Evaluation Model, XN-NF-85-74(P)(A), Exxon Nuclear Company, August 1986.
51. RODEX2 Fuel Rod Thermal-Mechanical Response Evaluation Model, XN-NF-81-58(P)(A) Supplements 1 and 2 Revision 2, Exxon Nuclear Company, May 1986.
52. General Electric Report NEDE-22290 Supplement 2, Production of Advanced Longer Life Control Rod in BWR 2-6 Plants.
53. General Electric Report NEDE-31578PA, Class III, GE Marathon Control Rod Assembly, October 1991.
54. General Electric Report NLM-CR-4505, Revision C, Class III, Tubricast Velocity Limits for Duralife and Marathon Control Blades, September 1998.

LSCS-UFSAR

55. Fuel Design Evaluation for Siemens Power Corporation ATRIUM-10 BWR Reload Fuel, EMF-95-52(P), Revision 2, December 1998.
56. Mechanical Design Evaluation for ATRIUM-10 BWR Reload Fuel to 54 MWd/KgU Assembly Exposure, EMF-98-006(P), January 1998.
57. Mechanical Design for BWR Fuel Channels, EMF-93-177(P)(A) Revision 1 and Supplement 1, August 2005
58. GE14 Compliance with Amendment 22 of NEDE-24011-P-A (GESTAR 11), NEDC – 32868P, Revision 1, September 2000.

LSCS-UFSAR

TABLE 4.2-1

TYPICAL LIMITING LHGR'S FOR GADOLINIA-URANIA FUEL RODS (kW/ft)

<u>EXPOSURE (MWd/tU)</u>	<u>INCIPIENT CENTER MELTING</u>	<u>1% PLASTIC STRAIN OF CLADDING</u>	<u>EXPECTED OPERATING MAXIMUM (4 wt% Gd₂O₃)</u>
0	18.4	23.0	~ 4
20,000	17.8	21.4	~ 11
40,000	16.7	18.2	~ 8

LSCS-UFSAR

TABLE 4.2-2a.

General Electric

STRESS INTENSITY LIMITS

	<u>YIELD STRENGTH (S_y)</u>	<u>ULTIMATE TENSILE STRENGTH (S_u)</u>
Primary membrane stress	2/3	1/2
Primary membrane plus bending stress intensity	1	1/2 to 3/4
Primary plug secondary stress intensity	2	1.0 to 1.5

TABLE 4.2-2b

FANP STRESS INTENSITY LIMITS*

	Stress Intensity Limits**	
	YIELD STRENGTH (σ_y)	ULTIMATE TENSILE STRENGTH (σ_u)
Primary membrane stress	2/3 σ_y	1/2 σ_y
Primary membrane plus bending stress intensity	1.0 σ_y	1/2 σ_u
Primary plug secondary stress intensity	2.0 σ_y	1.0 σ_u

* Characteristics of the stress categories are defines as follows:

- a) Primary stress is a stress developed by the imposed loading which is necessary to satisfy the laws of equilibrium between external and internal forces and moments. The basic characteristics of a primary stress is that it is not self-limiting. If a primary stress exceeds the yield strength of the material through the entire thickness, the prevention of failure is entirely dependent on the strain-hardening properties of the material.
- b) Secondary stress is a stress developed by the self-constraint of a structure. It must satisfy an imposed strain pattern rather than being in equilibrium with an external load. The basic characteristic of a secondary stress is that it is self-limiting. Local yielding and minor distortions can satisfy the discontinuity conditions due to thermal expansions which cause the stress to occur.

** The stress intensity is defined as twice the maximum shear stress and is equal to the largest algebraic difference between any two of the three principal stresses.

LSCS-UFSAR

TABLE 4.2-3

CONDITIONS OF DESIGN RESULTING FROM IN-REACTOR PROCESS
CONDITIONS COMBINED WITH EARTHQUAKE LOADING

REACTOR INITIAL CONDITIONS	CONDITIONS OF DESIGN		
	PERCENT OF SAFE SHUTDOWN EARTHQUAKE IMPOSED		
	<u>0%</u>	<u>50%</u>	<u>100%</u>
Startup Testing	Upset	--	--
Normal	Normal	Upset	Faulted
Abnormal	Upset	--	--

LSCS-UFSAR

TABLE 4.2-4(a)

DATA FOR THE 8x8R FUEL DESIGN

Core (Full Core Data)

Fuel cell spacing (control rod pitch), in.	12
Number of fuel assemblies	764
Total number of fueled rods	47368
Core power density (rated power), kW/l	50.0
Total core heat transfer area, ft ²	74872

Fuel Assembly Data

Overall length, in.	176
Nominal active fuel length, in.	150
Fuel rod pitch, in.	0.640
Space between fuel rods, in.	0.157
Fuel channel wall thickness, in.	0.100
Fuel bundle heat transfer area, ft ²	98.0
Channel width (inside), in.	5.278

Fuel Rod Data

Outside diameter, in.	0.483
Cladding inside diameter, in.	0.419
Cladding thickness, in.	0.032
Fission gas plenum length, in.	10.0
Pellet immersion density, % T.D.	95
Pellet outside diameter, in.	0.410
Pellet length, in.	0.410

Water Rod Data

Outside diameter, in.	0.591
Inside diameter, in.	0.531

LSCS-UFSAR

TABLE 4.2-4(b)

DATA FOR THE GE8x8NB (GE9B) FUEL DESIGN

Core (Full Core Data)

Fuel cell spacing (control rod pitch), in.	12
Number of fuel assemblies	764
Total number of fueled rods	45840
Core power density (rated power), kW/l	50.0
Total core heat transfer area, ft ²	approximately 71816

Fuel Assembly Data

Nominal active fuel length, in.	150
Fuel rod pitch, in.	0.640
Space between fuel rods, in.	0.157
Fuel channel wall thickness, in.	0.100*
Fuel bundle heat transfer area, ft ²	approximately 94
Channel width (inside), in.	5.278

Fuel Rod Data

Outside diameter, in.	0.486
Cladding inside diameter, in.	0.419
Cladding thickness, in.	0.032
Pellet immersion density, % T.D.	96.5
Pellet outside diameter, in.	0.411
Pellet length, in.	0.410

Water Rod Data

Outside diameter, in.	1.340
Inside diameter, in.	1.260

* Either 100 or 80 mil channels are used, depending on the reload.

LSCS-UFSAR

TABLE 4.2-4(c)

DATA FOR THE FANP ATRIUM-9B FUEL DESIGN

Core (Full Core Data)

Fuel cell spacing (control rod pitch), in.	12
Number of fuel assemblies	764
Total number of fueled rods	55008
Core power density (rated power), kW/l	50.0
Total core heat transfer area, ft ²	77426

Fuel Assembly Data

Overall length, in.	176
Nominal active fuel length, in.	149
Fuel rod pitch, in.	0.569
Space between fuel rods, in.	0.136
Fuel channel wall thickness, in.	0.08*
Fuel bundle heat transfer area, ft ²	101.343
Channel width (inside), in.	5.278

Fuel Rod Data

Outside diameter, in.	0.433
Cladding inside diameter, in.	0.3807
Cladding thickness, in.	0.026
Fission gas plenum length, in.	10.578
Pellet immersion density, % T.D.	96
Pellet outside diameter, in.	0.3737
Pellet length, in.	
Enriched, in.	0.393
Natural, in.	0.545

Water Box Data

Outside dimension, in.	1.516
Water box wall thickness,	0.0285

* Either 100 or 80 mil channels are used, depending on the reload.

LSCS-UFSAR

TABLE 4.2-4(d)

DATA FOR THE AREVA ATRIUM-10 FUEL DESIGN

Core (Full Core Data)

Fuel cell spacing (control rod pitch), in.	12
Number of fuel assemblies	764
Total number of fueled rods	69524
Core power density (rated power), kW/l	52.0
Total core heat transfer area, ft ²	86315

Fuel Assembly Data

Overall length, in.	176.386
Nominal active fuel length, in.	
• Full length fuel rods	149
• Part length fuel rods	90
Fuel rod pitch, in.	0.510
Space between fuel rods, in.	0.114
Fuel channel wall thickness, in.	0.100
Fuel bundle heat transfer area, ft ²	113.0
Channel width (inside), in.	5.278

Fuel Rod Data

Outside diameter, in.	0.3957
Cladding inside diameter, in.	0.3480
Cladding thickness, in.	0.024
Fission gas plenum length, in.	
• Full length fuel rod	11.52 (TIG)/ 11.53 (USW)
• Part length fuel rod	5.26 (TIG)/ 5.42 (USW)
Pellet immersion density, % T.D. (typical, pellet enrichment dependent)	96.26
Pellet outside diameter, in.	0.3413
Pellet length, in.	
Enriched, in.	0.413
Natural, in.	0.551

Water Box Data

Outside dimension, in.	1.378
Water box wall thickness,	0.0285

LSCS-UFSAR

TABLE 4.2-4(e)

DATA FOR THE GE14 FUEL DESIGN

Core (Full Core Data)

Fuel cell spacing (control rod pitch), in.	12	
Number of fuel assemblies	764	
Total number of fueled rods	70288	92*764
Core power density (rated power), kw/l	53.01	NEDE 31152P Rev8
Total core heat transfer area, ft ²	86332	113*764

Fuel Assembly Data

Nominal active fuel length, in.		
• Full length fuel rods	150	GE Dwg 217C1442
• Part length fuel rods	84	GE Dwg 217C1444
Fuel rod pitch, in.	0.510	NEDE 31152P Rev 8
Space between fuel rods, in.	0.106	NFM DIR-00-081, Nov 30, 2000, GE14 Design Review
Fuel channel wall thickness (corner/median), in.	0.120/0.075	NEDE 31152P Rev 8
Fuel bundle heat transfer area, ft ²	113	NEDE 31152P Rev 8
Channel width (inside), in.	5.278	NEDE 31152P Rev 8

Fuel Rod Data

Outside diameter, in.	0.404	NEDE 31152P Rev 8
Cladding inside diameter, in.	0.352	NEDE 31152P Rev 8
Cladding thickness, in.	0.026	NEDE 31152P Rev 8
Fission gas plenum length, in.		
• Full length fuel rod	9.64	GE Dwg 217C1442
• Part length fuel rod	10.94	GE Dwg 217C1444
Pellet immersion density, %T.D. (typical, pellet enrichment dependent)	97.0	NEDE 31152P Rev 8
Pellet outside diameter (cold), in.	0.345	GE Dwg 137C9061
Pellet length, in.	0.370	GE Dwg 137C9061

Water Rod Data

Outside diameter, in.	0.980	NEDE 31152P Rev 8
Inside diameter, in.	0.920	NEDE 31152P Rev 8

LSCS-UFSAR

TABLE 4.2-5
(SHEET 1 OF 2)

SITE FUEL RECEIVING INSPECTION *, **

FUEL INSPECTION OBJECTIVES

<u>CHARACTERISTIC</u>	<u>INTENDED METHOD</u>	<u>EXPECTED FREQUENCY</u>
Container Damage and Leak	Visual	100%
Bundle Damage	Visual	100%
Shipping Separators Removed	Visual	100%
Cleanliness	Visual	100%
Rod Integrity	Visual, gauge when required	100%
Lock Tab Washers	Visual	100%
Channel Integrity	Visual	100%
Channel Cleanliness	Visual	100%
Guard Integrity and Installation	Visual and Torque Wrench	100%
Spacer Damage	Visual	100% for first 5 bundles and every 20th thereafter, otherwise the middle 3 spacers.
Rod to Rod	Feeler gauge	100% of first 5 bundles and every 20th thereafter, otherwise two sections, all spaces, alternate the sections.
Rod-to-Simulated Channel	Simulated Channel and Feeler Gauge	100% of first 5 bundles and every 20th thereafter, otherwise 2 sections, 4 sides per section, alternate sections excluding end sections.

LSCS-UFSAR

TABLE 4.2-5
(SHEET 2 OF 2)

<u>CHARACTERISTIC</u>	<u>INTENDED METHOD</u>	<u>EXPECTED FREQUENCY</u>
Spring Length	Visual	100% for all bundles
	Gauge	100% for first 5 bundles and every fourth thereafter, otherwise visual inspection.
Finger Spring Seated in Pocket	Visual	100% for all bundles
	Gauge	100% for first 5 bundles and every fourth thereafter, otherwise visual inspection.

NOTE:

Deviations require 100% inspection of the next 5 bundles for that characteristic. Two deviations for a characteristic within 6 consecutive bundles require revision of the AQL (acceptable quality level) with the General Electric, Wilmington, North Carolina, U.S.A., facility.

Where a reduced inspection was performed, all inspection steps shall be designated S OK (stamped OK).

- * Current LaSalle fuel inspection procedures meet the requirements outlined in the fuel vendor's Quality plan, which may or may not be the same as the sampling rate in Table 4.2-5.
- ** These inspection objectives are specific to GE fuel. FANP fuel has similar inspection objectives for the FANP designs.

4.3 NUCLEAR DESIGN

4.3.1 Design Bases

The nuclear design bases are conveniently divided into two specific categories. The safety design bases are those which are required for the plant to operate from safety considerations. The second category is the power generation design bases which are required in order to meet the objective of producing power in an efficient manner.

4.3.1.1 Safety Design Bases

The safety design bases are requirements which protect the nuclear fuel from damage which could result in an undue release of radioactivity. In general, the safety bases fall into two categories: the reactivity bases which prevent an uncontrolled positive reactivity excursion, and the overpower bases which prevent the core from operating beyond the fuel integrity limits.

- a. The core system shall be capable of being rendered subcritical at any time or at core conditions with the highest worth control rod fully withdrawn.
- b. The negative feedback coefficient must be sufficient, in consort with other plant systems, to prevent fuel damage as a result of abnormal operational transients (see Chapter 15.0).
- c. The moderator void coefficient must be negative over the entire operating range. (Moderator temperature coefficient is not a limiting design feature.)
- d. Reactivity insertion limits are specified so that control rod worths are low enough to prevent damage to the nuclear process barrier (overpressure of the reactor pressure vessel) and to limit off-site release as a result of any single control rod drop from the full-in to the position of the control rod drive.
- e. Control rod withdrawal notch sizes are to be selected so that rod movement of one notch does not result in a reactor period which the operator cannot safely control.
- f. Sufficient burnable poison is included in the fuel design to ensure that the shutdown margin limits are met at the most reactive condition and time in core life.
- g. Power distribution throughout the core is controlled such that the design linear heat generation rate (LHGR,) the average planar linear heat generation rate (APLHGR), and the

LSCS-UFSAR

minimum critical power ratio (MCPR) are not violated during steady-state operation.

- h. The standby liquid control system (SLCS) is capable of rendering the core subcritical at any time (or any core conditions) from equilibrium full power independent of control rod actions.

4.3.1.2 Power Generation Design Bases

The core and fuel design must meet the following bases:

- a. The design shall have adequate excess reactivity to attain the desired fuel cycle burnup at rated power.
- b. The design shall be capable of operating at rated conditions without exceeding technical specification limits.
- c. The core and fuel design and the reactivity control system shall allow continuous, stable regulation of reactivity.
- d. The core and fuel design shall have adequate reactivity feedback to facilitate normal operation.
- e. The Doppler coefficient is evaluated as part of the total power coefficient of reactivity (and with accident reactivity characteristics). This large power coefficient is of sufficient magnitude to effectively damp any Xenon-related power oscillations.
- f. Chemical shim control or control curtains are not used at LSCS.
- g. There are no specific design limits on excess reactivity beyond the requirements of the shutdown criteria.

4.3.2 Description

4.3.2.1 Nuclear Design Description

The LaSalle County Station (LSCS) Unit 1 and 2 cores utilize a light-water moderated reactor, fueled with slightly enriched uranium dioxide. The use of a water moderator produces a neutron energy spectrum in which fissions are caused principally by thermal neutrons. At operating conditions the moderator boils, producing a spatially variable density of steam voids in the core. The BWR design provides a system for which reactivity changes are inversely proportional to the steam void content in the moderator.

This void feedback effect is one of the inherent safety features of the BWR system. Any system input which increases reactor power, either in a local or gross sense, produces additional steam voids which reduces reactivity and thereby reduces the power.

The fuel for a BWR is uranium dioxide which is slightly enriched with U-235 with the remainder U-238. Early in the fuel life the fissioning of the U-235 produces the majority of the energy. The presence of uranium-238 in the uranium dioxide fuel leads to the production of significant quantities of plutonium during core operation. This plutonium contributes to both fuel reactivity and reactor power production, i.e., approximately 50% at end of life. In addition, direct fissioning of uranium-238 by fast neutrons yields approximately 7% to 10% of the total power and contributes to an increase of delayed neutrons in the core.

In addition, the uranium-238 contributes a strong negative Doppler reactivity coefficient and limits the peak power in excursions.

The reactor core is approximately cylindrical, 12.5 feet high and 16 feet in diameter and composed of 764 fuel bundles, each approximately 5.5 in. x 5.5 in. in cross section on a 6-inch pitch. The present fuel loading scheme for each unit can be found in the current Technical Requirements Manual.

The GE 8x8NB (GE9B) fuel type contains 60 fuel rods and one large centrally located water rod. The layout and dimension are presented in Figure 4.1-2a for the GE 8x8NB fuel type. The FANP fuel bundle type ATRIUM-9B, which is based on a 9x9 fuel rod array, contains 72 fuel rods and an inner water channel with a square cross section. The general arrangement is presented in Figure 4.1-2b for the ATRIUM-9B fuel type. The FANP fuel bundle type ATRIUM-10, which is based on a 10x10 fuel rod array, contains 83 full length fuel rods and 8 part length fuel rods. The general arrangement is presented in Figure 4.1-2c. The GE14 fuel bundle, based on a 10x10 fuel rod array, contains 78 full-length fuel rods and 14 part-length fuel rods and has an integrated debris filter. The general GE14 fuel bundle lattice arrangement is presented in Figure 4.1-2d. The enrichment distribution of the fuel bundles is designed to meet the bases described in Subsection 4.3.1. Gadolinia in the form Gd_2O_3 is selectively placed in fuel rods to provide reactivity control and improve shutdown margin. The reactivity variations of the fuel bundles are designed to complement each other. The bundle rod enrichment distributions and gadolinia distributions are proprietary information and can be found in Reference 10 for GE fuel and Reference 14 for FANP fuel.

4.3.2.1.1 Fuel Nuclear Properties

The bundle reactivity is a complex function of several important physical properties. The important properties consist of the average bundle enrichment, the gadolinia rod location and Gd concentration, the void fraction and the accumulated exposure. The typical variation of reactivity, K-infinity as a function of void fraction and exposure,

LSCS-UFSAR

for the high enrichment bundle dominant gadolinia design is presented in Figure 4.3-2. At low exposure the reactivity effect due to void formation is readily apparent; however, at higher exposure, due to the effect of void history, the curves

cross. The primary reason for this difference is the higher ratio of plutonium formation at the higher void fraction. The typical isotopic concentrations as a function of exposure are presented in Figure 4.3-3 for the important heavy element isotopes.

Early in the fuel bundle life approximately 93% of the power is produced by fissions in U-235 with the remainder coming from fast fissions in U-238. At high exposures typical of discharge, the power production due to plutonium exceeds that of the U-235. The typical fraction of fissions in the important isotopes is shown in Figure 4.3-4.

Other typical bundle parameters such as neutron generation time and delayed neutron fraction as a function of exposure at core average voids are shown in Figures 4.3-5 and 4.3-6, respectively. More detailed neutronic parameter curves typical of the GE fuel presently in use of LaSalle can be found in Reference 2. For all fuel loaded in the core, specific values for these parameters can be obtained from the lattice physics neutronic calculation performed to characterize the neutronic design.

The variation of the core-wide nuclear characteristics is a function of the characteristics of each bundle in the core. With the three unique initial core bundles and the various reload situations, any description of the gross core characteristics can only be expressed in terms of the overall core performance.

4.3.2.2 Power Distributions

The core is designed such that the resultant operating power distributions meet the plant technical specifications. The primary criteria for thermal limits are the linear heat generation rate (LHGR), average planar linear heat generation rate (APLHGR) and the minimum critical power ratio (MCPR). Each of these is a function of both the gross three-dimensional power distribution and the local rod-to-rod power distribution. Sufficient design calculations are performed to ensure that the core meets these criteria. For design convenience, separate target peaking factors are used for the local and the gross power distributions. The local rod-to-rod peaking factor is defined as the ratio of the power density in the highest power rod in the lattice, i.e., a cross section through the bundle, to the average power density in the lattice. In addition, (for GE only) the local effects on MCPR are characterized by a quantity designated as R-Factor per Reference 3. For FANP methodology, the local power peaking dependency is characterized by the F-eff parameter which is based on power distribution constants used by FANP Critical Power Correlations to calculate the critical power ratio. (References 15 and 22). The gross power peaking is defined as the ratio of the maximum power density in any axial segment of any bundle in the core to the average power density in the core. Appropriate design allowances are included at the design stage to ensure that these limits are met. During operation of the plant, the power distributions are measured by the incore instrumentation system and thermal margins are calculated by the process computer.

4.3.2.2.1 Local Power Distribution

The local rod-to-rod power distribution is a direct function of the lattice fuel rod enrichment distribution. Near the outside of the lattice where the thermal flux peaks due to interbundle water gaps, low enrichment fuel rods are utilized to minimize power peaking. Closer to the center of the bundle, higher enrichment fuel rods are used to increase the power generation and flatten the power distribution. In addition, water rods or water boxes containing unvoided water are at the center of the lattice in order to increase the thermal flux and produce more power in the center of the lattice. The combination of these factors result in the relatively flat local power distribution. The local power tends to flatten with increasing void fraction. The presence of a control blade adjacent to the bundle significantly perturbs the local power distribution. The fuel rods which contain gadolinia produce relatively little power early in bundle life; however, as the gadolinia is depleted, the power in these rods increases to approximately the lattice average.

4.3.2.2.2 Radial Power Distribution

The integrated bundle power, commonly referred to as the radial power, is a primary factor for determining MCPR. At rated conditions the MCPR is directly proportional to the radial power peaking. The radial power distribution is a complex function of the control rod pattern in the core, the fuel bundle type and distribution, and the void condition for that bundle and power. A three-dimensional BWR simulator is used to calculate the three-dimensional power distribution in the core and the power is axially integrated to determine average bundle power.

The radial distribution is controlled by both the radial reactivity zones and the control rods. The control rods are withdrawn or inserted as reactivity control is needed.

4.3.2.2.3 Axial Power Distribution

The axial power distributions obtained in the analysis of a BWR are a function of the control rod pattern, the axial gadolinia and uranium and the exposure distribution. The effect of voids is to skew the power toward the bottom of the core, the effect of the bottom entry control rods is to reduce the power in the bottom of the core, and the effect of the gadolinia is to reduce the power near the bottom. Since the void distribution is determined primarily from the power shape, the two mechanisms for optimizing the axial power shape are the control rods and the gadolinia. Detailed three-dimensional calculations are performed to determine the gadolinia and uranium distribution which provides the axial power shape. A typical beginning of cycle axial power shape is shown in Figure 4.3-11 along with an end-of-cycle power shape.

For LaSalle Units 1 and 2, the exposure shape existing in the bundles which remain from the initial cycle provides the necessary power shaping. However, subsequent reload bundles may contain axially varying gadolinia and uranium.

4.3.2.2.4 Power Distribution Calculations

A full range of calculated power distributions along with the resultant exposure shapes and the corresponding control rod patterns is shown in Reference 4 for a typical BWR. In addition, the variation of these quantities as a function of power and flow is shown. For FANP methods, power distribution calculations are discussed in References 17 and 23.

4.3.2.2.5 Power Distribution Measurements

The measurement of the power distribution within the reactor core together with instrumentation correlations and operation limits are discussed in Reference 5 for GE fuel and References 17 and 23 for FANP fuel.

4.3.2.2.6 Power Distribution Accuracy

The accuracy of the calculated local rod-to-rod power distribution and of the radial, axial, and the gross three-dimensional power distribution calculations for GE methodology is discussed in the model reports referenced in Reference 1. (A study of power distributions in boiling water reactors is given in Reference 6). A similar discussion of power distribution uncertainties for FANP methodology is provided in References 17 and 23.

4.3.2.2.7 Power Distribution Anomalies

Stringent inspection procedures are implemented to ensure the correct assembly of the reactor core. Although operation with a misplacement of a bundle in the core would be a very improbable event, calculations have been performed in order to determine the effects of such accidents on linear heat generation rate and critical power ratio. These results are presented in Chapter 15.0.

The inherent design characteristics of the BWR are well suited to limit gross power tilting. The stabilizing nature of the large moderator void coefficient effectively reduces perturbations in the power distribution. In addition, the incore instrumentation system together with the on-line computer provide the operator with prompt information on power distribution so that he can readily use control rods or other means to limit the undesirable effects of power tilting. Because of these design characteristics, it is not necessary to allocate a specific margin in the peaking factor to account for power tilt. If, for some reason, the power distribution could not be maintained within normal limits using control rods, then the operating power would have to be reduced in conformance with the Technical Specifications.

4.3.2.3 Reactivity Coefficients

Reactivity coefficients, the differential changes in reactivity produced by differential changes in core conditions, are useful in calculating the response of the core to external disturbances. The base initial condition of the system and the postulated initiating event determine which of the several defined coefficients are significant in evaluating the response of the reactor.

The coefficients of interest, relative to BWR systems, are discussed herein individually with references to the types of events in which they significantly affect the response.

There are three primary reactivity coefficients which characterize the dynamic behavior of boiling water reactors over all operating states. These are the Doppler reactivity coefficient, the moderator temperature reactivity coefficient, and the moderator void reactivity coefficient. Also associated with the BWR is a power reactivity coefficient which is generally associated with spatial xenon stability; however, this coefficient is a combination of the Doppler and void reactivity coefficients in the power operating range.

4.3.2.3.1 Void Reactivity Coefficients

The most important of these coefficients is the void reactivity coefficient. The void coefficient must be large enough to prevent power oscillation due to spatial xenon changes yet small enough that pressurization transients do not unduly limit plant operation. In addition, the void coefficient in a BWR has the ability to flatten the radial power distribution and provides ease of reactor control due to the void feedback mechanism. The overall void coefficient is always negative during the complete operating range since the BWR design is undermoderated. The reactivity change due to the formation of voids results from the reduction in neutron slowing down due to the decrease in the water fuel ratio.

A detailed discussion of the methods used to calculate void reactivity coefficients, their accuracy, and their application to plant transient analysis is presented in Reference 1 for GE fuel. A similar discussion of void reactivity is included in References 23 and 18 for FANP methodology.

The moderator void reactivity coefficient as a function of percent voids is presented in Figure 4.3-12 for the end of the initial cycle. This represents the most negative value during the cycle. This curve is for Cycle 1, however, it is typical of subsequent fuel cycles.

4.3.2.3.2 Moderator Temperature Coefficient

The moderator temperature coefficient is the least important of the reactivity coefficients since its effect is limited to a very small portion of the reactor operating

range. Once the reactor reaches the power producing range, boiling begins and the moderator temperature remains essentially constant. As with the void coefficient the moderator temperature coefficient is associated with a change in the moderating power of the water. The temperature coefficient is negative for most of the operating cycle; however, near the end-of-cycle the overall moderator temperature coefficient may become slightly positive. This is due to the fact that the uncontrolled BWR lattice is slightly overmoderated near the end-of-cycle; this, combined with the fact that more control rods must be withdrawn from the reactor core near the end-of-cycle to establish criticality, may result in a slightly positive overall moderator temperature coefficient.

The range of values of moderator temperature coefficients encountered in current BWR lattices does not include any that are significant from the safety point of view. Typically, the temperature coefficient may range from $+4 \times 10^{-5} \Delta k/k^{\circ}F$ to $-14 \times 10^{-5} \Delta k/k^{\circ}F$, depending on base temperature and core exposure. The small magnitude of this coefficient, relative to that associated with steam voids and combined with the long time-constant associated with transfer of heat from the fuel to the coolant, makes the reactivity contribution of moderator temperature change insignificant during rapid transients.

For the reasons stated previously, current core design criteria do not impose limits on the value of the temperature coefficient, and effects of minor design changes on the coefficient in members of the same class of core usually are not calculated. A measure of design control over the temperature coefficient is exercised, however, by applying a design limit to the void coefficient. This constraint implies control over the water-to-fuel ratio of the lattice; this, in turn, controls the temperature coefficient.

Thus, imposing a quantitative limit on the void coefficient effectively limits the temperature coefficient.

4.3.2.3.3 Doppler Reactivity Coefficient

The Doppler reactivity coefficient is the change in reactivity due to a change in the temperature of the fuel. This is due to the broadening of the resonance absorption cross sections as the temperature increases. At beginning of life the Doppler contribution is due primarily to U-238, however the buildup of Pu-240 with exposure adds to the Doppler coefficient. A detailed discussion of the methods used to calculate the Doppler coefficient, their accuracy and their application to plant transient analyses is presented in Reference 1 for GE methods. A similar discussion of Doppler reactivity is provided in References 23 and 18 for FANP methodology. The application of the Doppler coefficient to the analysis of the rod drop accident is discussed in Reference 7 for GE methodology and Reference 18 for FANP methodology.

The variation in the Doppler reactivity coefficient as a function of average lattice fuel temperature for the Cycle 1 high enrichment bundle dominant fuel type is shown in Figure 4.3-13 for various lattice exposures. The curve is typical of other bundle types.

4.3.2.3.4 Power Coefficient

The power coefficient is determined from the composite of all the significant individual sources of reactivity change associated with a differential change in reactor thermal power assuming xenon reactivity remains constant. A typical value for the power coefficient is $-0.05 \Delta k/k \div \Delta P/P$. This value is well within the range required for adequately damping power and spatial-xenon disturbances. The power coefficient will vary from cycle to cycle.

4.3.2.4 Control Requirements

The core and fuel design in conjunction with the reactivity control system provide an inherently stable system in that it may be shutdown from all conditions.

The control rod system is designed to provide adequate control of the maximum excess reactivity anticipated during the equilibrium fuel cycle operation. Because fuel reactivity is a maximum and control is a minimum at ambient temperature, the shutdown capability is evaluated assuming a cold, xenon-free core. Safety design basis requires that the core, in its maximum reactivity condition, be subcritical with the control rod of highest worth fully withdrawn and all others fully inserted. This limit allows control rod testing at any time in core life and assures that the reactor can be made subcritical by control rods alone.

In addition to the control rod shutdown requirements, the standby liquid control system provides sufficient reactivity control to shut down the reactor from equilibrium full power at any time independent of control rod action. The negative reactivity worth of the gadolinia-containing fuel rods decreases with the depletion of the gadolinia in a nearly linear manner so that it closely matches the depletion of fissile material.

4.3.2.4.1 Shutdown Reactivity

To ensure that the safety design basis is satisfied, an additional target design margin is adopted: a bias-adjusted k_{eff} is calculated to be less than 0.99 with the rod of highest worth fully withdrawn. An example of shutdown margin as a function of fuel exposure is shown in Figure 4.3-14. This example is based on a two-year cycle with ATRIUM-9B and GE fuel.

The limiting criteria for shutdown reactivity margins are stated in Subsection 4.3.1.1. Figure 4.3-14 shows the calculated values of k_{eff} for the shutdown condition

(20° C, strongest rod withdrawn). The initial drop in k_{eff} shows the effect of the transition from clean core to equilibrium Xe and samarium. The presence of the burnable poison Gd_2O_3 is apparent from the rise in k_{eff} as the poison depletes. The k_{eff} peak and the point of burnable poison depletion are a function of the fuel specifications (enrichment level, gadolinia concentration, etc.).

The cold (20° C) reactor condition is the most limiting with regard to shutdown criteria. Heating the reactor to hot conditions will increase the shutdown margin by 0.02 Δk to 0.03 Δk . For this reason, shutdown margin calculations are not generally performed for hot conditions.

Reduction of control rod effectiveness during core lifetime is not a major concern with the BWR. The control rod worth remains essentially constant over the BWR operating cycle.

The accuracy with which shutdown reactivity is calculated is discussed in Reference 1 for GE methodology. A similar discussion of shutdown reactivity is included in Reference 23 and 18 for FANP methodology. Basically, the accuracy is characterized as a bias and an uncertainty. The bias is a reactivity correction applied directly to the calculated results. For example:

$$k_{\text{eff}} (\text{Expected}) = k_{\text{eff}} (\text{Calculated}) + \Delta k (\text{Bias})$$

This bias has been incorporated into the shutdown curve shown in Figure 4.3-14.

The one percent design margin target is satisfied after the bias correction is applied.

4.3.2.4.2 Reactivity Variations

The excess reactivity designed into a core is controlled by a control rod system supplemented by gadolinia-urania fuel rods. Each core is designed to permit a particular amount of energy extraction over a core cycle. The average fuel enrichment for the core load is chosen to provide excess reactivity in the fuel assemblies sufficient to overcome the neutron losses caused by core neutron leakage, moderator heating and boiling, fuel temperature rise, equilibrium xenon, and samarium poisoning, plus an allowance for fuel depletion.

Control rods are used during fuel burnup, partly to balance the power distribution effect of steam voids as indicated by the incore flux monitors. In combination, the control rod and void distributions are used to flatten gross power. The design provides considerable flexibility to control the gross distribution. This permits control of fuel burnup and isotopic composition throughout the core to the extent necessary to counteract the effects of voids on axial power distribution at the end of a fuel cycle, when the few control rods remain in the core.

Reactivity balances have not normally been used in describing BWR behavior because of the strong dependence of, for example, rod worth on temperature and void fraction; therefore, the design process does not produce components of a reactivity balance at the conditions of interest but instead gives the k representing all effects combined. Further, any listing of components of a reactivity balance is quite ambiguous unless the sequence of the changes is clearly defined.

Consider, for example, the reactivity effect of control rods and burnable poison. The combined worth of these two absorbers would be considerably different than the sum of their individual worths. Even this combined worth would be of questionable significance unless the path and conditions of other parameters (i.e., temperature, void, xenon, etc.) were completely specified. Many other illustrations could be presented showing that the reactivity balance approach, which may be appropriate in some types of reactors, is completely inappropriate in a BWR. This is related to the large potential excess reactivity in a BWR combined with the dependence of interaction (shadowing) factors on reactor state.

4.3.2.5 Control Rod Patterns and Reactivity Worths

4.3.2.5.1 Control Rod Withdrawal Sequences

To understand the definition of incremental control rod worth, the banked position (BP) method of control rod withdrawal utilized in the rod worth minimizer (RWM) must be completely understood. For this reason, a description of the BP withdrawal method precedes the discussion of control rod reactivity worth. The BP method is described in detail in Reference 8. To clarify this discussion, the control rod withdrawal sequence is divided into two steps. The first range of withdrawals covers all the rods inserted to the 50% or checkerboard control configurations, referred to as the startup range. The second step covers control rod withdrawals from the checkerboard through the power range control configurations, referred to as the RWM power range (50% rod density to 10% rated power).

Figures 4.3-15 through 4.3-18 show the control rod group assignments that are utilized in the BP withdrawal system. Figures 4.3-15 and 4.3-16 illustrate Groups 1 through 4 and Groups 5 through 10, respectively, for Sequence A. Figures 4.3-17 and 4.3-18 illustrate Groups 1 through 4 and Groups 5 through 10, respectively, for Sequence B.

Historically, ComEd utilized the generic General Electric Banked Position Withdraw Sequence methodology (References 1 and 8) to protect the 280 cal/gm fuel damage limit. This analysis was a bounding and conservative generic calculation. As with most generic analyses, it can also be unnecessarily restrictive. In the early 90's, ComEd received NRC approval (Reference 21) to perform in-house design calculations. Using this in-house ability, ComEd/Exelon began to perform cycle specific CRDA analyses. Using cycle specific calculations, Exelon is able to modify the

original BPWS sequence to remove some of the unnecessary conservatism (typically, elimination of some of the banked positions, Reference 20.) These sequences are referred to as the analyzed rod position sequence.

Control rod patterns analyzed in the cycle specific CRDA analyses follow predetermined sequencing rules. This sequence applies to all control rod movement from the all rods in condition to the Low Power Setpoint (LPSP). These rules include the designation of control rod groups. The banked positions are established to limit the maximum incremental control rod worth such that the 280 cal/gm design limit is not exceeded. Cycle specific analyses ensure that the 280 cal/gm fuel damage limit is not exceeded during worst case scenarios. These worst case scenarios account for a limited number of inoperable control rods with a specified separation criteria. Specific evaluations or analyses can be performed for atypical operating conditions, e.g. fuel leaker suppression.

4.3.2.5.1.1 Control Rod Withdrawal Sequences in the Startup Range

Typical control rod withdrawal sequences in the startup range are shown in Figures 4.3-15 and 4.3-17 for Sequences A and B, respectively. Given that Sequence A or B has been selected, the BPWS:

- a. Any of the control rod groups, 1, 2, 3, or 4, is selected as the first group of rods to be moved. Groups 1 and 2 must be fully withdrawn before any rods from Groups 3 or 4 can be moved or Groups 3 and 4 must be fully withdrawn before any rods from Groups 1 and 2 can be moved.
- b. The first 25% of the control rods to be moved (i.e., Groups 1 and 2 or Groups 3 and 4) are fully withdrawn.
- c. The second 25% of the control rods to be moved are to be notch-banked to predetermined positions (N_1 , N_2 , N_3 , and N_4).
- d. All control rods within a group must be withdrawn to this designated notch-bank position before withdrawing to the next notch-bank position.
- e. The notch positions N_1 , N_2 , N_3 , and N_4 , are flexible values and may vary between rod groups.

The highest control rod worth using the BP method is not limited to the worth associated with a control rod dropping from the fully inserted position to the full-out position. If all rods in a group are at bank position N_1 and one rod of the group is withdrawn to bank position N_2 , the furthest this control rod could drop, if it were decoupled from its drive and stuck at the full-in position, would be to N_2 . Without the BP methods, if the control rod bank were at N_4 , and one control rod drive

withdrawn to the full-out position, the control rod could drop from the fully inserted to the full-out position. Only incremental control rod worths are considered when the banked position system is employed. Neutronic coupling must also be taken into account when calculating maximum incremental control rod worth.

4.3.2.5.1.2 Control Rod Withdrawal Sequences in the RWM Power Range

The following rules are enforced by BPWS for rods in Groups 5-10:

- a. Movement of rods in Groups 5 through 10 requires that Groups 1 through 4 are fully withdrawn.
- b. Generally, any group within Groups 5 through 10 may be selected as the first group of control rods to be withdrawn; however, if rods in Groups 7 or 8 are moved first, rods in Groups 9 and 10 cannot be moved until all rods contained in Groups 5 and 6, and 7 or 8 are at notch position $\geq M_1$. Conversely, if rods in Groups 9 or 10 are moved first, rods in Groups 7 and 8 cannot be moved until all rods contained in Groups 5 and 6, and 9 or 10 are at notch position $\geq M_1$.
- c. Rod Group 5 and 6 are to be banked to notch positions 00-N₁-48.
- d. Any control rod contained within groups 7 through 10 can be withdrawn to any notch position with the restriction that any rod within the group cannot be moved beyond N₁ or N₂ or N₃ or N₄ without having the remainder of the rods assigned to the group positioned at N₁ or N₂ or N₃ or N₄, respectively.
- e. The order of control rod withdrawal within a group is arbitrary as long as all other conditions are met.
- f. Intermediate banking of groups within BPWS rules is acceptable as determined by a reactor engineer. The notch positions N₁, N₂, N₃ and N₄ are flexible values and may vary between rod groups. These notch positions, as well as M₁, may also vary from fuel cycle to fuel cycle.
- g. The rods within a group must be moved as a group to a BPWS notch banked position prior to moving any single rod to the next notch bank position.

Once the 50% control rod density point has been achieved under the BP method, the control rods remaining in the core, Groups 5 through 10 shown in Figures 4.3-16 and 4.3-18, are withdrawn following BPWS rules. In addition to the previous rules, the infinite lattice technique is utilized to minimize the occurrence and severity of short periods. This technique treats the core as if it were infinite, so that the peripheral rods, groups 5 and 6 are withdrawn with groups 7 and 8 or groups 9 and 10. This prevents the periphery from being undercontrolled or overcontrolled.

The generalized BPWS methodology described above is applied in the LSCS startup sequence to mitigate the scale of the control rod drop accident. This control rod withdrawal sequence is based on the BPWS Banked Position method. A single control rod withdrawal from full-in to full-out is prohibited procedurally by the predetermined withdrawal sequence as well as physically by the RWM. The predetermined rod withdrawal sequences in the power range are retained to optimize the power distribution and remain within technical specification limits. In doing this, the control rod worth is minimized.

4.3.2.5.1.3 Maximum Control Rod Worth Pattern with a Single Error in the RWM Power Range

The control rods assigned to groups in the RWM power range (Figures 4.3-16 and 4.3-18) are withdrawn in the Banked Position mode as are the second 25% of the control rods in the startup range. The banked mode requires that all control rods assigned to a given group be banked to the preassigned notch position, i.e., N_1 , N_2 , etc., as they are withdrawn to a specific position. Typically, if Group 7, shown in Figure 4.3-16, is to be withdrawn from its fully inserted position to notch 4, all rods of Group 7 would first be notch-banked at the applicable notch position. When all Group 7 rods are at that notch, the BPWS allows movement to the next notch. After all Group 7 rods are at the next notch, the BPWS allows movement to continue.

The maximum incremental control rod worth with the RWM operational is a function of neutronic coupling. The incremental worth (i.e., the worth of the rod from its fully inserted position to the position of its control rod drive) is the significant safety variable controlled by the RWM. This discussion is applicable only when taken in the context of the Banked Position mode of withdrawal.

4.3.2.5.2 Control Rod Worth Calculations

4.3.2.5.2.1 Control Rod Worth in the Startup Range and RWM Power Range

In the startup range incremental control rod worth calculations were performed using three-dimensional analysis which properly accounts for the spatial fuel, exposure, and gadolinia distributions. These multidimensional calculations also

properly account for the spatial power shifts that occur when the banked mode of rod withdrawal is employed.

The control rod worth is defined as the eigenvalue difference calculated with the subject rod fully inserted and with the rod withdrawn to its drive position. The maximum incremental control rod worth with the RWM operational in its RWM power range is presented in Table 4.3-1 for the initial cycle cores. Rod Worth is an input to the Control Rod Drop Accident Analysis. See section 15.4.9 for a discussion of this analysis.

4.3.2.5.2.2 Control Rod Worth in the Reactor Power Range > 10% Rated Power

In the reactor power range the rod worth calculations are affected by the formation of steam voids in the moderator; therefore, three-dimensional calculations which properly account for the void distribution, as well as the spatial fuel and gadolinia distributions were performed. When void formation is present, the incremental control rod worth is defined as the excess reactivity that occurs due to the instantaneous withdrawal of a control rod; therefore, no heat transfer or heat addition occurs and the void distribution remains constant at its initial value.

4.3.2.5.3 Scram Reactivity

The reactor protection system (RPS) responds to certain abnormal operational transients by initiating a scram. The RPS and the CRD system act quickly enough to prevent the initiating disturbance from causing fuel damage. The scram reactivity curve at the end of cycle 1 is shown in Figure 4.3-19.

At the hot operating condition the control rod, power, delayed neutron, and void distributions must all be properly accounted for as a function of time. Therefore, this protective response is calculated using a one-dimensional (axial) finite-differenced space-time model which is coupled with a single channel thermal-hydraulic model. The finite-differenced space-time model uses three prompt and six delayed neutron energy groups, and has been compared and verified by analysis of published results obtained using the industry standard computer code.

The transient thermal-hydraulic model employed for this calculation is described in Reference 1 and 19. It is sufficient to state here that the coupled neutronics and thermal-hydraulics properly account for the redistribution of the power, neutron flux, and voids during the scram.

4.3.2.5.4 Control Rod Withdrawal Sequences

Simplified shut down sequences that eliminate the group banking requirements have been generically bounded in Reference 24.

4.3.2.6 Criticality of Reactor During Refueling

4.3.2.6.1 Criticality of Reactor

The maximum allowable value of k_{eff} is < 1.000 at any time during refueling. For each reload cycle the maximum core reactivity during refueling is calculated with the highest worth rod withdrawn to show at least 0.38% $\Delta k/k$ margin. Control rod system interlock prevents the withdrawal of more than one rod while in the REFUEL mode.

4.3.2.6.2 Criticality of Fuel Assemblies

With regard to fuel storage and handling, the criticality analyses were performed on a generic basis. Refer to Sections 9.1.1.3, 9.1.2.1.3, and 9.1.2.2.3 for detailed discussions of the criticality analyses. For the dry condition, k_{eff} is < 0.90 . For fuel storage and handling the design requirements are that $k_{\text{eff}} < 0.95$ for normal conditions and abnormal conditions. Using procedural controls, reactor personnel are restricted from arranging four fuel bundles in a square array in the fuel handling facilities since this would result in k_{eff} approximately equal to 0.91 based on the generic study. The k_{eff} for a single fuel bundle was not evaluated; however, the effective multiplication factor for two bundles placed side by side was evaluated and found to be approximately 0.74. These fuel handling and storage calculations are very conservative since 16 to 20 fuel bundles would be required to establish a critical array assuming fresh fuel with gadolinia present.

4.3.2.7 Stability

4.3.2.7.1 Xenon Transients

The maximum xenon reactivity buildup on shutdown from full power and the rate of xenon reactivity burnout on return to full power when the maximum shutdown xenon buildup occurs were calculated for both the beginning-of-life and the end-of-cycle reactor conditions. The maximum rate of reactivity change is obtained by assuming an instantaneous return to full power. The results of these calculations are shown in Figure 4.3-20 for the beginning-of-life condition. From this analysis it was determined that the maximum reactivity addition caused by burnup of xenon was $+0.00010$ ($\Delta k/k$)/min. Assuming a control rod worth of 0.001 $\Delta k/k$ with an insertion rate of 3 in/sec, the reactivity addition by the control rod insertion is -0.00125 ($\Delta k/k$)/min. Therefore, a very weak control rod can easily compensate for a xenon-burnup reactivity addition.

Boiling water reactors do not have instability problems due to xenon. This has been demonstrated by operating BWR's for which xenon instabilities have never been observed (such instabilities would readily be detected by the LPRM's), by special tests which have been conducted on operating BWR's in an attempt to force the

reactor into xenon instability, and by calculations. All of these indicators have proven that xenon transients are highly damped in a BWR due to the large negative power coefficient.

The analysis and experiments conducted in this area are reported in Reference 9.

4.3.2.7.2 Thermal Hydraulic Stability

This subject is covered in Subsection 4.4.4.6.

4.3.2.8 Vessel Irradiation

The neutron fluences at the vessel have been calculated assuming continuous reactor operation at rated power for 40 years. The flux data used in these determinations are given in Table 4.3-2. Also, a 24 group breakdown of the core boundary neutron flux spectrum is shown in Table 4.3-3. The power distribution used to obtain the flux data is shown in Figures 4.3-21 and 4.3-22.

The method of fluence calculations is described in Subsection 4.1.4.5. The predicted maximum fluence for neutron energies greater than 1 MeV is 6.2×10^{17} neutrons/cm².

4.3.3 Analytical Methods

The analytical methods and nuclear data used to determine the nuclear characteristics are those in use for design and analysis of water moderated reactors.

The Lattice Physics Model (described in models referenced in Reference 1 for GE methodology and References 18 and 23 for FANP methodology) is used to calculate lattice reactivity characteristics, few group flux averaged cross sections and local rod-to-rod power and exposure distributions. These data are generated for various temperature, void, exposure and control conditions as required to represent the reactor core behavior.

The BWR Simulator (Reference 1 for GE methodology and Reference 18 and 23 for FANP methodology) is a large three-dimensional code which provides for spatially varying voids, control rods, burnable poisons, xenon, and exposure. This code is used to calculate three-dimensional power and exposure distributions, control rod patterns, and thermal-hydraulic characteristics throughout core life.

These methods have been compared extensively to experiments and plant operating data on the results are presented in the reports given in Reference 1 for GE fuel and References 15, 18, 19, 22 and 23 for FANP fuel.

LSCS-UFSAR

4.3.4 References

1. "General Electric Standard Application for Reactor Fuel (GESTAR II)," NEDE-24011-P-A, (latest approved revision).
2. Letter No. MFN-045-086, J. S. Charnley (GE) to H. N. Berkow (NRC), "Submittal of General Electric Neutronic Parameter Curves to Satisfy a Condition of the NRC Approval of Amendment 13 to GESTAR-II," June 23, 1986.
3. E. C. Eckert et al., "General Electric BWR Thermal Analysis Basis (GETAB) Data, Correlation, and Design Application," NEDO-10958, January 1977.
4. General Electric Standard Safety Analysis Report (GESSAR), Appendix 4A.
5. J. F. Carew, "Process Computer Performance Evaluation Accuracy," NEDO-20340, June 1974.
6. General Electric Company Topical Report NEDO-20944-P, "BWR/4 and BWR/5 Fuel Design," October 1976.
7. R. G. Stirn et al., "Rod Drop Accident Analysis for Large Boiling Water Reactors," NEDO-10527, General Electric Co., Atomic Power Equipment Department, March 1972 (also Supplement 1, July 1972 and Supplement 2, January 1973).
8. C. J. Paone, "Banked Position Withdrawal Sequence," NEDO-21231, January 1977.
9. R. L. Crowther, "Xenon Considerations in Design of Boiling Water Reactors," APED-5640, June 1968.
10. NEDE-31152, "GE Fuel Bundle Designs," (latest revision).
11. NEDE-31510P, "LSCS Units 1 & 2, Safer/GESTR-LOCA Loss of Coolant Accident Analysis," (as amended).
12. Letter from R. J. Stransky, NRR, to T. J. Kovach, CECo, Issuance of Amendment 88 to LaSalle Unit 1 Facility Operating License No. NPF-11 and Amendment 73 to LaSalle Unit 2 Facility Operating License No. NPF-18 and including Safety Evaluation Report dated December 4, 1992.
13. [Deleted]

LSCS-UFSAR

14. Cycle Specific FANP Fuel Design Report (applicable only to FANP reloads).
15. ANFB Critical Power Correlation, ANF-1125 (P)(A) and Supplements 1 and 2, Advanced Nuclear Fuels Corporation, April 1990; ANFB Critical Power Correlation Application for Co-Resident Fuel, EMF-1125(P)(A), Supplement 1, Appendix C, Siemens Power Corporation, August 1997; and ANFB Critical Power Correlation Determination of ATRIUM-9B Additive Constant Uncertainties, ANF-1125(P)(A) Supplement 1, Appendix E, Siemens Power Corporation, September 1998.
16. Intentionally Deleted
17. MICROBURN-B2 Based Impact of Failed/Bypassed LPRMs and TIPS, Extended LPRM Calibration Interval and Single Loop Operation on Measured Radial Bundle Power Uncertainty, EMF-2493(P), Revision 0, Siemens Power Corporation, December 2000.
18. Exxon Nuclear Methodology for Boiling Water Reactors – Neutronic Methods for Design and Analysis, XN-NF-80-19(P)(A) Volume 1 and Supplements 1 and 2, Exxon Nuclear Company, Richland, WA 99352, March 1983.
19. Exxon Nuclear Plant Transient Methodology for Boiling Water Reactors, XN-NF-79-71(P)(A), Revision 2 and Supplements 1, 2, and 3, Exxon Nuclear Company, Inc. March 1986.
20. ComEd letter, "Dresden Nuclear Power Station Units 2 and 3, Quad Cities Nuclear Power Station Units 1 and 2, LaSalle County Nuclear Power Station Units 1 and 2, Revised Control Rod Sequencing Methods, NRC Docket Nos. 50-237/249, 50-254/265, and 50-373/374", P.L. Piet to T.E. Murley, January 27, 1993.
21. Commonwealth Edison Topical Report NFSR-0091, "Benchmark of CASMO/MICROBURN BWR Nuclear Design Methods", Revision 0, Supplements 1 and 2, December 1991, March 1992, and May 1992, respectively; SER letter date March 22, 1993.
22. SPCB Critical Power Correlation, EMF-2209(P)(A) Revision 2, Siemens Power Corporation, September 2003.

LSCS-UFSAR

23. Siemens Power Corporation Methodology for Boiling Water Reactors: Evaluation and Validation of CASMO - 4/MICROBURN - B2, EMF-2158 (P)(A), Revision 0, October 1999.
24. "Improved BPWS Control Rod Insertion Process," NEDO-033091-A Revision 2, July 2004.

LSCS-UFSAR

TABLE 4.3-1

MAXIMUM INCREMENTAL ROD WORTHS FOR INITIAL CYCLE USING
BPWS FOR EACH OF THE GIVEN ROD GROUPS

<u>CORE CONDITION</u>	<u>CONTROL ROD GROUP*</u>	<u>BANKED AT NOTCH</u>	<u>CONTROL ROD (X,Y)</u>	<u>DROPS FROM→TO</u>	<u>Δk</u>
BOC-1 Sequence A G1 through G4 W/D all others at 0	7	12	26-35	0 → 48	.004658
BOC-1 Sequence A G1 through G4 W/D all others at 0	8	12	26-43	0 → 48	.002518
BOC-1 Sequence A G1 through G4 W/D G5 through G8 at 12 G10 at 0	9	4	30-31	0 → 8	.002154
BOC-1 Sequence A G1 through G4 W/D G5 through G8 at 12 G9 at 0	10	4	22-31	0 → 8	.002141

NOTE: The following assumptions were made to ensure that the rod worths were conservatively high for the BPWS:

- a. BOC
- b. HOT STARTUP¹
- c. NO XENON

* For definition of rod groups, see Figures 4.3-24 through 4.3-27.

LSCS-UFSAR

TABLE 4.3-2

NEUTRON FLUXES RELATED TO VESSEL IRRADIATION*

<u>NEUTRON ENERGY (MeV)</u>	<u>AVERAGE FLUX IN THE CORE (n/cm²-sec)</u>	<u>FLUX AT THE CORE BOUNDARY (n/cm²-sec)</u>	<u>FLUX INSIDE SURFACE OF VESSEL (n/cm²-sec)</u>
30	5.6 E + 12	1.6 E + 12	1.7 E + 8
1.0 - 3.0	4.4 E + 13	1.2 E + 13	3.2 E + 8
0.1 - 1.0	5.3 E + 13	1.3 E + 13	3.8 E + 8
Thermal -0.1	8.4 E + 13	2.3 E + 13	8.1 E + 8
Thermal	2.6 E + 13	2.8 E + 13	4.7 E + 9
>1.0	5.0 E + 13	1.4 E + 13	4.9 E + 8

* These values were not revised for Power Uprate.

LSCS-UFSAR

TABLE 4.3-3

24 GROUP MULTIGROUP NEUTRON FLUX AT THE CORE EQUIVALENT RADIUS*

<u>GROUP</u>	<u>LOWER ENERGY</u> <u>BOUND</u>		<u>FLUX</u> <u>(n/cm²-sec)</u>
1	10	MeV	4.4 E+10
2	6.07	MeV	5.7 E+11
3	3.68	MeV	2.0 E+12
4	2.23	MeV	4.1 E+12
5	1.35	MeV	4.4 E+12
6	821.0	KeV	4.0 E+12
7	498.0	KeV	4.1 E+12
8	302.0	KeV	3.0 E+12
9	183.0	KeV	2.5 E+12
10	111.0	KeV	2.0 E+12
11	67.4	KeV	1.6 E+12
12	40.8	KeV	1.3 E+12
13	24.8	KeV	1.2 E+12
14	15.0	KeV	1.2 E+12
15	9.12	KeV	1.1 E+12
16	5.53	KeV	1.1 E+12
17	3.35	KeV	1.1 E+12
18	2.03	KeV	1.0 E+12
19	1.01	KeV	1.4 E+12
20	249.0	eV	2.7 E+12
21	55.6	eV	2.8 E+12
22	12.4	eV	2.6 E+12
23	.625	eV	4.3 E+12
24	0	eV	2.8 E+13

*These values were not revised for Power Uprate.

4.4 THERMAL AND HYDRAULIC DESIGN

4.4.1 Design Bases

4.4.1.1 Safety Design Bases

Thermal hydraulic design of the LaSalle County Station (LSCS) core is established and based upon the following design bases:

- a. Actuation limits for the devices of the nuclear safety systems are employed such that no fuel damage occurs as a result of abnormal transients (Chapter 15.0). Specifically, the minimum critical power ratio (MCPR) operating limit is specified such that at least 99.9% of the fuel rods in the core will not experience boiling transition during the most severe abnormal operational transient. A 1% plastic strain limit is specified to ensure that clad overstraining does not occur.
- b. Thermal hydraulic safety limits are used in setting safety margins and the consequences of fuel barrier failure to public safety.
- c. The nuclear system must meet the requirements in 10CFR50, Appendix A, General Design Criterion 12 - Suppression of Reactor Power Oscillations.

4.4.1.2 Power Generation Design Bases

The thermal-hydraulic design of the core provides the following operational characteristics:

- a. ability to achieve rated core power output throughout the design life of the fuel without sustaining premature fuel failure, and
- b. flexibility to adjust core output over the range of plant load and load maneuvering requirements in a stable, predictable manner without sustaining fuel damage.

4.4.1.3 Requirements for Steady-State Conditions

Steady-State Limits

For purposes of maintaining adequate thermal-hydraulic margin during normal steady-state operation, the minimum critical power ratio must not be less than the required MCPR operating limit, the operational linear heat generation rate (LHGR) is maintained below the LHGR limit for the fuel type, and the maximum average

planar linear heat generation rate (MAPLHGR) must be maintained below the limits for the plant. This does not specify the operating power nor does it specify peaking factors. These parameters are determined subject to a number of constraints, including the thermal limits given previously. The core and fuel thermal-hydraulic design basis for steady-state operation, has been defined to provide margin between the steady-state operating condition and any fuel damage condition to accommodate uncertainties and to ensure that no fuel damage results, even during the worst anticipated transient conditions at any time in life. For LSCS, the operating limits for all three fuel thermal design limits are contained in the Core Operating Limits Report.

4.4.1.4 Requirements for Transient Conditions

Transient Limits

The transient thermal-hydraulic limits are established such that no fuel damage is expected to occur during the most severe abnormal operating transient. Fuel damage is defined as perforation of the cladding that permits release of fission products (Section 4.2). Mechanisms that cause fuel damage in reactor transients are:

- a. severe overheating of fuel cladding caused by inadequate cooling, and
- b. fracture of the fuel cladding caused by relative expansion of the uranium dioxide pellet inside the fuel cladding.

For design purposes, the transient thermal-hydraulic limit requirement is met if at least 99.9% of the fuel rods in the core do not experience boiling transition during any abnormal operating transient. No fuel damage is expected to occur even if a fuel rod actually experiences a boiling transition.

A value of 1% plastic strain of Zircaloy cladding has been established as the limit below which fuel damage from overstraining the fuel cladding is not expected to occur. Available data indicate that the threshold for damage is in excess of this value. The linear heat generation rate required to cause this amount of cladding strain decreases with burnup.

4.4.1.5 Summary of Design Bases

In summary, the steady-state thermal-hydraulic operating limits have been established to ensure that the design basis is satisfied for the most severe abnormal operational situation, whether a transient or an accident. Transient analyses are performed that demonstrate compliance with overpower transient limits assuming steady-state operation has been in compliance with steady state operating limits. An overpower which occurs during an abnormal operational transient must not

result in violation of the MCPR safety limit for the plant. Demonstration that the transient limits are not exceeded is sufficient to conclude that the thermal hydraulic design basis is satisfied.

The MCPR, LHGR and MAPLHGR limits are sufficiently general so that no other limits need to be stated. The cladding and fuel bundle integrity criterion is assured as long as MCPR, LHGR and MAPLHGR limits are met. There are no additional design criteria on coolant void fraction, core coolant flow-velocities, or flow distribution, nor are they needed. Core design and target rod patterns ensure CPRs remain above the MCPR limits, thereby ensuring bundle parameters (e.g., flow, power, void fraction) remain within prescribed ranges. The coolant flow velocities and void fraction become constraints upon the mechanical and physics design of reactor components and are partially constrained by stability and control requirements.

4.4.1.5.1 Fuel Cladding Integrity

The fuel cladding integrity is defined in Subsection 4.2.1. The fuel cladding integrity from a thermal hydraulic viewpoint is assured by the operating and transient MCPR requirements.

4.4.1.5.2 Fuel Assembly Integrity

The fuel channel provides adequate lateral structural support for the fuel bundle and protects the fuel rods and spacers from impact and abrasion. The upper tie-plate handle is capable of supporting the weight of the fuel assembly. Specific design characteristics are given in Section 4.2.

4.4.1.5.3 Fuel-Cladding Gap Characteristics

The subject of fuel to cladding gap characteristics is covered in Section 4.2.

4.4.2 Description of Thermal Hydraulic Design of Reactor Core

4.4.2.1 Summary Comparison

An evaluation of plant performance from a thermal and hydraulic standpoint is provided in Subsection 4.4.4.

Transient evaluations are given in Chapter 15. A tabulation of thermal and hydraulic parameters of the LSCS reactor initial core, along with a comparison to the initial core of other reactors of a similar design, are given in Table 4.4-1.

4.4.2.2 Critical Power Ratio

There are three different types of boiling heat transfer in water forced convection systems: nucleate boiling, transition boiling, and film boiling. Nucleate boiling, at lower heat transfer rate, is an extremely efficient mode of heat transfer, allowing

large quantities of heat to be transferred with a very small temperature rise at the heated wall. As heat transfer rate is increased the boiling heat transfer surface alternates between film and nucleate boiling, leading to fluctuations in heated wall temperatures. The point of departure from the nucleate boiling region into the transition boiling region is called the boiling transition. Transition boiling begins at the critical power, and is characterized by fluctuations in cladding surface temperature. Film boiling occurs at the highest heat transfer rates; it begins as transition boiling comes to an end. Film boiling heat transfer is characterized by stable wall temperatures which are higher than those experienced during nucleate boiling.

4.4.2.2.1 Boiling Correlations

4.4.2.2.1.1 GE Fuel

The occurrence of boiling transition is a function of the local steam quality, boiling length, mass flow rate, pressure, flow geometry, and local peaking pattern. General Electric has conducted extensive experimental investigations of these parameters. These parametric studies encompass the entire design range of these variables. In the experimental investigations, a boiling transition event was associated with a 25° F rise in rod surface temperature. The (critical) quality at which boiling transition occurs as a function of the distance from the equilibrium boiling boundary is predicted by the GEXL (General Electric Critical Quality X - Boiling Length) correlation. This correlation is based on accurate test data of full-prototype simulations of reactor fuel assemblies operating under conditions duplicating those in actual reactor designs. The GEXL correlation is a best fit to the data and is used together with a statistical analysis to assure adequate reactor thermal margins (References 1 and 11).

The figure of merit used for reactor design and operation is the critical power ratio (CPR). This is defined as the ratio of the bundle power which would produce equilibrium quality equal to but not exceeding the correlation value (critical quality), to the bundle power at the reactor condition of interest (i.e., the ratio of critical bundle power to operating bundle power). In this definition, the critical power is determined at the same mass flux, inlet temperature, and pressure which exist at the specified reactor condition.

The core is sized with sufficient coolant flow to assure that the MCPR is maintained greater than the operating limit at rated conditions.

4.4.2.2.1.2 FANP Fuel

In the FANP methodology, the fuel assembly critical power corresponding to a particular reactor operating state is determined from the SPCB (References 25 and 26) or ANF-B (Reference 17) critical power correlations.

LSCS-UFSAR

The ANF-B and SPCB correlations provides a generic tool for evaluating critical power and to assess thermal margin for all current domestic FANP BWR fuel designs. It is based on a data base characteristic of FANP product designs. The database contains data for FANP fuel designs with both axially uniform and nonuniform power profiles.

The ANF-B and SPCB critical power correlations are an empirical representation of planar average thermal-hydraulic fluid conditions at which boiling transition has been experimentally determined. The minimum heat flux required to produce boiling transition is predicted from fluid conditions of pressure, mass velocity, and enthalpy averaged over the plane of interest. The correlation contains correction factors for the effects of boiling transition due to a nonuniform axial heat flux profile and the grouping of relatively high-powered rods.

The test assemblies include full-length rods; typical BWR grid spacers; 4x4, 5x5, and 9x9 rod configurations; and a variety of rod diameters, assembly hydraulic diameters, rod-to-wall spacings, and rod-to-rod spacings. The database was compiled from data taken at two test laboratories: Columbia University and the ATLAS facility. The uniform axial data was used to develop the correlation, while the nonuniform axial data was used to validate the correlation with the Tong factor. Therefore, the correlation has been checked against independent test data.

The correlations address the effects of operating pressure, mass velocity, enthalpy, axial power profile, local power peaking and distribution, rod diameter, and fuel assembly hydraulic diameter and heated length on boiling transition.

The ANF-B and SPCB correlations have also been used to predict the number of rods experiencing boiling transition (predict multiple indications) for the test database. The probability of boiling transition for each rod in a test section was determined from the critical power prediction based on that rod. The probabilities for all the rods in the test assembly, as predicted by ANF-B and SPCB, were then summed to yield the prediction of the total number of rods experiencing boiling transition. The ANF-B and SPCB correlations were found to conservatively overpredict the expected number of rods that experience boiling transition (References 16, 17, 25 and 26).

4.4.2.3 Maximum Average Planar Linear Heat Generation Rate (MAPLHGR)

The MAPLHGR limit for fuel assures that the peak cladding temperature of fuel following a postulated design basis loss-of-coolant accident (LOCA) will not exceed the peak cladding temperature (PCT) and maximum oxidation limits specified in 10CFR50.46. The calculational procedure used to establish the MAPLHGR limits is based on a LOCA analysis. The analysis is performed using calculational models

LSCS-UFSAR

which are consistent with the requirements of Appendix K to 10CFR50. The models are described in Reference 20 for FANP and Reference 12 for GE.

The PCT following a postulated LOCA is primarily a function of the average heat generation rate of all the rods of a fuel assembly at any axial location and not strongly influenced by the rod-to-rod power distribution within the assembly.

The MAPLHGR limits for two-loop operation for a particular cycle are specified in the COLR.

For single-loop operation, an APLHGR limit corresponding to the product of the two-loop limit and a reduction factor specified in the COLR can be conservatively used to ensure that the PCT for single-loop operation is bound by the PCT for two-loop operation.

4.4.2.3.1 Design Power Distribution

Thermal-hydraulic design of the reactor -- including the selection of the core size and effective heat transfer area, the design steam quality, the total recirculation flow, the inlet subcooling, and the specification of internal flow distribution -- is based on the concept and application of a design power distribution. The design power distribution represents a conservative thermal operating state at rated conditions and includes design allowances for the combined effects (on the fuel rod, and the fuel assembly heat flux and temperature) of the gross and local steady-state power density distributions and adjustments of the control rods.

The design power distribution is used in conjunction with flow and pressure drop distribution computations to determine the thermal conditions of the fuel and the enthalpy conditions of the coolant throughout the core.

The design power distribution is based on detailed calculations of the neutron flux distribution.

The core average and maximum void fractions are dependent on the reactor operating state and power distributions. Typical average and maximum void fraction results for FANP fuel can be found in Reference 13.

4.4.2.4 Void Fraction Distribution

The core average and maximum void fractions for the initial core at rated condition are given in Table 4.4-1. The typical axial distribution of core void fractions for the average radial channel and the maximum radial channel (end of node value) is given in Table 4.4-2. The core average and maximum exit value are also provided. Similar distributions for steam quality are provided in Table 4.4-3. The core average axial power distributions used to produce these tables are given in Table 4.4-2a.

4.4.2.5 Core Coolant Flow Distribution

Correct distribution of core coolant flow among the fuel assemblies is accomplished by the use of an accurately calibrated fixed orifice at the inlet of each fuel assembly. The orifices are located in the fuel support piece. They serve to control the flow distribution and, hence, the coolant conditions within prescribed bounds throughout the design range of core operation.

The core is divided into two orificed flow zones. The outer zone is a narrow, reduced-power region around the periphery of the core. The inner zone consists of the core center region. No other control of flow and steam distribution other than that incidentally supplied by adjusting the power distribution with the control rods, is used or needed. The orifices can be changed during refueling, if necessary.

The sizing and design of the orifices ensure stable flow in each fuel assembly during all phases of operation at normal operating conditions.

Design core flow distribution calculations are made using the design power distribution which consists of a hot and average powered assembly in each of the two orifice zones. Typical design bundle powers and resulting relative flow distributions are given in Table 4.4-4.

The flow distribution to the fuel assemblies is calculated on the assumption that the pressure drop from lower plenum to upper plenum (across all fuel assemblies) is the same. This assumption has been confirmed by measuring the flow distribution in a modern boiling water reactor as reported in Reference 2.

There is reasonable assurance, therefore, that the calculated flow distribution throughout the core is in close agreement with the actual flow distribution of an operating reactor. The use of the design power distribution discussed previously ensures that the chosen orificing covers the range of normal operation. The expected shifts in power production during core life are less severe and are bounded by the design power distribution.

4.4.2.6 Core Pressure Drop and Hydraulic Loads

The pressure drop across various core components under steady-state design conditions is included in Table 4.4-1 for the initial core. Initial Cycle analyses for the most limiting conditions, the recirculation line break and the steamline break, are reported in Chapter 15. For SAFER/GESTR information, see Reference 12. For core pressure drop information for FANP fuel, see Reference 13.

The components of bundle pressure drop considered are friction, local, elevation, and acceleration pressure drops. Pressure drop measurements made in operating reactors confirm that the total measured core pressure drop and calculated core pressure drop are in good agreement.

Subsections 4.4.2.6.1 through 4.4.2.6.4 describe the pressure drop models that were used by GE for the initial core. FANP utilizes similar pressure drop correlations and methodology. For more detail on these correlations and methodologies see References 14 and 15.

4.4.2.6.1 Friction Pressure Drop

Friction pressure drop is calculated using the relationship:

$$\Delta P_f = \frac{w^2}{2g\rho} \frac{fL}{D_H A_{ch}^2} \phi_{TPF}^2 \quad (4.4-1)$$

where:

Δp_f	=	friction pressure drop, psi,
w	=	mass flow rate,
g	=	acceleration of gravity,
ρ	=	water density,
D_H	=	channel hydraulic diameter,
A_{ch}	=	channel flow area,
L	=	length,

LSCS-UFSAR

- f = friction factor, and
- ϕ_{TPF}^2 = two phase friction multiplier.

This formulation is similar to that used throughout the nuclear power industry. The formulation for the two-phase multiplier is based on data which compares closely to that found in the open literature (Reference 3).

4.4.2.6.2 Local Pressure Drop

The local pressure drop is defined as the irreversible pressure loss associated with an area change such as the orifice, lower tie-plate, and spacers of a fuel assembly.

The general local pressure drop model is similar to the friction pressure drop and is given by:

$$\Delta P_L = \frac{w^2}{2g\rho} \frac{K}{A^2} \phi_{\text{TPL}}^2 \quad (4.4-2)$$

where:

- ΔP_L = local pressure drop, psi;
- K = local pressure drop loss coefficient;
- A = reference area for local loss coefficient; and
- ϕ_{TPL}^2 = two-phase local multiplier

and w, g, and ρ are defined the same as for friction. This basic calculation is similar to that used throughout the nuclear power industry. The formulation for the two-phase multiplier is similar to that reported in the open literature (Reference 4) with the addition of empirical constants to adjust the results to fit data taken at General Electric Company for the specific designs of the BWR fuel assembly.

4.4.2.6.3 Elevation Pressure Drop

$$\Delta P_E = \bar{\rho} \Delta L; \bar{\rho} = \rho_f (1 - \bar{\alpha}) + \rho_g \bar{\alpha} \quad (4.4 - 3)$$

LSCS-UFSAR

The elevation pressure drop is based on the well-known relationship where:

$$\begin{aligned} \Delta P_E &= \text{elevation pressure drop, psi;} \\ \Delta L &= \text{incremental length;} \\ \bar{\rho} &= \text{average coolant density;} \\ \bar{\alpha} &= \text{average void fraction over length } -L; \text{ and} \\ \rho_f, \rho_g &= \text{saturated water and vapor density, respectively.} \end{aligned}$$

4.4.2.6.4 Acceleration Pressure Drop

A reversible pressure change occurs when an area change is encountered, and an irreversible loss occurs when the fluid is accelerated through the boiling process. The basic formulation for the reversible pressure change resulting from a flow area change is given by:

$$\Delta P_{ACC} = (1 - \sigma^2) \frac{w^2}{2g\rho A_2^2}; \quad \sigma = \frac{A_2}{A_1} \quad (4.4-4)$$

where:

$$\begin{aligned} \Delta P_{ACC} &= \text{acceleration pressure drop,} \\ A_2 &= \text{final flow area, and} \\ A_1 &= \text{initial flow area} \end{aligned}$$

and other terms are as previously defined. The basic formulation for the acceleration pressure change due to density change is:

$$\Delta P_{ACC} = \frac{w^2}{g A_{ch}^2} \left[\left(\frac{1}{\rho_M} \right)_{OUT} - \left(\frac{1}{\rho_M} \right)_{IN} \right] \quad (4.4 - 5)$$

where:

$$\frac{1}{\rho_M} = \frac{x^2}{\rho_g \alpha} + \frac{(1-x)^2}{\rho_f (1-\alpha)},$$

ρ_M = momentum density, and
 x = steam quality

and other terms are as previously defined. The total acceleration pressure drop in boiling water reactors is on the order of a few percent of the total pressure drop.

4.4.2.7 Correlation and Physical Data

The General Electric Company has obtained substantial amounts of physical data in support of the pressure drop and thermal hydraulic loads discussed in Subsection 4.4.2.6. Correlations have been developed to fit this data to the formulations discussed.

Subsection 4.4.2.7.1 through 4.4.2.7.3 describe the thermal hydraulic correlations used by GE for the initial core. FANP has also qualified their thermal hydraulic correlations for use in calculating pressure drop, void fraction, and heat transfer in References 14 and 15.

4.4.2.7.1 Pressure Drop Correlations

The General Electric Company has taken significant amounts of friction pressure drop data in multirod geometries representative of modern BWR plant fuel bundles and correlated both the friction factor and two-phase multipliers on a best fit basis using the pressure drop formulations reported in Subsections 4.4.2.6.1 and 4.4.2.6.2. Tests are performed in single-phase water to calibrate the orifice and the lower tie-plate, and in both single- and two-phase flow to arrive at best fit design values for spacer and upper tie-plate pressure drop.

The range of test variables is specified to include the range of interest to boiling water reactors. New data are taken whenever there is a significant design change to ensure the most applicable methods are in use at all times.

Applicability of the single-phase and two-phase hydraulic models discussed in Subsections 4.4.2.6.1 and 4.4.2.6.2 is confirmed by prototype (64-rod bundle) flow tests. The typical range of the test data is summarized in Table 4.4-5.

4.4.2.7.2 Void Fraction Correlation

The void fraction correlation is similar to models used throughout the nuclear power industry and includes effects of pressure, flow direction, mass velocity, quality, and subcooled boiling.

4.4.2.7.3 Heat Transfer Correlation

The Jens-Lottes (Reference 5) heat transfer correlation is used in fuel design to determine the cladding-to-coolant heat transfer coefficient for nucleate boiling.

4.4.2.8 Thermal Effects of Operational Transients

The evaluation of the core's capability to withstand the thermal effects resulting from anticipated operational transients is covered in Chapter 15 and Appendix G.

In summary, all transients due to normal operation and to single operator error or equipment malfunction result in MCPR greater than the transient MCPR limit.

4.4.2.9 Uncertainties in Estimates

Uncertainties in thermal-hydraulic parameters are considered in the statistical analysis which is the basis for setting the transient MCPR limit such that at least 99.9% of the fuel rods in the core are expected not to experience boiling transition during any abnormal operating transient. The statistical model and analytical procedure are described in detail in References 1 and 11. The uncertainties considered and their input values for the analysis are given in References 1 and 11. For FANP fuel, the statistical models and the methodology for calculating the MCPR safety limit are described in References 16, 17, 21, 25 and 26.

4.4.2.9.1 Transition Boiling Uncertainties

The fuel cladding employed for the nuclear fuel is Zircaloy. This material is selected primarily for its nuclear properties. Zircaloy also has good corrosion and strength properties at normal operating conditions. However, continued operation at the elevated temperatures possible in the transition and film boiling regimes could cause gradual reduction in strength and accelerated corrosion, resulting in damage to the cladding.

The boiling transition does not necessarily correspond to the fuel damage threshold, especially in the high steam-quality range. Boiling transition is identified as the heat transfer rate below which cladding overheating does not occur. Damage would not actually occur until well into the film boiling regime. For example, during inpile tests (Reference 6), Zircaloy-clad uranium dioxide fuel was purposely operated at heat transfer rates well into film boiling for a total time exceeding 5 minutes, then operated at typical boiling water reactor conditions for 10 days. Post-irradiation examination showed evidence of overheating but no cladding failure. To ensure good performance and long life of the cladding, conservative limits have been established to ensure that normal operations remain well below the transition boiling regime.

4.4.2.9.2 Variation of Fuel Damage Limit

Incipient center melting of the uranium dioxide pellet occurs at a higher kW/ft than the peak LHGR during any abnormal operating transient. If UO₂ center melting occurs and the molten uranium dioxide is redistributed and densified, the damage limit for strain can reduce to a lower value. The redistribution and densification phenomena are functions of time and temperature. Plant transients of short duration in the molten range do not result in appreciable redistribution or densification. For the plant events that meet the transient MCPR limit, there is no appreciable change in the kW/ft damage limit.

4.4.2.9.3 Effects of Misoriented Fuel Bundle

The concern with a misoriented assembly is primarily that the redistribution of power among the fuel pins could lead to higher local powers than indicated by the core monitoring system. In addition, a misorientation could lead to slightly higher assembly powers as well. A detailed description of this evaluation may be found in section 15.4.7.

4.4.2.10 Flux Tilt Considerations

For flux tilt considerations, refer to Subsection 4.3.2.2.7.

4.4.3 Description of the Thermal and Hydraulic Design of the Reactor Coolant System

The thermal and hydraulic design of the reactor coolant system is described in this subsection.

4.4.3.1 Plant Configuration Data

The descriptive summary of the reactor coolant system is given in Section 5.1. That overview describes the reactor coolant pressure boundary and the reactor coolant equipment used for the various coolant requirements encountered in both normal and abnormal operations. The engineered safety functions are described in Chapter 6.0 with system details and analysis shown there. The reactor recirculation loops are described in detail in Subsection G.2.3 of Appendix G; The main steam and feedwater systems are treated in Section 5.4. Plant configuration data are included in these chapters.

Table 4.4-7 provides the flow path length, height, liquid level, minimum elevations, and minimum flow areas for each major flow path volume within the reactor vessel and recirculation loops of the reactor coolant system. Table 4.4-8 provides the lengths and sizes of all safety injection lines to the reactor coolant system.

4.4.3.2 Operating Restrictions on Pumps

See Subsection G.2.2 of Appendix G.

4.4.3.3 Power-Flow Operating Map

See Subsection G.2.3 of Appendix G.

4.4.3.4 Temperature-Power Operating Map (PWR)

Not applicable.

4.4.3.5 Load-Following Characteristics

See Subsection G.2.4 of Appendix G.

4.4.3.6 Thermal and Hydraulic Characteristics Summary Table

A summary of the thermal and hydraulic characteristics of the reactor coolant system for the initial core and the initial cores of other reactors of similar design is included in Table 4.4-1.

4.4.4 Evaluation

The thermal-hydraulic design of the reactor core and reactor coolant system is based upon an objective of no fuel damage during normal operation or during abnormal operational transients. This design objective is demonstrated by analysis in the following sections.

4.4.4.1 Critical Heat Flux

Table 4.4-1 provides data on maximum heat flux, average heat flux, heat transfer areas, and other parameters affecting heat transfer of the initial core. The concept of critical heat flux has been used in the determination of operationally significant power distribution constraints. These are given in terms of the linear heat generation rate and minimum critical power ratio as discussed in the following subsections.

4.4.4.2 Core Hydraulics

See Subsection G.2.3 of Appendix G.

4.4.4.3 Influence of Power Distribution

The design constraints imposed by the maximum average planar linear heat generation rate, the core power density, and the local peaking factor limit the gross

peaking factor (radial x axial). There are many combinations of radial and axial peaking factors that satisfy this design constraint, but each will have a different effect on the MCPR. In general, the MCPR decreases as the radial peaking (bundle power) increases and as the axial peak location moves to the top of the core. For example, for a 1.96 gross factor, a flat (1.0) axial and a 1.96 radial would give a relatively low CPR, whereas a 1.0 radial and a 1.96 axial peaked in the bottom of the core would give a relatively high CPR. These extremes are obviously not suited to design because they are not representative of realistic reactor behavior. Therefore, the design radial peaking factor is selected higher than that likely to be encountered in reactor operation, and the combination of this radial with the design axial profile is also more limiting than that expected during operating conditions.

4.4.4.4 Core Thermal Response

The thermal response of the core evaluated for expected transient conditions is covered in Chapter 15. All expected abnormal operational transients are conservatively evaluated to ensure that the integrity of the vessel and fuel is not compromised. These transients are analyzed at varying power and flow conditions within the analyzed power-to-flow map.

4.4.4.5 Analytical Methods

The analytical methods, thermodynamic data, and hydrodynamic data used in determining the thermal and hydraulic characteristics of the core are similar to those used throughout the nuclear power industry.

Core thermal-hydraulic analyses are performed with the aid of a digital computer program. This program models the reactor core through a hydraulic description of orifices, lower tie-plates, fuel rods, fuel rod spacers, upper tie-plates, fuel channel, and the core bypass flow paths.

The methods discussed in section 4.4.4.5.1 through 4.4.4.5.3 describe the analytical methods for GE. However, the descriptions below are typical for the nuclear industry. These descriptions apply generally to FANP methods. Further detailed descriptions of FANP methods can be found in References 14, 17, 25 and 26.

4.4.4.5.1 Reactor Model

The orifice, lower tie-plate, fuel rod spacers, and upper tie-plate are hydraulically represented as being separate, distinct local losses of zero thickness. The fuel channel cross section is represented by a square section with enclosed area equal to the unrodded cross-sectional area of the actual fuel channel. The fuel channel assembly consists of three basic axial regions. The first and most important is the active fuel region which consists of the fuel rods, nonfueled rods, and fuel-rod spacers. The second is the nonfueled region consisting of nonfueled rods and the upper tie-plate.

LSCS-UFSAR

The third region represents the unrodded portion of the fuelchannel above the upper tie-plate. The active fuel region is considered in independent axial segments or nodes over which fuel thermal properties are assumed constant and coolant properties are assumed to vary linearly. The code can handle 12 fuel channel types and 10 types of bypass flow paths. In normal analyses the fuel assemblies are modeled by four channel types--a hot central orifice region channel type, an average central orifice region channel type, a hot peripheral orifice region type and an average peripheral orifice region type. Usually there is one fuel assembly representing each of the hot types. The average types then make up the balance of the core.

The computer program iterates on flow through each flow path (fuel assemblies and bypass paths) until the total differential pressure (plenum to plenum) across each path is equal, and the sum of the flows through each path equals the total core flow.

Orificing is selected to optimize the core flow distribution between orifice regions as discussed in Subsection 4.4.2.5. The core design pressure is determined from the required turbine throttle pressure, the steamline pressure drop, steam dryer pressure drop, and the steam separator pressure drop. The core inlet enthalpy is determined from the reactor and turbine heat balances. The core power distribution is determined as per Subsection 4.4.2.3. The required core flow is then determined by applying the procedures of this section and specifications such that the thermal limits of Reference 11 are satisfied and the nominal expected bypass flow fraction is approximately 10%. The results of applying these methods and specifications are:

- a. flow for each bundle type,
- b. flow for each bypass path,
- c. core pressure drop,
- d. fluid property axial distribution for each bundle type, and
- e. CPR calculations for each bundle type.

4.4.4.5.2 System Flow Balances

The basic assumption used by the code in performing the hydraulic analysis is that the flow entering the core will divide itself between the fuel bundles and the bypass flow paths such that each assembly and bypass flow path experience the same pressure drop.

The bypass flow paths considered are described in Table 4.4-9 and shown in Figure 4.2-2. Due to the large flow area, the pressure drop in the bypass region above the core plate is essentially all elevation head. Thus, the sum of the core plate differential pressure and the bypass region elevation head is equal to the core differential pressure.

The total core flow less the control rod cooling flow enters the lower plenum through the jet pumps. A fraction of this passes through the various bypass paths. The remainder passes through the orifice in the fuel support (experiencing a pressure loss) where more flow is lost through the fit-up between the fuel support and the lower tie-plate into the bypass region. The majority of the flow continues through the lower tie-plate (experiencing a pressure loss) where some flow is lost through the flow path defined by the fuel channel and lower tie-plate, and restricted by the finger springs, into the bypass region.

The flow through the bypass flow paths are expressed by the form:

$$W = C_1 \Delta P^{1/2} + C_2 \Delta P^C + C_3 \Delta P^2 \quad (4.4 - 6)$$

Full scale tests have been performed to establish the flow coefficients for the major flow paths. These tests simulate actual plant configurations which have several parallel flow paths and, therefore, the flow coefficients for the individual paths could not be separated. However, analytical models of the individual flow paths were developed as an independent check of the tests. The models were derived for actual BWR design dimensions and considered the effects of dimensional variations. These models predicted the test results when the "as-built" dimensions were applied. When using these models for hydraulic design calculations, nominal drawing dimensions are used. This is done to yield the most accurate prediction of the expected bypass flow. With the large number of components in a typical BWR core, deviations from the nominal dimensions will tend to statistically cancel, resulting in a total bypass flow best represented by that calculated using nominal dimensions.

The balance of the flow enters the fuel bundle from the lower tie plate and passes through the fuel rod channel spaces. A small portion of the in-channel flow enters the non-fueled rod through orifice holes just above the lower tie-plate. This flow, normally referred to as the water-rod flow, remixes with the active coolant channel flow below the upper tie-plate.

4.4.4.5.3 System Heat Balances

Within the fuel assembly, heat balances on the active coolant are performed nodally. Fluid properties are expressed as the bundle average at the particular node of interest and are based on Reference 7. In evaluating fluid properties a constant pressure model is used.

The core power is divided into two parts: an active coolant power and a bypass flow power. The bypass flow is heated by neutron-slowing down and gamma heating in the water and by heat transfer through the channel walls. Heat is also transferred to the bypass flow from structures and control elements which are themselves heated by gamma absorption and by (n, α) reactions in the control material. The fraction of total reactor power deposited in the bypass region is very nearly 2%. A similar phenomena occurs with the fuel bundle to the active coolant and the water rod flows. The net effect is that approximately 96% of the core power is conducted through the fuel cladding and appears as heat flux.

The power is allocated to the individual fuel bundles using a relative power factor. The power distribution along the length of the fuel bundle is specified with axial power factors which distribute the bundle's power among the axial nodes. A nodal location power or peaking factor is used to establish the peak heat flux at each nodal location. Relative, axial, and local peaking factors are more thoroughly discussed in Subsection 4.3.2.

The relative (radial) and axial power distributions when used with the bundle flow determine the axial coolant property distribution resulting in sufficient information to calculate the pressure drop components within each fuel assembly type. Once the equal pressure drop criterion has been satisfied, the critical bundle power (the power which would result in critical quality existing at some point in the bundle using the correlation expressed in References 1 and 11) is determined by an iterative process for each fuel type.

In applying the above methods to core design, the number of bundles (for a specified core thermal power) and bundle geometry (8 x 8, rod diameter, etc.) are selected based on power density and linear heat generation rate limits.

4.4.4.5.4 Uncertainties in Design Analyses

The effects of uncertainties in design values and on calculational results are accounted for in the statistical analysis on which the MCPR limits are based.

4.4.4.6 Reactor Stability Analysis

4.4.4.6.1 Introduction

There are many definitions of stability, but for feedback processes and control systems it can be defined as follows: a system is stable if, following a disturbance, the transient settles to a steady, noncyclic state.

A system may also be acceptably safe even if oscillatory, provided that any limit cycle of the oscillations is less than a prescribed magnitude. Instability then, is either a continual departure from a final steady-state value or greater-than-prescribed limit cycle about the final steady-state value.

The mechanism for instability can be explained in terms of frequency response. Consider a sinusoidal input to a feedback control system which for the moment has the feedback disconnected. If there were no time lags or delays between input and output, the output would be in phase with the input. Connecting the output so as to subtract from the input (negative feedback or 180° out-of-phase connection) would result in stable closed loop operation. However, natural laws can cause phase shift between output and input and should the phase shift reach 180°, the feedback signal would be reinforcing the input signal rather than subtracting from it. If the feedback signal were equal to or larger than the input signal (loop gain equal to one or greater), the input signal could be disconnected and the system would continue to oscillate. If the feedback signal were less than the input signal (loop gains less than one), the oscillations would die out.

The design of the BWR is based on the premise that power oscillations can be readily detected and suppressed.

4.4.4.6.2 Description

Three types of stability considered in the design of boiling water reactors are (1) reactor core (reactivity) stability, (2) channel hydrodynamic stability, and (3) total system stability. Reactivity feedback instability of the reactor core could drive the reactor into power oscillations. Hydrodynamic channel instability could impede heat transfer to the moderator and drive the reactor into power oscillations. The total system stability considers control system dynamics combined with basic process dynamics. The criteria is demonstrated if it is analytically demonstrated that no divergent oscillation develops within the system as a result of calculated step disturbances of any critical variable, such as steam flow, pressure, neutron flux, and recirculation flow, or that the divergent oscillation can be detected and suppressed.

Stability is expressed in terms of two compatible parameters. First is the decay ratio x_2/x_0 , designated as the ratio of the magnitude of the second overshoot to the first overshoot resulting from a step perturbation. A plot of the decay ratio is a graphic representation of the physical responsiveness of the system, which is readily evaluated in a time-domain analysis. Second is the damping coefficient ζ_n , the definition of which corresponds to the pole pair closest to the $j\omega$ axis in the s-plane for the system closed loop transfer function. This parameter also applies to the frequency-domain interpretation. The damping coefficient is related to the decay ratio as shown in Figure 4.4-1.

4.4.4.6.3 Solution Description for Thermal-Hydraulic Stability

BWR cores may exhibit thermal-hydraulic instabilities in certain portions of the core power and recirculation flow operating domain. The instabilities and the solutions devised to detect and suppress them are discussed in Reference 22 and 23. |

LSCS-UFSAR

LSCS has adopted the solution Option III, designated as the Oscillation Power Range Monitor (OPRM). The OPRM complies with GDC-12, as discussed in Section 3.1.2.2.3.

The overall design philosophy of the OPRM is to generate an alarm in the control room if it detects core instabilities (based on period-based algorithm only), and to generate an automatic suppression system trip if the instabilities reach an amplitude that could threaten the fuel safety limits.

The overall objective of the oscillation detection algorithm is to reliably detect expected instabilities at a low magnitude such that mitigation can occur well before the MCPR Safety Limit is exceeded, while avoiding spurious trips during expected neutron flux transients. The algorithm is based on the detection of the three known characteristics that BWR neutron flux oscillations exhibit. These characteristics are the amplitude or absolute magnitude, growth rate, and periodic behavior. Only the period based detection algorithm is used in the safety analysis. The other algorithms provide defense in depth and additional protection against unanticipated oscillations. Details of the algorithm can be found in References 22 and 23.

The OPRM consists of a microprocessor that analyzes signals from LPRMs. Since LPRMs are evenly distributed throughout the reactor core, they are capable of responding to any neutron flux oscillations that can create an MCPR concern. Individual LPRMs readily respond to a wide variety of normal operating maneuvers and expected events, and are also subject to electrical interference. For these reasons, each OPRM may use multiple LPRMs as a means of maintaining a strong response to a neutron flux oscillation while minimizing the susceptibility to false signals associated with a single LPRM, or may utilize a detection algorithm designed to achieve the same objective. The OPRM is automatically bypassed at high flow or low power conditions, where core instabilities are unlikely to occur, to avoid spurious actuation.

4.4.4.6.4 Stability Criteria

The following discussion on stability is based on the original design bases, which did not assume an inherent tendency towards oscillations. They are presented here for historic perspective. The new design, in compliance with the NRC Generic Letter 94-02, is based on the detection and suppression methodology, and is discussed above in Section 4.4.4.6.3.

Stability criteria are established to demonstrate compliance with the requirements set forth in 10CFR50 Appendix A, General Design Criterion (GDC) 12.

These stability compliance criteria consider potential limit cycle response within the limits of safety system and/or operator intervention and the OPRM assures that for BWR fuel designs this operating mode does not result in specified acceptable

LSCS-UFSAR

fuel design limits being exceeded. The onset of power oscillations for which corrective actions are necessary is reliably and readily detected and suppressed by operator actions and/or automatic system functions.

To ensure compliance of the GE BWR design with GDC 12 requirements, the following stability acceptance criteria have been established.

- (1) Neutron flux limit cycles which oscillate up to the 120% APRM high neutron flux scram set point or up to the LPRM upscale alarm trip (without initiating scram) prior to operator mitigating action, shall not result in exceeding specified acceptable fuel design limits.
- (2) The individual channels shall be designed and operated to be hydrodynamically stable or more stable than the reactor core for all expected operating conditions.

Calculations which predict that core-wide limit cycles will not occur (decay ratio < 0.8) also demonstrate compliance with GDC-12.

This criteria is presently used for LSCS two recirculation loop operation. For single recirculation loop operation, the plant is monitored per General Electric SIL-380 (Reference 8).

These criteria shall be satisfied for all attainable conditions of the reactor that may be encountered in the course of plant operation. For stability purposes, the most severe conditions to which these criteria will be applied correspond to natural circulation flow at a power corresponding to the extrapolated APRM rod block intercept condition.

The licensing basis is to generate a trip signal during oscillations of sufficiently low amplitude to provide margin to the MCPR safety limits for all expected modes of BWR oscillations. The OPRM oscillation recognition algorithm is intended to discriminate between true stability-related neutron flux oscillations and other flux variations that may be expected during plant operation. Extensive evaluation of operating plant data is done to determine the combination of algorithm and OPRM setpoints, which meet the design objectives. The final algorithm/setpoint design is subjected to in-plant testing with the trip function disabled.

The OPRM assures that for BWR fuel designs, this operating mode does not result in specified acceptable fuel design limits being exceeded. The onset of power oscillations for which corrective actions are necessary is reliably and readily detected and suppressed by operator actions and/or automatic system functions.

4.4.4.6.5 Expected Oscillation Modes

The OPRM is capable of responding to the expected modes of BWR stability-related oscillations. The expected oscillation modes are as follows (Reference 13, Section 6.1):

- Core-wide, in which the average neutron flux in all fuel assemblies oscillates in phase.
- First Order Side-by-Side or a regional oscillation where the neutron flux on one side of the reactor oscillates 180° out of phase with the flux on the other side.
- First Order Precession a regional oscillation where the axis of zero oscillation amplitude rotates azimuthally, or the two reactor regions of peak oscillation amplitude shift from one location to another at a frequency lower than the oscillation frequency.

Other modes of oscillation are not expected in a BWR.

4.4.4.6.6 Analysis Approach

The total system stability analysis evaluates the relative stability of the total system, from time responses generated by applying step changes to the input variables to the total system stability model. The observed time response of an output variable of a high order dynamic system represents a superposition of the system's several response modes. The relative intensity of each particular mode in the time response is determined by the zeroes (the roots of the numerator) of the transfer function relating a given output variable to a particular input. Therefore, in judging the relative stability of the system, the observer should separate the distinct modes in the time response and apply the stability criterion to each modal response. The approach used here, of disturbing one input variable and applying the stability criterion to the resulting system response is a good approximation to modal separation. It is particularly applicable in calculating stability since, as a system tends toward instability a single oscillatory mode tends to dominate the observed time response (Reference 9).

Reference 15 describes the process used to calculate a conservative final MCPR value for an anticipated stability-related oscillation. It involves the determination of initial MCPR by a cycle-specific evaluation and the calculation of hot bundle oscillation magnitude. The licensing criterion is met when the final MCPR is greater than the MCPR safety limit. Appropriate reload parameters are checked every cycle to determine the initial MCPR. This methodology provides a conservative means of demonstrating with a high probability and confidence that the MCPR safety limits will not be violated for anticipated oscillations. The use of the MCPR safety limit to provide protection against possible fuel damage is exceedingly conservative (Reference 24, Section 4.5.2).

4.4.4.6.7 Mathematical Model

This mathematical model applies to the initial core analysis. The mathematical model representing the core examines the linearized reactivity response of a reactor system with density-dependent reactivity feedback caused by boiling. In addition, the hydrodynamics of various hydraulically coupled reactor channels or regions are examined separately on an axially multinoded basis by grouping various channels that are thermodynamically and hydraulically similar. This interchannel hydrodynamic interaction or coupling exists through pressure variations in the inlet plenum, such as can be caused by disturbances in the flow distribution between regions or channels. This approach provides a reasonably accurate, three-dimensional representation of the reactor's hydrodynamics.

The core model, shown in block diagram form in Figure 4.4-2, solves the dynamic equations that represent the reactor core in the frequency domain. From the solution of these dynamic equations, the reactivity and individual channel hydrodynamic stability of the boiling water reactor is determined for a given reactor flow rate, power distribution, and total power. This gives the most basic understanding of the inherent core behavior (and hence the system behavior) and is the principal consideration in evaluating the stable performance of the reactor. As

new experimental or reactor operating data are obtained, the model is refined to improve its capability and accuracy.

The plant model considers the entire reactor system, neutronics, heat transfer, hydraulics, and the basic processes, as well as associated control systems such as the flow controller, pressure regulator, feedwater controller, etc. Although the control systems may be stable when analyzed individually, final control system settings must be made in conjunction with the operating reactor so that the entire system is stable. The plant model yields results that are essentially equivalent to those achieved with the core model and allows the addition of the controllers, which have adjustable features permitting the attainment of the desired performance.

The plant model solves the dynamic equations that present the BWR system in the time domain. The variables, such as steam flow and pressure, are represented as a function of time. The extensiveness of this model (Reference 10) is shown in block diagram form in Figure 4.4-3. Many of the blocks are extensive systems in themselves. The model is periodically refined as new experimental or reactor operating data are obtained to improve its capability and accuracy.

4.4.4.6.8 Initial Core Analysis Results

The results of the two recirculation pump operation core and channel stability analysis is given in the Reload Licensing Package for each cycle. The plant stability analysis is performed only for the initial core and is described below.

The plant stability analysis was performed by assuming that the reactor is initially operating at the most sensitive condition, corresponding to natural circulation flow and a power level at the rod block limit. The nuclear system is then subjected to step disturbances from control rods, pressure regulator setpoint, and level controller setpoint. These time responses are shown in Figures 4.4-6 through 4.4-8. It is clear that the decay ratio is less than the stability criterion.

For expected normal operating modes, the time response of each of the important variables of the reactor system (neutron flux, pressure, and steam flow) to small step disturbances can be underdamped, but must analytically show a decay ratio of less than 0.25 in order to satisfy the operational design guide limit. Using final design parameters each of the following disturbances are analytically imposed, one at a time, using the model previously described for time domain analysis:

- a. a pressure setpoint change of at least 5 psi,
- b. a control rod position change equivalent to a local power change of at least 5% of point (of the magnitude of power at the time of the disturbance),

LSCS-UFSAR

- c. a load demand change of at least 5% of point, and
- d. a reactor water level setpoint change of at least 6 inches.

Using actual design parameters, calculated responses of important nuclear system variables to step disturbances from control rod reactivity, pressure regulator setpoint, level controller setpoint, and turbine load setpoint are tested for rated power-flow conditions and at the nominal power corresponding to the lower end of the automatic power-flow control path.

Results of the analysis for 105% rated power and 100% rated flow are shown in Figures 4.4-9 through 4.4-12. It is evident that the response meets the stability criterion. Figures 4.4-13 through 4.4-16 show the results of analysis at the low limit of the automatic flow-control range.

It is concluded that for all normal operating points over the flow-control range the decay ratio of the total system responses is less than one-fourth, good dynamic performance is expected, and the ratio conforms with the stability criterion.

4.4.5 Testing and Verification

See Subsection G.4.3 of Appendix G.

The OPRM, which is installed to detect and suppress thermal-hydraulic Instabilities, is extensively tested using available data from several BWR plants. After installation, the plant is operated for a period of time with the OPRM trip function disabled while OPRM performance is monitored for susceptibility to spurious trips. The OPRM trip function is enabled following approval of the associated Technical Specification.

4.4.6 Instrumentation Requirements

See Subsections 7.7.3.2 and 7.6.3.4 of Chapter 7.

4.4.6.1 Loose Parts Monitoring System

(Deleted)

This page intentionally left blank.

|

4.4.7 References

1. "General Electric BWR Thermal Analysis Basis (GETAB): Data, Correlation, and Design Application," January 1977 (NEDE-10958-PA and NEDO-10958A).
2. "Core Flow Distribution in a Modern Boiling Water Reactor as Measured in Monticello," NEDO-10299, AEC Topical Report NEDO-10299, January 1971.
3. R. C. Martinelli and D. E. Nelson, "Prediction of Pressure Drops During Forced Connection Boiling of Water," ASME Trans., 70, pp. 695-702, 1948.
4. C. J. Baroozy, "A Systematic Correlation for Two-Phase Pressure Drop," Heat Transfer Conference, Preprint No. 37, AICLE, Los Angeles, 1966.
5. W. H. Jens and P. A. Lottes, "Analysis of Heat Transfer, Burnout, Pressure Drop, and Density Data for High Pressure Water," USAEC Report - 4627, 1972.

LSCS-UFSAR

6. S. Levy et al., "Experience with BWR Fuel Rods Operating Above Critical Flux," Nucleonics, April 1965.
7. 1967 International Standard Steam Water Properties.
8. General Electric Service Information Letter (SIL) No. 380, "BWR Core Thermal Hydraulic Stability," Rev. 1, dated February 10, 1984.
9. Zadeh and Desoer, "Linear System Theory," McGraw-Hill Book Co., 1963.
10. "Analytical Methods of Plant Transient Evaluations for General Electric Boiling Water Reactor," NEDO-10802, General Electric Company, BWR Systems Department, February 1973.
11. "General Electric Standard Application for Reactor Fuel," NEDE-P-A, (Latest approved revision).
12. GE Document, "SAFER/GESTR-LOCA, Loss-of-Coolant Accident Analysis, LaSalle County Station Units 1 & 2," NEDC-31510P, as amended & revised.
13. Cycle specific Fuel Design Report (FANP fuel only).
14. Exxon Nuclear Methodology for Boiling Water Reactors: THERMEX Thermal Limits Methodology, Summary Description, XN-NF-80-19(A), Volume 3, Revision 2, Exxon Nuclear Company, Inc., Richland, WA (January 1987).
15. Generic Mechanical Design Criteria for BWR Fuel Design, ANF-89-98(P)(A), Revision 1 and Supplement 1, Advanced Nuclear Fuels Corporation, Richland, WA (May 1995).
16. Advanced Nuclear Fuels Critical Power Methodology for Boiling Water Reactors, ANF-524(P)(A), Revision 2 and Supplements, Advanced Nuclear Fuels Corporation, November 1990.
17. ANFB Critical Power Correlation, ANF-1125 (P)(A) and Supplements 1 and 2, Advanced Nuclear Fuels Corporation, April 1990; ANFB Critical Power Correlation Application for Co-Resident Fuel, EMF-1125(P)(A), Supplement 1, Appendix C, Siemens Power Corporation, August 1997; and ANFB Critical Power Correlation Determination of ATRIUM-9B Additive Constant Uncertainties, ANF-1125(P)(A) Supplement 1, Appendix E, Siemens Power Corporation, September 1998.

LSCS-UFSAR

18. Siemens Power Corporation Methodology for Boiling Water Reactors: Evaluation and Validation of CASMO-4 / MICROBURN-B2 EMF-2158(P)(A) Revision 0, Siemens Power Corporation, October 1999.
19. Exxon Nuclear Methodology for Boiling Water Reactors - Neutronic Methods for Design and Analysis, XN-NF-80-19(P)(A) Volume 1 and Supplements 1 and 2, Exxon Nuclear Company, March 1983.
20. BWR Jet Pump Model Revision for RELAX, ANF-91-048(P)(A), Supplements 1 and 2, Siemens Power Corporation, October 1997.
21. MICROBURN-B2 Based Impact of Failed / Bypassed LPRMs and TIPs, Extended LPRM Calibration Interval, and Single Loop Operation Measured Radical Bundle Power Uncertainty, EMF-2493(P) Revision 0, Siemens Power Corporation, December 2000.
22. NEDO-31960, "BWR Owners Group Long-Term Stability Solutions Licensing Methodology," June 1991.
23. NEDO 31960, "BWR Owners Group Long-Term Stability Solutions Licensing Methodology," Supplement 1, March 1992.
24. NEDO-32465-A, "BWR Owners' Group Reactor Stability Detect and Suppress Solution Licensing Basis Methodology and Reload Application," August 1996.
25. SPCB Critical Power Correlation, EMF-2209(P)(A) Revision 2, Siemens Power Corporation, September 2003.
26. Application of Siemens Power Corporation's Critical Power Correlation to Co-Resident Fuel, EMF-2245(P)(A), Revision 0, Siemens Power Corporation, August 2000.

LSCS-UFSAR

TABLE 4.4-1
(SHEET 1 OF 2)

THERMAL AND HYDRAULIC DESIGN CHARACTERISTICS
OF THE REACTOR CORE
(INITIAL CORE DATA)

	<u>238-732</u> BWR/6	<u>218-592</u> BWR/6	<u>218-560</u> ZPS-1	<u>251-764</u> WPPSS NP No. 2	<u>251-784</u> BWR/6	<u>251-764</u> LSCS
<u>GENERAL OPERATING</u>						
<u>CONDITIONS</u>						
Reference design thermal output, MWt	3579	2894	2436	3323	3833	3323
Power level for engineered safety features, MWt	3758	3039	2550	3489	4025	3489
Steam flow rate, at 420° F final feedwater temperature, millions lb/hr	15.396	12.451	10.477	14.295	16.488	14.166
Core coolant flow rate, millions lb/hr	105.0	84.5	78.5	108.5	113.5	108.5
Feedwater flow rate, millions lb/hr	15.358	12.42	10.448	14.256	16.488	14.127
System pressure, nominal in steam dome, psia	1040	1040	1020	1020	1040	1020
System pressure, nominal core design, psia	1055	1055	1035	1035	1055	1035
Coolant saturation temperature at core design pressure, °F	551.1	551.1	548.8	548.8	551.1	548.8
Average power density, kW/liter	56	56	50.51	51.2	56.0	48.17
Specific power, kW/kg (U total)	25.9	25.9	23.7	23.7	25.9	23.7
Maximum thermal output, kW/ft	13.4	13.4	13.4	13.4	13.4	13.4
Average thermal output, kW/ft	6.04	6.04	5.45	5.45	6.04	5.33
Core total heat transfer area, ft ²	73,409	59,369	55,401	75,582	78,624	74,871
Maximum heat flux, Btu/hr-ft ²	354,000	354,000	354,000	354,000	354,000	361,000
Average heat flux, Btu/hr-ft ²	159,550	159,550	143,900	143,920	159,550	143,740

LSCS-UFSAR

TABLE 4.4-1
(SHEET 2 OF 2)

	<u>238-732</u> BWR/6	<u>218-592</u> BWR/6	<u>218-560</u> ZPS-1	<u>251-764</u> WPPSS NP No. 2	<u>251-784</u> BWR/6	<u>251-764</u> LSCS
<u>GENERAL OPERATING CONDITIONS</u>						
Core inlet enthalpy, at 420° F FFWT, Btu/lb	527.8	527.8	527.4	527.6	528.1	527.5
Core inlet temperature, at 420° F FFWT, °F	533.0	533.0	532.6	532.8	533.3	532.8
Core maximum exit voids within assemblies, %	76	76	75	75	76	76
Core average void fraction, active coolant	0.428	0.429	0.418	0.415	0.427	0.418
Active coolant flow area per assembly, in ²	15.50	15.50	15.50	15.50	15.50	15.82
Core average inlet velocity, ft/sec	7.2	7.2	7.0	7.1	7.2	6.77
Maximum inlet velocity, ft/sec	7.6	7.6	7.4	7.5	7.6	7.2
Total core pressure drop, psi	25.7	25.5	27.3	27.5	25.8	24.8
Core support plate pressure drop, psi	21.3	21.1	22.9	23.1	21.4	19.61
Average orifice pressure drop						
Central region, psi	8.6	8.5	11.2	11.4	8.7	8.13
Peripheral region, psi	17.3	17.2	19.6	19.8	17.5	16.66
Maximum channel pressure loading, psi	14.5	14.5	13.7	13.7	14.6	12.84
<u>TYPICAL POWER PEAKING FACTOR</u>						
Maximum relative assembly power	1.40	1.40	1.40	1.40	1.40	1.40
Local peaking factor	1.13	1.13	1.24	1.15	1.13	1.15
Axial peaking factor	1.40	1.40	1.40	1.40	1.40	1.40
Gross peaking factor	1.96	1.96	1.96	1.96	1.96	1.96
Total peaking factor	2.22	2.22	2.43	2.	2.22	2.25

LSCS-UFSAR

TABLE 4.4-2

TYPICAL VOID DISTRIBUTION*
(INITIAL CORE)

<u>NODE</u>	<u>CORE AVERAGE (AVERAGE NODE VALUE)</u>	<u>MAXIMUM CHANNEL (END OF NODE VALUE)</u>
Bottom 1	0.000	0.0
2	0.001	0.032
3	0.018	0.122
4	0.065	0.230
5	0.136	0.325
6	0.212	0.401
7	0.281	0.462
8	0.341	0.511
9	0.391	0.552
10	0.433	0.587
11	0.469	0.616
12	0.499	0.641
13	0.525	0.662
14	0.547	0.681
15	0.566	0.696
16	0.582	0.708
17	0.595	0.719
18	0.606	0.728
19	0.616	0.736
20	0.624	0.742
21	0.631	0.748
22	0.637	0.753
23	0.643	0.757
Top 24	0.647	0.761

* Core average value = 0.419
 Maximum exit value = 0.761
 Active fuel length = 150 inches

LSCS-UFSAR

TABLE 4.4-2a

AXIAL POWER DISTRIBUTION USED TO
GENERATE VOID AND QUALITY DISTRIBUTIONS (TYPICAL)

	<u>NODE</u>	<u>AXIAL POWER-FACTOR</u>
Bottom of core	1	0.54
	2	0.83
	3	1.02
	4	1.17
	5	1.26
	6	1.33
	7	1.37
	8	1.39
	9	1.40
	10	1.39
	11	1.38
	12	1.34
	13	1.29
	14	1.21
	15	1.10
	16	0.99
	17	0.89
	18	0.79
	19	0.71
	20	0.64
	21	0.58
	22	0.52
	23	0.46
Top of core	24	0.40

LSCS-UFSAR

TABLE 4.4-3
(SHEET 1 OF 2)

FLOW QUALITY DISTRIBUTION (TYPICAL)*

Core average value = 0.074
 Maximum exit value = 0.281
 Active fuel length = 150 inches

<u>NODE</u>	<u>CORE AVERAGE (AVERAGE NODE VALUE)</u>	<u>MAXIMUM CHANNEL (END OF NODE VALUE)</u>
BOTTOM 1	0.00	0.00
2	0.000	0.001
3	0.000	0.006
4	0.002	0.017
5	0.006	0.032
6	0.013	0.049
7	0.022	0.067
8	0.032	0.085
9	0.044	0.103
10	0.053	0.121
11	0.063	0.139
12	0.073	0.157
13	0.083	0.173
14	0.093	0.189
15	0.101	0.203
16	0.109	0.216
17	0.117	0.228
18	0.123	0.238
19	0.129	0.248
20	0.134	0.256
21	0.138	0.263

LSCS-UFSAR

TABLE 4.4-3
(SHEET 2 OF 2)

<u>NODE</u>	<u>CORE AVERAGE (AVERAGE NODE VALUE)</u>	<u>MAXIMUM CHANNEL (END OF NODE VALUE)</u>
22	0.142	0.270
23	0.146	0.276
TOP 24	0.150	0.281

* These flow quality distribution values are typical for the initial core. The GE9 and GE14 fuel has an active fuel length of 150 inches. The ATRIUM-9B and ATRIUM-10 fuel have an active fuel length of 149.0 inches. This design characteristic difference in combination with changes in power distribution and reactor core state produce different flow quality distributions. These differences are included in transient and core design methodology.

LSCS-UFSAR

TABLE 4.4-4

CORE FLOW DISTRIBUTION (TYPICAL)

<u>OFFICE ZONE</u> <u>DESCRIPTION</u>	<u>CENTRAL</u> <u>HOT</u>	<u>CENTRAL</u> <u>AVERAGE</u>	<u>PERIPHERAL</u> <u>HOT</u>	<u>PERIPHERAL</u> <u>AVERAGE</u>
Relative Assembly Power	1.4	1.04	0.95	0.70
Relative Assembly Flow	0.93	1.06	0.55	0.57

LSCS-UFSAR

TABLE 4.4-5

TYPICAL RANGE OF TEST DATA

<u>MEASURED PARAMETER</u>	<u>TEST CONDITIONS</u>
<u>ADIABATIC TESTS</u>	
Spacer single-phase loss coefficient	$N_{Re^*} = 0.5 \times 10^5$ to 3.5×10^5
Lower tie plate + orifice single-phase loss coefficient	$T = 100$ to 500°F
Upper tie plate single-phase friction factor	
Spacer two-phase loss coefficient	$P = 800$ to 1400 psia
Two-phase friction multiplier	$G = 0.5 \times 10^6$ to 1.5×10^6 lb/h-ft ²
	$X = 0$ to 40%
<u>DIABATIC TESTS</u>	
Heated bundle pressure drop	$P = 800$ to 1400 psia
	$G = 0.5 \times 10^6$ to 1.5×10^6 lb/h-ft ²

* Reynolds Number

LSCS-UFSAR

TABLE 4.4-6

THIS PAGE LEFT INTENTIONALLY BLANK.

TABLE 4.4-6

REV. 4 - APRIL 1988

LSCS-UFSAR

TABLE 4.4-7

REACTOR COOLANT SYSTEM GEOMETRICAL DATA

	FLOW PATH LENGTH (in.)	HEIGHT AND LIQUID LEVEL (in.)	ELEVATION OF BOTTOM OF EACH VOLUME* (in.)	MINIMUM FLOW AREAS (ft ²)
A. Lower Plenum	216	216 216	-172.5	71.5
B. Core	164	164 164	44	142.0
C. Upper Plenum and Separators	178	178	208	49.5
D. Dome (Above Normal Water Level)	312	312	386.0	343.5
E. Downcomer Area	321	321 321	-51.0	79.5
F. Recirculation Loops and Jet Pumps (one loop)	108.5 ft (one loop)	403	-394.5	132.5 in ²

*Reference point is recirculation nozzle outlet centerline.

LSCS-UFSAR

TABLE 4.4-8

LENGTHS AND SIZES OF SAFETY INJECTION LINES

	<u>LINE OD (inches)</u>	<u>LINE LENGTH (feet)</u>
I. HPCS Line		
A. Pump discharge to valve	16	146.0
B. Inside containment to RPV	12	101.5
Total		247.5
II. LPCI Lines		
A. Loop A		
1. Pump discharge to valve*	18/12	182.0
2. Inside containment to RPV	12	101.5
Total		283.5
B. Loop B		
1. Pump discharge to valve*	18/12	388.5
2. Inside containment to RPV	12	84.5
Total		473.0
C. Loop C		
1. Pump discharge to valve*	18	344.0
2. Inside containment to RPV	12	77.0
Total		421.0
III. LPCS Line		
A. Pump discharge to valve*	16	282.5
B. Inside containment to RPV	12	84.5
Total		367.0

* Valve located as near as possible to outside of containment wall.

LSCS-UFSAR

TABLE 4.4-9

BYPASS FLOW PATHS

<u>FLOW PATH DESCRIPTION</u>	<u>DRIVING PRESSURE</u>	<u>NUMBER OF PATHS</u>
1a. Between Fuel Support and the Control Rod Guide Tube (Upper Path)	Core Plate Differential	One/Control Rod
1b. Between Fuel Support and the Control Rod Guide Tube (Lower Path)	Core Plate Differential	One/Control Rod
2. Between Core Plate and the Control Rod Guide Tube	Core Plate Differential	One/Control Rod
3. Between Core Support and the Incore Support Instrument Guide Tube	Core Plate Differential	One/Instrument
4. Between Core Plate and Shroud	Core Plate Differential	One
5. Between Control Rod Guide Tube and Control Rod Drive Housing	Core Plate Differential	One/Control Rod
6. Between Fuel Support and Lower Tie-Plate	Channel Wall Differential Plus Lower Tie-Plate Differential	One/Channel
7. Control Rod Drive Coolant	Independent of of Core	One/Control Rod
8. Between Fuel Channel and Lower Tie-Plate	Channel Wall Differential	One/Channel
9. Holes in Lower Tie-Plate	Lower Tie-Plate/ Bypass Region Differential	Two/Assembly

4.5 REACTOR MATERIALS

4.5.1 Control Rod System Structural Materials

4.5.1.1 Material Specifications

The following material listing applies to the control rod drive mechanism supplied for this application. The position indicator and minor nonstructural items are omitted.

- a. Cylinder, Tube and Flange Assembly

Flange	ASME SA 182 Grade F304
Plugs	ASME SA 182 Grade F304
Cylinder	ASTM A269 Grade TP 304
Outer Tube	ASTM A269 Grade TP 304
Tube	ASTM A351 Grade CF-3
Spacer	ASTM A351 Grade CF-3

- b. Piston Tube Assembly

Piston Tube	ASTM A479 Grade XM-19
Stud	ASTM A276 Type 304
Head	ASME SA 182 Grade F304
Ind. Tube	ASME SA 312 Type 316
Cap	ASME SA 182 Grade F304.

- c. Drive Assembly

Coupling Spud	Inconel X-750
Index Tube	ASTM A479 Grade XM-19
Piston Head	Armco17-4 PH
Coupling	ASME SA 312 Grade TP 304 or ASTM A511 Grade MT 304
Magnet Housing	ASME SA 312 Grade TP 304 or ASTM A511 Grade MT 304.

- d. Collet Assembly

Collet Piston	ASTM A269 Grade TP 304 or ASME SA 312 Grade TP 304
Finger	Inconel X-750
Retainer	ASTM A260 Grade TP 304 or ASTM A511 Grade MT 304
Guide Cap	ASTM A269 Grade TP 304.

LSCS-UFSAR

e. Miscellaneous Parts

Stop Piston	ASTM A276 Type 304
Connector	ASTM A276 Type 304
O-Ring Spacer	ASME SA 240 Type 304
Nut	ASME SA 193 Grade B8
Barrel	ASTM A269 Grade TP 304 or ASME SA 312 Grade TP 304 or ASME SA 240 Type 304
Collet Spring	Inconel X-750
Ring Flange	ASME SA 182 Grade F304.

The materials listed under ASTM specification number are all in the annealed condition (with the exception of the outer tube in the cylinder, tube and flange assembly), and their properties are readily available. The outer tube is approximately 1/8 hard, and has a tensile of 90,000/125,000 psi, yield of 50,000/85,000 psi, and minimum elongation of 25%.

The coupling spud, collet fingers and collet spring are fabricated from Inconel X-750 in the annealed or equalized condition, and heat treated to produce a tensile of 165,000 psi minimum, yield of 105,000 psi minimum and elongation of 20% minimum. The piston head is Armco 17-4 PH in condition H-1100, with a tensile of 140,000 psi minimum, yield of 115,000 psi minimum and elongation of 15% minimum.

These are widely used materials, whose properties are well known. All have been successfully used for the past 10 to 15 years in similar drive mechanisms. The parts are readily accessible for inspection, and replaceable if necessary.

4.5.1.2 Special Materials

No cold worked austenitic stainless steels with a yield strength greater than 90,000 psi are employed in the control rod drive system. Hardenable martensitic stainless steels are not used. Armco 17-4 PH (precipitation hardened stainless steel) is used for the piston head. This material is aged to the H-1100 condition to produce resistance to stress corrosion cracking in the BWR environments. Armco 17-4 PH (H-1100) has been successfully used for the past 10 to 15 years in BWR drive mechanisms.

4.5.1.3 Processes, Inspections and Tests

All austenitic stainless steel used in the control rod drive system is solution annealed material with one exception, the outer tube in the cylinder, tube, and flange assembly (Subsection 4.5.1.1). Proper solution annealing is verified by

LSCS-UFSAR

testing per ASTM-A262, "Recommended Practices for Detecting Susceptibility to Intergranular Attack in Stainless Steels."

Two special processes are employed which subject selected components to temperatures in the sensitization range:

- a. The cylinder (cylinder, tube and flange assembly) and the retainer (collet assembly) are hard surfaced with Colmonoy 6.
- b. The following components are nitrided to provide a wear resistant surface:
 1. tube (cylinder, tube and flange assembly),
 2. piston tube (piston tube assembly),
 3. index tube (drive line assembly), and
 4. collet piston and guide cap (collet assembly).

Colmonoy hard surfaced components have performed successfully for the past 10 to 15 years in drive mechanisms. Nitrided components have accumulated 8 years of BWR service. It is normal practice to remove some control rod drives at each refueling outage. At this time, both the Colmonoy hard surfaced parts and nitrided surfaces are accessible for visual examination. In addition, dye penetrant examinations have been performed on nitrided surfaces of the longest service drives. This inspection program is adequate to detect any incipient defects before they could become serious enough to cause operating problems.

4.5.1.4 Control of Delta Ferrite Content

All Type 308 weld metal is purchased to a specification which requires a minimum of 5% delta ferrite. This amount of ferrite is adequate to prevent any microfissuring (hot cracking) in austenitic stainless steel welds.

4.5.1.5 Protection of Materials During Fabrication, Shipping and Storage

All the control rod drive parts listed previously (Subsection 4.5.1.1) are fabricated under a process specification which limits contaminants in cutting, grinding and tapping coolants and lubricants. It also restricts all other processing materials (marking inks, tape, etc.) to those which are completely removable by the applied cleaning process. All contaminants are then required to be removed by the appropriate cleaning process prior to any of the following:

- a. any processing which increases part temperature above 200° F,

LSCS-UFSAR

- b. assembly which results in decrease of accessibility for cleaning,
or
- c. release of parts for shipment.

The specification for packaging and shipping the control rod drive provides the following.

The drive is rinsed in hot deionized water and dried in preparation for shipment. The ends of the drive are then covered with a vapor-tight barrier with desiccant. Packaging is designed to protect the drive and prevent damage to the vapor barrier. The planned storage period considered in the design of the container and packaging is 2 years. This packaging has been qualified and in use for a number of years. Periodic audits have indicated satisfactory protection.

Site or warehouse storage specifications require inside heated storage comparable to level B of ANSI 45.2.2.

4.5.2 Reactor Internals Materials

4.5.2.1 Material Specifications

Materials used for steam dryer and core structure are as follows:

Plate, Sheet and Strip	ASTM A240 Type 304
Bolts	ASTM A193 Grade B8
Nuts	ASTM A194 Grade 8
Forgings	ASTM A182 Grade F304
Bar	ASTM A276 Type 304
Bar	ASTM A479 Type 304
Pipe	ASTM A312 Grade TP 304
Tube	ASTM A269, A249, or A213 Grade TP 304
Pipe Fittings	ASTM A403 Grade WPW 304 or WP 304
Pipe Fittings (cast)	ASTM A351 Grade CF8

The following materials are employed in other reactor internal structures:

- a. Steam Separator. All materials are Type 304, 304L, or 316L stainless steel

Plate, Sheet and Strip	ASTM A240, Type 304
---------------------------	---------------------

LSCS-UFSAR

Forgings	ASTM A182, Grade F304
Bars	ASTM A479 Type 304
Pipe	ASTM A312 Grade TP 304
Tube	ASTM A269 Grade TP 304
Bolting	
Material	ASTM A193 Grade B8
Nuts	ASTM A194 Grade 8
Castings	ASTM A351 Grade CF8

- b. Jet Pump Assemblies. The components in the jet pump assemblies are a riser, inlet, mixer, diffuser, adaptor, and brackets. All these components are fabricated with Type 304 stainless steel to the following specifications:

Castings	ASTM A351 Grade CF8
Bars	ASTM A276 Type 304
Bolts	ASTM A193 Grade B8 or B8M
Sheet and Plate	ASTM A240 Type 304
Tubing	ASTM A269 Grade TP 304
Pipe	ASTM A358 Type 304 and ASTM A312 Grade TP304
Weld Coupling	ASTM A403 Grade WP304
Forgings	ASTM A182 Grade F304

Auxiliary Wedges The frames are fabricated from Type 304, 304L, 316, or 316L stainless steel.

The sliding components are fabricated from XM-19 or Alloy X-750.

Slip Joint Clamps The clamp frames are fabricated per ASTM A-182 Grade F XM-19. The sub-components are fabricated per ASTM B-637 UNS N07750 Type 3.

Due to damage repaired during L1R08, the following unique features are associated with Unit 1 jet pump 9.

- The damaged “Stellite-6” hard faced surface on the restrainer bracket pad was removed.
- Two auxiliary wedges are located on the riser restrainer bracket. The frames are fabricated from ASTM A-240 or A-479 Type 304 stainless steel (0.02% max).

LSCS-UFSAR

- carbon) and the sliding component is fabricated from Alloy X-750 in accordance with ASTM B-637 UNS N077550 Type 3;
- The replacement inlet mixer wedge is fabricated from ASTM A-240 or A-479 Type 304 stainless steel (0.02% max carbon). Both of the wedge bearing surfaces are hard faced with “Stellite-21”.
- In L2R10, inlet-mixer wedges and mounting hardware fabricated from Alloy X-750 and solution heat treated 300 series austenitic stainless steel (0.02% max. carbon) materials were installed in all of the Unit 2 jet pumps.
- During L1R11, jet pump riser brace clamps were installed on Unit 1 jet pumps 5/6 and 9/10 to mitigate crack indications by structurally replacing the upper and lower riser brace yoke to riser pipe welds designated as RS-8 and RS-9. The clamp components are fabricated from ASME SA-479/ASTM A479, ASME SA-240/ASTM A240, or ASME SA-182/ASTM A182 Type 316 stainless steel. The bolting components are fabricated from ASME SA-479/ASTM A479, or ASME SA-240/ASTM A240 Type XM-19 stainless steel. The ratchet springs and nuts are fabricated from ASME SB-670/ASTM B-637 Grade UNS N07750, Type 3 Alloy X-750.

LSCS-UFSAR

Identification and justification for using materials in the jet pump assemblies which are not included in Appendix I to Section III of ASME B&PV Code are provided as follows:

- a. The inlet mixer adaptor casting, the wedge casting, bracket casting adjusting screw, and the diffuser collar casting are Type 304 hard surfaced with Stellite 6 for slip fit joints.
- b. The adaptor is a bimetallic component made by welding a Type 304 forged ring to a forged Inconel 600 ring, made to Specification ASTM B166.
- c. The inlet contains a pin, insert, and beam made of Inconel X-750 to Specification ASTM B637 Grade 688 or UNS N07750 Type 3 (beam), and ASTM A370 Grade E38 and E55 (pin and insert).
- d. The jet pump beam bolt is stainless steel Type 316L.
- e. The jet pump beam keeper, screws, plate and pins are 304L, XM-19, or X-750.

4.5.2.2 Controls on Welding

All welding of the reactor internals is performed in accordance with the ASME Section IX B&PV Code. Interpass temperature does not exceed 370° F. Processes used are GTAW, SMAW, GMAW, and SAW. All welds except intermittent and tack welds are examined by liquid penetrant in accordance with ASME Section III. All welding filler material has a minimum of 5% ferrite as determined by the Schaeffler diagram.

4.5.2.3 Nondestructive Examination of Wrought Seamless Tubular Products

Wrought seamless tubular products were supplied in accordance with the applicable ASTM/ASME material specifications. These specifications require a hydrostatic test on each length of tubing. No special NDT was performed on the tubes.

4.5.2.4 Fabrication and Processing of Austenitic Stainless Steel

All materials have been solution heat treated and either water or air quenched. Where an air cool was used, a sample of each heat and heat treatment lot was tested in accordance with ASTM A262 practice A or E. There was no heating above 800° F after the final heat treatment, except for thermal cutting or welding.

4.5.2.5 Regulatory Guide Conformance Assessment

This information is addressed in Appendix B of the FSAR.

4.6 FUNCTIONAL DESIGN OF REACTIVITY CONTROL SYSTEMS

4.6.1 Information for Control Rod Drive Systems (CRDS)

4.6.1.1 Control Rod Drive System Design

4.6.1.1.1 Design Bases

4.6.1.1.1.1 General Design Bases

4.6.1.1.1.1.1 Safety Design Bases

The control rod drive mechanical system meets the following safety design bases:

- a. Design provides for a sufficiently rapid control rod insertion so that no fuel damage results from any abnormal operating transient.
- b. Design includes positioning devices, each of which individually supports and positions a control rod.
- c. Each positioning device:
 1. prevents its control rod from initiating withdrawal as a result of a single malfunction; collet piston stuck in upper position or stuck open withdraw valve will allow drive to continue withdrawal if initiating signal already given (Subsection 4.6.2.3);
 2. is individually operated so that a failure in one positioning device does not affect the operation of any other positioning device;
 3. is individually hydraulically energized when rapid control rod insertion (scram) is signaled so that failure of power sources external to the positioning device does not prevent other positioning devices' control rods from being inserted; and
 4. is locked to its control rod to prevent undesirable separation.

4.6.1.1.1.2 Power Generation Design Basis

The control rod system drive design provides for positioning the control rods to control power generation in the core.

4.6.1.1.2 Description

The control rod drive system (CRDS) controls gross changes in core reactivity by incrementally positioning neutron absorbing control rods within the reactor core in response to manual control signals. It is also required to quickly shut down the reactor (scram) in emergency situations by rapidly inserting withdrawn control rods into the core in response to a manual or automatic signal. The control rod drive system consists of locking piston, control rod drive mechanisms, and the CRD hydraulic system (including hydraulic control units, interconnecting piping, instrumentation, and electrical controls).

4.6.1.1.2.1 Control Rod Drive Mechanisms

The CRD mechanism (drive) used for positioning the control rod in the reactor core is a double-acting, mechanically latched, hydraulic cylinder using water as its operating fluid. (See Figures 4.6-1, 4.6-2, 4.6-3, and 4.6-4.) The individual drives are mounted on the bottom head of the reactor pressure vessel. The drives do not interfere with refueling and are operative even when the head is removed from the reactor vessel. The drives are also readily accessible for inspection and servicing. The bottom location makes maximum utilization of the water in the reactor as a neutron shield and gives the least possible neutron exposure to the drive components. Using water from the condensate storage tank as the operating fluid eliminates the need for special hydraulic fluid. Drives are able to utilize simple piston seals whose leakage does not contaminate the reactor water and does cool the drive mechanisms and their seals.

The drives are capable of inserting or withdrawing a control rod at a slow, controlled rate, as well as providing rapid insertion when required. A mechanism on the drive locks the control rod in 6-inch increments of stroke over the length of the core.

A coupling spud at the top end of the drive index tube (piston rod) engages and locks into a mating socket at the base of the control rod. The weight of the control rod is sufficient to engage and lock this coupling. Once locked, the drive and rod form an integral unit that must be manually unlocked by specific procedures before components can be separated.

The drive holds its control rod in distinct latch positions until the hydraulic system actuates movement to a new position. Withdrawal of each rod is limited by the seating of the rod in its guide tube. Withdrawal to the overtravel limit can be

accomplished only if the rod and drive are uncoupled and will result in a control room alarm.

The individual rod indicators, grouped in one control panel display, correspond to relative rod locations in the core. A separate, smaller display is located just below the large display on the vertical part of the benchboard. This display presents the positions of the control rod selected for movement and the other rods in the affected rod group.

For display purposes the control rods are considered in groups of four adjacent rods centered around a common core volume. Each group is monitored by four LPRM strings (Subsection 7.7.6). Rod groups at the periphery of the core may have less than four rods. The small rod display shows the positions, in digital form, of the rods in the group to which the selected rod belongs. A white light indicates which of the four rods is the one selected for movement.

4.6.1.1.2.2 Drive Components

Figure 4.6-2 illustrates the operating principle of a drive. Figures 4.6-3 and 4.6-4 illustrate the drive in more detail. The main components of the drive and their functions are described in the following paragraphs.

4.6.1.1.2.2.1 Drive Piston

The drive piston is mounted at the lower end of the index tube. This tube functions as a piston rod. The drive piston and index tube make up the main moving assembly in the drive. The drive piston operates between positive end stops, with a hydraulic cushion provided at the upper end only. The piston has both inside and outside seal rings and operates in an annular space between an inner cylinder (fixed piston tube) and an outer cylinder (drive cylinder). Because the type of inner seal used is effective in only one direction, the lower sets of seal rings are mounted with one set sealing in each direction.

A pair of nonmetallic bushings prevents metal-to-metal contact between the piston assembly and the inner cylinder surface. The outer piston rings are segmented step-cut seals with expander springs holding the segments against the cylinder wall. A pair of split bushings on the outside of the piston prevents piston contact with the cylinder wall. The effective piston area for downtravel, or withdrawal, is approximately 1.2 in² vs. 4.1 in² for uptravel, or insertion. This difference in driving area tends to balance the control rod weight and assures a higher force for insertion than for withdrawal.

4.6.1.1.2.2.2 Index Tube

The index tube is a long hollow shaft made of nitrided Type 304 stainless steel. Circumferential locking grooves, spaced every 6 inches along the outer surface, transmit the weight of the control rod to the collet assembly.

4.6.1.1.2.2.3 Collet Assembly

The collet assembly serves as the index tube locking mechanism. It is located in the upper part of the drive unit. This assembly prevents the index tube from accidentally moving downward. The assembly consists of the collet fingers, a return spring, a guide cap, a collet housing (part of the cylinder, tube, and flange), and the collet piston. LaSalle is the first domestic facility which contains the redesigned collet retainer tube. The collet retainer tube is fabricated from cast American Society for Testing and Materials A 351 CF-3 alloy with Colmonoy hardfacing, and the index tube and piston tube are fabricated from XM-19 alloy.

Locking is accomplished by fingers mounted on the collet piston at the top of the drive cylinder. In the locked or latched position the fingers engage a locking groove in the index tube.

The collet piston is normally held in the latched position by a force of approximately 150 pounds supplied by a spring. Metal piston rings are used to seal the collet piston from reactor vessel pressure. The collet assembly will not unlatch until the collet fingers are unloaded by a short, automatically sequenced, drive-in signal. A pressure, approximately 180 psi above reactor vessel pressure, must then be applied to the collet piston to overcome spring force, slide the collet up against the conical surface in the guide cap, and spread the fingers out so they do not engage a locking groove.

A guide cap is fixed in the upper end of the drive assembly. This member provides the unlocking cam surface for the collet fingers and serves as the upper bushing for the index tube.

If reactor water is used during a scram to supplement accumulator pressure, it is drawn through a filter on the guide cap.

4.6.1.1.2.2.4 Piston Tube

The piston tube is an inner cylinder, or column, extending upward inside the drive piston and index tube. The piston tube is fixed to the bottom flange of the drive and remains stationary. Water is brought to the upper side of the drive piston through this tube. A series of orifices at the top of the tube provides progressive water shutoff to cushion the drive piston at the end of its scram stroke.

4.6.1.1.2.2.5 Stop Piston

A stationary piston, called the stop piston, is mounted on the upper end of the piston tube. This piston provides the seal between reactor vessel pressure and the space above the drive piston. It also functions as a positive end stop at the upper limit of control rod travel. A stack of spring washers just below the stop piston helps absorb the final mechanical shock at the end of control rod travel. The piston rings are similar to the drive piston outer rings. A bleed-off passage to the center of the piston tube is located between the two pairs of rings. This arrangement allows seal leakage from the reactor vessel (during a scram) to be bled directly to the discharge line. The lower pair of seals is used only during the cushioning of the drive piston at the upper end of the stroke.

The center tube of the drive mechanism forms a well to contain the position indicator probe. This probe is an aluminum extrusion attached to a cast aluminum housing. Mounted on the extrusion are hermetically sealed, magnetically operated, position indicator switches. Each switch is sheathed in a braided glass sleeve, and the entire probe assembly is protected by a thin-walled stainless steel tube. The switches are actuated by a ring magnet located at the bottom of the drive piston.

The drive piston, piston tube, and indicator tube are all of nonmagnetic stainless steel, allowing the individual switches to be operated by the magnet as the piston passes. One switch is located at each position corresponding to an index tube groove, thus allowing indication at each latching point. An additional switch is located at each midpoint between latching points to indicate the intermediate positions during drive motion. Thus, indication is provided for each 3 inches of travel. Duplicate switches are provided for the full-in and full-out positions. One additional switch (an overtravel switch) is located at a position below the normal full-out position. Because the limit of downtravel is normally provided by the control rod itself as it reaches the backseat position, the drive can pass this position and actuate the overtravel switch only if it is uncoupled from its control rod. A convenient means is thus provided to verify that the drive and control rod are coupled after installation of a drive or at any time during plant operation.

4.6.1.1.2.2.6 Flange and Cylinder Assembly

A flange and cylinder assembly is made up of a heavy flange welded to the drive cylinder. A sealing surface on the upper face of this flange forms the seal to the drive housing flange. The seals contain reactor pressure and the two hydraulic control pressures. Teflon coated, stainless steel rings are used for these seals. The drive flange contains the integral ball, or two-way, check (ball-shuttle) valve. This valve directs either the reactor vessel pressure or the driving pressure, whichever is higher, to the underside of the drive piston. Reactor vessel pressure is admitted to this valve from the annular space between the drive and drive housing through passages in the flange.

Water used to operate the collet piston passes between the outer tube and the cylinder tube. The inside of the cylinder tube is honed to provide the surface required for the drive piston seals.

Both the cylinder tube and outer tube are welded to the drive flange. The upper ends of these tubes have a sliding fit to allow for differential expansion.

The upper end of the index tube is threaded to receive a coupling spud. The coupling (Figure 4.6-1) accommodates a small amount of angular misalignment between the drive and the control rod. Six spring fingers allow the coupling spud to enter the mating socket on the control rod. A plug then enters the spud and prevents uncoupling.

4.6.1.1.2.2.7 Lock Plug

Two means of uncoupling are provided. With the reactor vessel head removed, the lock plug can be raised against the spring force of approximately 50 pounds by a rod extending up through the center of the control rod to an unlocking handle located above the control rod velocity limiter. The control rod, with the lock plug raised, can then be lifted from the drive.

The lock plug can also be pushed up from below, if it is desired to uncouple a drive without removing the reactor pressure vessel head for access. In this case, the central portion of the drive mechanism is pushed up against the uncoupling rod assembly, which raises the lock plug and allows the coupling spud to disengage the socket as the drive piston and index tube are driven down.

The control rod is heavy enough to force the spud fingers to enter the socket and push the lock plug up, allowing the spud to enter the socket completely and the plug to snap back into place. Therefore, the drive can be coupled to the control rod using only the weight of the control rod. However, with the lock plug in place, a force in excess of 50,000 pounds is required to pull the coupling apart.

4.6.1.1.2.3 Materials of Construction

Factors that determine the choice of construction materials are discussed in the following subsections.

4.6.1.1.2.3.1 Index Tube

The index tube must withstand the locking and unlocking action of the collet fingers. A compatible bearing combination must be provided that is able to withstand moderate misalignment forces. The reactor environment limits the choice of materials suitable for corrosion resistance. The column and tensile loads

can be satisfied by an annealed AISI-300 series stainless steel. The wear and bearing requirements are provided by Malcomizing the complete tube. To obtain suitable corrosion resistance, a carefully controlled process of surface preparation is employed.

4.6.1.1.2.3.2 Coupling Spud

The coupling spud is made of Inconel-750 that is aged for maximum physical strength and the required corrosion resistance. Because misalignment tends to cause chafing in the semispherical contact area, the part is protected by a thin chromium plating (Electrolized). This plating also prevents galling of the threads attaching the coupling spud to the index tube.

4.6.1.1.2.3.3 Collet Fingers

Inconel-750 is used for the collet fingers, which must function as leaf springs when cammed open to the unlocked position. Colmonoy 6 hard facing provides a long wearing surface, adequate for design life, to the area contacting the index tube and unlocking cam surface of the guide cap.

4.6.1.1.2.3.4 Seals and Bushings

Graphitar 14 is selected for seals and bushings on the drive piston and stop piston. The material is inert and has a low friction coefficient when water lubricated. Because some loss of Graphitar strength is experienced at higher temperatures, the drive is supplied with cooling water to hold temperatures below 250° F. The Graphitar is relatively soft, which is advantageous when an occasional particle of foreign matter reaches a seal. The resulting scratches in the seal reduce sealing efficiency until worn smooth, but the drive design can tolerate considerable water leakage past the seals into the reactor vessel.

4.6.1.1.2.3.5 Summary

All drive components exposed to reactor vessel water are made of AISI-300 series stainless steel except the following:

- a. Seals and bushings on the drive piston and stop piston are Graphitar 14.
- b. All springs and members requiring spring action (collet fingers, coupling spud, and spring washers) are made of Inconel-750.
- c. The ball check valve is a Haynes Stellite cobalt-base alloy.
- d. Elastomeric O-ring seals are ethylene propylene.

LSCS-UFSAR

- e. Collet piston rings are Haynes 25 alloy.
- f. Certain wear surfaces are hard-faced with Colmonoy 6.
- g. Nitriding by a proprietary new Malcomizing process and chromium plating are used in certain areas where resistance to abrasion is necessary.
- h. The drive piston head is made of Armco 17-4PH.

Pressure-containing portions of the drives are designed and fabricated in accordance with requirements of Section III of the ASME Boiler and Pressure Vessel Code.

4.6.1.1.2.4 Control Rod Drive Hydraulic System

The control rod drive hydraulic system (Drawing Nos. M-100 and M-146) controls the pressure and flow to and from the drives through hydraulic control units (HCU). The water discharged from the drives during a scram flows through the HCU's to the scram discharge volume. The water discharged from a drive during a normal control rod positioning operation flows through the HCU into the exhaust header, a reverse flow then occurs from the exhaust header through the insert/exhaust directional solenoid valves (121) into the latched CRD's. There are as many HCU's as the number of control rod drives.

4.6.1.1.2.4.1 Hydraulic Requirements

The CRD hydraulic system design is shown in Drawing Nos. M-100 and M-146 and Figures 4.6-5 and 4.6-6. The hydraulic requirements, identified by the function they perform, are as follows:

- a. An accumulator hydraulic charging pressure of approximately 1400 to 1500 psig is required. Flow to the accumulators is required only during scram reset or system startup.
- b. Drive pressure of approximately 250 psi above reactor vessel pressure is required. A flow rate of approximately 4 gpm to insert a control rod and 2 gpm to withdraw a control rod is required.
- c. Cooling water to the drives is required at approximately 15 psi above reactor vessel pressure and at a flow rate of 0.20 to 0.34 gpm per drive unit. (Cooling water can be interrupted for short periods without damaging the drive.)

LSCS-UFSAR

- d. The scram discharge volume is sized to receive and contain all the water discharged by the drives during a scram; a minimum volume of 3.34 gallons per drive is required.
- e. The CRD System provides approximately 0.05 gpm to the condensing chambers reference legs for the narrow range, wide range, and fuel zone reactor vessel level instrumentation (UFSAR Section 7.7.1.2.2).

4.6.1.1.2.4.2 System Description

The CRD hydraulic systems provide the required functions with the pumps, filter, valves, instrumentation, and piping shown in Drawing Nos. M-100 and M-146 and described in the following paragraphs.

Duplicate components are included, where necessary, to ensure continuous system operation if an inservice component requires maintenance.

The control rod drive hydraulic system also supplies a purge flow to the reactor water cleanup pumps to prevent settling of sediment in the base of each of the two pumps. This flow is taken from the charging water header and becomes part of the RWCU process fluid once it enters the pump. It is not returned to the CRD hydraulic system. (Drawings M-97 and M-143, Sheet 1, and M-100 and M-146, Sheet 1). This purge flow is not required for operation of the pumps.

4.6.1.1.2.4.2.1 Supply Pump

One supply pump pressurizes the system. The condensate system is the normal source of water from the hotwell reject line. However, during shutdown conditions, the pump suction is from the condensate storage tank. One spare pump is provided for standby. A discharge check valve prevents backflow through the nonoperating pump. A portion of the pump discharge flow is diverted through a minimum flow bypass line to the condensate storage tank. This flow is controlled by an orifice and is sufficient to prevent immediate pump damage if the pump discharge is inadvertently closed. An additional recirculation line is provided for the supply pumps. This line provides a means of maintaining the pump manufacturer's recommended minimum flow, during unit outage time periods when CRD system flow demand is minimal. Flow in this line is controlled by a severe service manual control valve, which is closed during normal plant operation. This line is used concurrently with the previously mentioned minimum flow bypass line to the condensate storage tank.

Condensate water is processed by two filters in the system. The pump suction filter is a cleanable element type with a 25-micron absolute rating. The drive water filter downstream of the pump is a cleanable element type with a 50-micron absolute rating. A differential pressure indicator and control room alarm monitor the filter element as it collects foreign material.

4.6.1.1.2.4.2.2 Accumulator Charging Pressure

Accumulator charging pressure is established by the discharge pressure of the system supply pump. During scram the scram inlet (and outlet) valves open and permit the stored energy in the accumulators to discharge into the drives. The resulting pressure decrease in the charging water header allows the CRD supply pump to run out (i.e., flow rate to increase substantially) into the control rod drives via the charging water header. The flow sensing system upstream of the accumulator charging header detects high flow and closes the flow control valve. This action maintains increased flow through the charging water header.

Pressure in the accumulator charging header is monitored in the control room with a pressure indicator and a low/high pressure alarm. An automatic scram is initiated when the charging water header pressure drops below 1157 psig for more than approximately 10 seconds.

The automatic scram on low pressure in the charging water header is not active in the run mode because the accumulators are not required for scram at operating pressures. The automatic scram is also not active in the shutdown mode since no control rods may be withdrawn in this mode. In all other modes, the automatic scram on low charging-water-header pressure remains active.

During normal operation the flow control valve maintains a constant system flow rate. This flow is used for drive flow, drive cooling, and system stability.

4.6.1.1.2.4.2.3 Drive Water Pressure

Drive water pressure required in the drive header is maintained by the drive pressure control valve, which is manually adjusted from the control room. A flow rate of approximately 6 gpm (the sum of the flow rate required to insert and withdraw a control rod) normally passes from the drive water pressure stage through two solenoid-operated stabilizing valves (arranged in parallel) and then goes into the cooling water line. The flow through one stabilizing valve equals the drive insert flow; that of the other stabilizing valve equals the drive withdrawal flow. When operating a drive, the required flow is diverted to that drive by closing the appropriate stabilizing valve. Thus, flow through the drive pressure control valve is always constant.

Flow indicators in the drive water header and in the line downstream from the stabilizing valves allow the flow rate through the stabilizing valves to be adjusted when necessary. Differential pressure between the reactor vessel and the drive pressure stage is indicated in the control room.

4.6.1.1.2.4.2.4 Cooling Water Header

The cooling water header is located downstream from the drive pressure control valve. When not moving a CRD, all system flow returns to vessel through the cooling water header.

The flow through the flow control valve is virtually constant. Therefore, once adjusted, the drive pressure control valve maintains the required pressure independent of reactor pressure. Changes in setting of the pressure control valves are required only to adjust for changes in the cooling requirements of the drives, as their seal characteristics change with time. A flow indicator in the control room monitors cooling water flow. A differential pressure indicator in the control room indicates the difference between reactor vessel pressure and drive cooling water pressure. Although the drives can function without cooling water, seal life is shortened by long term exposure to reactor temperatures. The temperature of each drive is recorded in the control room, and excessive temperatures are annunciated.

4.6.1.1.2.4.2.5 Return Line

The H₂O discharged from the HCU during a normal control rod positioning operation is discharged back to the RPV through the insert/exhaust directional solenoid valves of adjoining HCUs.

4.6.1.1.2.4.2.6 Scram Discharge Volume

The scram discharge volume consists of header piping which connects to each HCU and drains into an instrument volume. The header piping is sized to receive and contain all the water discharged by the drives during a scram, independent of the instrument volume. Each header pipe is designed with a hydrolazing port having 3/4" threaded plugs to allow the lines to be flushed occasionally, to prevent radiation build-up. During normal plant operation the scram discharge volume is empty and vented to atmosphere through its open vent and drain valves. When a scram occurs, upon a signal from the safety circuit, these vent and drain valves are closed to conserve reactor water. Lights in the control room indicate the position of these valves.

During a scram, the scram discharge volume partly fills with water discharged from above the drive pistons. While scrammed, the control rod drive seal leakage from the reactor continues to flow into the scram discharge volume until the discharge volume pressure equals the reactor vessel pressure. A check valve in each HCU prevents reverse flow from the scram discharge header volume to the drive. When the initial scram signal is cleared from the reactor protection system, the scram discharge volume signal is overridden with a keylock override switch, and the scram discharge volume is drained and returned to atmospheric pressure.

LSCS-UFSAR

Remote manual switches in the pilot valve solenoid circuits allow the discharge volume vent and drain valves to be tested without disturbing the reactor protection system. Closing the scram discharge volume valves allows the outlet scram valve seats to be leak tested by timing the accumulation of leakage inside the scram discharge volume.

There are two instrument volumes associated with the scram discharge volume. Four level switches and two analog trip systems connected to each instrument volume to monitor the volume for abnormal water level. Each analog trip system consists of a transmitter and a trip unit. The level switches are set at three different levels. At the lowest level, a level switch actuates to indicate that the volume is not completely empty during postscram draining or to indicate that the volume starts to fill through leakage accumulation at other times during reactor operation. At the second level, one level switch produces rod withdrawal block to prevent further withdrawal of any control rod when leakage accumulates to approximately half the capacity of the instrument volume. The remaining two level switches and the trip units are interconnected with the reactor protection system (RPS) trip channels and will initiate a reactor scram should water accumulation fill the instrument volume. The liquid level switches are float type and transmitters are differential pressure type. Each differential pressure transmitter/trip unit combinations are powered from separate ESS Division sources that are independent of the Reactor Protection system power supply.

Redundant Vent & Drain Valves, placed in series, are located in the vent and drain piping for the scram discharge volume.

This system configuration addresses the concerns identified in IE Bulletin No. 80-17.

4.6.1.1.2.4.3 Hydraulic Control Units

Each hydraulic control unit (HCU) furnishes pressurized water on signal to a drive unit. The drive then positions its control rod as required. Operation of the electrical system that supplies scram and normal control rod positioning signals to the HCU is described in Subsection 7.7.2. Operation of the electrical system which supplies ATWS signals to the HCU is described in Subsection 7.6.5.

The basic components in each HCU are: manual, pneumatic, and electrical valves; an accumulator; related piping; electrical connections; filters; and instrumentation (Drawing Nos. M-100 and M-146 and Figure 4.6-7). The components and their functions are described in the following paragraphs.

4.6.1.1.2.4.3.1 Insert Drive Valve

The insert drive valve is solenoid-operated and opens on an insert signal. The valve supplies drive water to the bottom side of the main drive piston.

4.6.1.1.2.4.3.2 Insert Exhaust Valve

The insert exhaust valve also opens by solenoid on an insert signal. The valve discharges water from above the drive piston to the exhaust water header.

4.6.1.1.2.4.3.3 Withdraw Drive Valve

The withdraw drive valve is solenoid-operated and opens on a withdraw signal. The valve supplies drive water to the top of the drive piston.

4.6.1.1.2.4.3.4 Withdraw Exhaust Valve

The solenoid-operated withdraw exhaust valve opens on a withdraw signal and discharges water from below the main drive piston to the exhaust header. It also serves as the settle valve. The valve opens following any normal drive movement (insert or withdraw) to allow the control rod and its drive to settle back into the nearest latch position.

4.6.1.1.2.4.3.5 Speed Control Valves

The speed control valves regulate the control rod insertion and withdrawal rates during normal operation. They are manually adjustable flow control valves used to regulate the water flow to and from the volume beneath the main drive piston. A correctly adjusted valve does not require readjustment except to compensate for changes in drive seal leakage.

4.6.1.1.2.4.3.6 Scram Pilot Valves

The scram pilot valves are operated from the reactor protection system trip system. Two scram pilot valves control both the scram inlet valve and the scram exhaust valve. The scram pilot valves are identical, three-way, solenoid-operated, normally energized valves. On loss of electrical signal to the pilot valves, such as the loss of external a-c power, the inlet ports close and the exhaust ports open on both pilot valves. The pilot valves (Drawing Nos. M-100 and M-146) are arranged so that the trip system signal must be removed from both valves before air pressure can be discharged from the scram valve operators. This prevents the inadvertent scram of a single drive in the event of a failure of one of the solenoid pilot valves.

4.6.1.1.2.4.3.7 Scram Inlet Valve

The scram inlet valve opens to supply pressurized water to the bottom of the drive piston. This quick opening globe valve is operated by an internal spring and system pressure. It is closed by air pressure applied to the top of its diaphragm operator.

LSCS-UFSAR

A position indicator switch on this valve energizes a light in the control room as soon as the valve starts to open.

As the scram inlet valve and the scram exhaust valve start to open, position indication switches on the valves through the multiplexed-acknowledged word, which is decoded in the display memory module, energize a light on the full-core display in the main control room.

4.6.1.1.2.4.3.8 Scram Exhaust Valve

The scram exhaust valve opens slightly before the scram inlet valve, exhausting water from above the drive piston. The exhaust valve opens faster than the inlet valve because of a high air pressure spring setting in the valve operator. Otherwise the valves are similar.

4.6.1.1.2.4.3.9 Scram Accumulator

The scram accumulator stores sufficient energy to fully insert a control rod at lower vessel pressures. At higher vessel pressures the accumulator pressure is assisted or supplanted by reactor vessel pressure. The accumulator is a hydraulic cylinder with a free-floating piston. The piston separates the water on top from the nitrogen below. A check valve in the accumulator charging line prevents loss of water pressure in the event supply pressure is lost.

During normal plant operation, the accumulator piston is seated at the bottom of its cylinder. Loss of nitrogen decreases the nitrogen pressure, which actuates a pressure switch and sounds an alarm in the control room. To ensure that the accumulator is always able to produce a scram, it is continuously monitored for water leakage. A float-type level switch actuates an alarm if water leaks past the piston barrier and collects in the accumulator instrumentation block.

4.6.1.1.2.4.3.10 Alternate Rod Insertion Scram Valves

The alternate rod insertion (ARI) scram valves are redundant to the existing RPS scram backup valves C11-F110A&B, and scram discharge volume vent and drain pilot valves C11-F379 & F387. The ARI valves provide an alternate means of initiating control rod insertion during an ATWS event. The ARI valves have direct current solenoid dual coil operators. The valves are provided with position switches to indicate valve open/closed status in the main control room. The valves perform three functions during an ATWS trip:

1. Block the instrument air supply line to the pilot scram valves.
2. Exhaust the air from the pilot scram air header to 5 psig in 15 seconds.

3. Exhaust air header to the scram discharge volume vent and drain valves, permitting these valves to close.

4.6.1.1.2.5 Control Rod Drive System Operation

The control rod drive system performs rod insertion, rod withdrawal, and scram. These operational functions are described as follows.

4.6.1.1.2.5.1 Rod Insertion

Rod insertion is initiated by a signal from the operator to the insert valve solenoids. This signal causes both insert valves to open. The insert drive valve applies reactor pressure plus approximately 90 psi to the bottom of the drive piston. The insert exhaust valve allows water from above the drive piston to discharge to the exhaust header.

As is illustrated in Figure 4.6-3, the locking mechanism is a ratchet-type device and does not interfere with rod insertion. The speed at which the drive moves is determined by the flow through the insert speed control valve, which is set for approximately 4 gpm for a shim speed (nonscram operation) of 3 in/sec. During normal insertion, the pressure on the downstream side of the speed control valve is 90 to 100 psi above reactor vessel pressure. However, if the drive slows for any reason, the flow through and pressure drop across the insert speed control valve will decrease; the full differential pressure (260 psi) will then be available to cause continued insertion. With 260-psi differential pressure acting on the drive piston, the piston exerts an upward force of 1040 pounds.

4.6.1.1.2.5.2 Rod Withdrawal

Rod withdrawal is, by design, more involved than insertion. The collet finger (latch) must be raised to reach the unlocked position (Figure 4.6-3). The index tube notches and the collet fingers are shaped so that the downward force on the index tube holds the collet fingers in place. The index tube must be lifted before the collet fingers can be released. This is done by opening the drive insert valves (in the manner described in the preceding paragraph) for approximately 1 second. The withdraw valves are then opened, applying driving pressure above the drive piston and opening the area below the piston to the exhaust header. Pressure is simultaneously applied to the collet piston. As the piston raises, the collet fingers are cammed outward, away from the index tube, by the guide cap.

The pressure required to release the latch is set and maintained at a level high enough to overcome the force of the latch return spring plus the force of reactor pressure opposing movement of the collet piston. When this occurs, the index tube is unlatched and free to move in the withdraw direction. Water displaced by the drive piston flows out through the withdraw speed control valve, which is set to give

the control rod a shim speed of 3 in/sec. The maximum control rod drive withdrawal speed is 5.14 in/sec when the Operating Limit MCPR established in the Core Operating Limits Report (COLR) is set greater than or equal to the value corresponding to a RWE - at Power analysis for an "unblocked" condition. Otherwise, the maximum control rod drive withdrawal speed is 3.6 in/sec. See subsection 15.4.2.3 for additional details. The entire valving sequence is automatically controlled and is initiated by a single operation of the rod withdraw switch.

4.6.1.1.2.5.3 Scram

During a scram the scram pilot valves and scram valves are operated as previously described. With the scram valves open, accumulator pressure is admitted under the drive piston, and the area over the drive piston is vented to the scram discharge volume.

The large differential pressure (initially approximately 1500 psi and always several hundred psi, depending on reactor vessel pressure) produces a large upward force on the index tube and control rod. This force gives the rod a high initial acceleration and provides a large margin of force to overcome any possible friction. After the initial acceleration is achieved, the drive continues at a nearly constant velocity. This characteristic provides a high initial rod insertion rate. As the drive piston nears the top of its stroke, the piston seals close off the large passage (buffer orifices) in the stop piston tube, and the drive slows.

Prior to a scram signal the accumulator in the hydraulic control unit has approximately 1450-1510 psig on the water side, and ≥ 980 and < 1200 psig on the nitrogen side. As the inlet scram valve opens, the full water side pressure is available at the control rod drive acting on a 4.1 in² area. As CRD motion begins, this pressure drops to the gas-side pressure less line losses between the accumulator and the CRD. At low vessel pressures, the accumulator completely discharges with a resulting gas-side pressure of approximately 575 psig. Reactor pressure provides the force necessary to scram the reactor when reactor pressure exceeds scram accumulator pressure.

The control-rod-drive accumulators are required to scram the control rod when the reactor pressure is low. When the reactor pressure is low, the accumulator retains sufficient stored energy to ensure the complete insertion of the control rod in the required time. The accumulator is not required in order to scram the control rod in time when the reactor is close to or at full operating pressure. In this instance, the reactor pressure alone will scram the control rod in the required time. However, the accumulator does provide an additional energy boost to the reactor pressure in providing scram action at vessel pressures less than accumulator pressures.

The control rod drive system, with accumulators, was designed to meet the scram time requirements specified in Technical Specification.

4.6.1.1.2.6 Instrumentation

The general functional requirements for the control rod drive are discussed in Subsection 4.6.1.1.2.4.1.

4.6.1.2 Control Rod Drive Housing Supports

4.6.1.2.1 Safety Objective

The control rod drive (CRD) housing supports prevent any significant nuclear transient in the event a drive housing breaks or separates from the bottom of the reactor vessel.

4.6.1.2.2 Safety Design Bases

The CRD housing supports meet the following safety design bases:

- a. Following a postulated CRD housing failure, control rod downward motion is limited so that any resulting nuclear transient cannot be sufficient to cause fuel damage.
- b. The clearance between the CRD housings and the supports is sufficient to prevent vertical contact stresses caused by thermal expansion during plant operation.

4.6.1.2.3 Description

The CRD housing supports are shown in Figure 4.6-8. Horizontal beams are installed immediately below the bottom of the reactor vessel, between the rows of CRD housings. The beams are supported by brackets welded to the steel form liner of the drive room in the reactor support pedestal.

Hanger rods, approximately 10-feet long and 1-3/4-inches in diameter, are supported from the beams on stacks of disc springs. These springs compress approximately 2 inches under the design load.

LSCS-UFSAR

The support bars are bolted between the bottom ends of the hanger rods. The spring pivots at the top, and the beveled, loose-fitting ends on the support bars prevent substantial bending moment in the hanger rods if the support bars are overloaded.

Individual grids rest on the support bars between adjacent beams. Because a single-piece grid would be difficult to handle in the limited work space and because it is necessary that control rod drives, position indicators, and incore instrumentation components be accessible for inspection and maintenance, each grid is designed for in-place assembly or disassembly. Each grid assembly is made from two grid plates, a clamp, and a bolt. The top part of the clamp guides the grid to its correct position directly below the respective CRD housing that it would support in the postulated accident.

When the support bars and grids are installed, a gap of approximately 1-1/2 inch at room temperature is provided between the grid and the bottom contact surface of the control rod drive flange. During system heatup, this gap is reduced by a net downward expansion of the housings with respect to the supports. In the hot operating condition, the gap is reduced approximately 1/4 inch.

In the postulated CRD housing failure, the CRD housing supports are loaded when the lower contact surface of the CRD flange contacts the grid. The resulting load is then carried by two grid plates, two support bars, four hanger rods, their disc springs, and two adjacent beams.

The American Institute of Steel Construction (AISC) Manual of Steel Construction, "Specification for the Design, Fabrication and Erection of Structural Steel for Buildings," was used in designing the CRD housing support system. However, to provide a structure that absorbs as much energy as practical without yielding, the allowable shear, tension and bending stresses used 1.5 times the AISC allowable stresses.

For purposes of mechanical design, the postulated failure resulting in the highest forces is an instantaneous circumferential separation of the CRD housing from the reactor vessel, with an internal pressure of 1086 psig (reactor vessel operating pressure) acting on the area of the separated housing. The weight of the separated housing, control rod drive, and blade, plus the pressure of 1086 psig acting on the area of the separated housing, gives a force of approximately 32,000 pounds. This force is multiplied by an impact factor that conservatively assumes the housing travels through a 1-1/2 inch gap before it contacts the supports. The total force of approximately 120,000 pounds is then treated as a static load in design.

LSCS-UFSAR

All CRD housing support subassemblies are fabricated of commonly available structural steel, except for the following items:

	<u>Material</u>
a. grid bars	ASTM-A-441,
b. disc springs	Schnorr, Type BS-125-71-8, and
c. hex bolts and nuts	ASTM-A-307.

4.6.2 Evaluations of the CRDS

4.6.2.1 Failure Mode and Effects Analysis

Engineering standards for electrical and physical separation, a design with high safety factors, and the unitary design approach for the CRD modules using ASME standards have each contributed toward an effective and proven CRDS for the control and safe shutdown of BWR's designed by GE. An analysis of failure modes and effects has not been completed for the LSCS units because the CRDS design has a proven history beginning with Dresden-1. Further analytical evaluations are believed to be of less value than the accrual of real operating data and the incorporation of generic improvements based on actual experience. LSCS utilized this approach in lieu of FMEA.

4.6.2.2 Protection from Common Mode Failures

Based on NEDO-10189, NEDO-10349, and NEDO-20626, General Electric concludes that the complete failure of the BWR control rod scram system due to common mode failure is of such extremely low probability that no change in BWR design to account for the event is warranted.

EGC does not believe the ATWS to be a credible event; nevertheless, the LSCS design includes three provisions to assist shutdown in this unlikely event: tripping of the recirculation pumps, scram discharge volume upgrades, and the addition of alternate rod insertion (ARI) and main steam isolation valve closure modifications. These modifications adequately prevent and, additionally, contribute to the mitigation of ATWS events.

4.6.2.3 Safety Evaluation

4.6.2.3.1 Control Rod Drives

4.6.2.3.1.1 Evaluation of Scram Time

The rod scram function of the control rod drive system provides the negative reactivity insertion required by safety design basis in Subsection 4.6.1.1.1.1.1,

Item c, part 1. The scram time shown in the description is adequate as shown by the transient analyses of Chapter 15.0.

4.6.2.3.1.2 Analysis of Malfunction Relating to Rod Withdrawal

There are no known single malfunctions that cause the unplanned withdrawal of even a single control rod; providing initiating signal has not been given (Subsections 4.6.1.1.1.1.1, Item c, part 1, and 4.6.2.3.1.2.10). However, if multiple malfunctions are postulated, studies show that an unplanned rod withdrawal can occur at withdrawal speeds that vary with the combination of malfunctions postulated. In all cases the subsequent withdrawal speeds are less than that assumed in the rod drop accident analysis as discussed in Chapter 15.0. Therefore, the physical and radiological consequences of such rod withdrawals are less than those analyzed in the rod drop accident.

4.6.2.3.1.2.1 Drive Housing Fails at Attachment Weld

The bottom head of the reactor vessel has a penetration for each control rod drive location. A drive housing is raised into position inside each penetration and fastened by welding. The drive is raised into the drive housing and bolted to a flange at the bottom of the housing. The housing material is seamless, Type 304 stainless steel pipe with a minimum tensile strength of 75,000 psi. The basic failure considered here is a complete circumferential crack through the housing wall at an elevation just below the J-weld.

Static loads on the housing wall include the weight of the drive and the control rod, the weight of the housing below the J-weld, and the reactor pressure acting on the 6-inch diameter cross-sectional area of the housing and the drive. Dynamic loading results from the reaction force during drive operation.

If the housing were to fail as described, the following sequence of events is foreseen. The housing would separate from the vessel. The control rod, drive, and housing would be blown downward against the support structure by reactor pressure acting on the cross-sectional area of the housing and the drive. The downward motion of the drive and associated parts would be determined by the gap between the bottom of the drive and the support structure and by the deflection of the support structure under load. In the current design, maximum deflection is limited to 3.65 inches. If the collet were to remain latched, no further control rod ejection would occur (Reference 4); the housing would not drop far enough to clear the vessel penetration. Reactor water would leak at a rate of approximately 220 gpm through the 0.03-inch diametral clearance between the housing and the vessel penetration.

If the basic housing failure were to occur while the control rod is being withdrawn (this is a small fraction of the total drive operating time) and if the collet were to stay unlatched, the following sequence of events is foreseen. The housing would

separate from the vessel. The drive and housing would be blown downward against the control rod drive housing support.

Calculations indicate that the steady-state rod withdrawal velocity would be 0.3 ft/sec. During withdrawal, pressure under the collet piston would be approximately 250 psi greater than the pressure over it. Therefore, the collet would be held in the unlatched position until driving pressure was removed from the pressure-over port.

4.6.2.3.1.2.2 Rupture of Hydraulic Line(s) to Drive Housing Flange

There are three types of possible rupture of hydraulic lines to the drive housing flange: (1) pressure-under line break; (2) pressure-over line break; and (3) coincident breakage of both of these lines.

4.6.2.3.1.2.2.1 Pressure-Under Line Break

For the case of a pressure-under line break, a partial or complete circumferential opening is postulated at or near the point where the line enters the housing flange. Failure is more likely to occur after another basic failure wherein the drive housing or housing flange separates from the reactor vessel. Failure of the housing, however, does not necessarily lead directly to failure of the hydraulic lines.

If the pressure-under line were to fail and if the collet were latched, no control rod withdrawal would occur. There would be no pressure differential across the collet piston and, therefore, no tendency to unlatch the collet. Consequently, the associated control rod could not be inserted or withdrawn.

The ball check valve is designed to seal off a broken pressure-under line by using reactor pressure to shift the check ball to its upper seat. If the ball check valve were prevented from seating, reactor water would leak to the atmosphere. Because of the broken line, cooling water could not be supplied to the drive involved. Loss of cooling water would cause no immediate damage to the drive. However, prolonged exposure of the drive to temperatures at or near reactor temperature could lead to deterioration of material in the seals. High temperature would be indicated to the operator by the thermocouple in the position indicator probe. A second indication would be high cooling water flow.

If the basic line failure were to occur while the control rod is being withdrawn, the hydraulic force would not be sufficient to hold the collet open, and spring force normally would cause the collet to latch and stop rod withdrawal. However, if the collet were to remain open, calculations indicate that the steady-state control rod withdrawal velocity would be 2 ft/sec.

4.6.2.3.1.2.2.2 Pressure-Over Line Break

The case of the pressure-over line breakage considers the complete breakage of the line at or near the point where it enters the housing flange. If the line were to break, pressure over the drive piston would drop from reactor pressure to atmospheric pressure. Any significant reactor pressure (approximately 600 psig or greater) would act on the bottom of the drive piston and fully insert the drive. Insertion would occur regardless of the operational mode at the time of the failure. After full insertion, reactor water would leak past the stop piston seals. This leakage would exhaust to the atmosphere through the broken pressure-over line. The leakage rate of 1000 psi reactor pressure is estimated to be 4 gpm nominal but not more than 10 gpm, based on experimental measurements. If the reactor were hot, drive temperature would increase. This situation would be indicated to the reactor operator by the drift alarm, by the fully inserted drive, by a high drive temperature (indicated on a recorder in the control room), and by operation of the drywell sump pump.

4.6.2.3.1.2.2.3 Simultaneous Breakage of the Pressure-Over and Pressure-Under Lines

For the simultaneous breakage of the pressure-over pressure-under lines, pressures above and below the drive piston would drop to zero, and the ball check valve would close the broken pressure-under line. Reactor water would flow from the annulus outside the drive, through the vessel ports, and to the space below the drive piston. As in the case of pressure-over line breakage, the drive would then insert at a speed dependent on reactor pressure. Full insertion would occur regardless of the operational mode at the time of failure. Reactor water would leak past the drive seals and out the broken pressure-over line to the atmosphere, as described previously. Drive temperature would increase. Indication in the control room would include the drift alarm, the fully-inserted drive, the high drive temperature on a recorder in the control room, and operation of the drywell sump pump.

4.6.2.3.1.2.3 All Drive Flange Bolts Fail in Tension

Each control rod drive is bolted to a flange at the bottom of a drive housing. The flange is welded to the drive housing. The CRD mechanism is bolted to the CRD housing flange by 8 bolts. Each bolt has significantly high load carrying capacity compared to the actual load.

If a progressive or simultaneous failure of all bolts were to occur, the drive would separate from the housing. The control rod and the drive would be blown downward against the support structure. Impact velocity and support structure loading would be slightly less than that for drive housing failure because reactor pressure would

act on the drive cross-sectional area only and the housing would remain attached to the reactor vessel. The drive would be isolated from the cooling water supply. Reactor water would flow downward past the velocity limiter piston, through the large drive filter, and into the annular space between the thermal sleeve and the drive. For worst-case leakage calculations, the large filter is assumed to be deformed or swept out of the way so it would offer no significant flow restriction. At a point near the top of the annulus, where pressure would have dropped to 350 psi, the water would flash to steam and cause choke-flow conditions. Steam would flow down the annulus and out the space between the housing and the drive flanges to the atmosphere. Steam formation would limit the leakage rate to approximately 840 gpm.

If the collet were latched, control rod ejection would be limited to the distance the drive can drop before coming to rest on the support structure. There would be no tendency for the collet to unlatch because pressure below the collet piston would drop to zero. Pressure forces, in fact, exert 1435 pounds to hold the collet in the latched position.

If the bolts failed during control rod withdrawal, pressure below the collet piston would drop to zero. The collet, with 1650 pounds return force, would latch and stop rod withdrawal.

4.6.2.3.1.2.4 Weld Joining Flange to Housing Fails in Tension

The failure considered is a crack in or near the weld that joins the flange to the housing. This weld extends through the wall and completely around the housing. The flange material is forged, Type 304 stainless steel, with a minimum tensile strength of 75,000 psi. The housing material is seamless, Type 304 stainless steel pipe, with a minimum tensile strength of 75,000 psi. The conventional, full-penetration weld of Type 308 stainless steel has a minimum tensile strength approximately the same as that for the parent metal. The design pressure and temperature are 1250 psig and 575° F. Reactor pressure acting on the cross-sectional area of the drive, the weight of the control rod, drive, and flange, and the dynamic reaction force during drive operation result in a maximum tensile stress at the weld of approximately 6000 psi.

If the basic flange-to-housing joint failure occurred, the flange and the attached drive would be blown downward against the support structure. The support structure loading would be slightly less than that for drive housing failure because reactor pressure would act only on the drive cross-sectional area. Lack of differential pressure across the collet piston would cause the collet to remain latched and limit control rod motion to approximately 3.65 inches. Downward drive movement would be small and, therefore, most of the drive would remain inside the housing. The pressure-under and pressure-over lines are flexible enough to withstand the small displacement and remain attached to the flange. Reactor

water would follow the same leakage path described above for the flange-bolt failure, except that exit to the atmosphere would be through the gap between the lower end of the housing and the top of the flange. Water would flash to steam in the annulus surrounding the drive. The leakage rate would be approximately 840 gpm.

If the basic failure were to occur during control rod withdrawal (a small fraction of the total operating time) and if the collet were held unlatched, the flange would separate from the housing. The drive and flange would be blown downward against the support structure. The calculated steady-state rod withdrawal velocity would be 0.13 ft/sec. Because pressure-under and pressure-over lines remain intact, driving water pressure would continue to the drive, and the normal exhaust line restriction would exist. The pressure below the velocity limiter piston would drop below normal as a result of leakage from the gap between the housing and the flange. This differential pressure across the velocity limiter piston would result in a net downward force of approximately 70 pounds. Leakage out of the housing would greatly reduce the pressure in the annulus surrounding the drive. Thus, the net downward force on the drive piston would be less than normal. The overall effect of these events would be to reduce rod withdrawal to approximately one-half of normal speed. With a 560-psi differential across the collet piston, the collet would remain unlatched; however, it should relatch as soon as the drive signal is removed.

4.6.2.3.1.2.5 Housing Wall Ruptures

This failure is a vertical split in the drive housing wall just below the bottom head of the reactor vessel. The flow area of the hole is considered equivalent to the annular area between the drive and the thermal sleeve. Thus, flow through this annular area, rather than flow through the hole in the housing, would govern leakage flow. The housing is made of Type 304 stainless steel seamless pipe, with a minimum tensile strength of 75,000 psi. The maximum hoop stress of 11,900 psi results primarily from the reactor design pressure (1250 psig) acting on the inside of the housing.

If such a rupture were to occur, reactor water would flash to steam and leak through the hole in the housing to the atmosphere at approximately 1030 gpm. Choke-flow conditions would exist as described previously for the flange-bolt failure. However, leakage flow would be greater because flow resistance would be less; that is, the leaking water and steam would not have to flow down the length of the housing to reach the atmosphere. A critical pressure of 350 psi causes the water to flash to steam.

No pressure differential across the collet piston would tend to unlatch the collet; but the drive would insert as a result of loss of pressure in the drive housing causing a pressure drop in the space above the drive piston.

If this failure occurred during control rod withdrawal, drive withdrawal would stop, but the collet would remain unlatched. The drive would be stopped by a reduction of the net downward force action on the drive line. The net force reduction would occur when the leakage flow of 1030 gpm reduces the pressure in the annulus outside the drive to approximately 540 psig, thereby reducing the pressure acting on top of the drive piston to the same value. A pressure differential of approximately 710 psi would exist across the collet piston and hold the collet unlatched as long as the operator held the withdraw signal.

4.6.2.3.1.2.6 Flange Plug Blows Out

To connect the vessel ports with the bottom of the ball check valve, a hole of 3/4-inch diameter is drilled in the drive flange. The outer end of this hole is sealed with a plug of 0.812-inch diameter and 0.25-inch thickness. A full-penetration, Type 308 stainless steel weld holds the plug in place. The postulated failure is a full circumferential crack in this weld and subsequent blowout of the plug.

If the weld were to fail, the plug were to blow out, and the collet remained latched, there would be no control rod motion. There would be no pressure differential across the collet piston acting to unlatch the collet. Reactor water would leak past the velocity limiter piston, down the annulus between the drive and the thermal sleeve, through the vessel ports and drilled passage, and out the open plug hole to the atmosphere at approximately 320 gpm. Leakage calculations assume only liquid flows from the flange. Actually, hot reactor water would flash to steam and choke-flow conditions would exist. Thus, the expected leakage rate would be lower than the calculated value. Drive temperature would increase and initiate an alarm in the control room.

If this failure were to occur during control rod withdrawal and if the collet were to stay unlatched, calculations indicate that control rod withdrawal speed would be approximately 0.24 ft/sec. Leakage from the open plug hole in the flange would cause reactor water to flow downward past the velocity limiter piston. A small differential pressure across the piston would result in an insignificant driving force of approximately 10 pounds, tending to increase withdraw velocity.

A pressure differential of 295 psi across the collet piston would hold the collet unlatched as long as the driving signal was maintained.

Flow resistance of the exhaust path from the drive would be normal because the ball check valve would be seated at the lower end of its travel by pressure under the drive piston.

4.6.2.3.1.2.7 Drive Pressure Control Valve Closure (Reactor Pressure, 0 psig)

The pressure to move a drive is generated by the pressure drop of practically the full system flow through the drive pressure control valve. This valve is a motor-operated valve with a normally closed, standby manually operated valve in parallel. The motor-operated valve is adjusted to a fixed opening, to develop a normal pressure (260 psig in excess of normal reactor pressure) on the upstream side of the motor-operated valve. In the event of motor-operated valve failure, this valve can be isolated (upstream and downstream gate valves) and its function replaced by the manually operated standby valve.

If the flow through the drive pressure control valve were to be stopped, as by a valve closure or flow blockage, the drive pressure would increase to the shutoff pressure of the supply pump. The occurrence of this condition during withdrawal of a drive at zero vessel pressure will result in a drive pressure increase from 260 psig to no more than 1700 psig. Calculations indicate that the drive would accelerate from a nominal 3 in/sec to approximately 6 in/sec. A pressure differential of 1670 psi across the collet piston would hold the collet unlatched. Flow would be upward, past the velocity limiter piston, but retarding force would be negligible. Rod movement would stop as soon as the driving signal was removed.

4.6.2.3.1.2.8 Ball Check Valve Fails to Close Passage to Vessel Ports

Should the ball check valve sealing the passage to the vessel ports be dislodged and prevented from reseating following the insert portion of a drive withdrawal sequence, water below the drive piston would return to the reactor through the vessel ports and the annulus between the drive and the housing rather than through the speed control valve. Because the flow resistance of this return path would be lower than normal, the calculated withdrawal speed would be 2 ft/sec. During withdrawal, differential pressure across the collet piston would be approximately 40 psi. Therefore, the collet would tend to latch and would have to stick open before continuous withdrawal at 2 ft/sec, could occur. Water would flow upward past the velocity limiter piston, generating a small retarding force of approximately 120 pounds.

4.6.2.3.1.2.9 Hydraulic Control Unit (HCU) Valve Failures

Various failures of the valves in the HCU can be postulated, but none could produce differential pressures approaching those described in the preceding paragraphs and none alone could produce a high velocity withdrawal. Leakage through either one or both of the scram valves produces a pressure that tends to insert the control rod rather than to withdraw it. If the pressure in the scram discharge volume should exceed reactor pressure following a scram, a check valve in the line to the scram discharge header prevents this pressure from operating the drive mechanisms.

4.6.2.3.1.2.10 Collet Fingers Fail to Latch

When the drive withdraw signal is removed, the drive continues to withdraw at a fraction of normal speed. Without some initiating signal there is no known means for the collet fingers to become unlocked. If the drive withdrawal valve fails to close following a rod withdrawal, it would have the same effect as failure of the collet fingers to latch in the index tube. Because the collet fingers remain locked until they are unloaded, accidental opening of the drive withdrawal valve does not unlock them.

4.6.2.3.1.2.11 Withdrawal Speed Control Valve Failure

Normal withdrawal speed is determined by differential pressures in the drive and is set for a nominal value of 3 in/sec. Withdrawal speed is maintained by the pressure regulating system and is independent of reactor vessel pressure. Tests have shown that accidental opening of the speed control valve to the full-open position produces a velocity of approximately 6 in/sec.

The control rod drive system prevents rod withdrawal and it has been shown above that only multiple failures in a drive unit and in its control unit could cause an unplanned rod withdrawal.

4.6.2.3.2 Scram Reliability of CRDS

High scram reliability is the result of a number of features of the CRD system. For example:

- a. Two sources of scram energy are used to insert each control rod when the reactor is operating: accumulator pressure and reactor vessel pressure.
- b. Each drive mechanism has its own scram and pilot valves so only one drive can be affected if a scram valve fails to open. Two pilot valves are provided for each drive. Both pilot valves must be deenergized to initiate a scram.
- c. The reactor protection system and the HCU's are designed so that the scram signal and mode of operation override all others.
- d. The alternate rod insertion (ARI) system provides an alternate means of exhausting the scram air header and closing the vent and drain valves of the scram discharge volume, thereby providing an additional reactor scram mechanism which is diverse, redundant and independent of the reactor protection system.

- e. The collet assembly and index tube are designed so they will not restrain or prevent control rod insertion during scram.
- f. The scram discharge volume is monitored for accumulated water and will scram the reactor before the volume is reduced to a point that could interfere with a scram.

4.6.2.3.2.1 Reliability Analysis

A reliability analysis was performed to demonstrate that the ARI design meets the design failure rate criteria of 10^{-6} failures to actuate per reactor-year (reference 5). The probability of spurious actuation was shown to be more than a factor of 10 less likely than the probability of failure to actuate. The basis for demonstrating the 10^{-6} criteria was the complete electrical independence of the ARI system from the electrical portion of the reactor protection system (RPS) including power supplies. When determining the overall electrical system failure probability (ARI and RPS), the independence results in an overall failure probability well beyond any practical means of engineering judgement ($\sim 10^{-11}$ failures to actuate per demand). Note that the mechanical portion of the CRD is unchanged by the ARI modification and now becomes the limiting factor in the overall scram system reliability. Hence, the ARI modification provides a conservative means of demonstrating adequate ATWS prevention for the expected ATWS initiators.

The charging water header pressure is monitored with a low pressure alarm to provide warning to control room operators of an impending reactor scram due to low charging-water-header pressure.

The scram assures that sufficient energy remains in the accumulators to shut down the reactor.

4.6.2.3.2.2 Control Rod Support and Operation

As described previously, each control rod is independently supported and controlled as required by safety design bases.

4.6.2.3.3 Control Rod Drive Housing Supports

4.6.2.3.3.1 Safety Evaluation

Downward travel of the CRD housing and its control rod following the postulated housing failure equals the sum of these distances: (1) the compression of the disc springs under dynamic loading, and (2) the initial gap between the grid and the bottom contact surface of the CRD flange. If the reactor were cold and pressurized, the downward motion of the control rod would be limited to the spring compression

(approximately 2 inches) plus a gap of approximately 1-1/2 inch. If the reactor were hot and pressurized, the gap would be reduced approximately 1/4 inch and the spring compression would be slightly less than in the cold condition. In either case, the control rod movement following a housing failure is substantially limited below one drive notch movement (6 inches). Sudden withdrawal of any control rod through a distance of one drive notch at any position in the core does not produce a transient sufficient to damage any radioactive material barrier.

The CRD housing supports are in place during power operation and when the nuclear system is pressurized. If a control rod is ejected during shutdown, the reactor remains subcritical because it is designed to remain subcritical with any one control rod fully withdrawn at any time.

At plant operating temperature, a gap of approximately 1-1/4 inch exists between the CRD housing and the supports. At lower temperatures the gap is greater. Because the supports do not contact any of the CRD housing except during the postulated accident condition, vertical contact stresses are prevented.

4.6.3 Testing and Verification of the CRDS

4.6.3.1 Control Rods

4.6.3.1.1 Testing and Inspection

The tests performed on control rods plus their related surveillance program are covered in Subsection 4.6.3.2.

4.6.3.2 Control Rod Drives

4.6.3.2.1 Testing and Inspection

4.6.3.2.1.1 Development Tests

The development drive (one prototype) testing to date included more than 5000 scrams and approximately 100,000 latching cycles. One prototype was exposed to simulated operating conditions for 5000 hours. These tests demonstrated the following:

- a. The drive easily withstands the forces, pressures, and temperatures imposed.
- b. Wear, abrasion, and corrosion of the nitrated Type 304 stainless parts are negligible. Mechanical performance of the nitrated surface is superior to that of materials used in earlier operating reactors.

LSCS-UFSAR

- c. The basic scram speed of the drive has a satisfactory margin above minimum plant requirements at any reactor vessel pressure.
- d. Usable seal lifetimes in excess of 1000 scram cycles can be expected.

4.6.3.2.1.2 Factory Quality Control Tests

Quality control of welding, heat treatment, dimensional tolerances, material verification, and similar factors is maintained throughout the manufacturing process to ensure reliable performance of the mechanical reactivity control components. Some of the quality control tests performed on the control rods, control rod drive mechanisms, and hydraulic control units are listed as follows:

- a. Control rod absorber tube tests:
 - 1. Material integrity of the tubing and end plug is verified by ultrasonic inspection.
 - 2. The boron-10 fraction of the boron content of each lot of boron-carbide is verified.
 - 3. Weld integrity of the finished absorber tubes is verified by helium leak-testing.
- b. Control rod drive mechanism tests:
 - 1. Pressure welds on the drives are hydrostatically tested in accordance with ASME codes.
 - 2. Electrical components are checked for electrical continuity and resistance to ground.
 - 3. Drive parts that cannot be visually inspected for dirt are flushed with filtered water at high velocity. No significant foreign material is permitted in effluent water.
 - 4. Seals are tested for leakage to demonstrate correct seal operation.
 - 5. Each drive is tested for shim motion, latching, and control rod position indication.

LSCS-UFSAR

6. Each drive is subjected to scram timing tests as required by Technical Specifications to verify correct scram performance.
- c. Hydraulic control unit tests:
1. Hydraulic systems are hydrostatically tested in accordance with the applicable code.
 2. Electrical components and systems are tested for electrical continuity and resistance to ground.
 3. Correct operation of the accumulator pressure and level switches is verified.
 4. The unit's ability to perform its part of a scram is demonstrated.
 5. Correct operation and adjustment of the insert and withdrawal valves is demonstrated.

4.6.3.2.1.3 Operational Tests

After installation, all rods and drive mechanisms can be tested through their full stroke for operability.

During normal operation, each time a control rod is withdrawn, the operator can observe the incore monitor indications to verify that the control rod is following the drive mechanism. All control rods that are partially withdrawn from the core can be tested for rod-following by inserting or withdrawing the rod and returning it to its original position, while the operator observes the incore monitor indications.

To make a positive test of control rod to control rod drive coupling integrity, the operator can withdraw a control rod to the end of its travel and then attempt to withdraw the drive to the overtravel position. Failure of the drive to overtravel demonstrates rod-to-drive coupling integrity.

Hydraulic supply subsystem pressures can be observed from instrumentation in the control room. Scram accumulator pressures can be observed on the nitrogen pressure gauges.

4.6.3.2.1.4 Acceptance Tests

The information in this subsection is being maintained for historical purposes only, as it is related to pre-startup testing.

Criteria for acceptance of the individual control rod drive mechanisms and the associated control and protection systems will be incorporated in specifications and test procedures covering three distinct phases: (1) preinstallation, (2) after installation prior to startup, and (3) during startup testing.

The preinstallation specification will define criteria and acceptable ranges of such characteristics as seal leakage, friction, and scram performance under fixed test conditions which must be met before the component can be shipped.

The after-installation, prestartup tests include normal and scram motion and are primarily intended to verify that piping, valves, electrical components, and instrumentation are properly installed. The test specifications will include criteria and acceptable ranges for drive speed, times settings, scram valve response times, and control pressures. These tests are intended more to document system condition than as tests of performance.

As fuel is placed in the reactor, the startup test procedure will be followed. The tests in this procedure are intended to determine that the initial operational characteristics meet the limits of the specifications over the range of primary coolant temperatures and pressures from ambient to operating. The detailed specifications and procedures have not as yet been prepared but will follow the general pattern established for such specifications and procedures in BWR's presently under construction and in operation.

4.6.3.2.1.5 Surveillance Tests

The surveillance requirements (SR) for the control rod drive system are recommended as follows:

- a. Sufficient control rods shall be withdrawn, following a refueling outage when core alterations are performed, to demonstrate with the technical specification design margin that the core can be made subcritical at any time in the subsequent fuel cycle with the strongest operable control rod fully withdrawn and all other operable rods fully inserted.
- b. Each partially or fully withdrawn control rod shall be exercised as defined in the Technical Specifications. When any control rod is immovable as a result of excessive friction or mechanical interference, a determination must be made and appropriate action taken.

The weekly control rod exercise test serves as a periodic check against deterioration of the control rod system and also verifies

LSCS-UFSAR

the ability of the control rod drive to scram because if a rod can be moved with drive pressure, it will scram since higher pressure is applied during scram. The frequency of exercising the control rods under the conditions of three or more control rods valved out of service provides even further assurance of the reliability of the remaining control rods.

- c. The coupling integrity shall be verified for each withdrawn control rod as follows:
 - 1. when the rod is first withdrawn, observe any indicated response of the nuclear instrumentation; and
 - 2. when the rod is fully withdrawn the first time, observe that the drive will not go to the overtravel position.

Observation of a response from the nuclear instrumentation during an attempt to withdraw a control rod indicates indirectly that the rod and drive are coupled. The overtravel position feature provides a positive check on the coupling integrity, for only an uncoupled drive can reach the overtravel position.

- d. During operation, accumulator pressure and level at the normal operating value are verified.

Experience with control rod drive systems of the same type indicates that weekly verification of accumulator pressure and level is sufficient to assure operability of the accumulator portion of the control rod drive system.

- e. After each major refueling outage, each operable control rod shall be subjected to scram time tests from the fully withdrawn position.

Experience indicates that the scram times of the control rods do not significantly change over the time interval between refueling outages. A test of the scram times at each refueling outage is sufficient to identify any significant lengthening of the scram times.

Routine accumulator surveillance is performed to authenticate the discharge pressure of the CRD pump and its associated hydraulic accumulator. Accumulator hydraulic pressure retention above the analysis value of 1157 psig is observed after a CRD pump trip to assure scram action via charging-water-

header pressure supplied from the accumulator. The 1157 psig value for this CRD-accumulator auto scram was selected because it exceeds the analytical point where the control rod maximum insertion times were defined.

4.6.3.3 Control Rod Drive Housing Supports

4.6.3.3.1 Testing and Inspection

CRD housing supports are removed for inspection and maintenance of the control rod drives. The operational condition during which CRD housing supports can be removed is controlled by the Technical Specifications. When the support structure is reinstalled, it is inspected for correct assembly with particular attention to maintaining the correct gap between the CRD flange lower contact surface and the grid.

4.6.4 Information for Combined Performance of Reactivity Systems

4.6.4.1 Vulnerability to Common Mode Failures

Protection of the CRDS from common mode failures is described in Subsection 4.6.2.2, and in GE's "BWR Scram System Reliability Analysis," dated September 30, 1976 (Proprietary) which was provided to Mr. D. F. Ross (NRC) by Mr. E. A. Hughes (GE) by letter of the same date. The evaluation of the ECCS and SLCS against common mode failures is presented in Section 6.3 and Subsection 9.3.5 respectively. In addition, no balance-of-plant failure will prevent reactivity shutdown. Therefore, no common mode failures need be considered in Chapter 15.0.

4.6.4.2 Accidents Taking Credit for Two or More Reactivity Control Systems

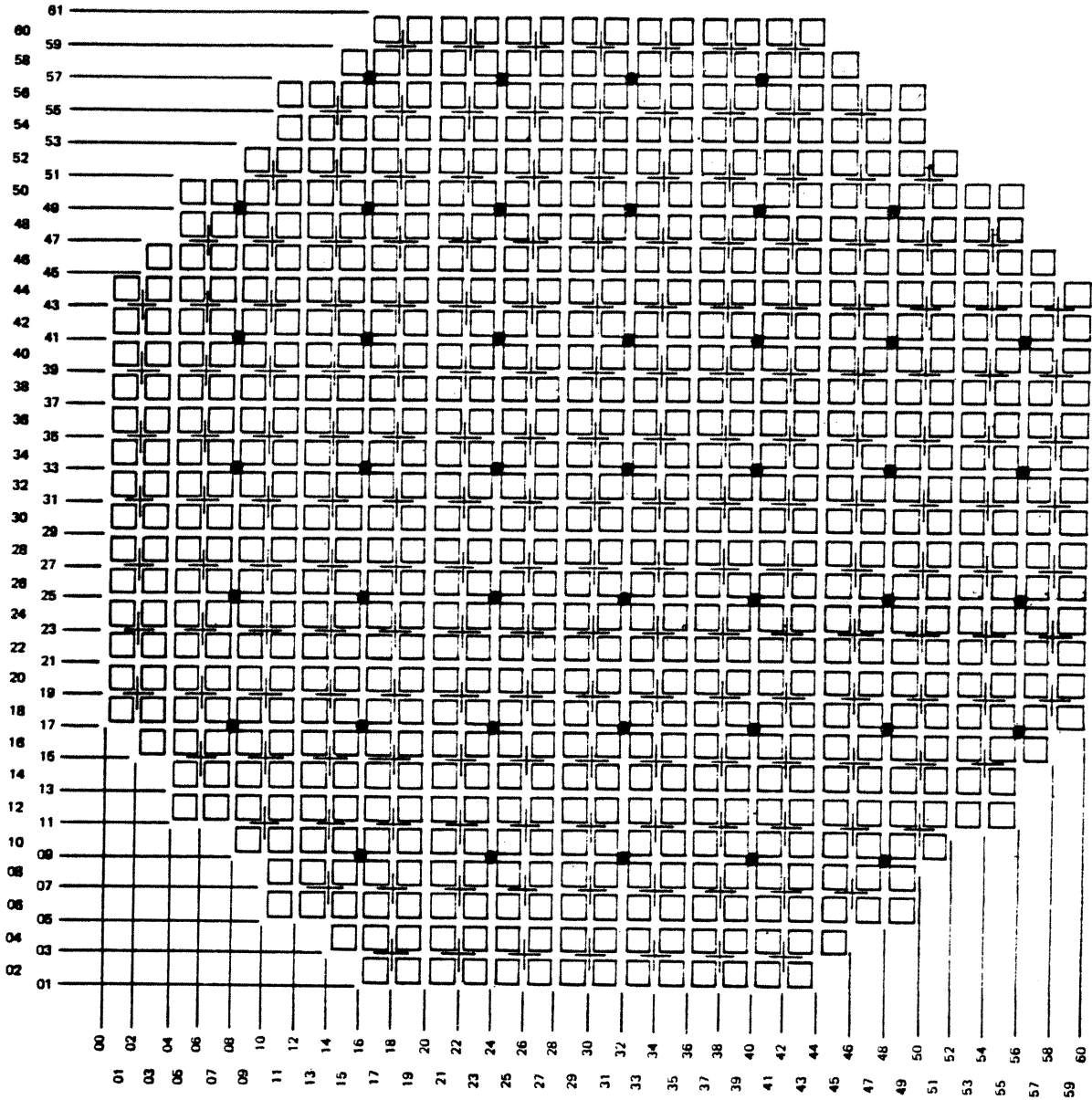
There are no postulated accidents evaluated in Chapter 15.0 that take credit for two or more reactivity control systems preventing or mitigating the accident.

4.6.5 Evaluation of Combined Performance

As indicated in Subsection 4.6.4.2, credit is not taken for multiple reactivity control systems for any postulated accidents in Chapter 15.0.

4.6.6 References

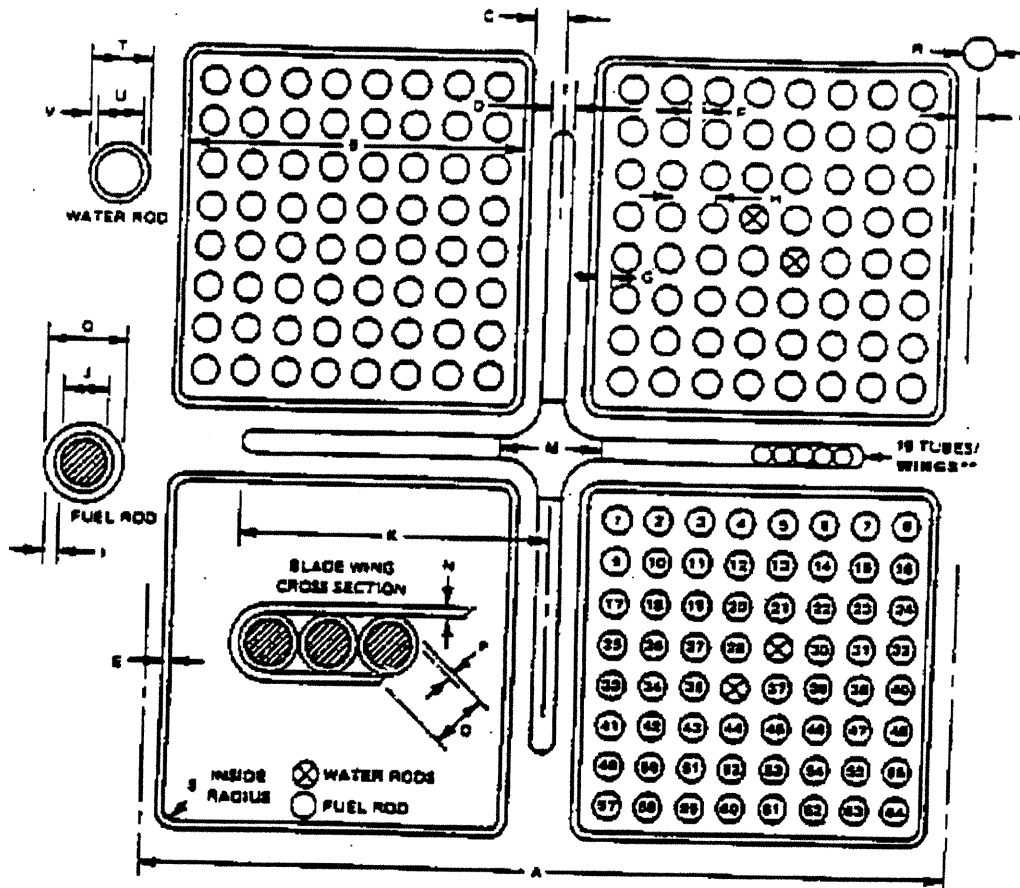
1. J. P. Fritz, "Testing of Cruciform Control Rods for BWR/6," NEDO-10565, GE APED, April 1972.
2. R. J. Benche, "Visual and Photographic Examination of Dresden 1 High Exposure Control Rod B87," NEDO-10541, April 1972.
3. R. G. Stirn et al., "Rod Drop Accident Analysis for Large Boiling Water Reactors," NEDO-10527, General Electric Co., Atomic Power Equipment Department, March 1972.
4. J. E. Benecki, "Impact Testing on Collet Assembly for Control Rod Drive Mechanism 7RD B144A," General Electric Company, Atomic Power Equipment Department, APED-5555, November 1967.
5. "Reliability Evaluation Analysis - Unit 2 Alternate Rod Insertion System", COM-0249-R-003, February 1983.



NUMBER OF FUEL ASSEMBLIES 764
 NUMBER OF CONTROL RODS 185
 NUMBER OF LPRM STRINGS 43

LA SALLE COUNTY STATION
 UPDATED FINAL SAFETY ANALYSIS REPORT

FIGURE 4.1-1
 CORE ARRANGEMENT



DIM. IDENT.	A	B	C*	D**	E*	F	G	H
DIM. INCHES	12.0	5.278	0.261	0.260	0.100	0.157	0.1575	0.640

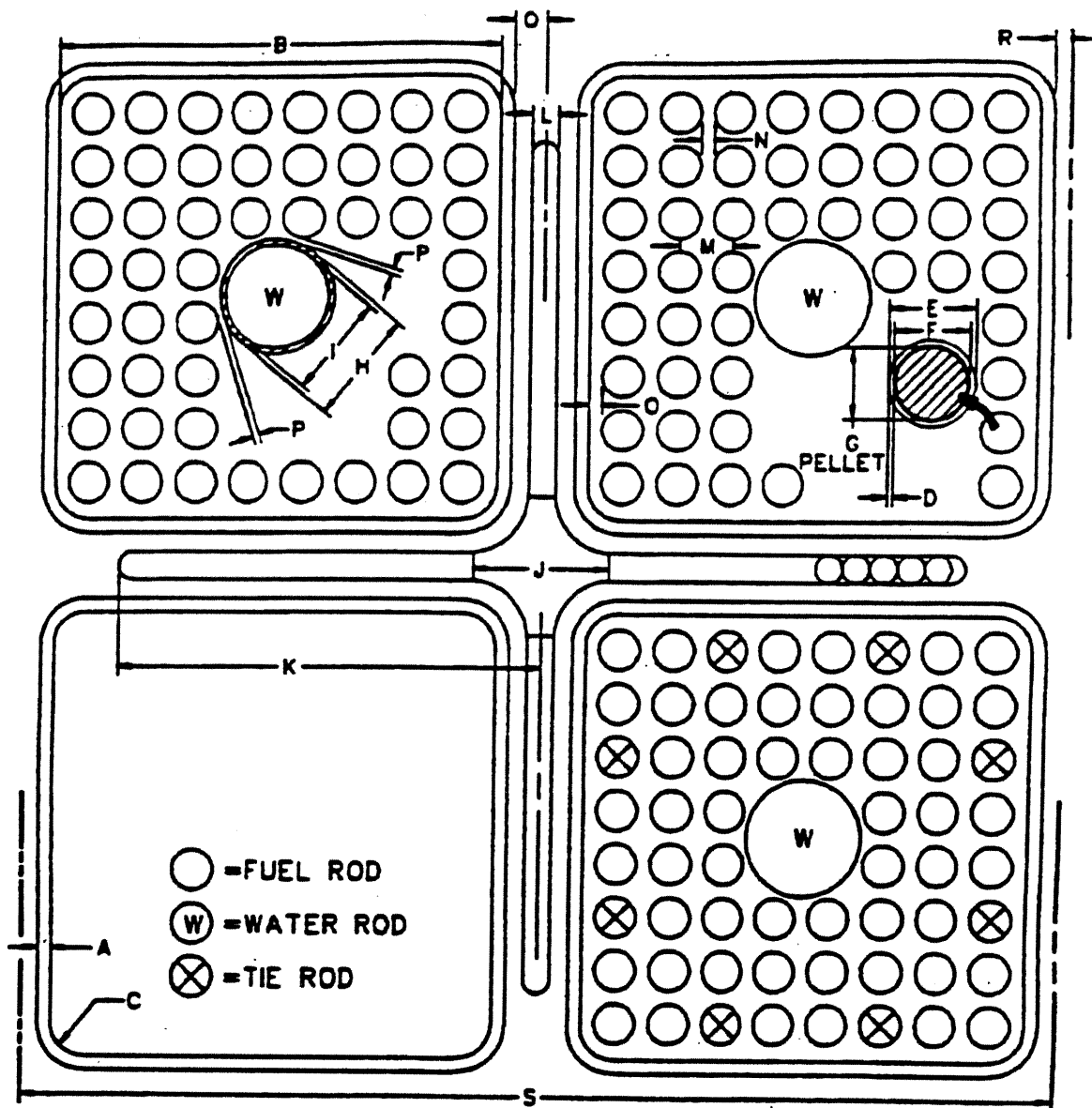
DIM. IDENT.	I	J	K**	L	M**	N**	O**	P*
DIM. INCHES	0.032	0.410	4.875		1.58	0.030	0.188	0.025

DIM. IDENT.	Q	R	S	T	U	V
DIM. INCHES	0.483	1.062	0.380	0.591	0.531	0.030

* This value is based on 100 mil channels. Channel thickness can be 80 or 100 mil.

** This data is based on GE original equipment control blades. Different control blade design are also utilized.

LASALLE COUNTY STATION
 UPDATED FINAL SAFETY ANALYSIS REPORT
 FIGURE 4.1-2
 CORE CELL GE 8X8R FUEL TYPE



DIM. I.D.	CHANNEL			FUEL ROD			PELLET	WATER ROD	
	A*	B	C	D	E	F	G	H	I
DIM. INCHES	0.100	5.278	0.380	0.032	0.483	0.419	0.411	1.340	1.260

DIM. I.D.	CONTROL ROD*			BUNDLE LATTICE				CELL*		
	J**	K**	L**	M	N	O	P	O*	R	S
DIM. INCHES	1.55	4.905	0.312	0.640	0.157	0.158	0.100	0.261	0.261	12.00

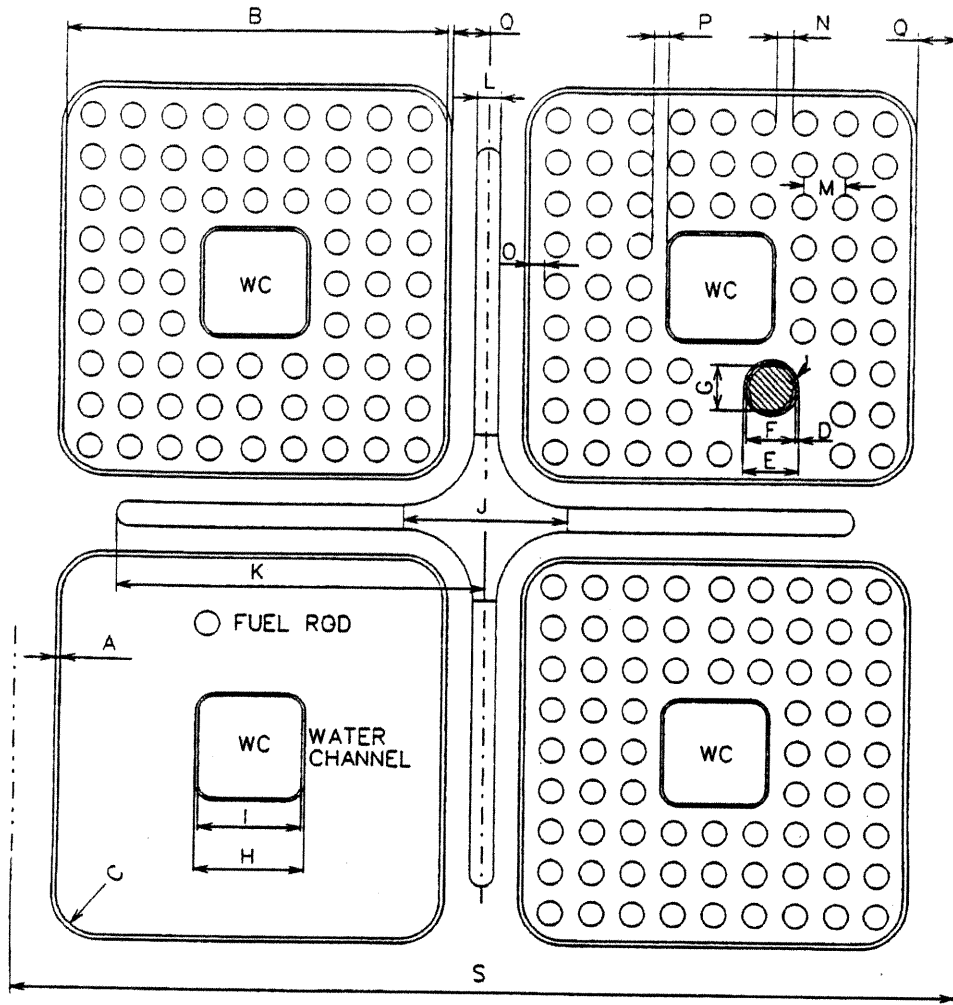
• This value is based on 100 mil channels. Channel thickness vary from 80 to 100 mil.

** This data is based on GE original equipment control blades. Different control blade designs are also utilized.

LASALLE COUNTY STATION
 UPDATED FINAL SAFETY ANALYSIS REPORT
 FIGURE 4.1-2a
 CORE CELL GE 8X8NB FUEL TYPE

LSCS-UFSAR

ATRIUM-9B DESIGN



	CHANNEL			FUEL ROD			PELLET	WATER CHANNEL	
DIM. I.D.	A**	B	C	D	E	F	G	H	I
DIM INCHES	0.080	5.278	0.380	*	*	*	*	*	*

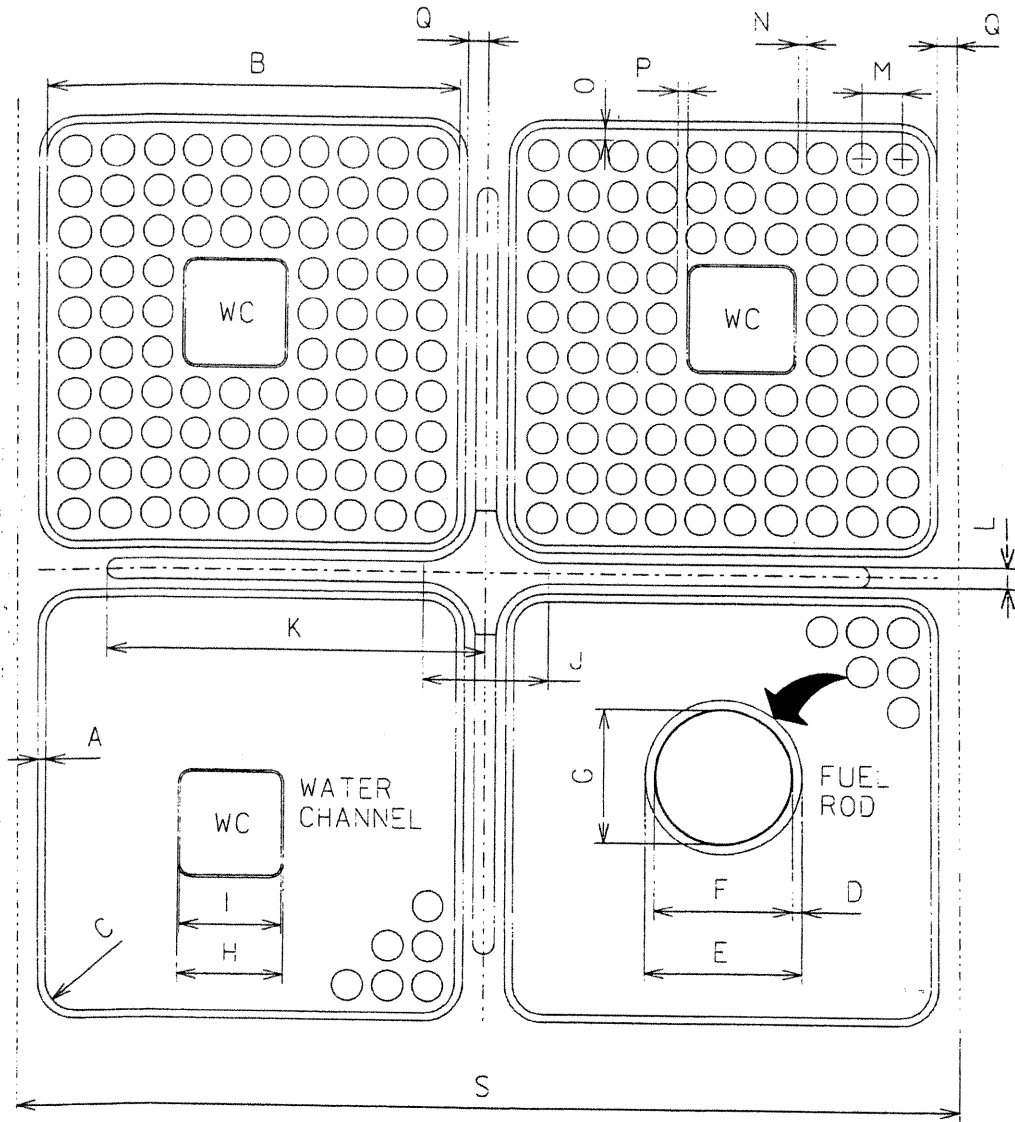
	CONTROL BLADE*			BUNDLE LATTICE				CELL*	
DIM. I.D.	J	K	L	M	N	O	P	Q**	S
DIM INCHES	1.58	4.875	0.260	*	*	*	*	0.281	12.00

*See Reference 25.

**This value is based on 80 mil channels. Channel thickness can be 80 or 100 mil.

LASALLE COUNTY STATION
 UPDATED FINAL SAFETY ANALYSIS REPORT
 FIGURE 4.1-2b
 CORE CELL FANP ATRIUM-9B FUEL

LSCS-UFSAR



FSTC01601.DGN

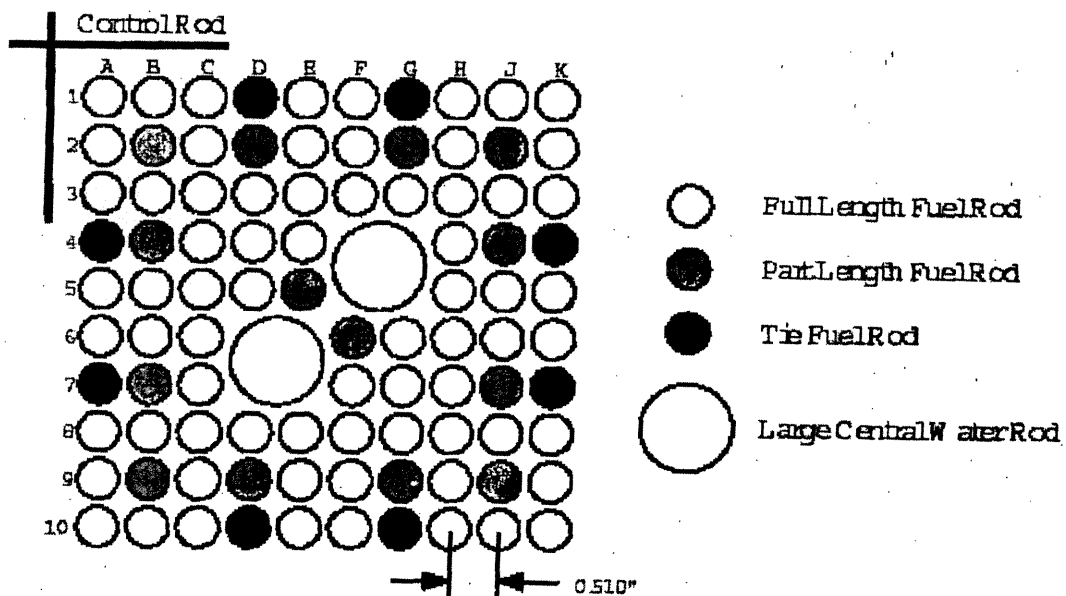
	CHANNEL			FUEL ROD			PELLET	WATER CHANNEL	
DIM I.D.	A	B	C	D	E	F	G	H	I
DIM INCHES	0.100	5.278	0.38	*	*	*	*	*	*
	CONTROL BLADE			BUNDLE LATTICE				CELL	
DIM I.D.	J	K	L	M	N	O	P	Q	S
DIM INCHES	1.58	4.875	0.260	*	*	*	*	0.261	12.0

* See Reference 26

LASALLE COUNTY STATION
 UPDATED FINAL SAFETY ANALYSIS REPORT

FIGURE 4.1-2c

CORE CELL FANP ATRIUM-10 FUEL

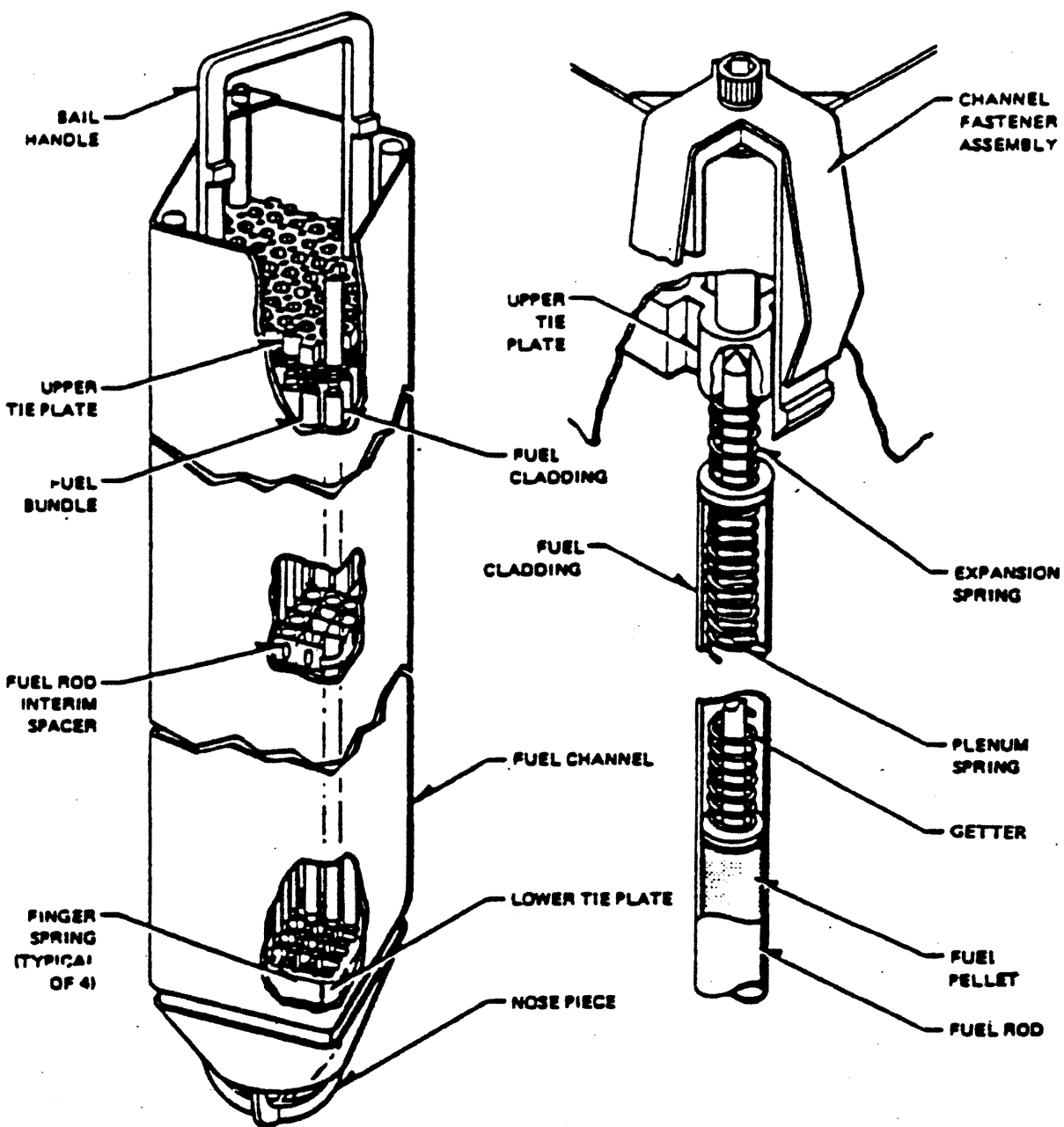


Notes: 1) View of bundle lattice looking down from top.
 2) Channel fastener is at A1 corner.

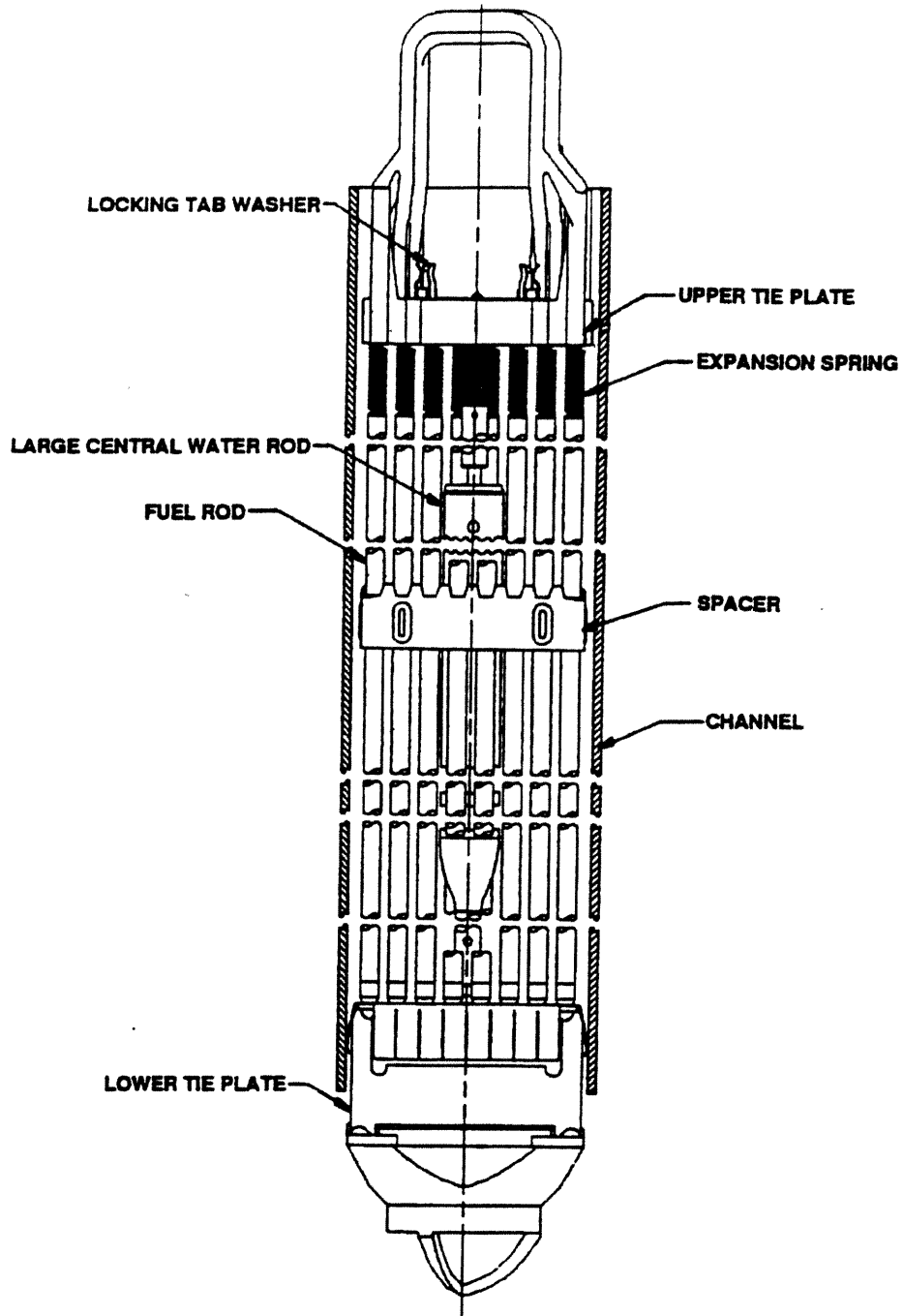
LASALLE COUNTY STATION
 UPDATED FINAL SAFETY ANALYSIS REPORT

FIGURE 4.1-2d

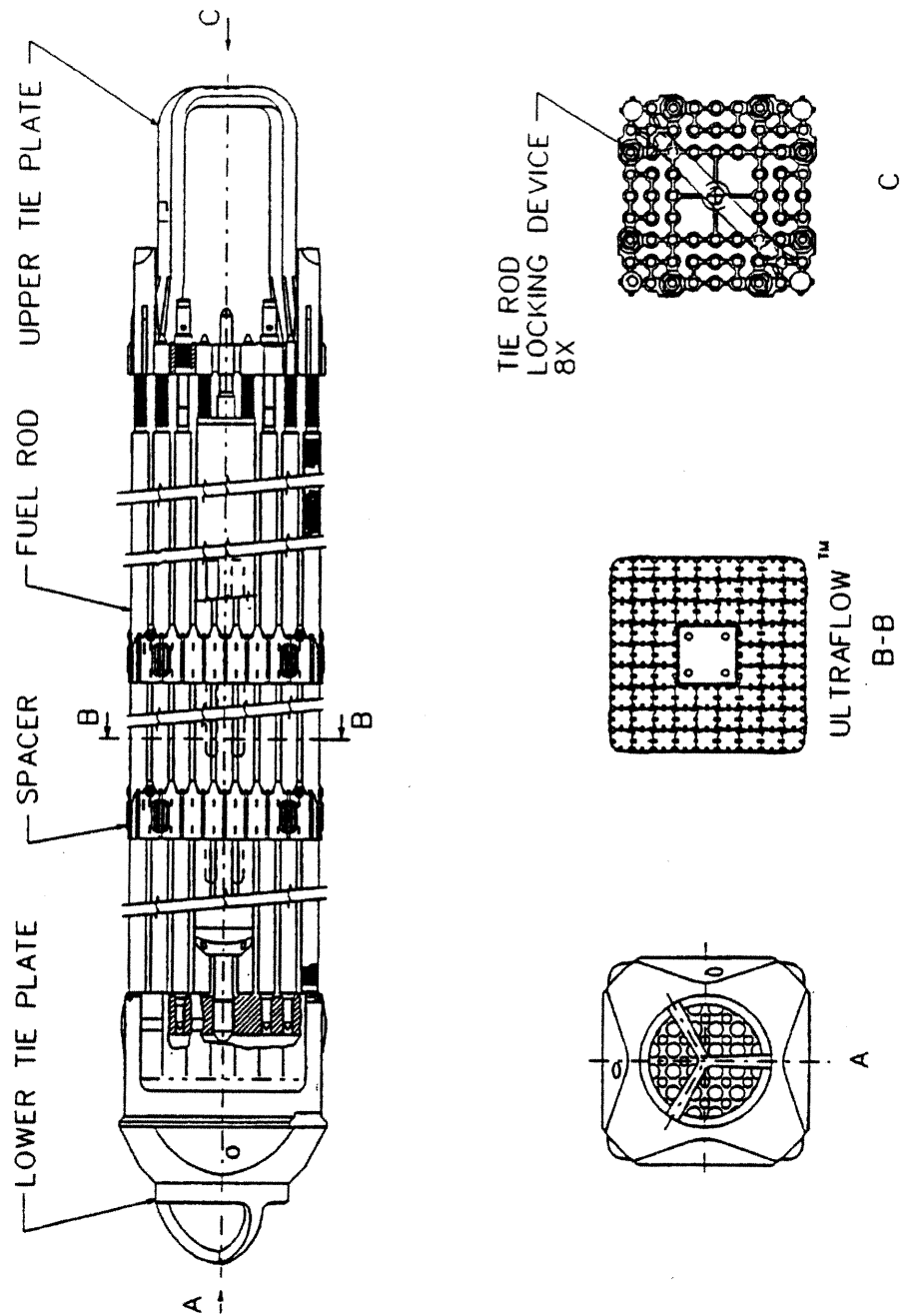
GE14 LATTICE ARRANGEMENT



LASALLE COUNTY STATION
UPDATED FINAL SAFETY ANALYSIS REPORT
FIGURE 4.1-3
(TYPICAL) FUEL ASSEMBLY (GE 8X8R SHOWN)



LASALLE COUNTY STATION UPDATED FINAL SAFETY ANALYSIS REPORT
FIGURE 4.1-3a
FUEL ASSEMBLY GE 8x8NB FUEL TYPE

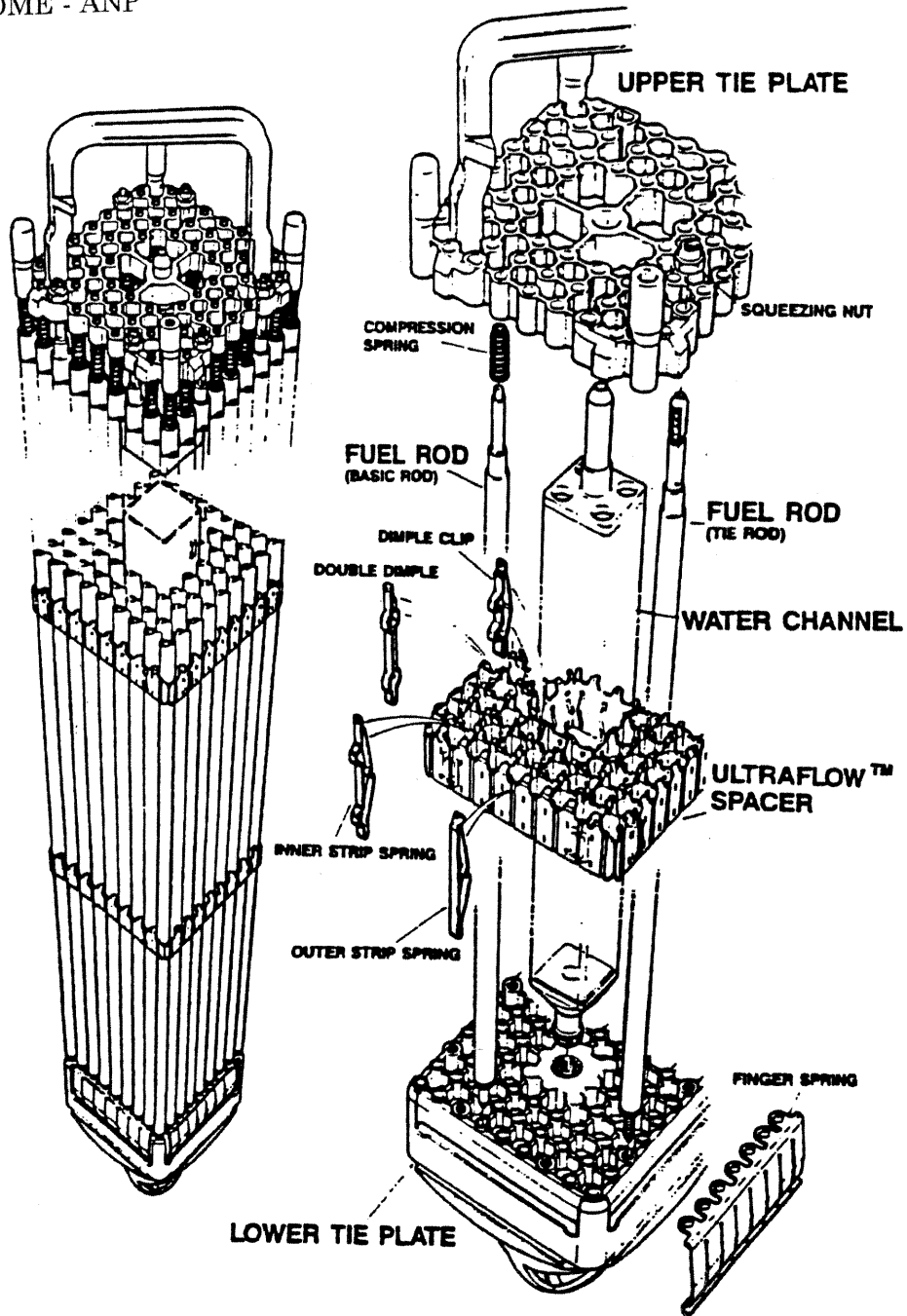


LASALLE COUNTY STATION
UPDATED FINAL SAFETY ANALYSIS REPORT

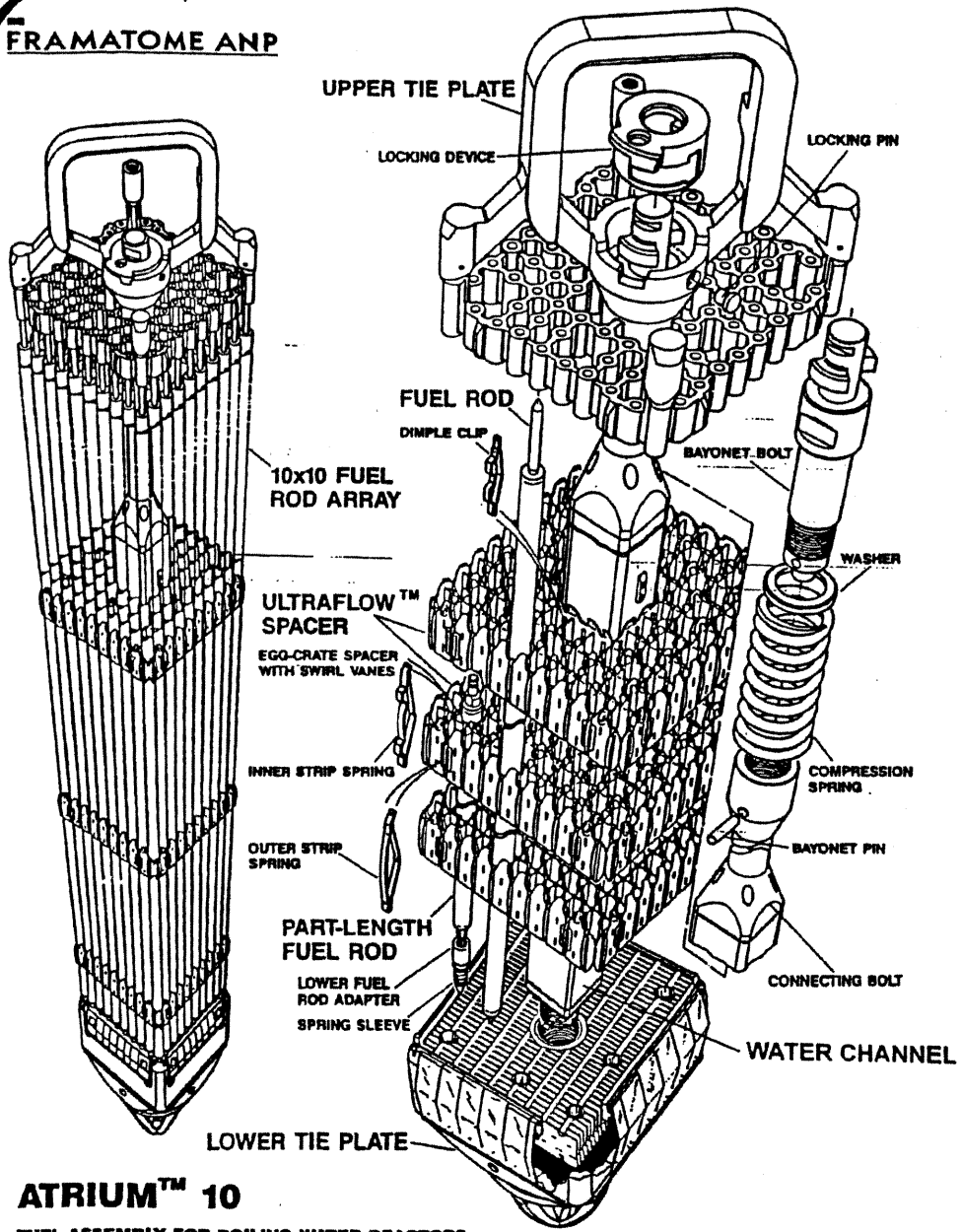
FIGURE 4.1-3b

FUEL ASSEMBLY FANP ATRIUM-9B FUEL

FRAMATOME - ANP



LASALLE COUNTY STATION
UPDATED FINAL SAFETY ANALYSIS REPORT
FIGURE 4.1-3c
FUEL ASSEMBLY FANP ATRIUM-9B FUEL



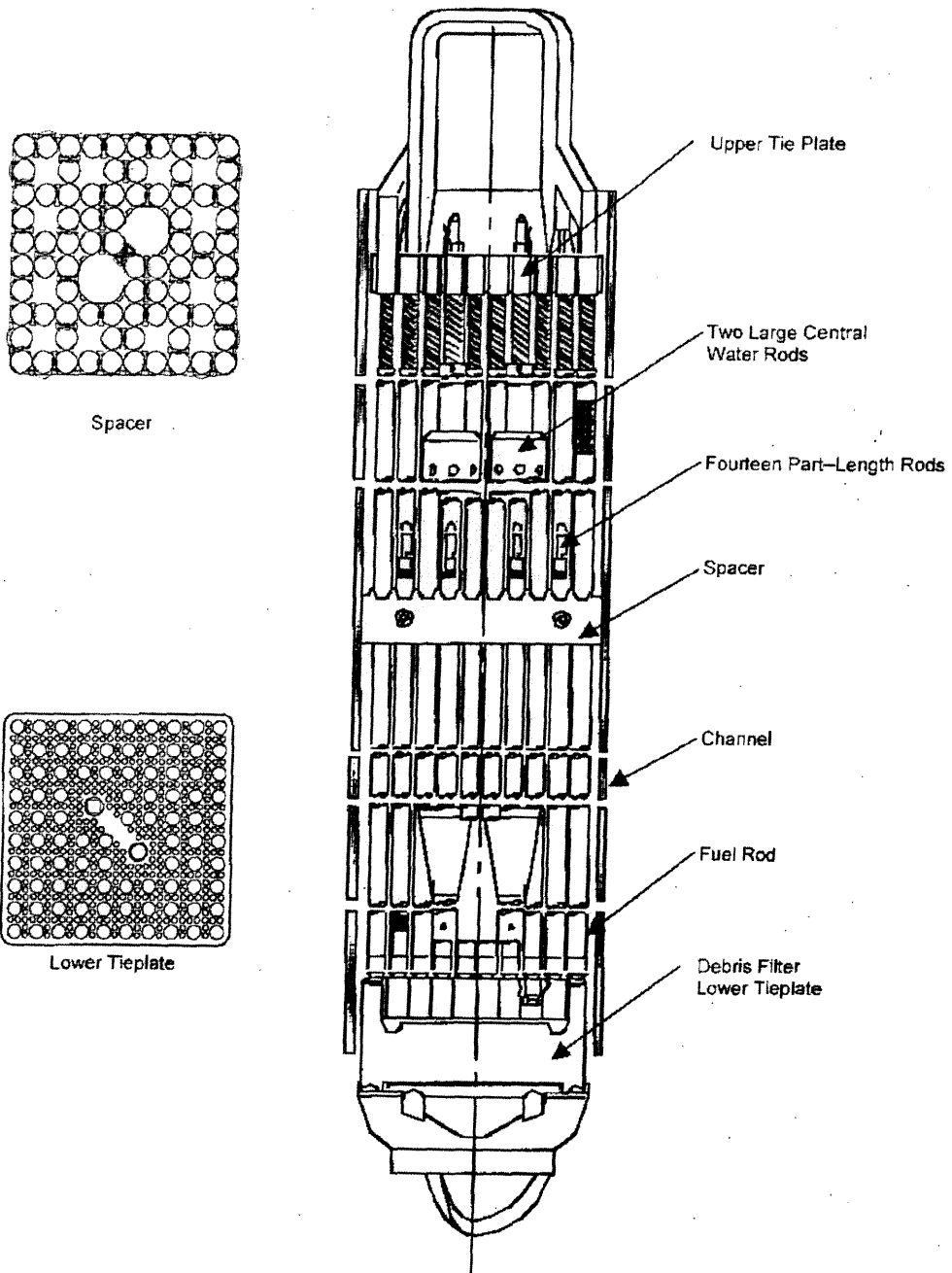
ATRIUM™ 10

FUEL ASSEMBLY FOR BOILING WATER REACTORS

LASALLE COUNTY STATION
UPDATED FINAL SAFETY ANALYSIS REPORT

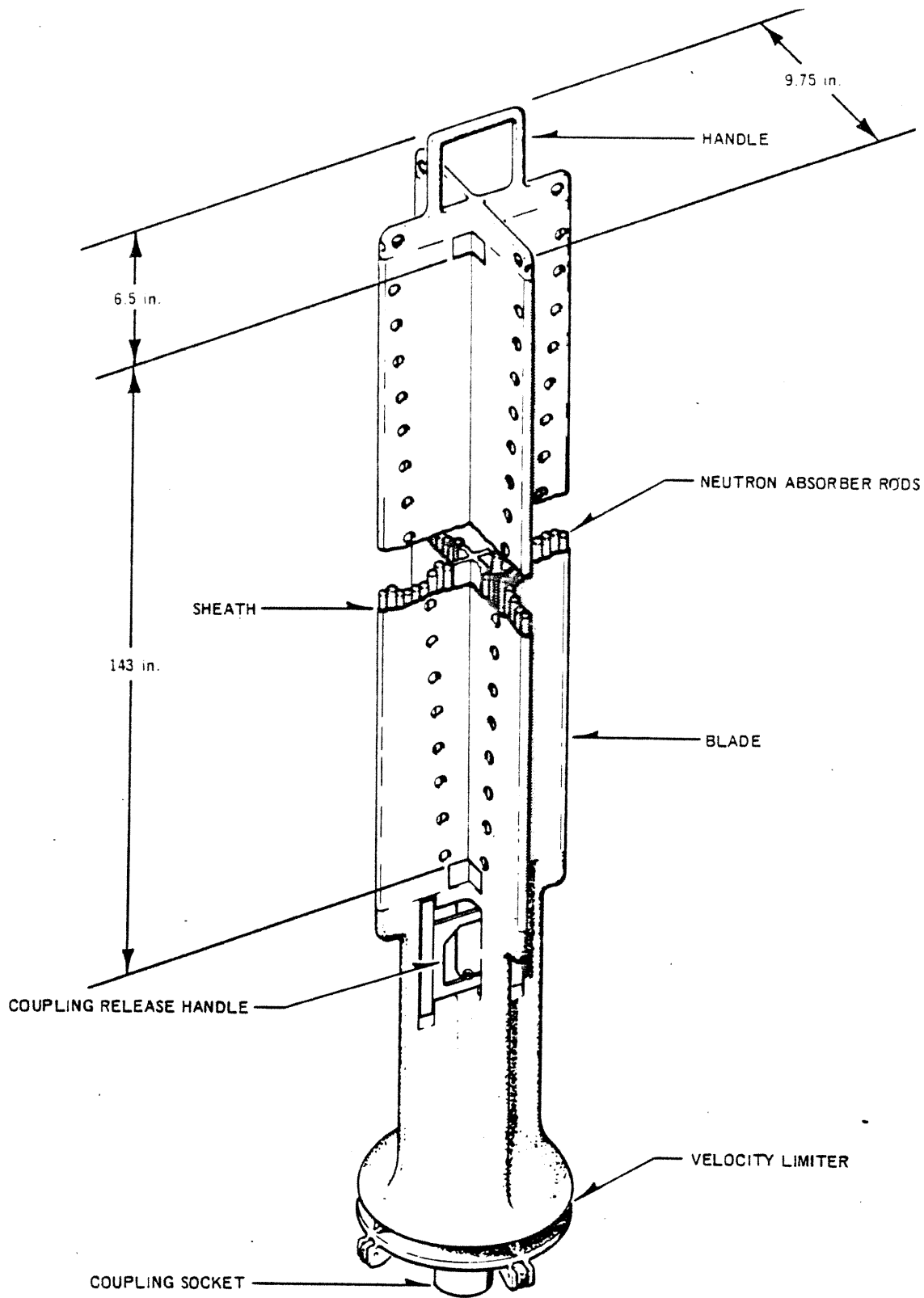
FIGURE 4.1-3d

FUEL ASSEMBLY FANP ATRIUM-10 FUEL



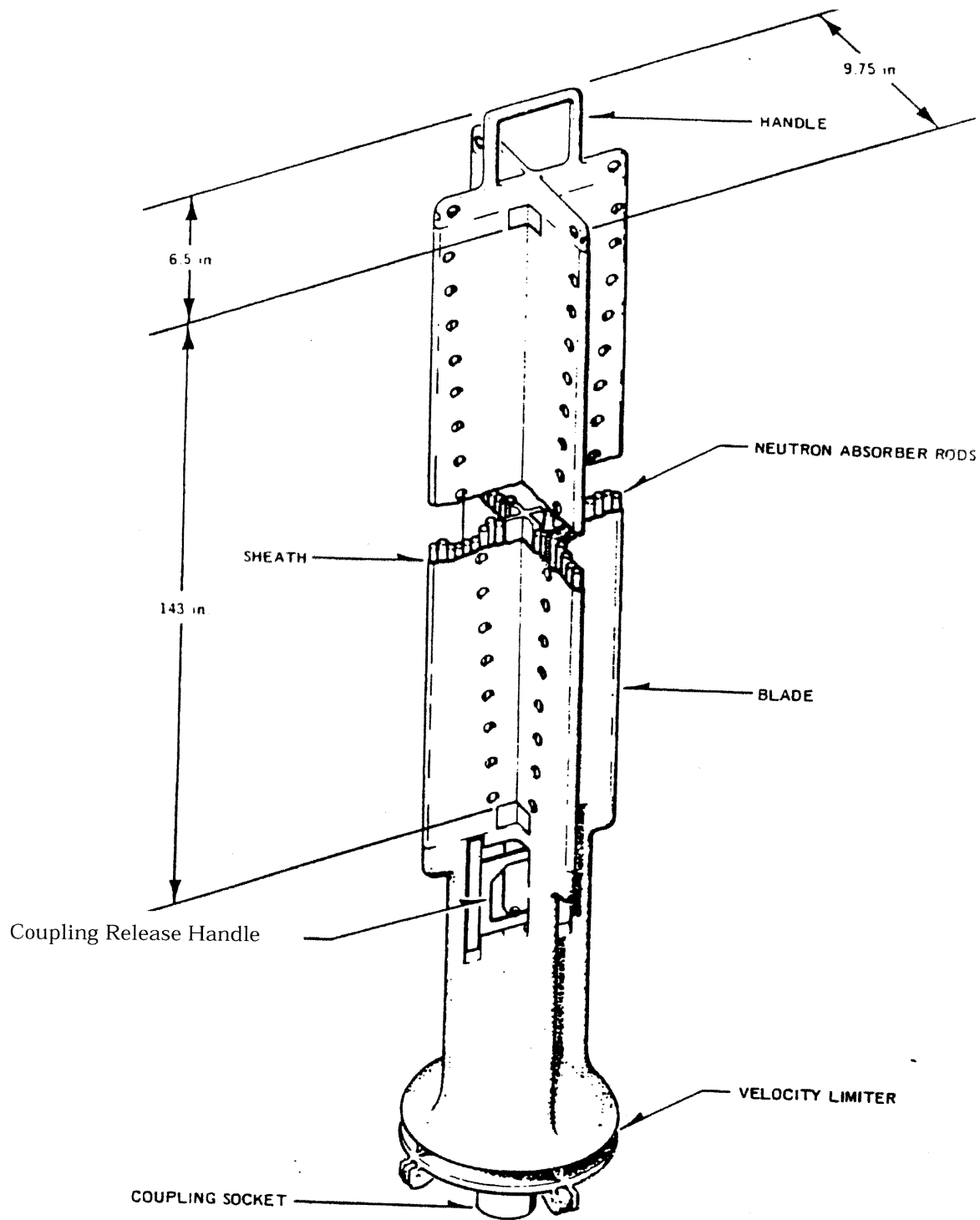
LASALLE COUNTY STATION
UPDATED FINAL SAFETY ANALYSIS REPORT

FIGURE 4.1-3e
GE14 Fuel Bundle (Typical)

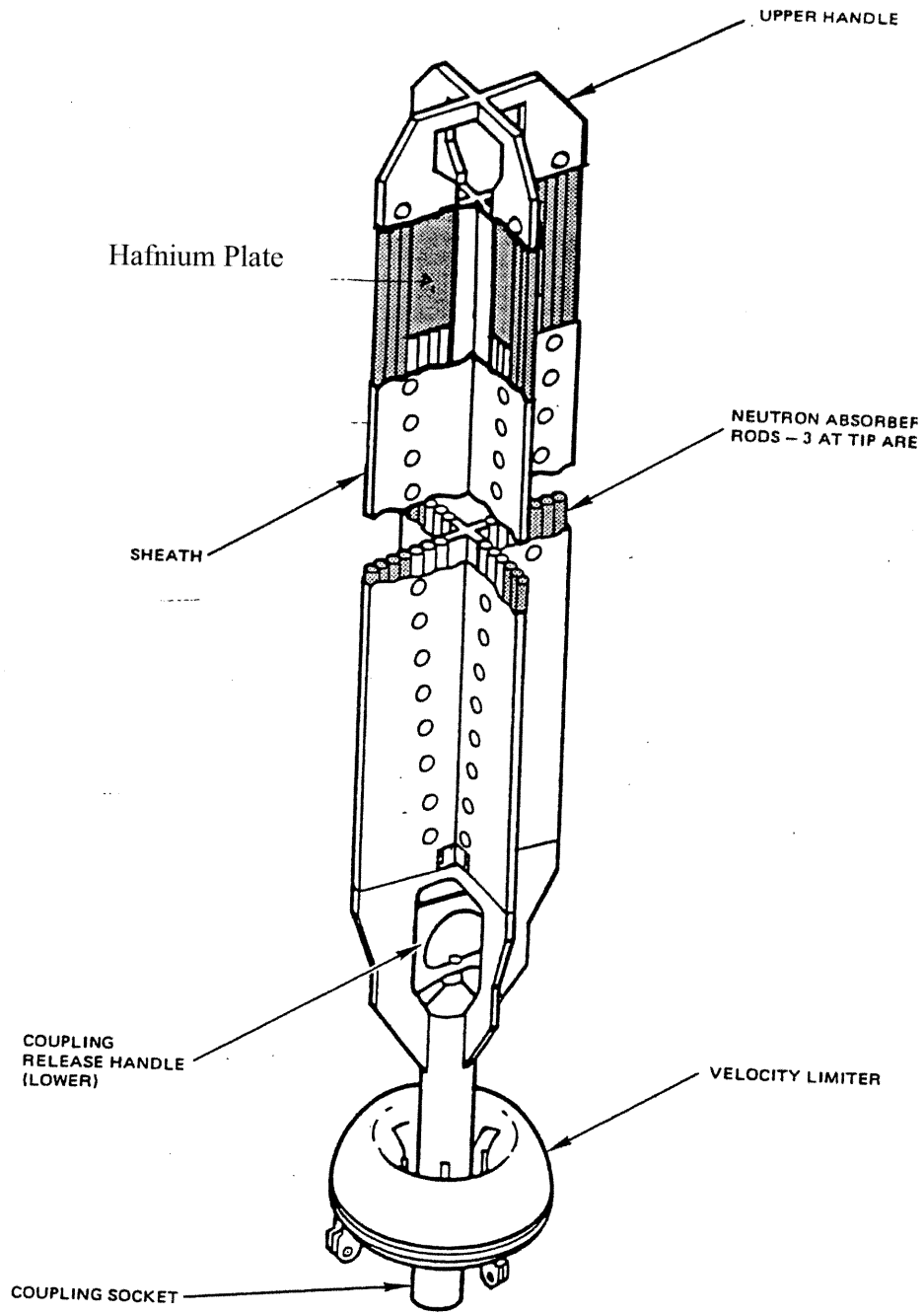


LA SALLE COUNTY STATION
 UPDATED FINAL SAFETY ANALYSIS REPORT

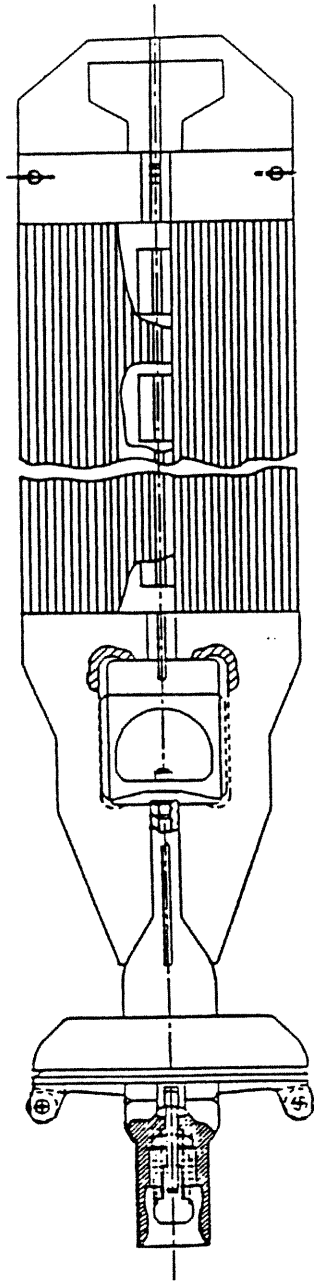
FIGURE 4.1-4
 GENERAL ELECTRIC
 CONTROL ROD ASSEMBLY



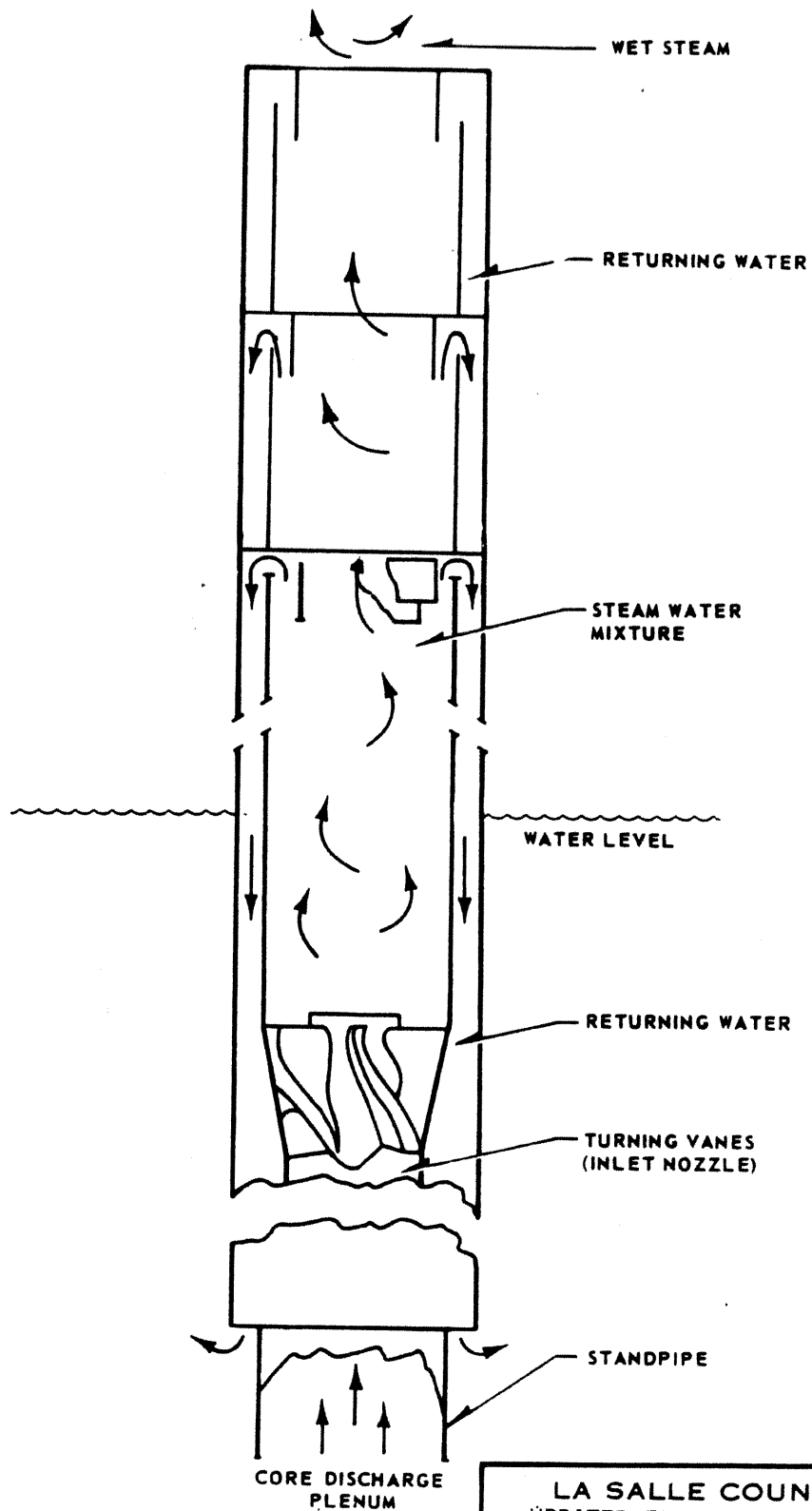
LASALLE COUNTY STATION UPDATED FINAL SAFETY ANALYSIS REPORT
FIGURE 4.1-4a GENERAL ELECTRIC ORIGINAL EQUIPMENT CONTROL ROD ASSEMBLY



LASALLE COUNTY STATION UPDATED FINAL SAFETY ANALYSIS REPORT
FIGURE 4.1-4b GENERAL ELECTRIC TYPICAL DURALIFE 215 CONTROL ROD ASSEMBLY

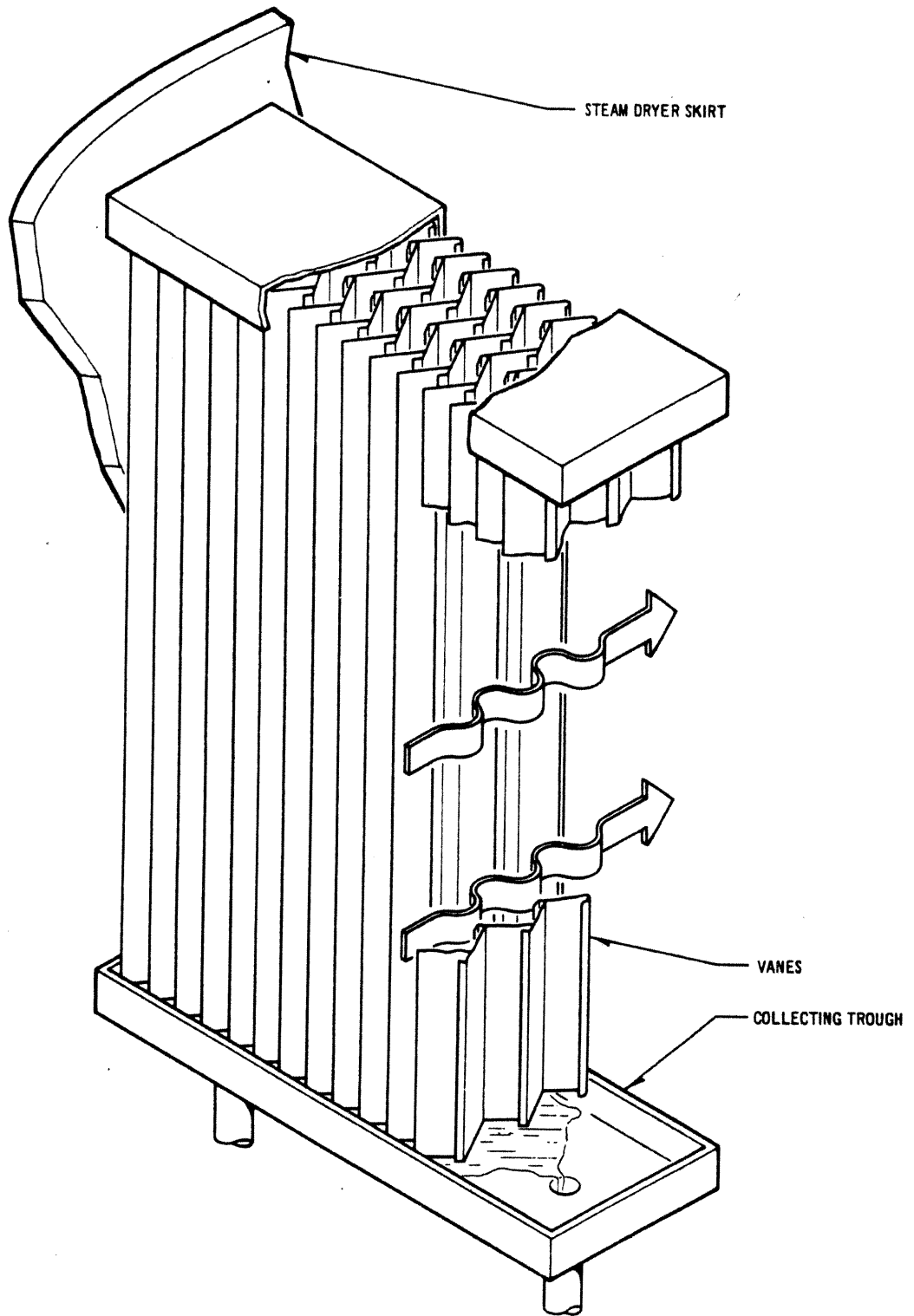


LASALLE COUNTY STATION UPDATED FINAL SAFETY ANALYSIS REPORT
FIGURE 4.1-4c GENERAL ELECTRIC TYPICAL MARATHON CONTROL ROD ASSEMBLY



LA SALLE COUNTY STATION
 UPDATED FINAL SAFETY ANALYSIS REPORT

FIGURE 4.1-5
 STEAM SEPARATOR

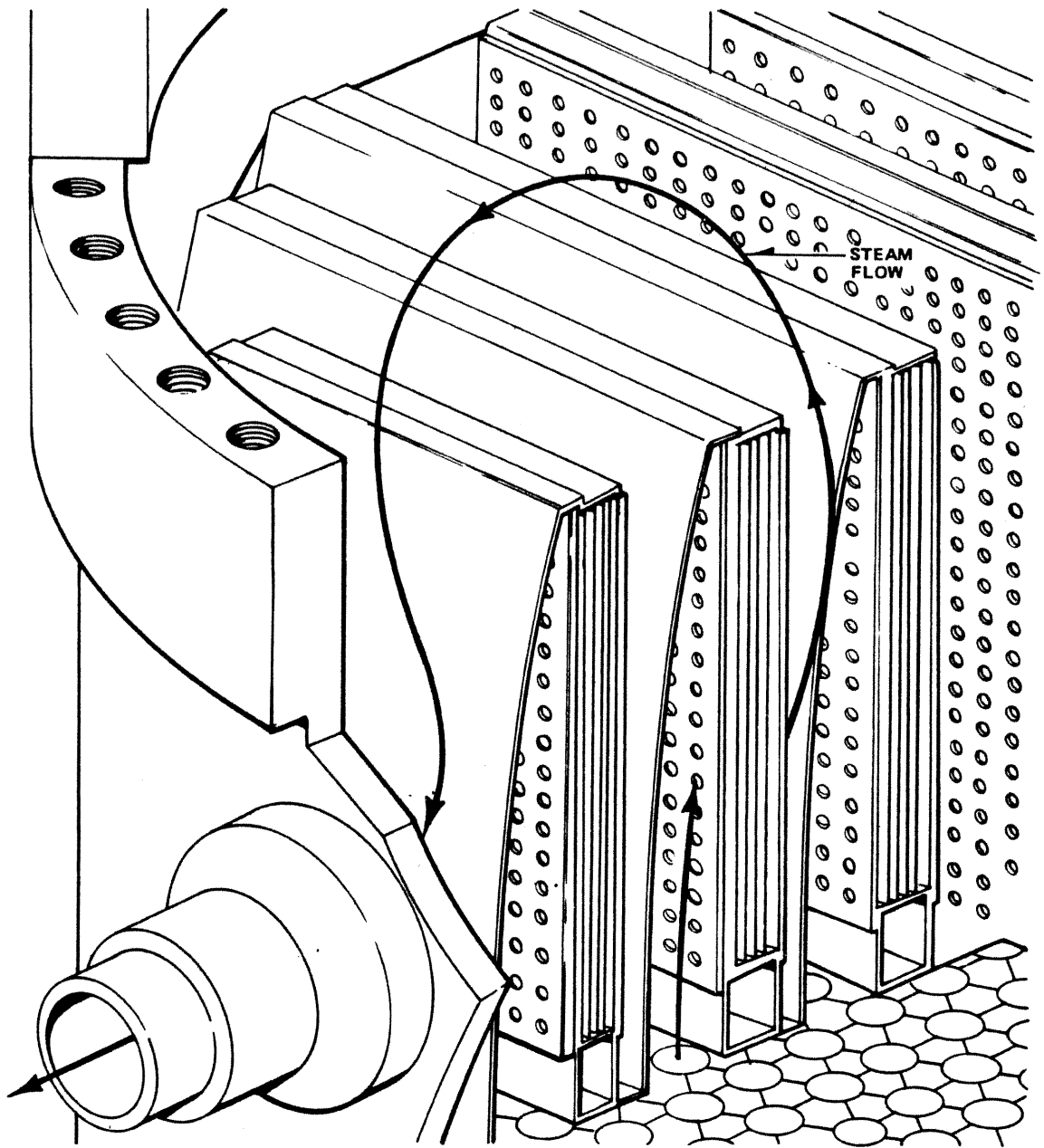


LA SALLE COUNTY STATION
UPDATED FINAL SAFETY ANALYSIS REPORT

FIGURE 4.1-6

STEAM DRYER

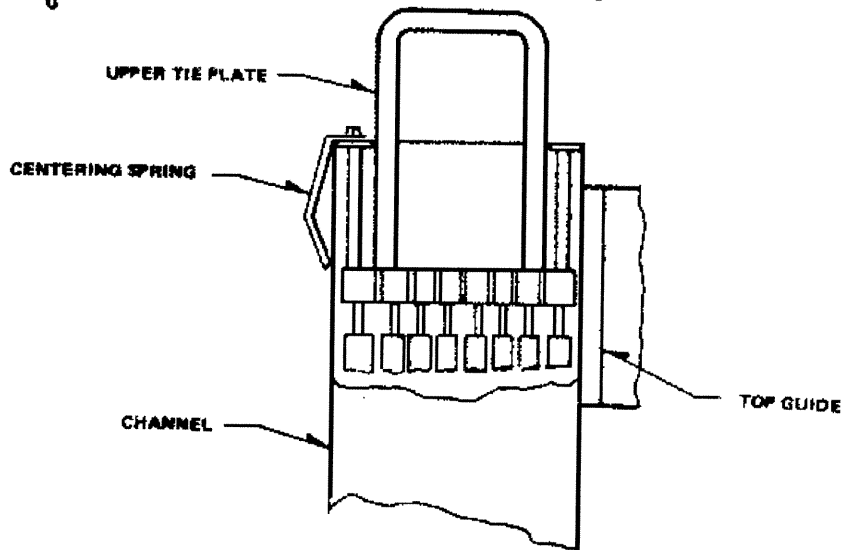
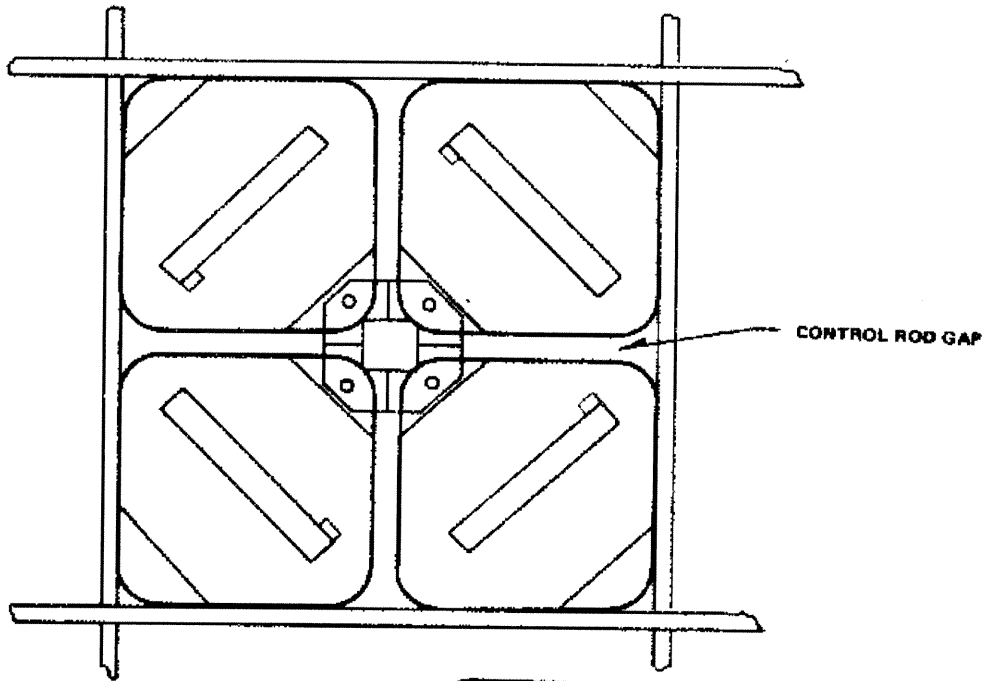
REV. 0 - APRIL 1984



LA SALLE COUNTY STATION
UPDATED FINAL SAFETY ANALYSIS REPORT

FIGURE 4.1-7
STEAM DRYER PANEL

REV. 0 - APRIL 1984

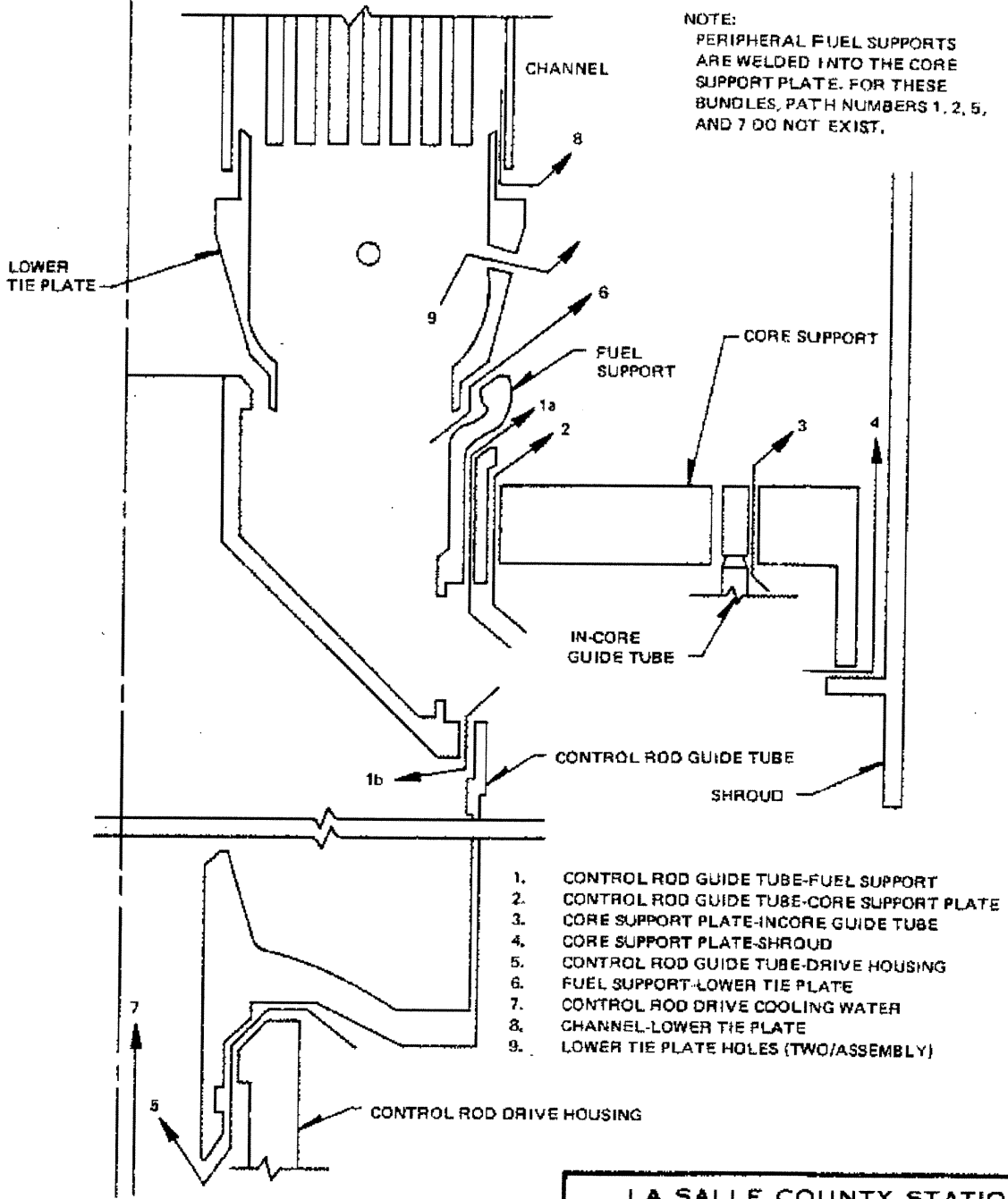


LA SALLE COUNTY STATION
 UPDATED FINAL SAFETY ANALYSIS REPORT

FIGURE 4.2-1
 SCHEMATIC OF FOUR BUNDLE
 CELL ARRANGEMENT

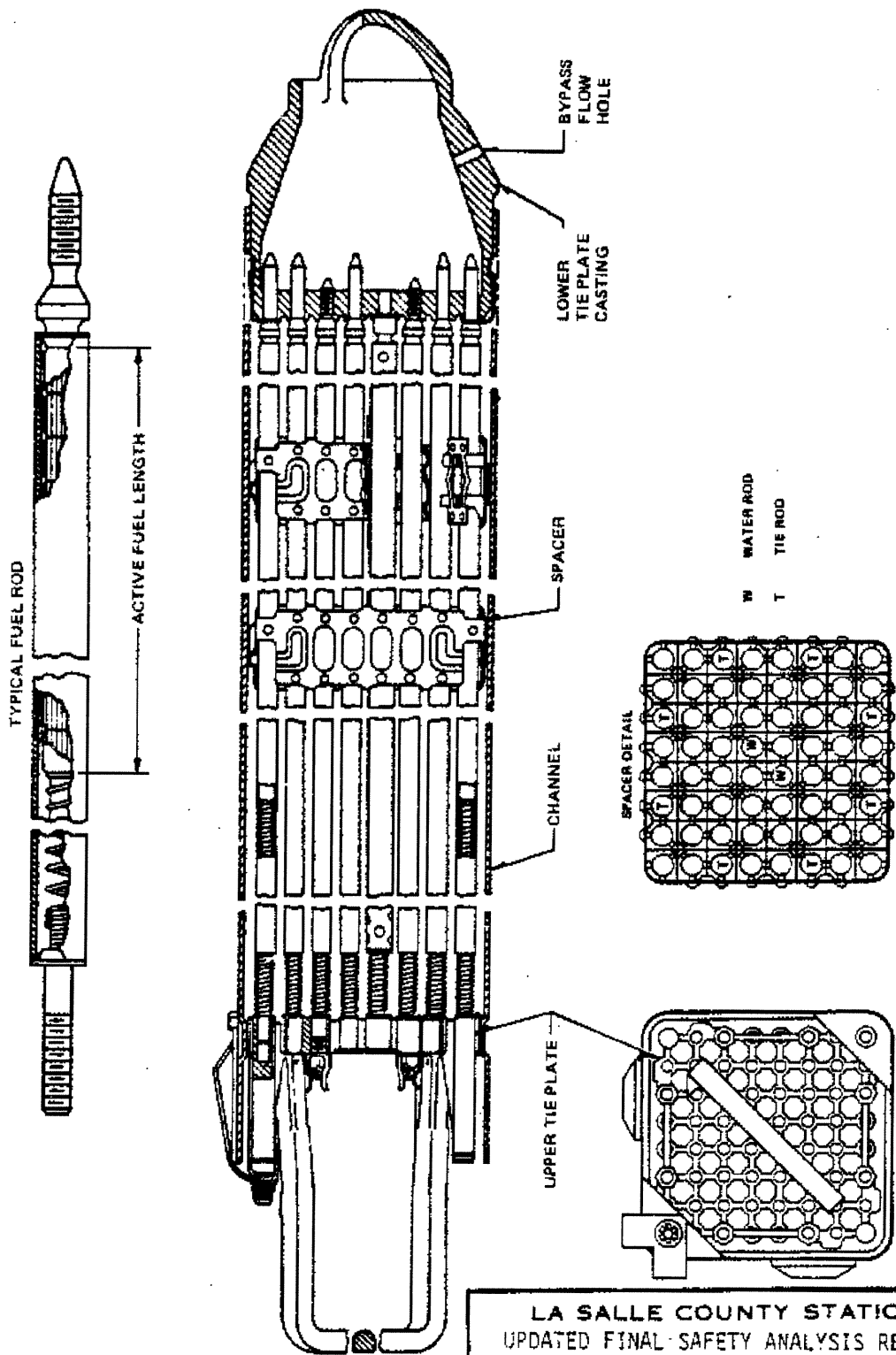
REV. 0 - APRIL 1984

SCHMATIC OF REACTOR ASSEMBLY SHOWING THE LEAKAGE FLOW PATHS



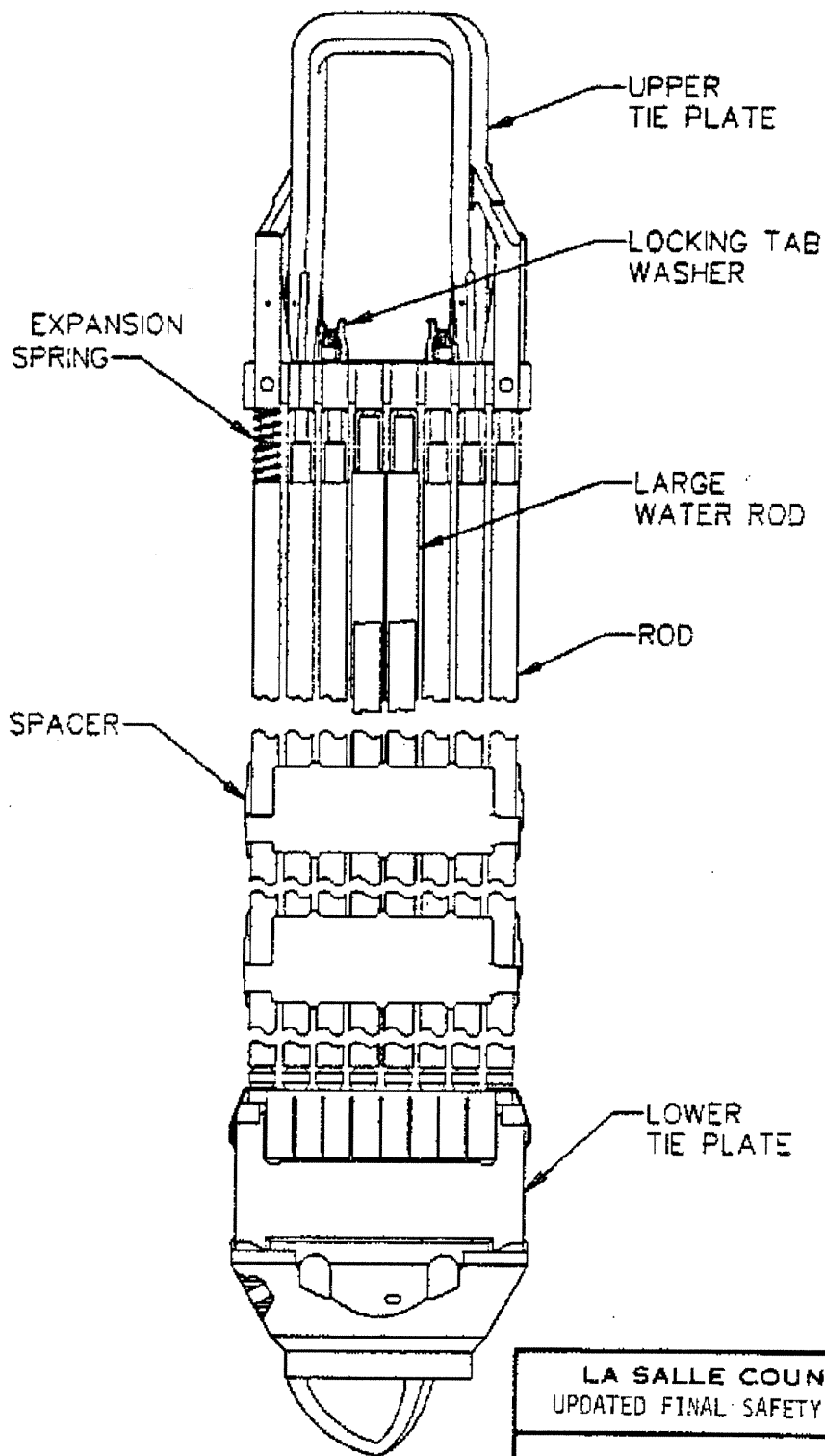
LA SALLE COUNTY STATION
UPDATED FINAL SAFETY ANALYSIS REPORT

FIGURE 4.2-2
BYPASS FLOW PATHS



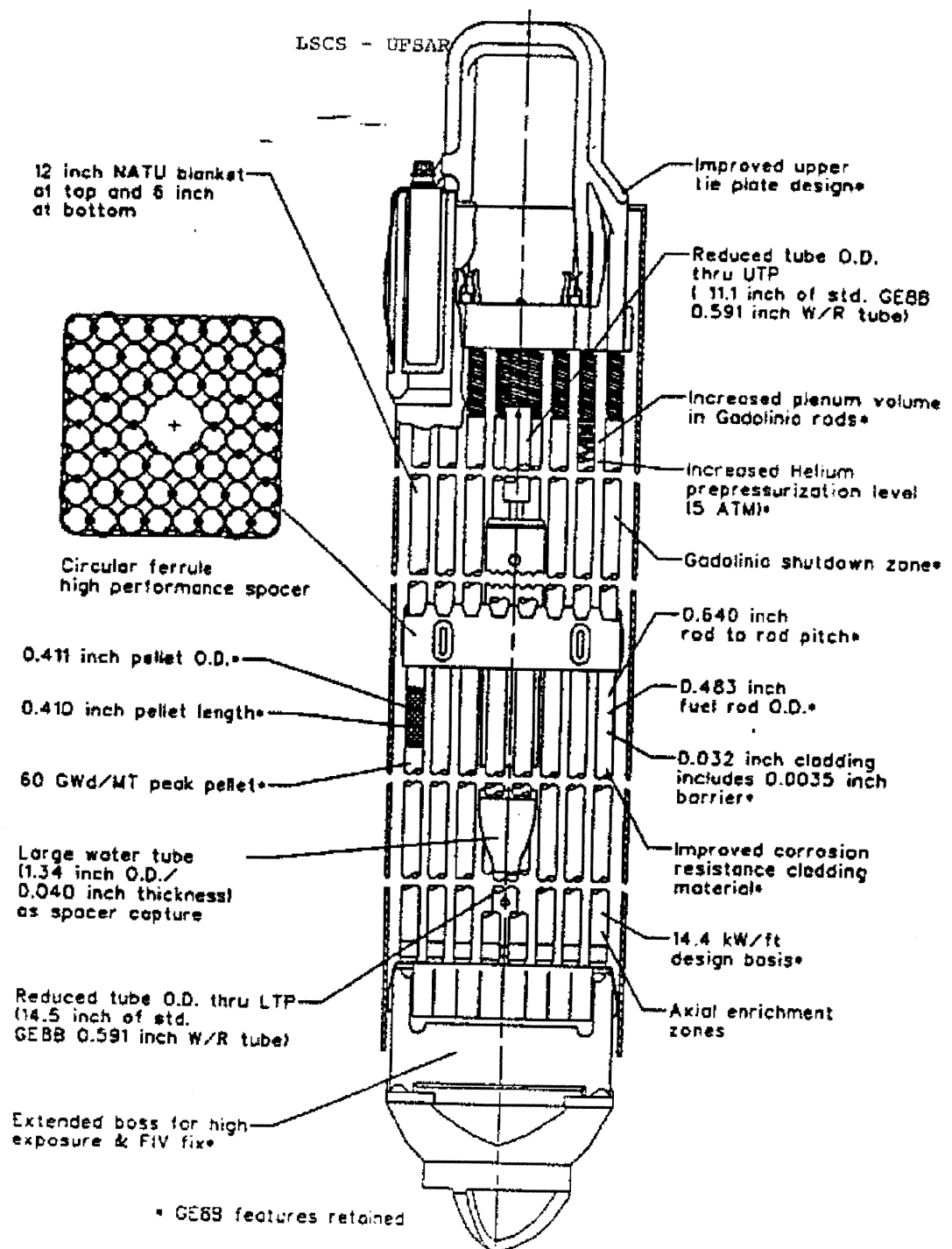
LA SALLE COUNTY STATION
 UPDATED FINAL SAFETY ANALYSIS REPORT

FIGURE 4.2-3
 FUEL BUNDLE
 8X8R AND 8P8X8R FUEL TYPES



LA SALLE COUNTY STATION
 UPDATED FINAL SAFETY ANALYSIS REPORT

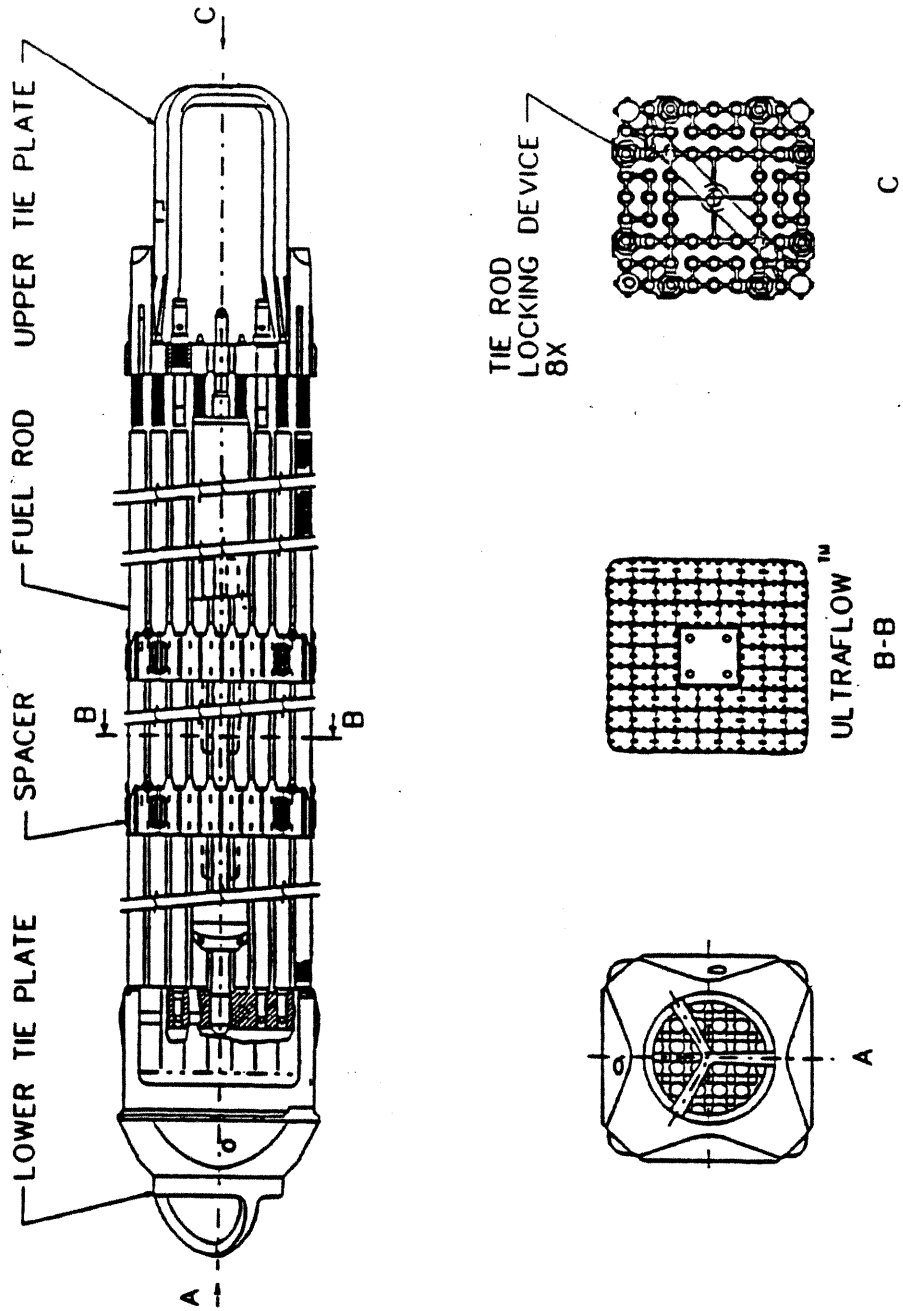
FIGURE 4.2-3a
 FUEL BUNDLE
 GE 8X8B3 FUEL TYPE



LA SALLE COUNTY STATION
 UPDATED FINAL SAFETY ANALYSIS REPORT

FIGURE 4.2-3b

Fuel Bundle
 GE BX8NB Fuel Type

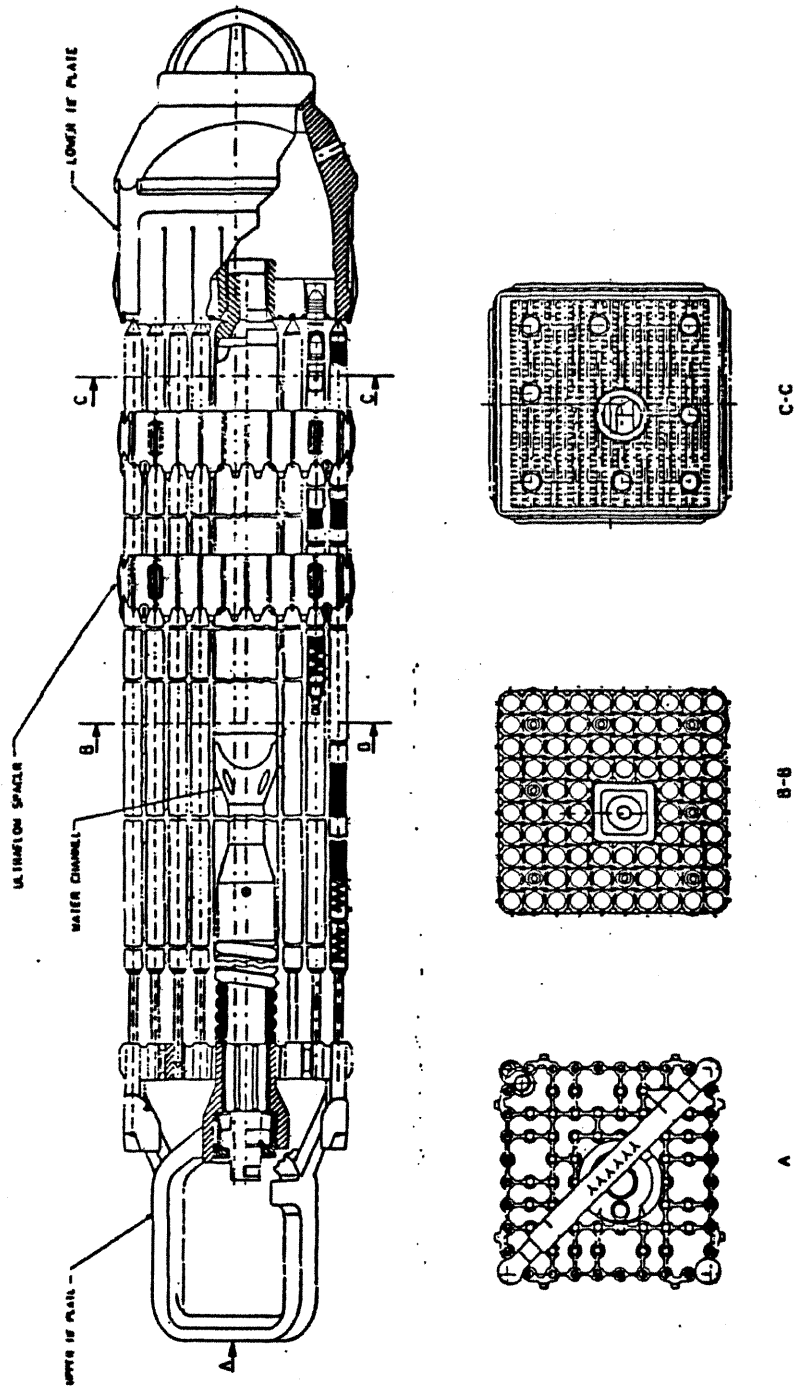


LASALLE COUNTY STATION
UPDATED FINAL SAFETY ANALYSIS REPORT

FIGURE 4.2-3c

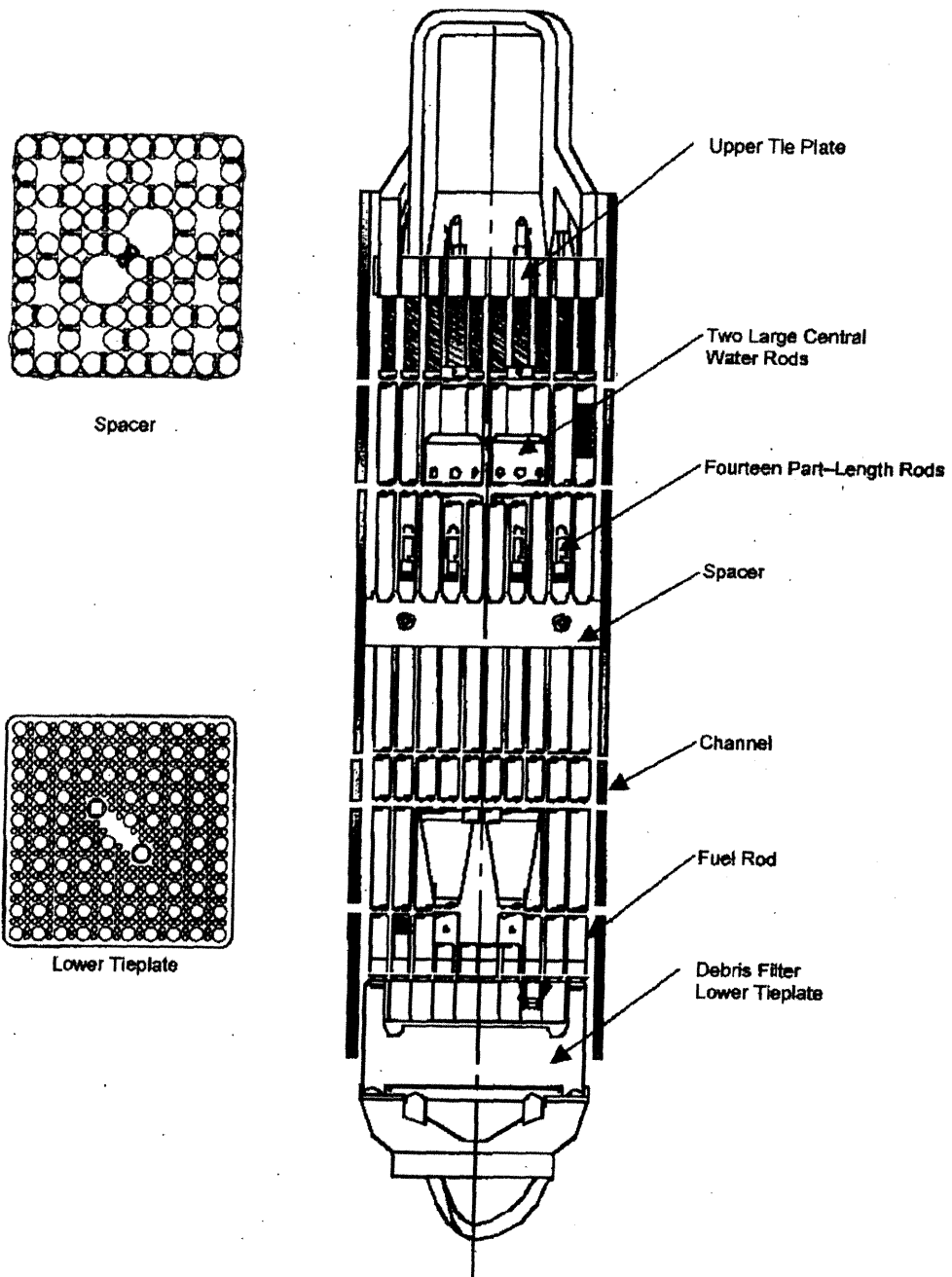
FUEL BUNDLE FANP ATRIUM-9B TYPE

LSCS-UFSAR



LASALLE COUNTY STATION
UPDATED FINAL SAFETY ANALYSIS REPORT
FIGURE 4.2-3d
FUEL BUNDLE FANP ATRIUM-10 TYPE

LSCS-UFSAR



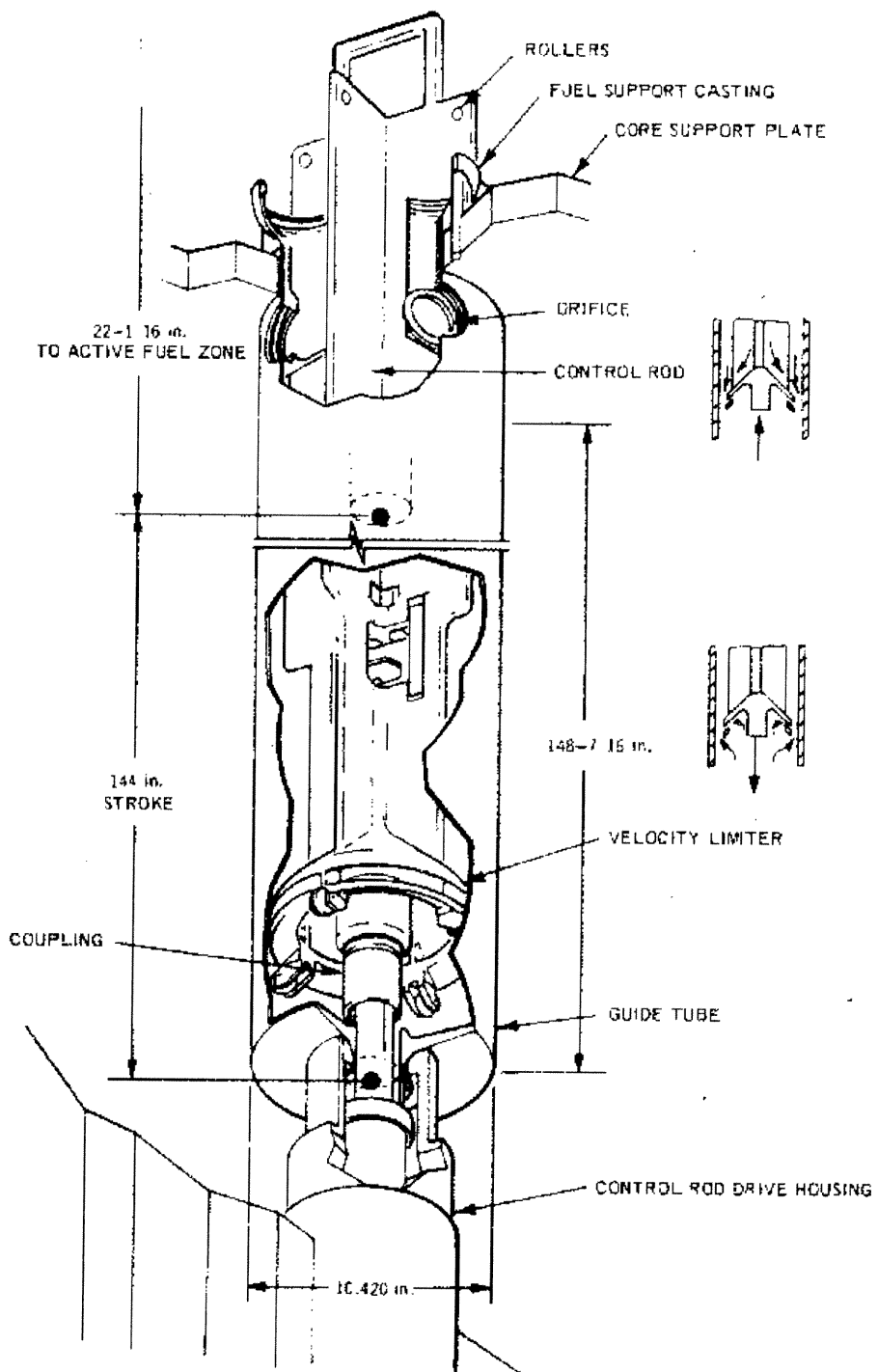
LASALLE COUNTY STATION
UPDATED FINAL SAFETY ANALYSIS REPORT

FIGURE 4.2-3e

GE14 Fuel Bundle (Typical)

Page Intentionally Left Blank

LASALLE COUNTY STATION UPDATED FINAL SAFETY ANALYSIS REPORT
FIGURE 4.2-4
DELETED

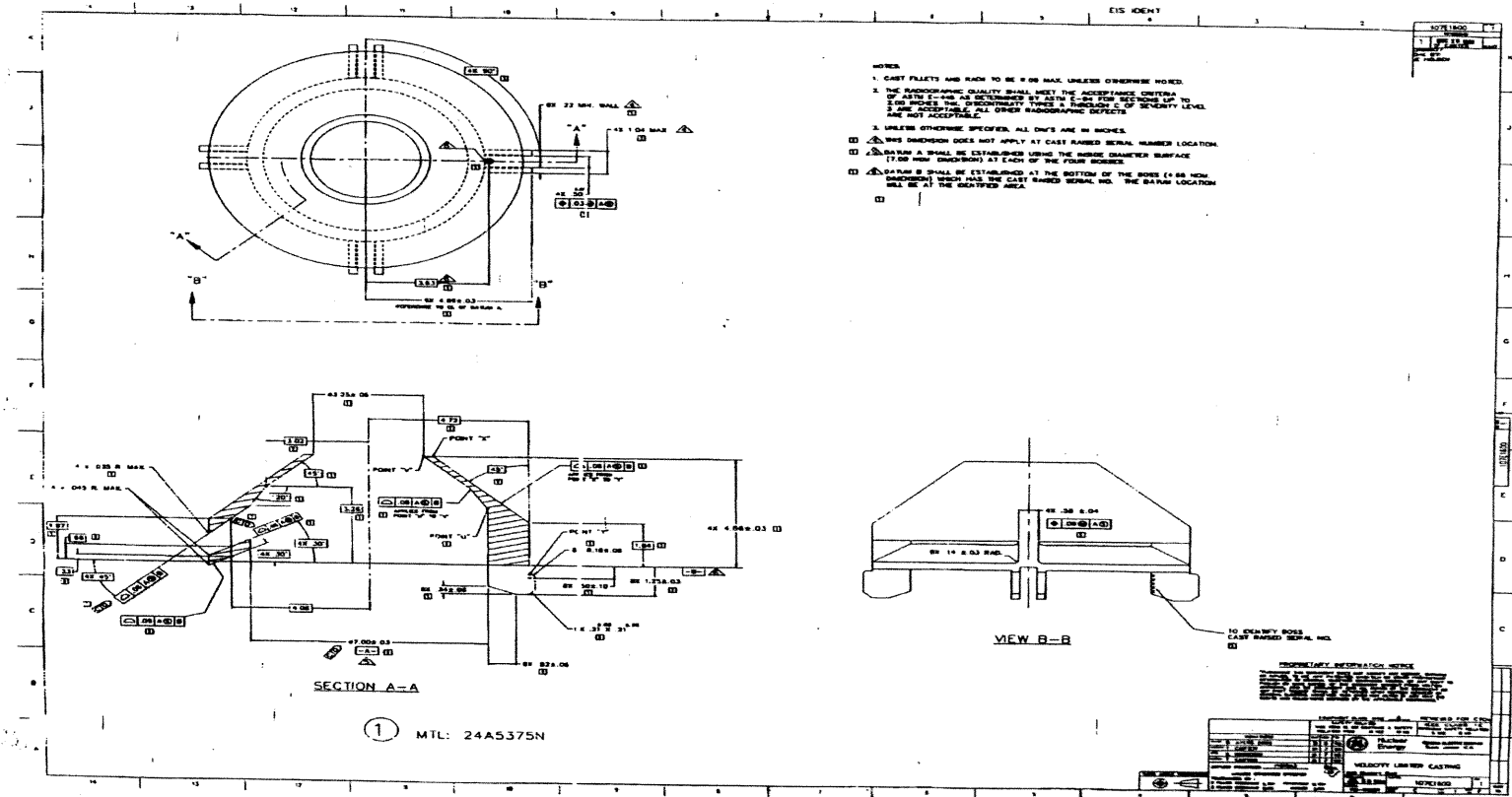


LA SALLE COUNTY STATION
 UPDATED FINAL SAFETY ANALYSIS REPORT

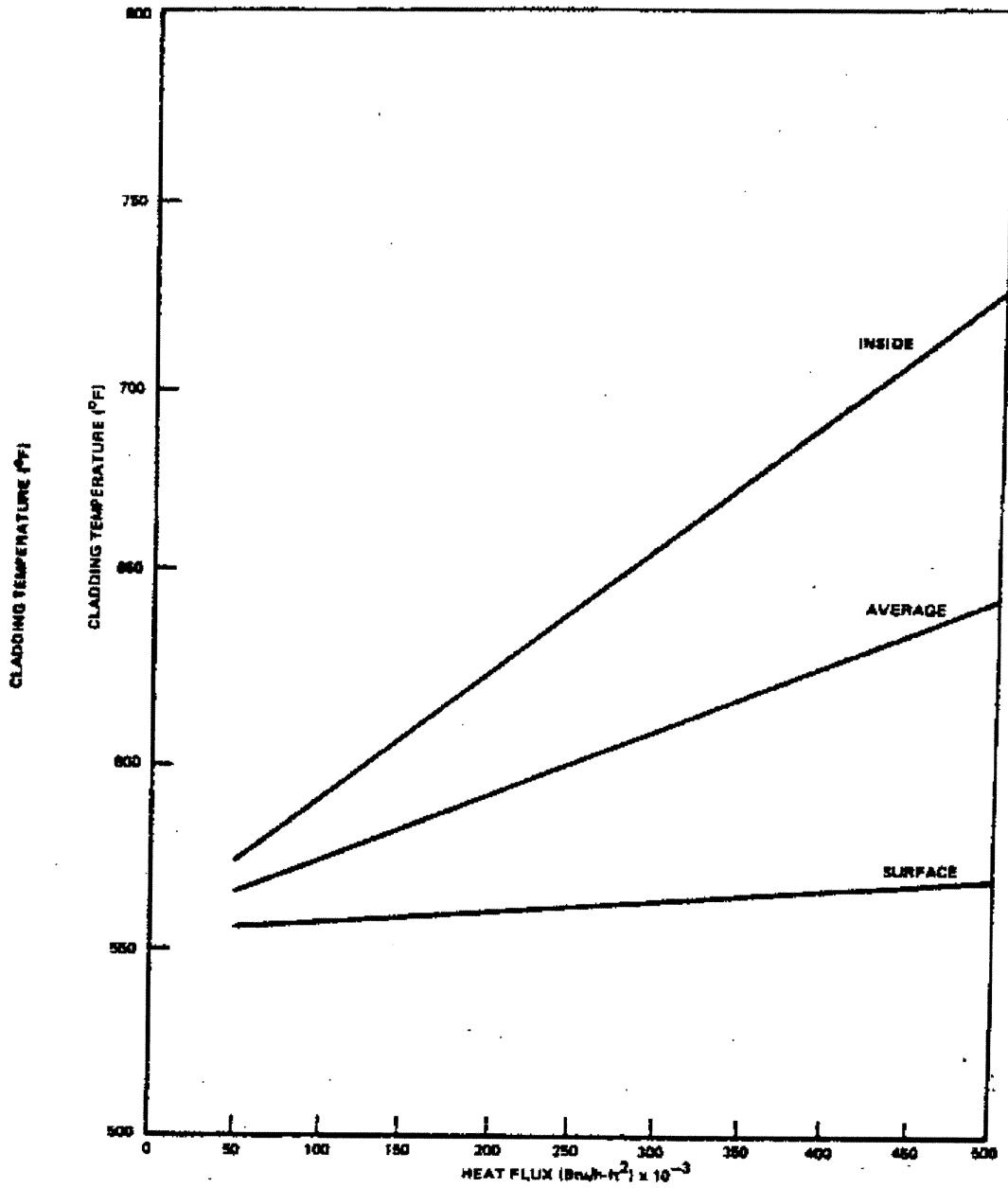
FIGURE 4.2-5

CONTROL ROD VELOCITY LIMITER

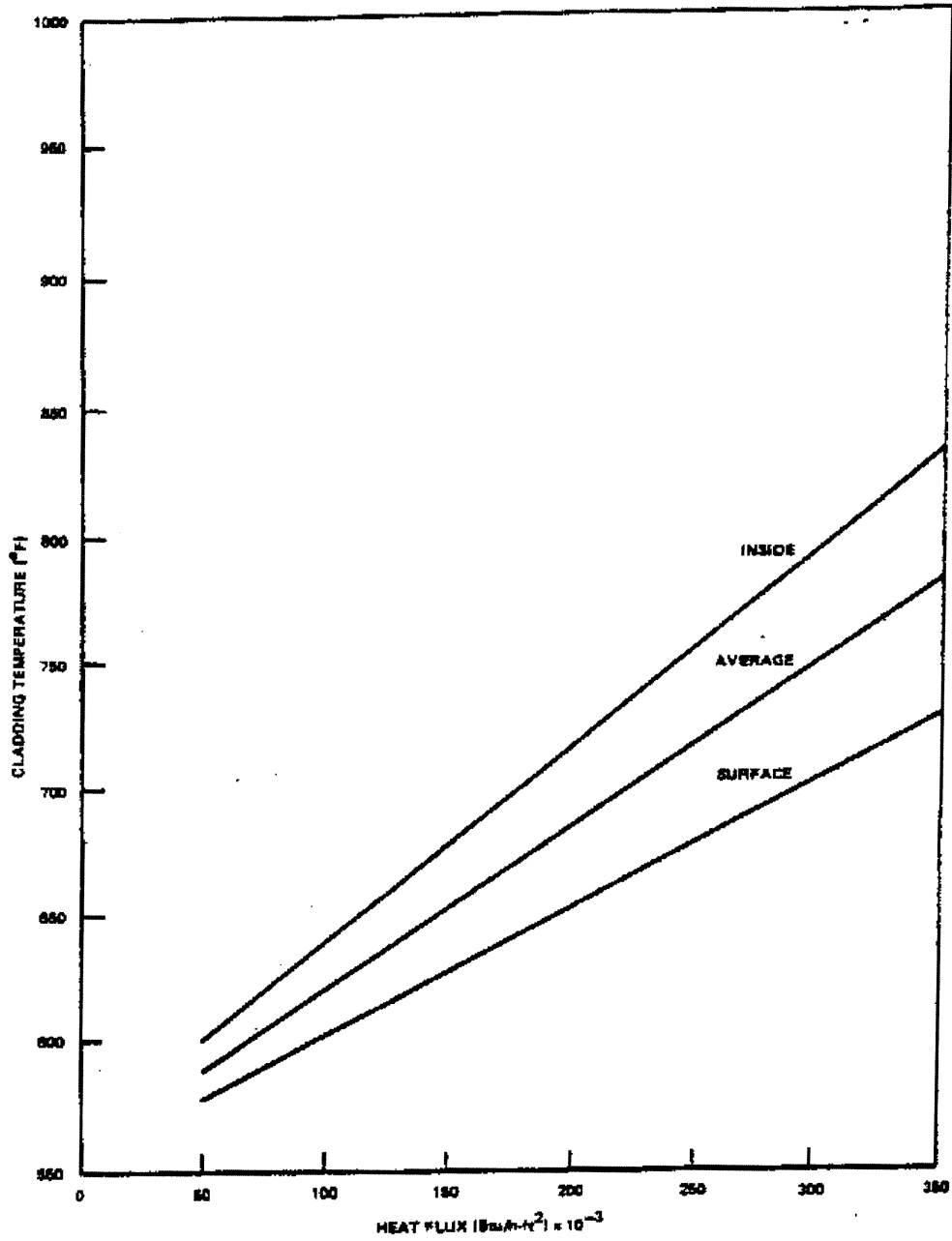
REV. 0 - APRIL 1984



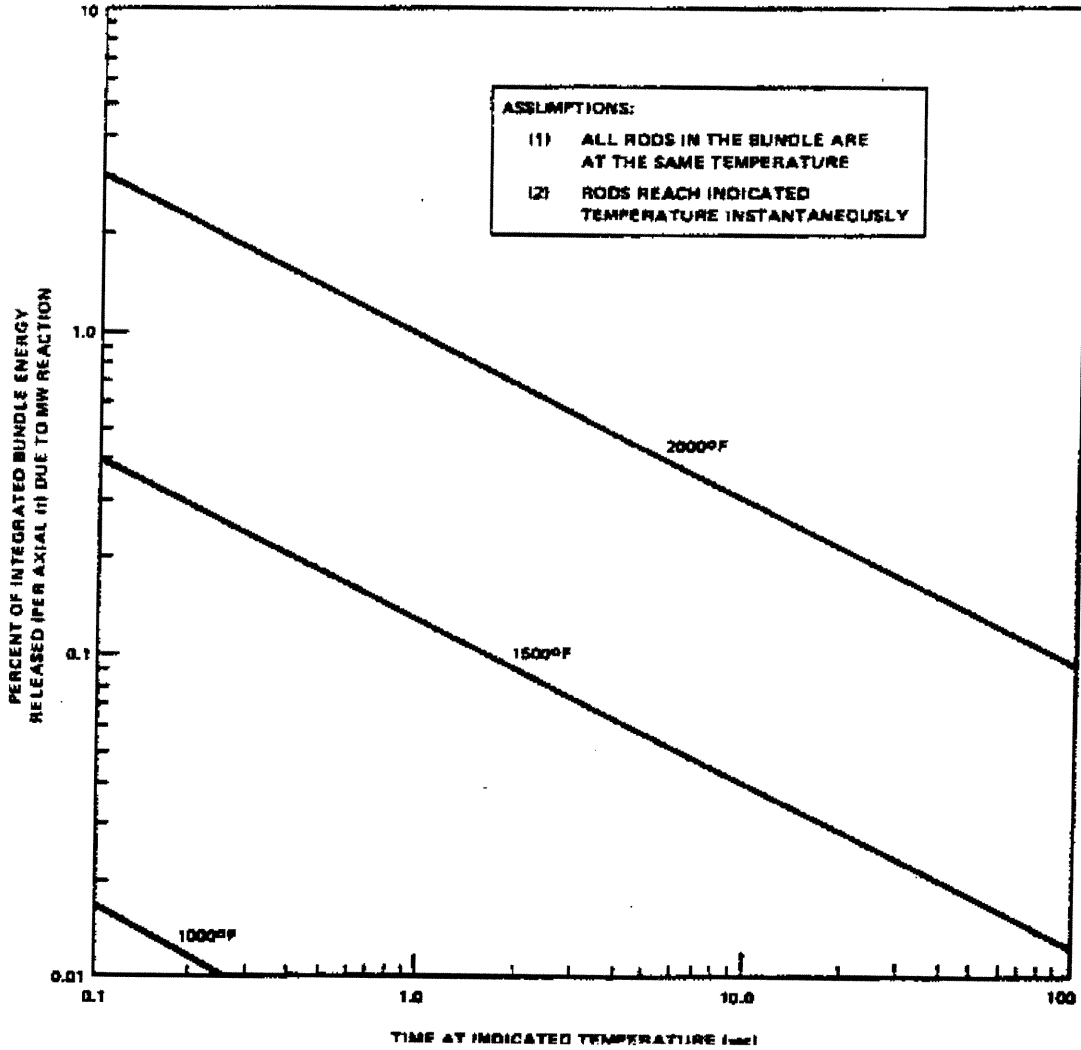
LASALLE COUNTY STATION
 UPDATED FINAL SAFETY ANALYSIS REPORT
 FIGURE 4.2-5a
 FABRICAST VELOCITY LIMITER



LASALLE COUNTY STATION
UPDATED FINAL SAFETY ANALYSIS REPORT
FIGURE 4.2-6
(TYPICAL)
CLADDING TEMPERATURE VS. HEAT FLUX - BOL 8X8R
FUEL TYPE



LASALLE COUNTY STATION
UPDATED FINAL SAFETY ANALYSIS REPORT
FIGURE 4.2-7
(TYPICAL)
CLADDING TEMPERATURE VS. HEAT FLUX - LATE LIFE
8X8R FUEL TYPE



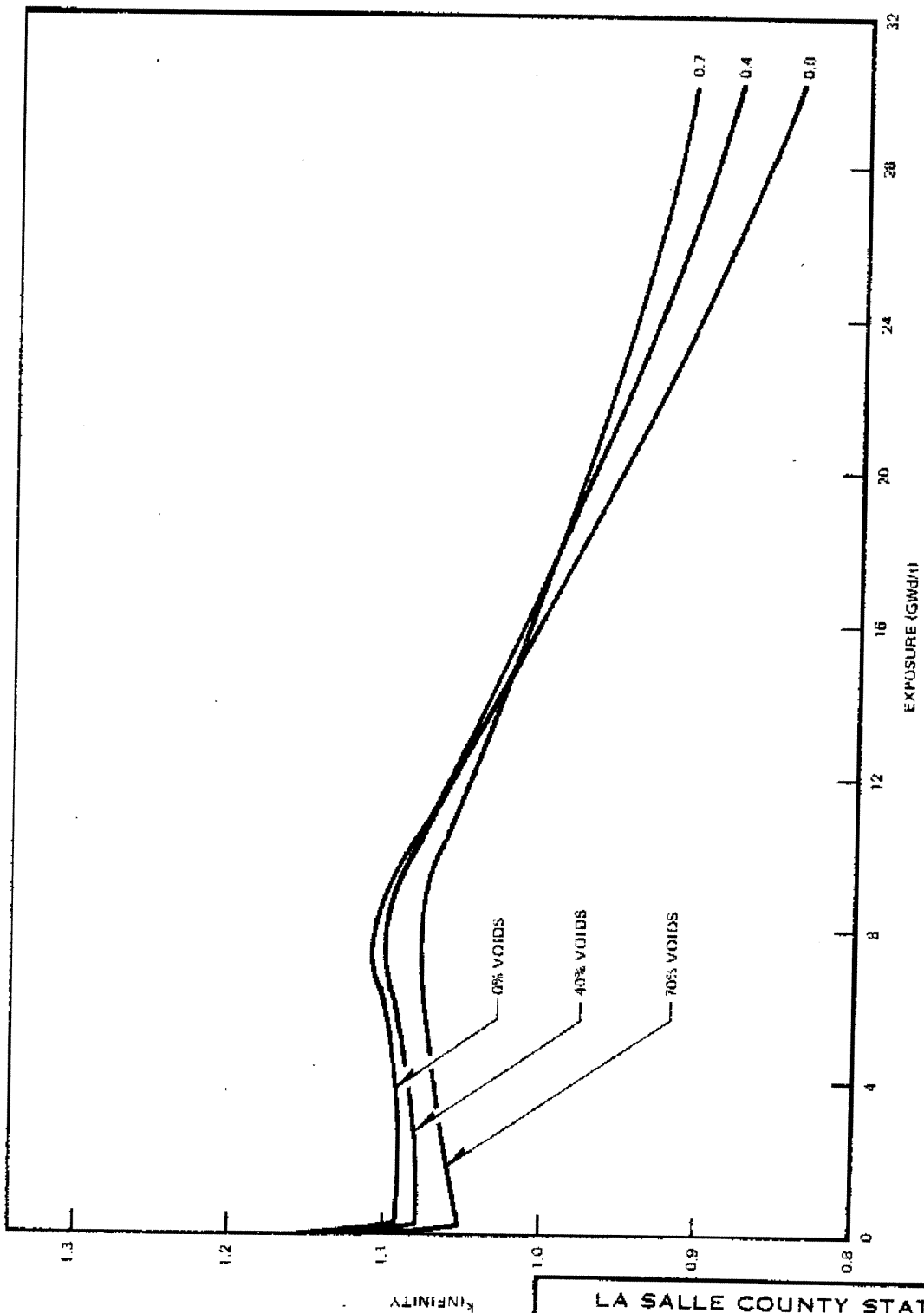
LASALLE COUNTY STATION
UPDATED FINAL SAFETY ANALYSIS REPORT
FIGURE 4.2-8
ENERGY RELEASE AS A FUNCTION OF TIME
(TYPICAL)

THIS PAGE INTENTIONALLY LEFT BLANK

LASALLE COUNTY STATION UPDATED FINAL SAFETY ANALYSIS REPORT
FIGURE 4.3-1a UNIT 1 CORE LOADING MAP

THIS PAGE INTENTIONALLY LEFT BLANK

LASALLE COUNTY STATION UPDATED FINAL SAFETY ANALYSIS REPORT
FIGURE 4.3-1b UNIT 2 CORE LOADING MAP

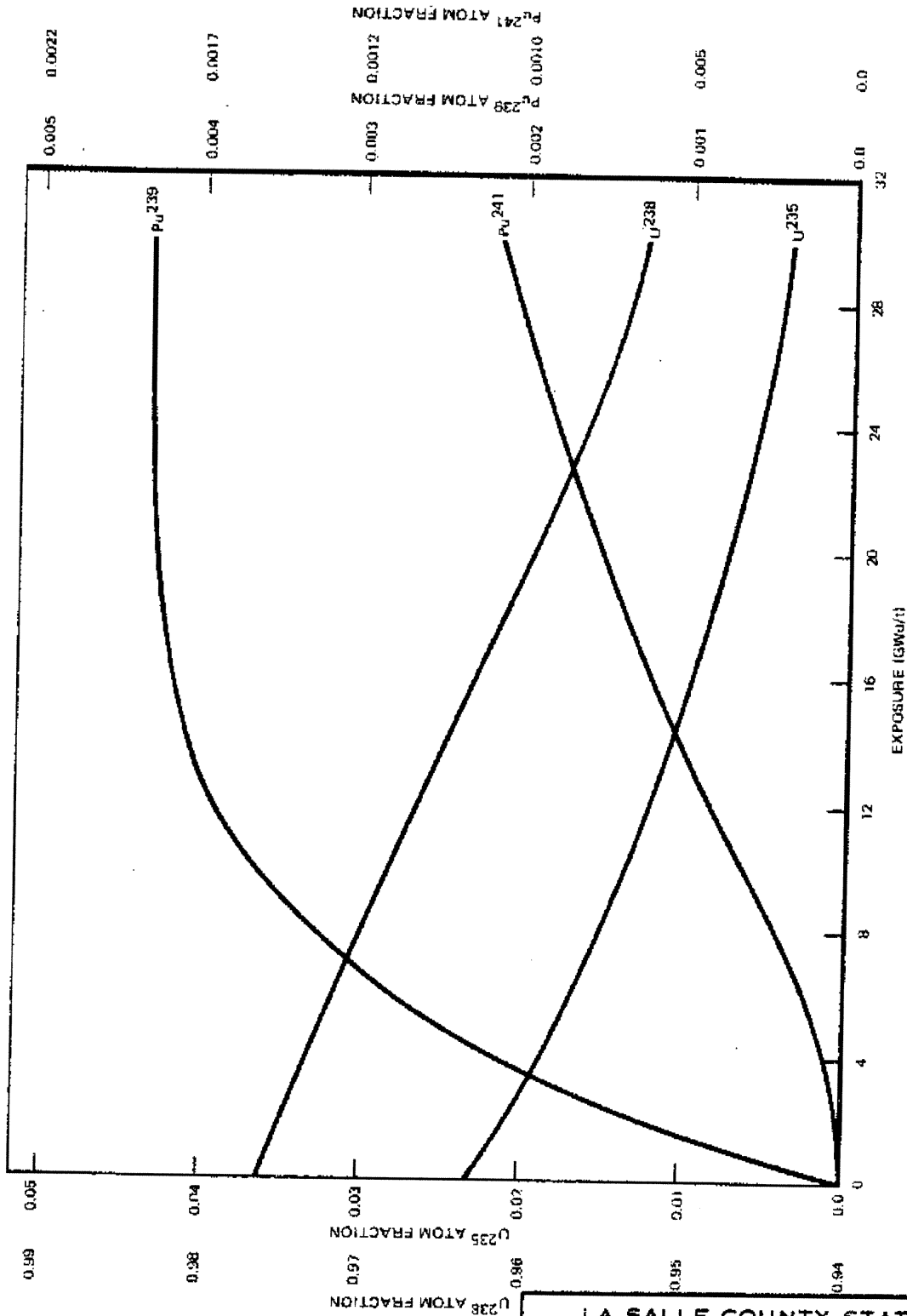


LA SALLE COUNTY STATION
 UPDATED FINAL SAFETY ANALYSIS REPORT

FIGURE 4.3-2

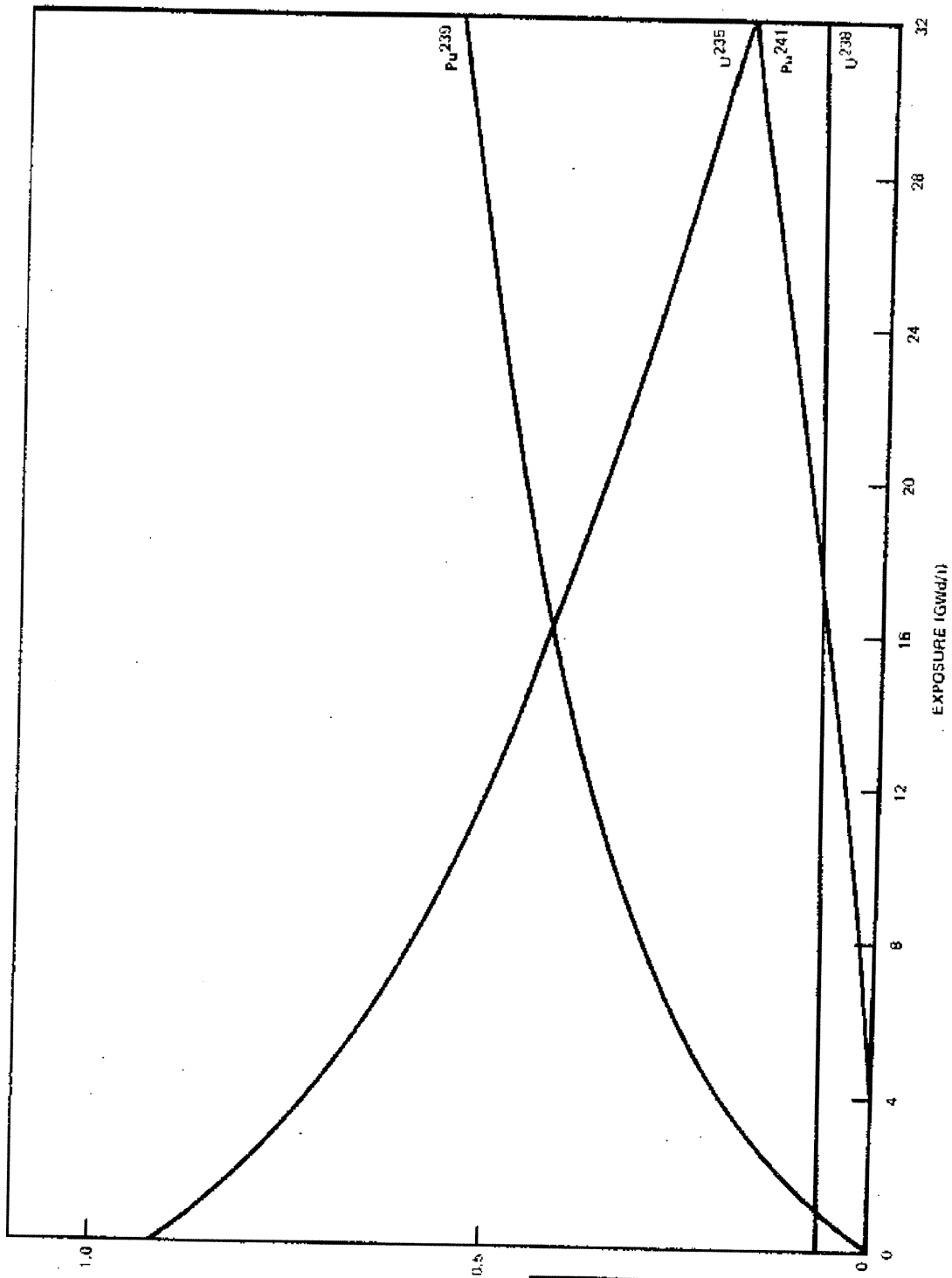
K_{∞} AS A FUNCTION OF EXPOSURE AT
 VARIOUS VOID FRACTIONS, HIGH ENRICHMENT,
 DOMINANT FUEL TYPE (TYPICAL)

REV. 4 - APRIL 1988



LA SALLE COUNTY STATION
 UPDATED FINAL SAFETY ANALYSIS REPORT
 FIGURE 4.3-3
 ATOM FRACTION AS A FUNCTION OF
 EXPOSURE, HIGH ENRICHMENT, DOMINANT
 FUEL TYPE, 40% VOIDS (TYPICAL)

REV. E - APRIL 1988



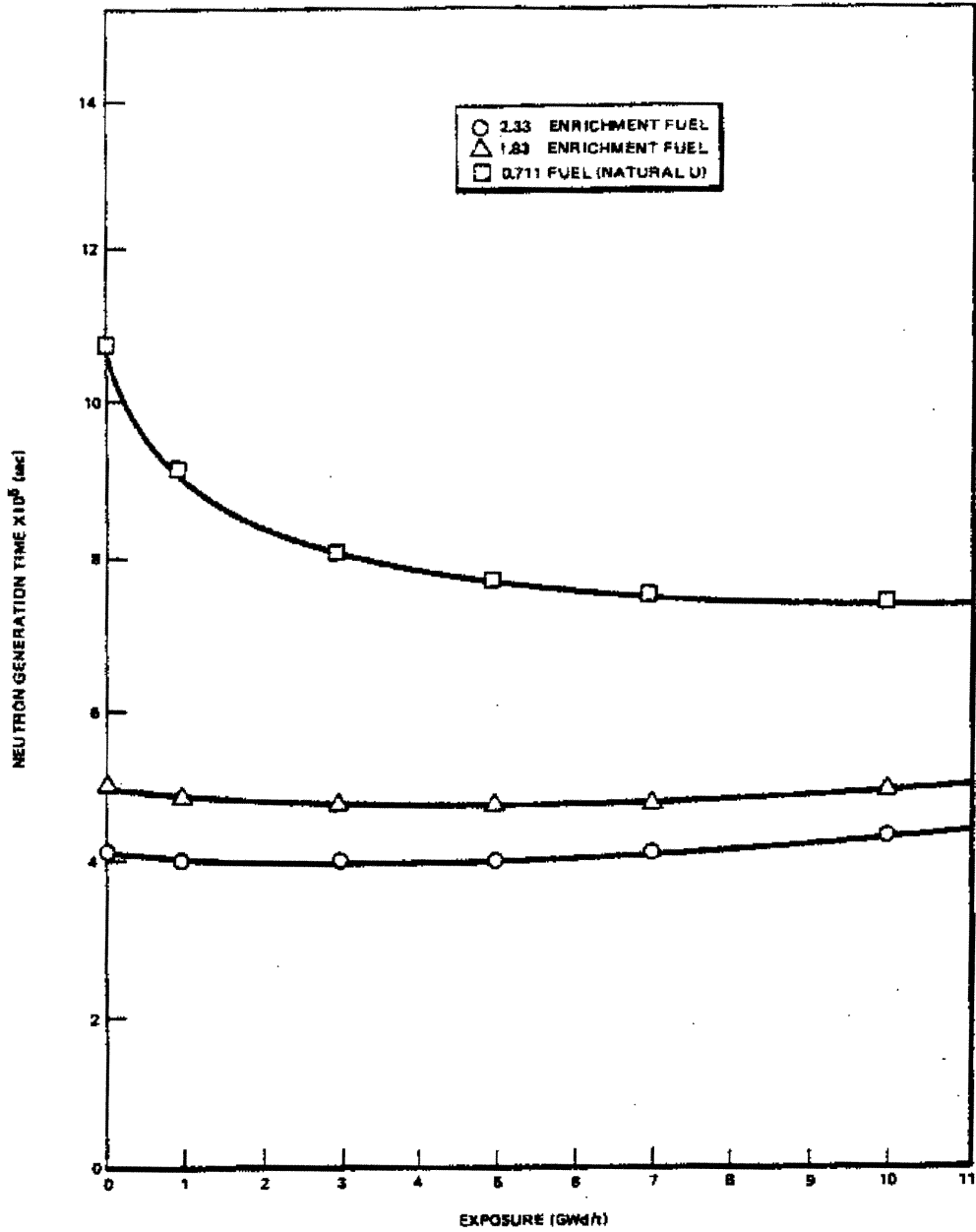
FISSION FRACTIONS

LA SALLE COUNTY STATION
 UPDATED FINAL SAFETY ANALYSIS REPORT

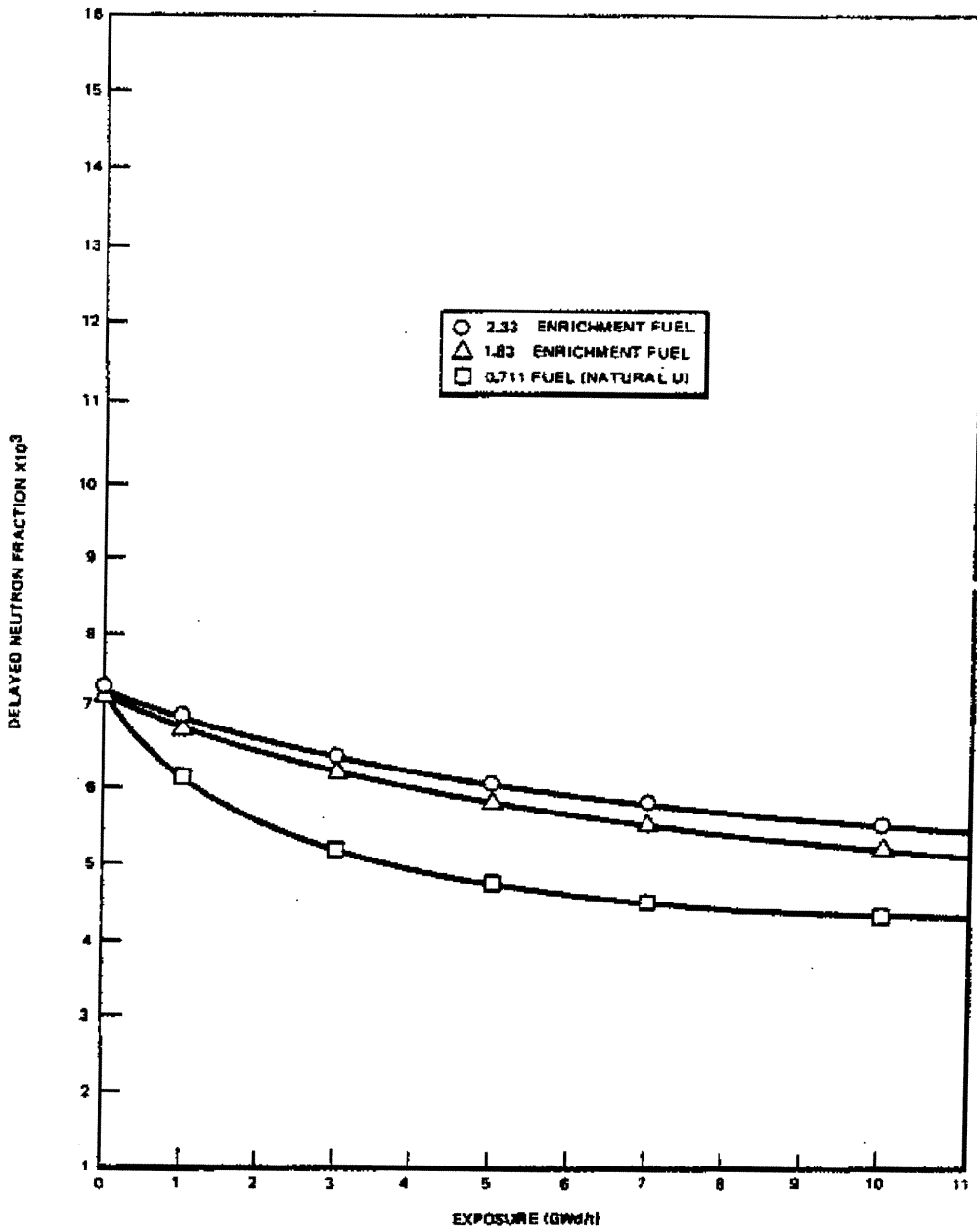
FIGURE 4.3-4

FISSION FRACTION AS A FUNCTION OF
 EXPOSURE, HIGH ENRICHMENT, DOMINANT
 FUEL TYPE, 40% VOIDS (TYPICAL)

REV. 4 - APRIL 1988



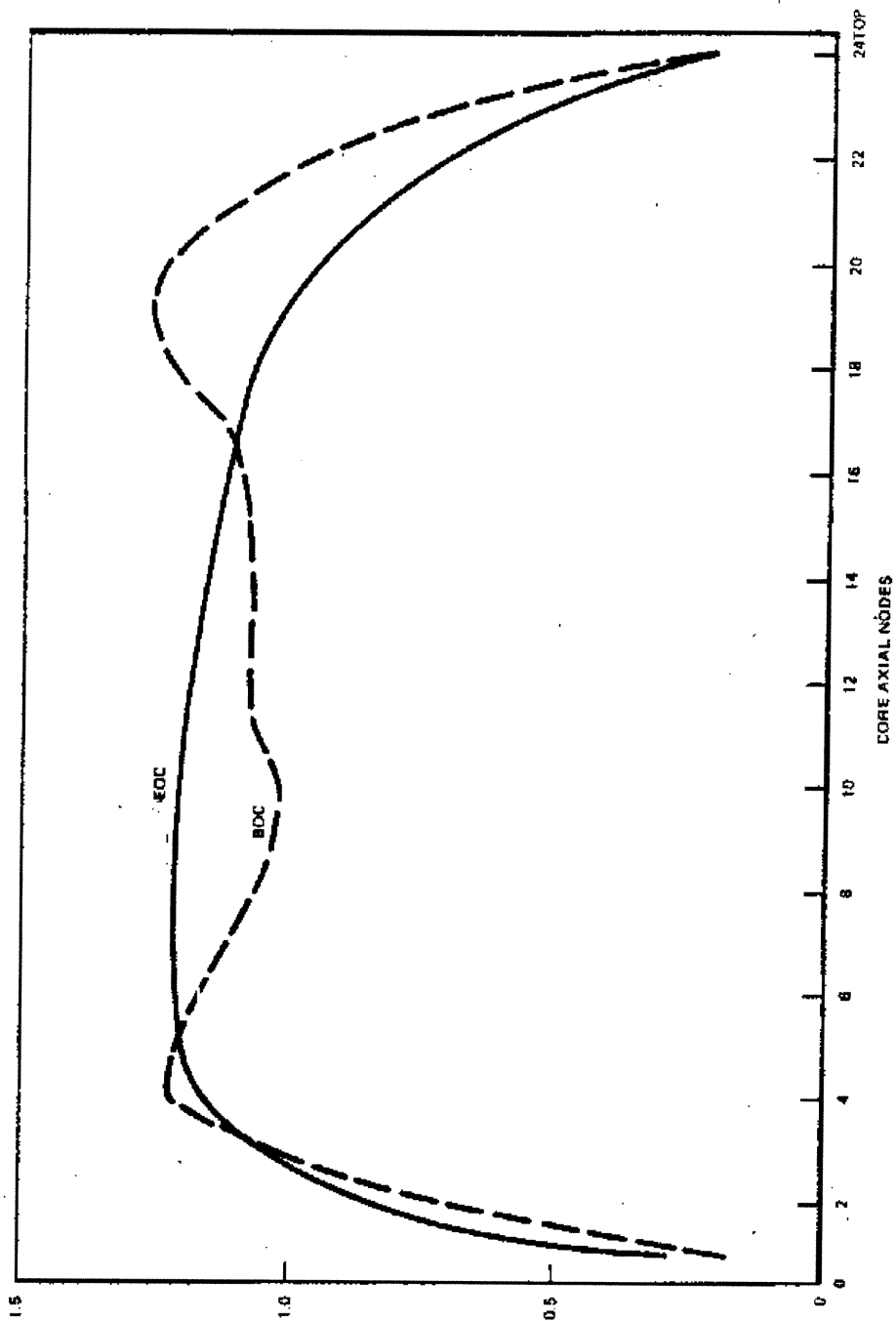
LASALLE COUNTY STATION
UPDATED FINAL SAFETY ANALYSIS REPORT
FIGURE 4.3-5
(TYPICAL)
NEUTRON GENERATION TIME VS. EXPOSURE AT
40 PERCENT VOIDS



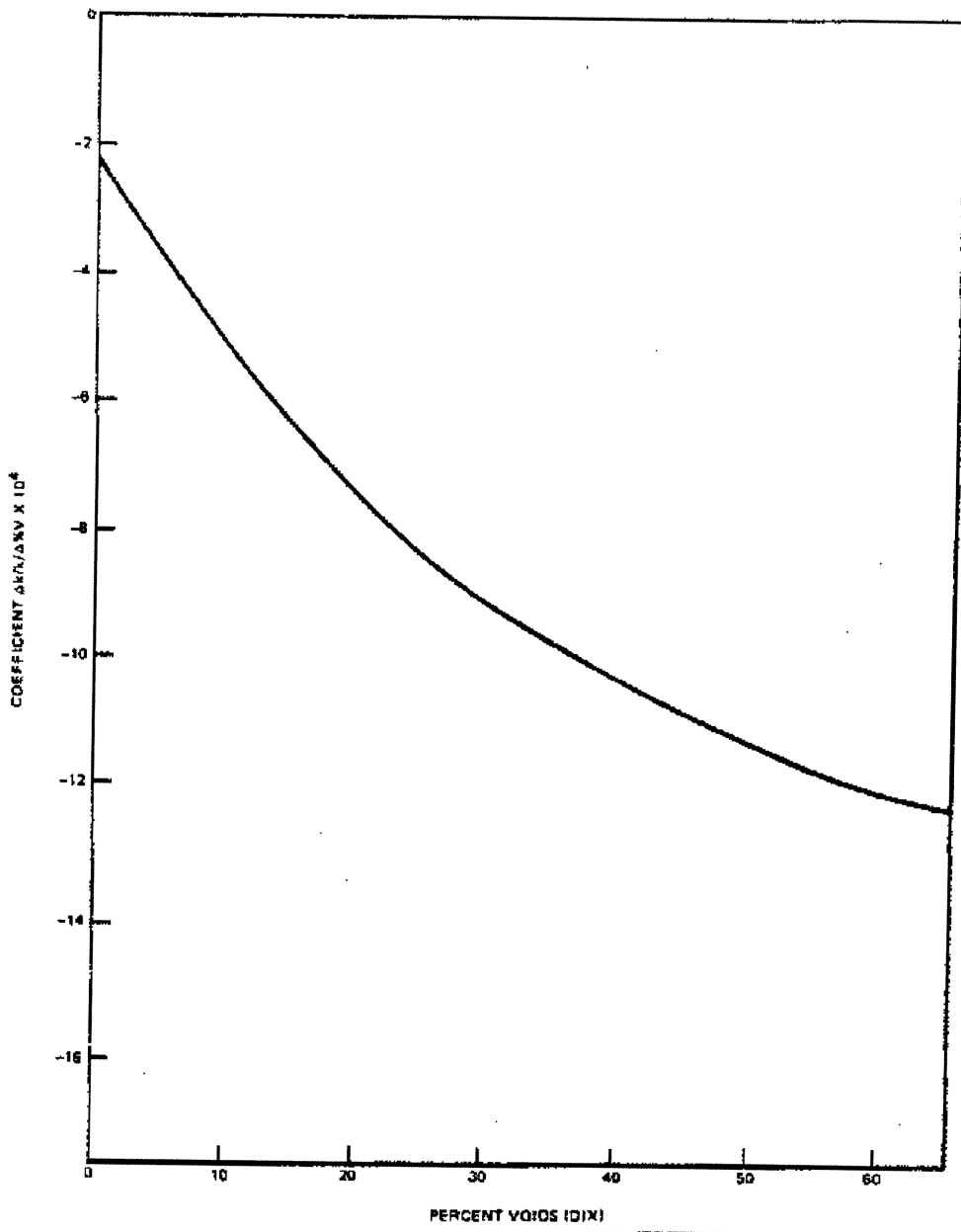
LASALLE COUNTY STATION
UPDATED FINAL SAFETY ANALYSIS REPORT
FIGURE 4.3-6
(TYPICAL)
DELAYED NEUTRON FRACTION VS. EXPOSURE AT
40 PERCENT VOIDS

THIS PAGE INTENTIONALLY LEFT BLANK

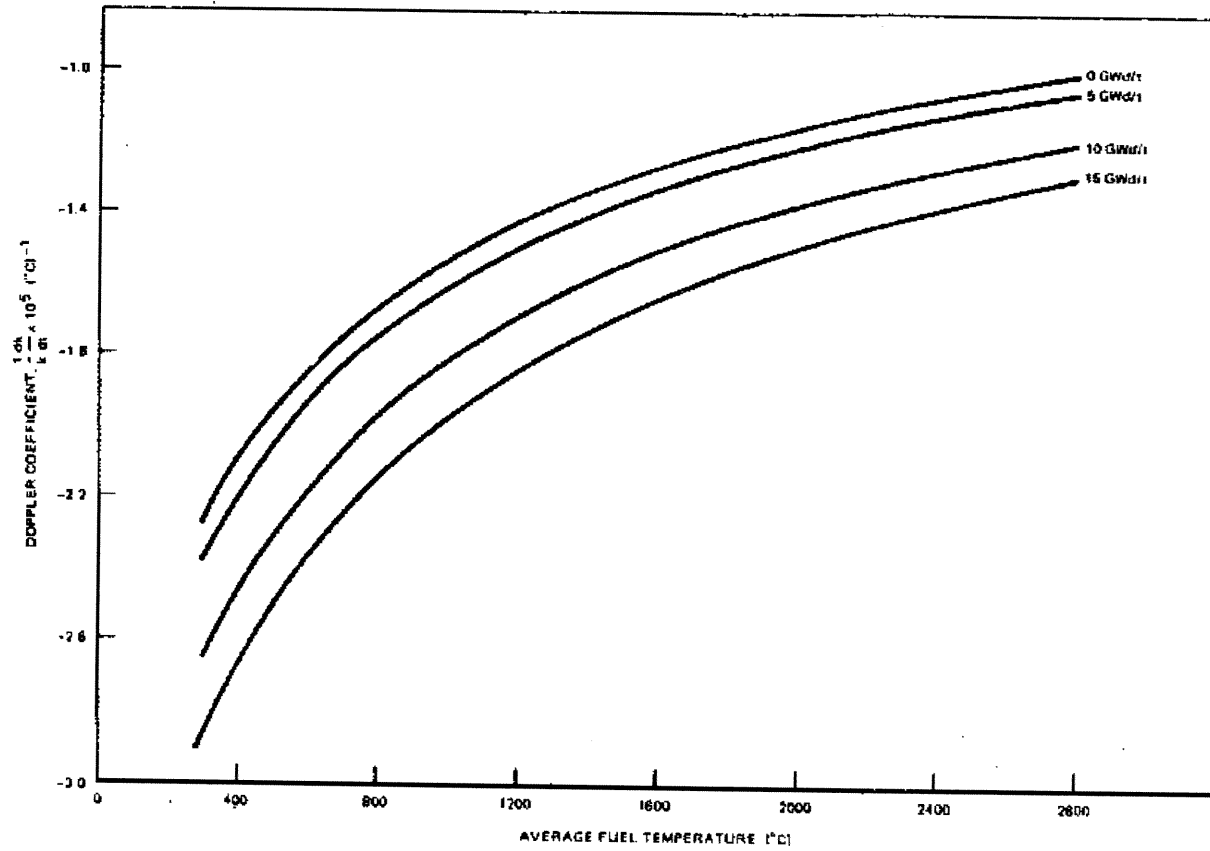
|



LASALLE COUNTY STATION
UPDATED FINAL SAFETY ANALYSIS REPORT
FIGURE 4.3-11
(TYPICAL)
BEGINNING OF CYCLE AND END OF CYCLE CORE
AVERAGE AXIAL POWER - 764 CORE, BWR/4 AND BWR/5



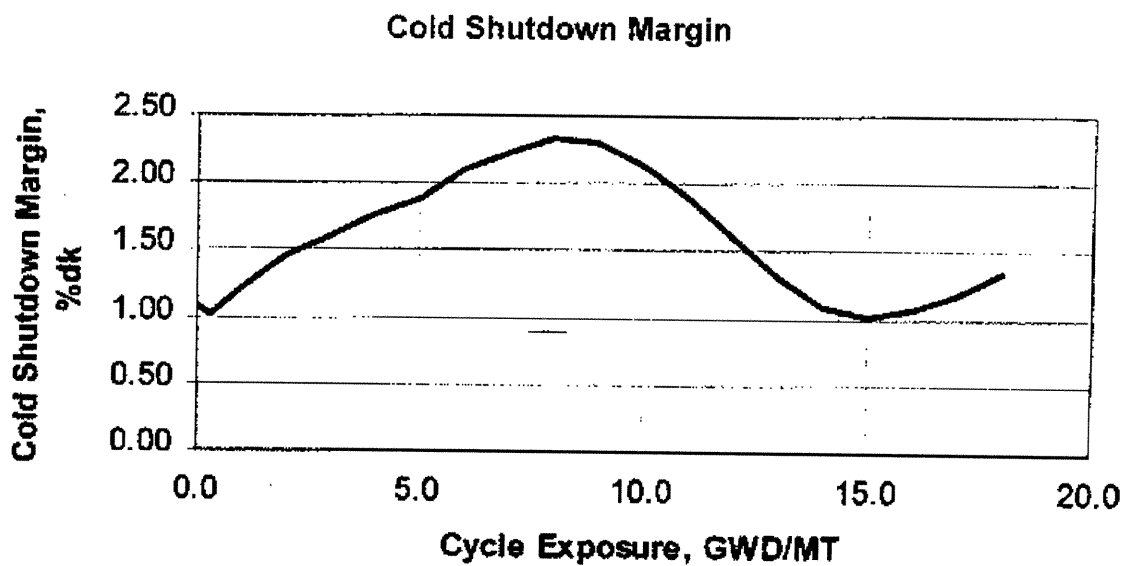
LASALLE COUNTY STATION
UPDATED FINAL SAFETY ANALYSIS REPORT
FIGURE 4.3-12
MODERATOR VOID REACTIVITY COEFFICIENT AT EOC-1
INITIAL CYCLE



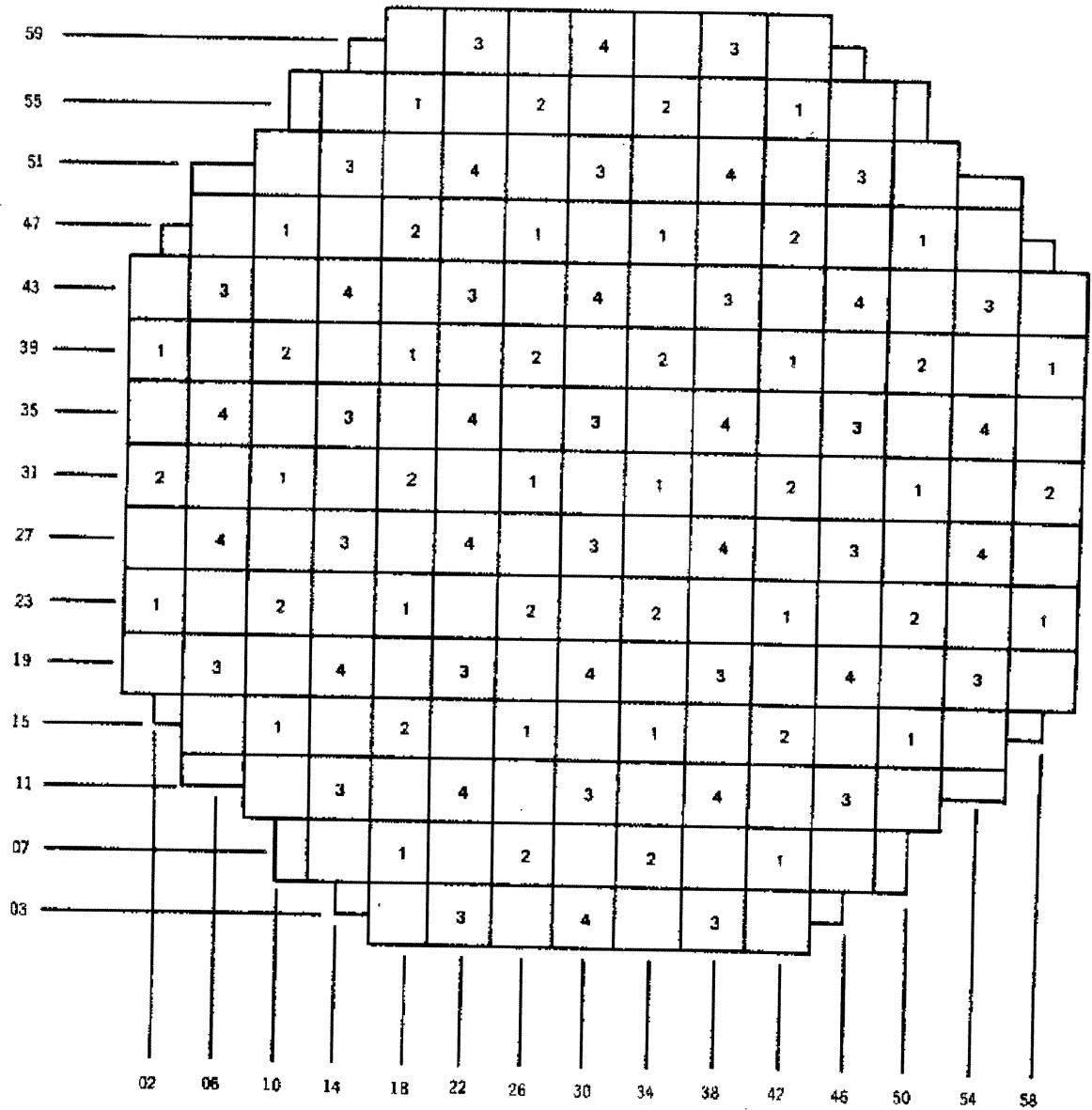
LASALLE COUNTY STATION
 UPDATED FINAL SAFETY ANALYSIS REPORT

FIGURE 4.3-13

DOPPLER REACTIVITY COEFFICIENT AS A FUNCTION OF
 FUEL EXPOSURE AND AVERAGE FUEL TEMPERATURE AT
 AN AVERAGE VOID CONTENT OF 40% HIGH ENRICHMENT
 (INITIAL CYCLE)



LASALLE COUNTY STATION UPDATED FINAL SAFETY ANALYSIS REPORT
FIGURE 4.3-14
EXAMPLE OF A COLD SHUTDOWN MARGIN CURVE

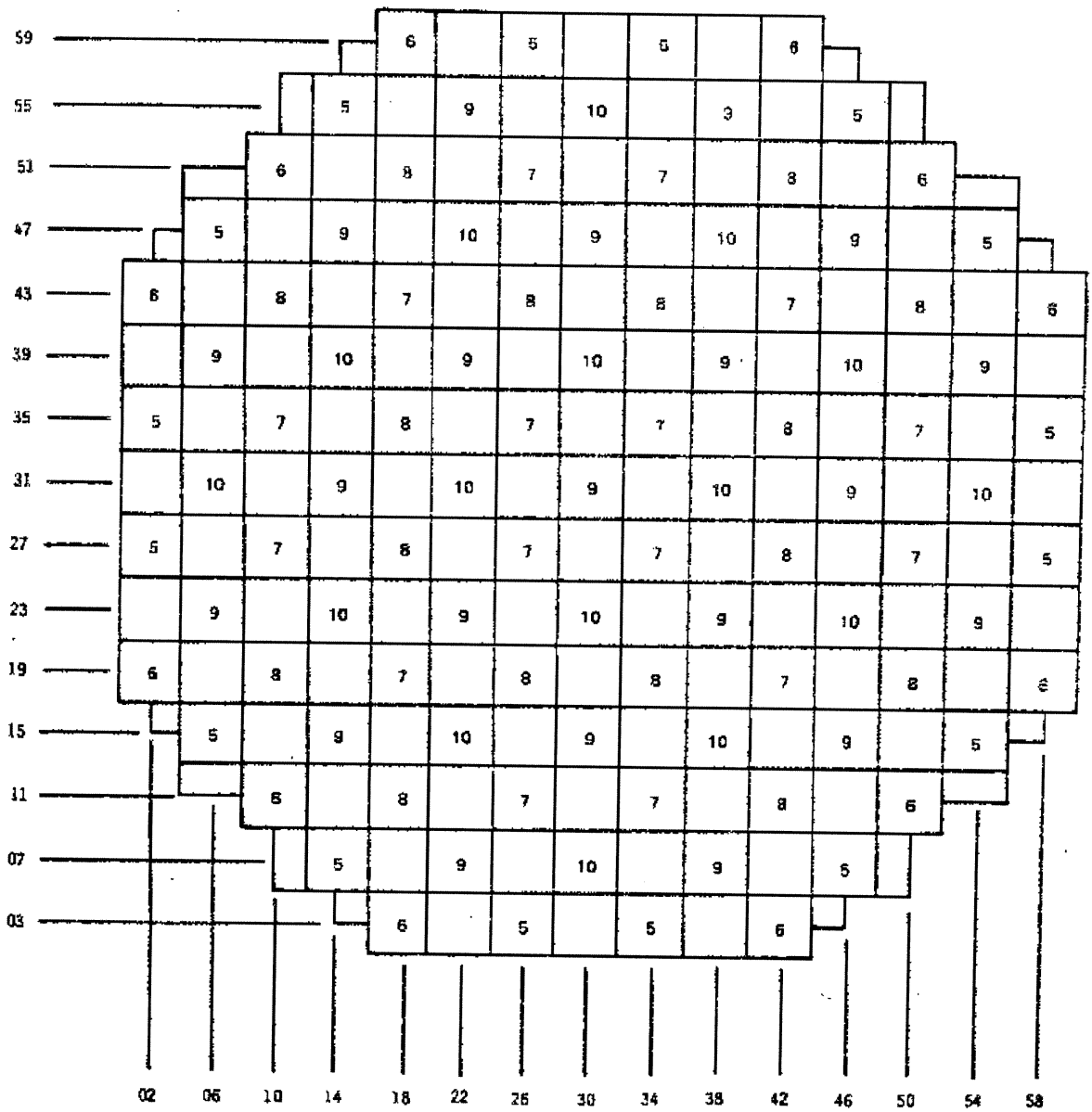


LA SALLE COUNTY STATION
 UPDATED FINAL SAFETY ANALYSIS REPORT

FIGURE 4.3-15

CONTROL ROD ASSIGNMENTS FOR
 GROUPS 1 THROUGH 4 (SEQUENCE A)

REV. 0 - APRIL 1984

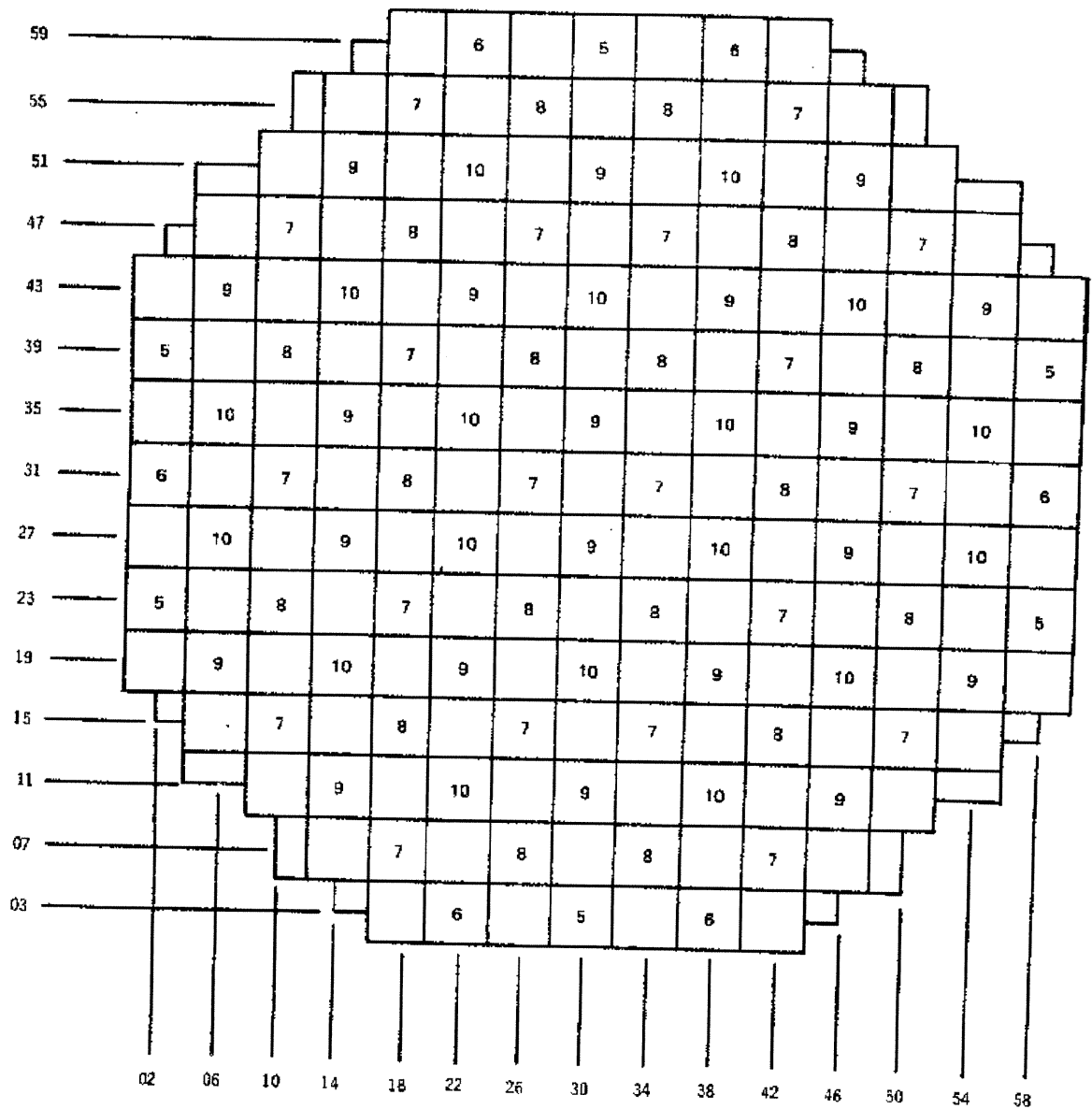


LA SALLE COUNTY STATION
 UPDATED FINAL SAFETY ANALYSIS REPORT

FIGURE 4.3-16

CONTROL ROD ASSIGNMENTS FOR
 GROUPS 5 THROUGH 10 (SEQUENCE A)

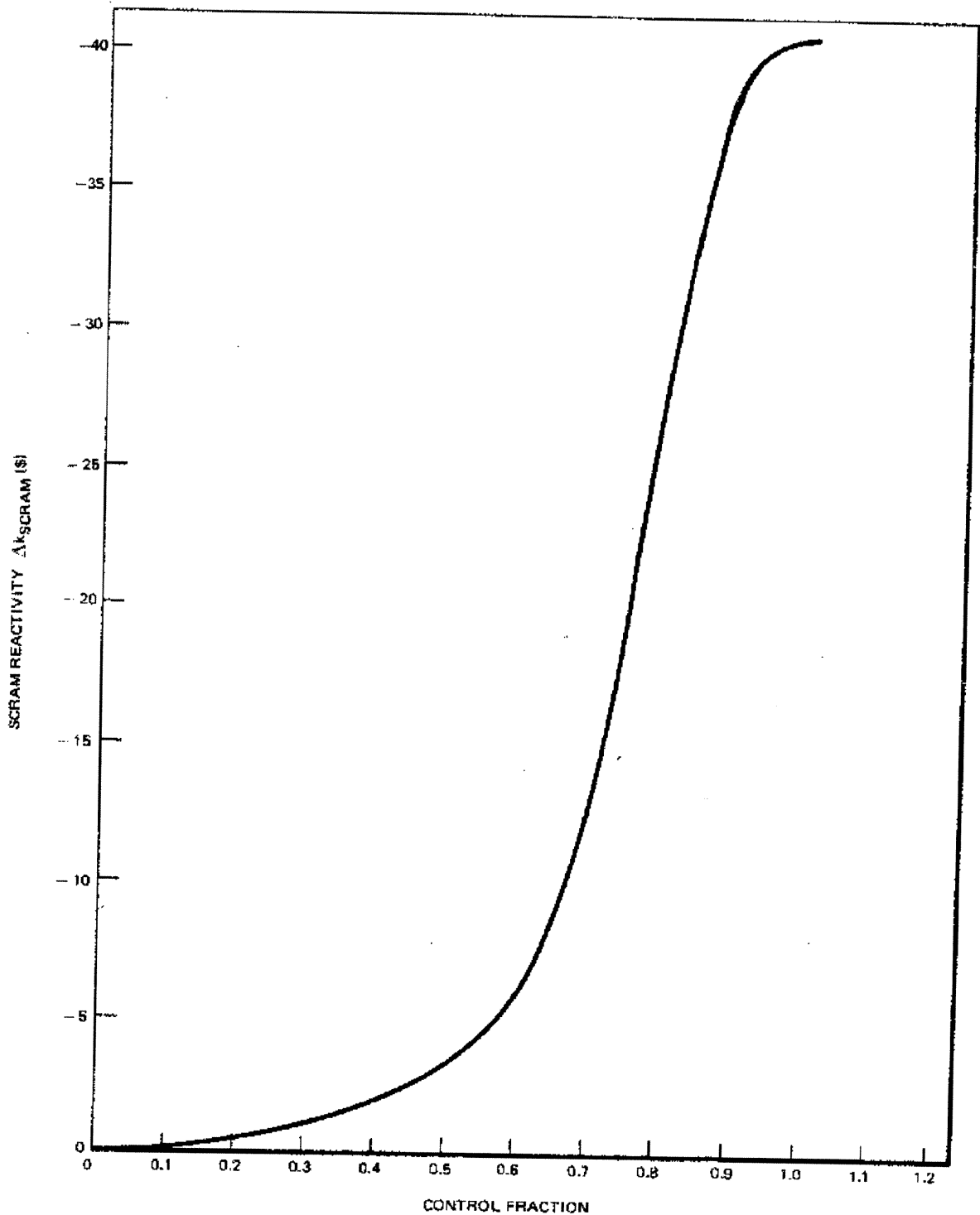
REV. 0 - APRIL 1984



LA SALLE COUNTY STATION
 UPDATED FINAL SAFETY ANALYSIS REPORT

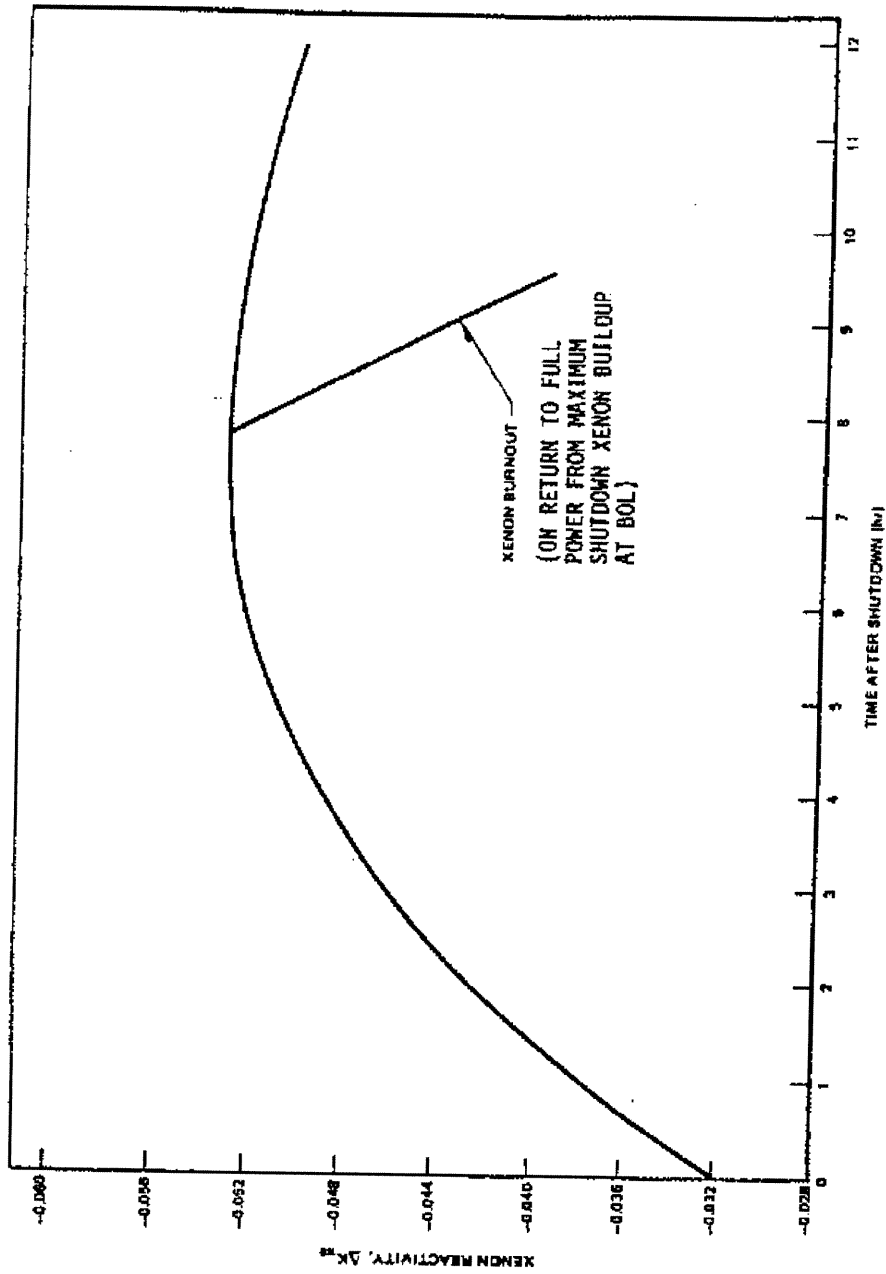
FIGURE 4.3-18

CONTROL ROD ASSIGNMENTS FOR
 GROUPS 5 THROUGH 10 (SEQUENCE B)

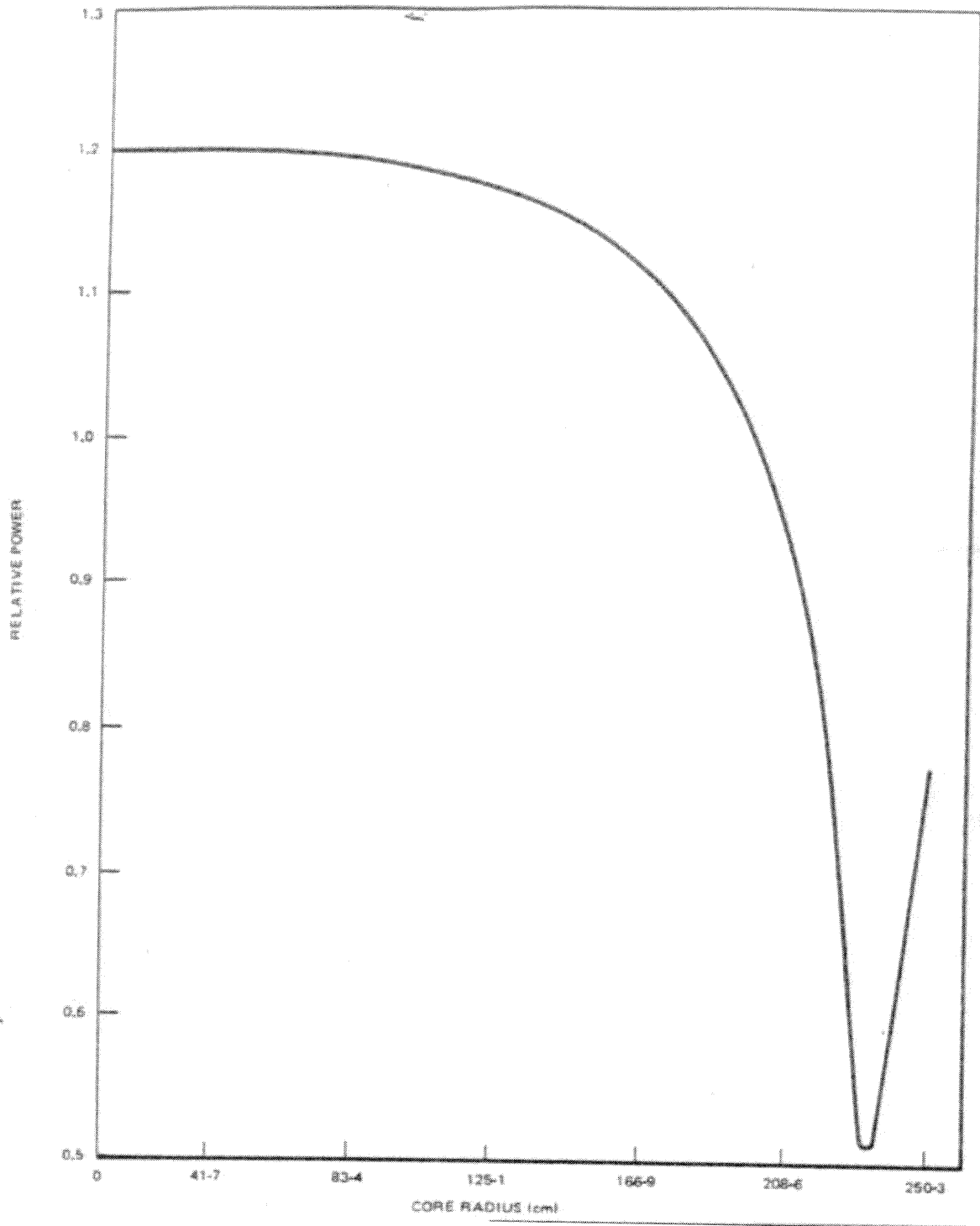


LA SALLE COUNTY STATION
UPDATED FINAL SAFETY ANALYSIS REPORT
FIGURE 4.3-19
HOT OPERATING EOC-1 SCRAM REACTIVITY

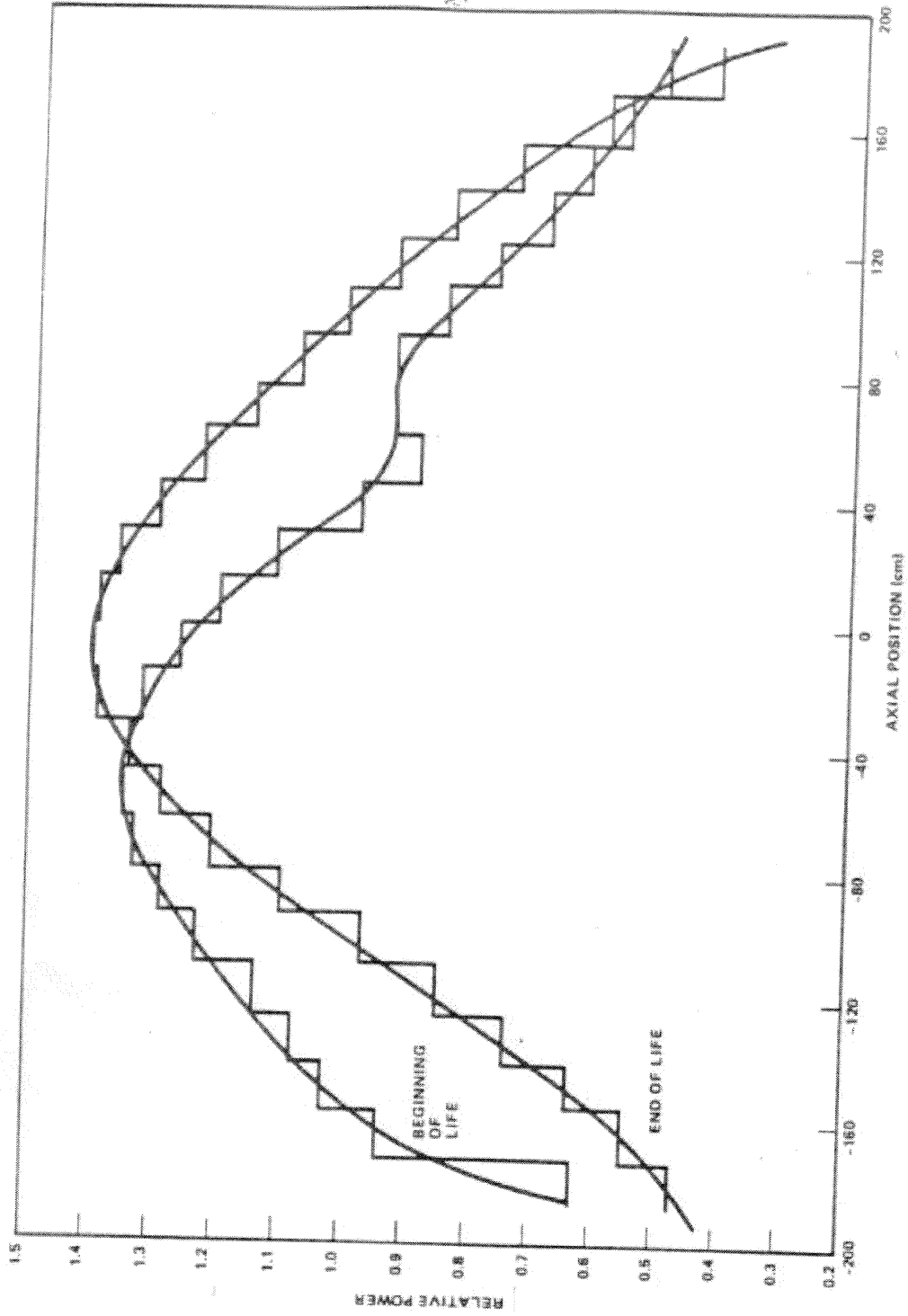
REV. 0 - APRIL 1984



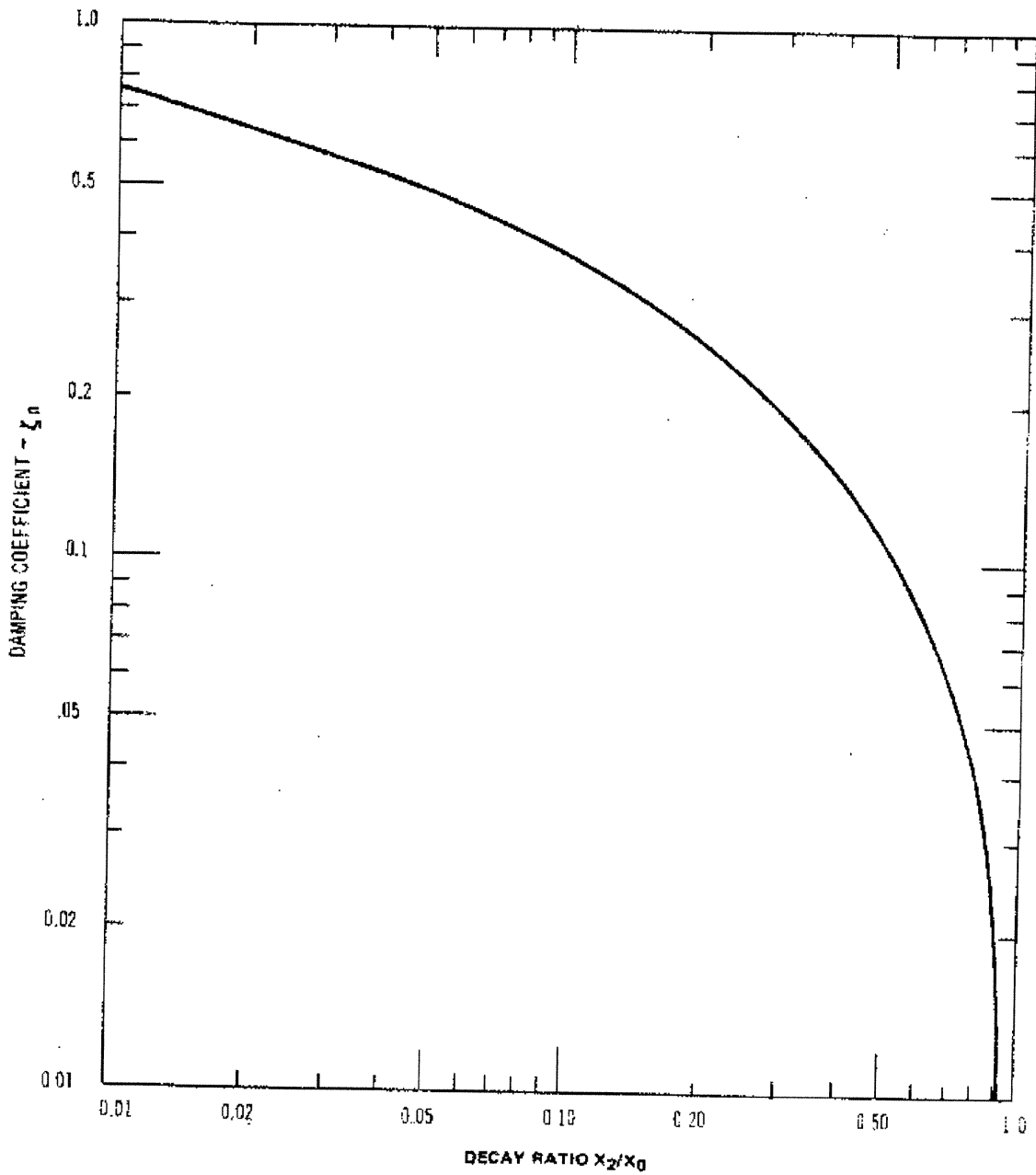
LASALLE COUNTY STATION
UPDATED FINAL SAFETY ANALYSIS REPORT
FIGURE 4.3-20
XENON REACTIVITY BUILDUP AND BURNOUT AFTER
SHUTDOWN (TYPICAL)



LASALLE COUNTY STATION
UPDATED FINAL SAFETY ANALYSIS REPORT
FIGURE 4.3-21
TYPICAL
RADIAL POWER DISTRIBUTION



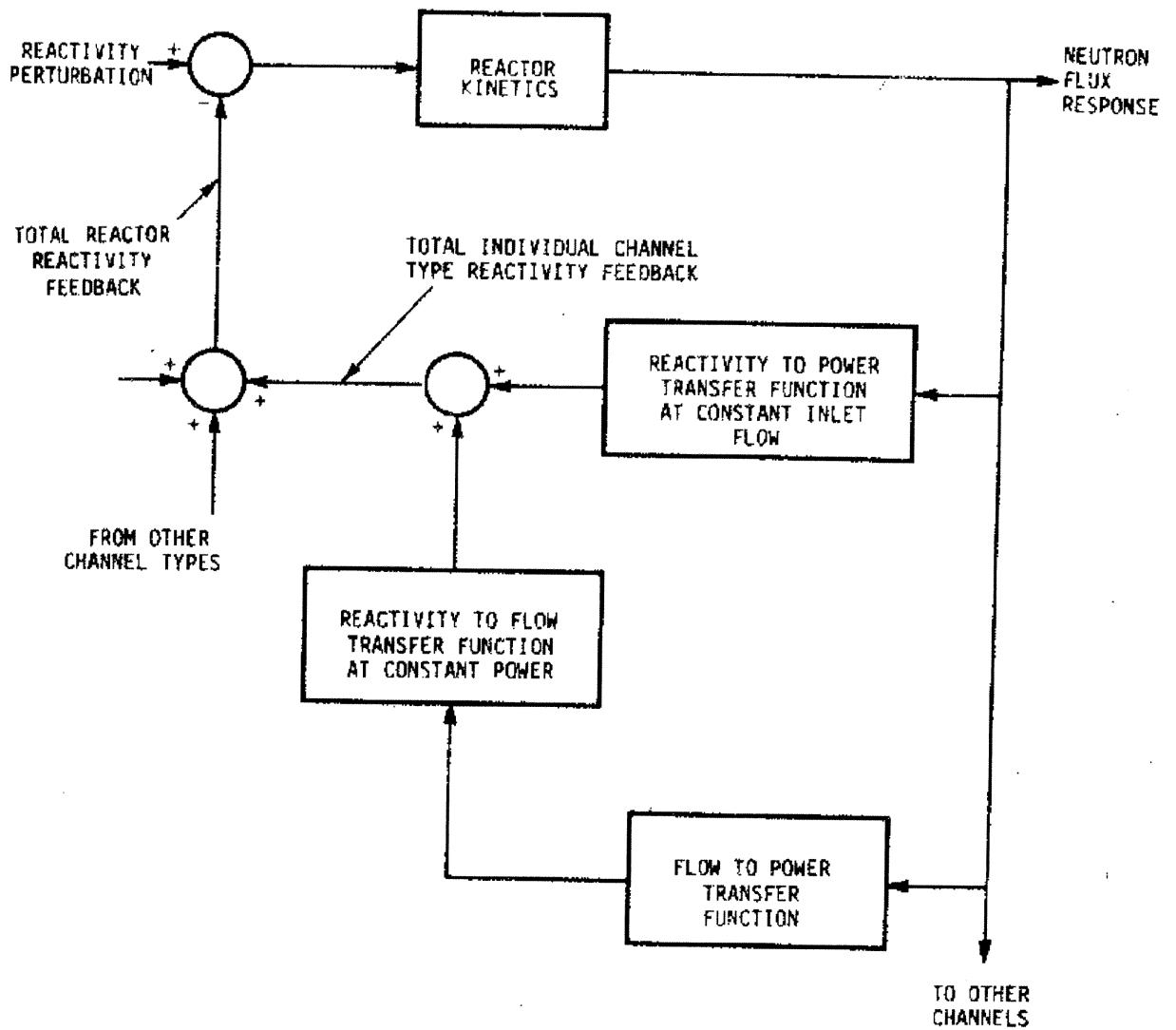
LASALLE COUNTY STATION
UPDATED FINAL SAFETY ANALYSIS REPORT
FIGURE 4.3-22
TYPICAL
AXIAL POWER DISTRIBUTION



LA SALLE COUNTY STATION
 UPDATED FINAL SAFETY ANALYSIS REPORT

FIGURE 4.4-1
 DAMPING COEFFICIENT VS. DECAY
 RATIO (SECOND ORDER SYSTEMS)

REV. 0 - APRIL 1984

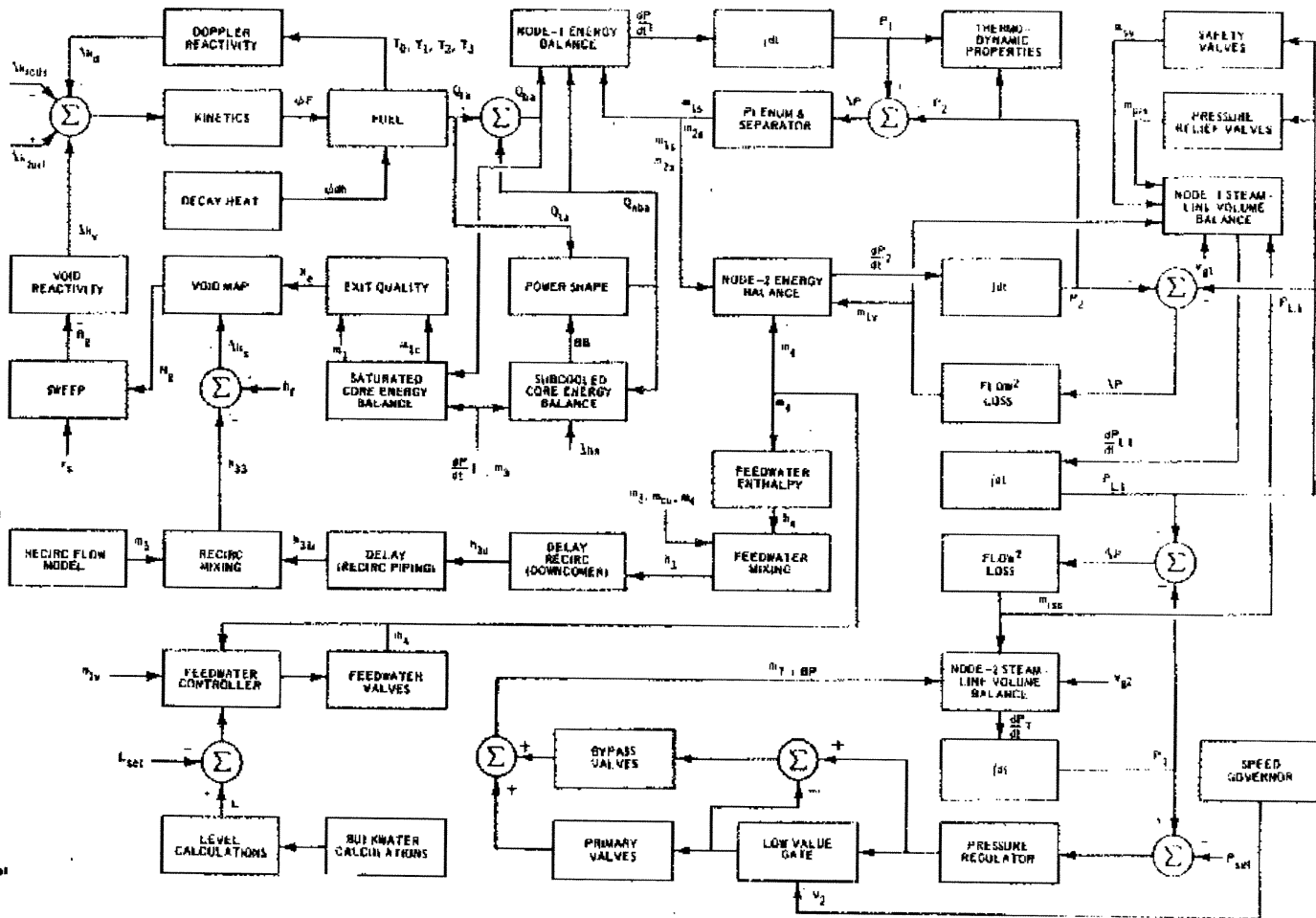


LA SALLE COUNTY STATION
 UPDATED FINAL SAFETY ANALYSIS REPORT

FIGURE 4.4-2
 HYDRODYNAMIC AND CORE STABILITY MODEL

REV. 0 - APRIL 1984

- E_d Enthalpy of downcomer fluid
- E_{fw} Feedwater enthalpy
- E_{kin} Kinetic energy
- E_{rec} Delayed enthalpy—enthalpy of fluid at entrance to recirculation loops
- E_{rec} Enthalpy of fluid in 1st recirculation loop
- L_{set} Reactor vessel water level
- L_{set} Level set point
- m_3 Recirculation mass flow rate
- m_4 Feedwater mass flow rate
- m_{21} Core exit—steam mass flow rate
- m_{22} Separator steam flow rate
- m_{23} Vessel steam flow
- m_{24} Separator, saturated water mass flow rate
- m_{25} Steam flow to the turbine and bypass
- m_{26} Saturated vapor condenser mass flow rate
- m_{27} Pressure relief valve mass flow rate
- m_{28} Safety valve mass flow rate
- P_1 Pressure, Node 1 (core)
- P_2 Pressure, Node 2 (separator)
- P_{L1} Pressure—downcomer Node 1
- P_1 Turbine pressure—steamline Node 2
- P_{set} Pressure set point
- Q_{ba} Steaming active heat (heat to saturated region of the core)
- Q_{sub} Nonsteaming active heat (heat to subcooled region of the core)
- Q_{tot} Total active core heat
- R_0 Core average void fraction
- T_0 Fuel temperature—center of fuel rod
- T_1 Fuel temperature—Radius r_1 of fuel rod
- T_2 Fuel temperature—Radius r_2 of fuel rod
- T_3 Fuel temperature—Radius r_3 of fuel rod
- v_2 Speed governor demand signal
- v_{11} Specific volume—Node 1 steamline
- v_{12} Heated subcooled
- v_{13} Doppler reactivity
- v_{fuel} Fuel reactivity
- v_{rods} Control rod reactivity
- m_{30} Steam flow through isolation valve
- v_{14} Void reactivity
- Q_{21} Decay heat
- τ_1 Newton time which produces heat in the fuel
- τ_2 Swept time constant
- BB Boiling boundary



LA SALLE COUNTY STATION
 UPDATED FINAL SAFETY ANALYSIS REPORT

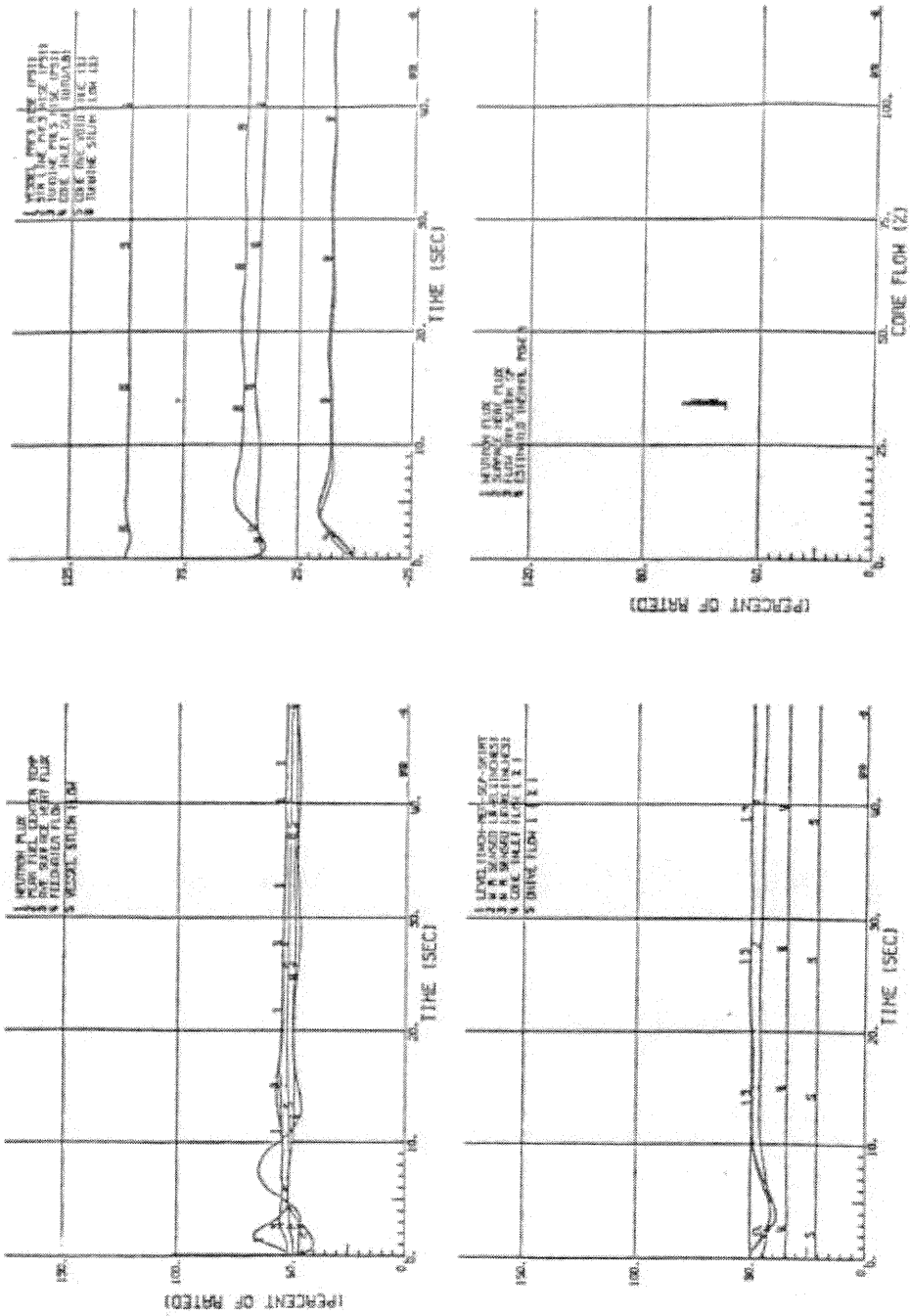
FIGURE 4.4-3
 MODEL BLOCK DIAGRAM WITH VALVE
 FLOW CONTROL

THIS PAGE INTENTIONALLY LEFT BLANK

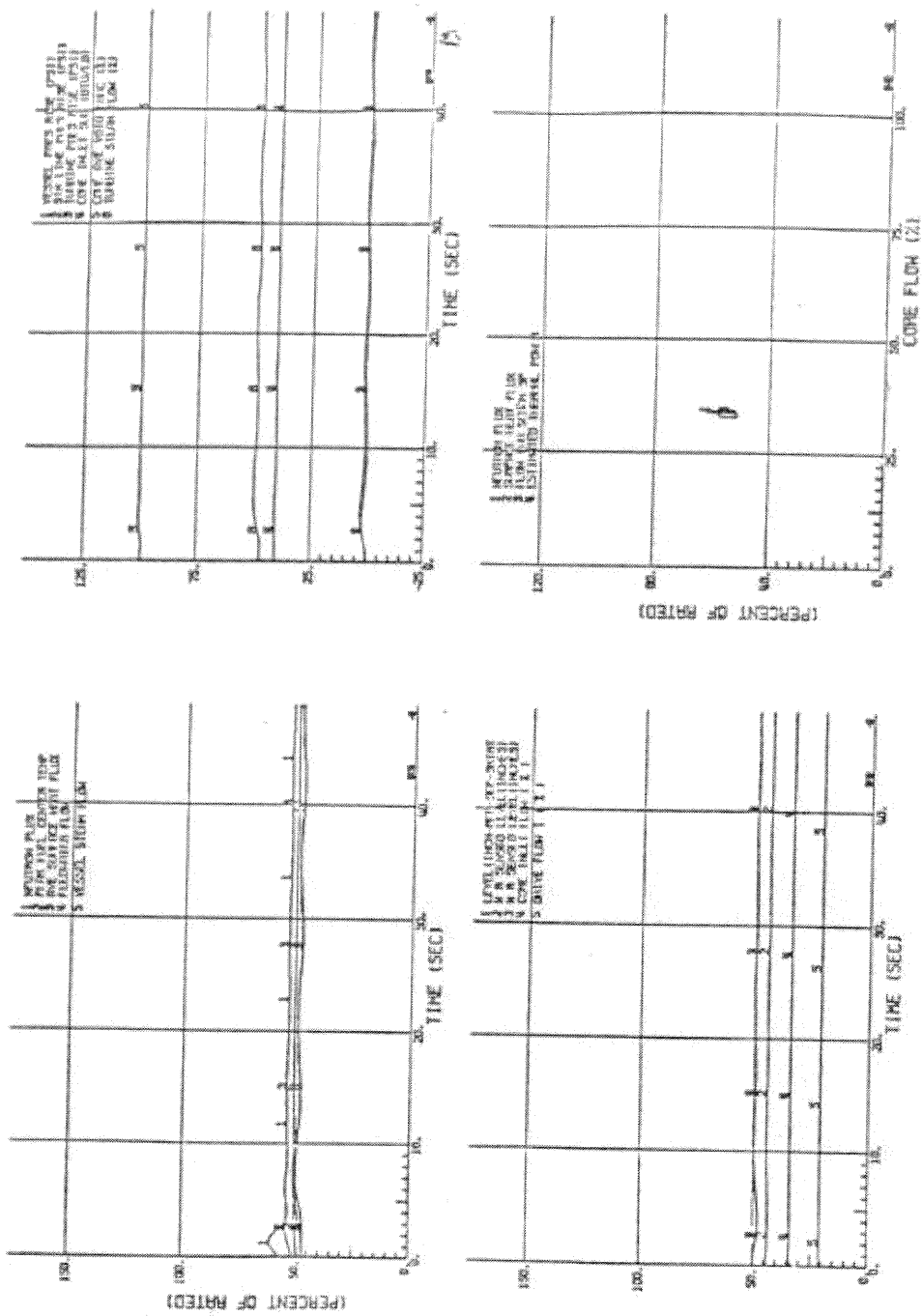
|

THIS PAGE INTENTIONALLY LEFT BLANK

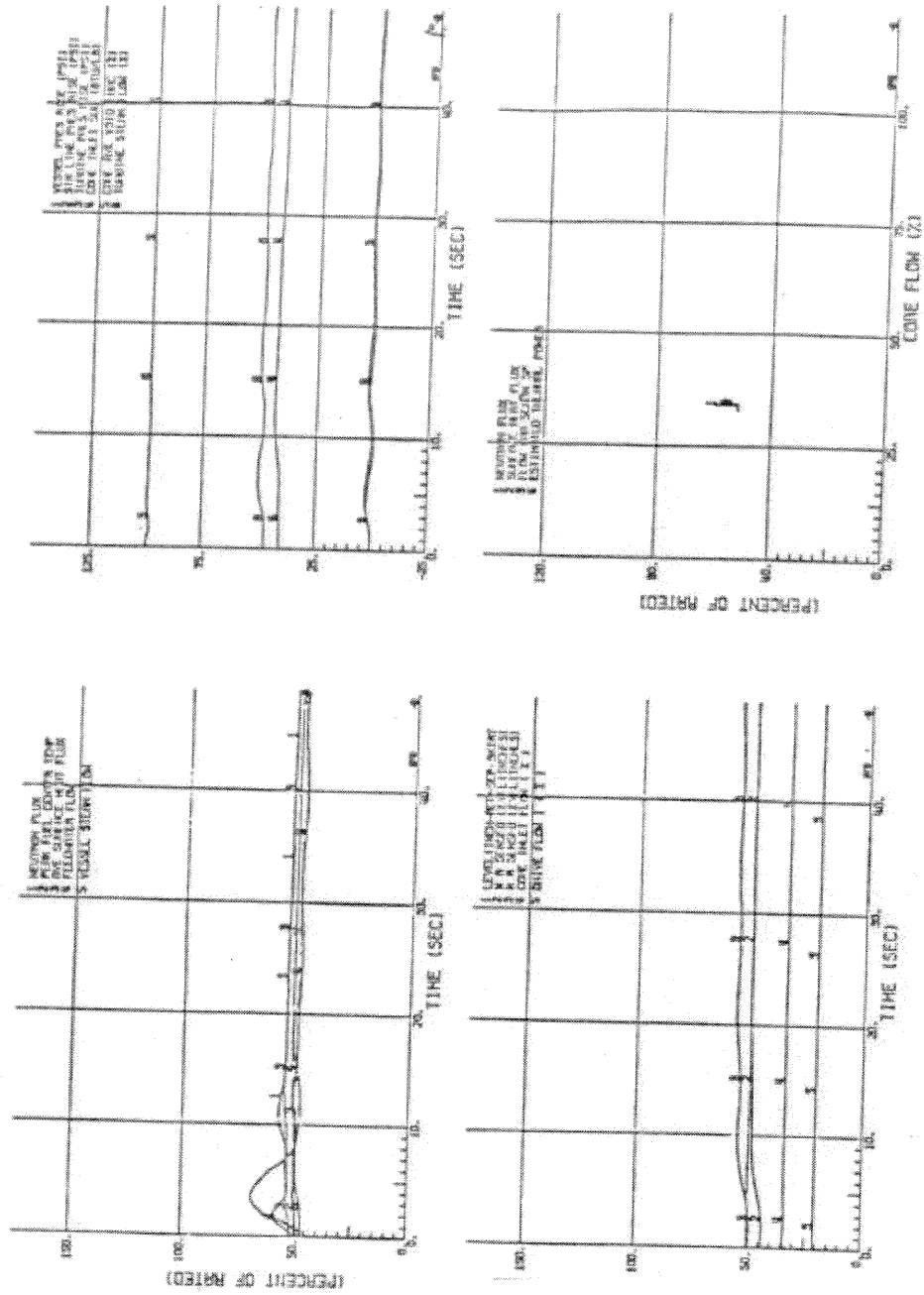
|



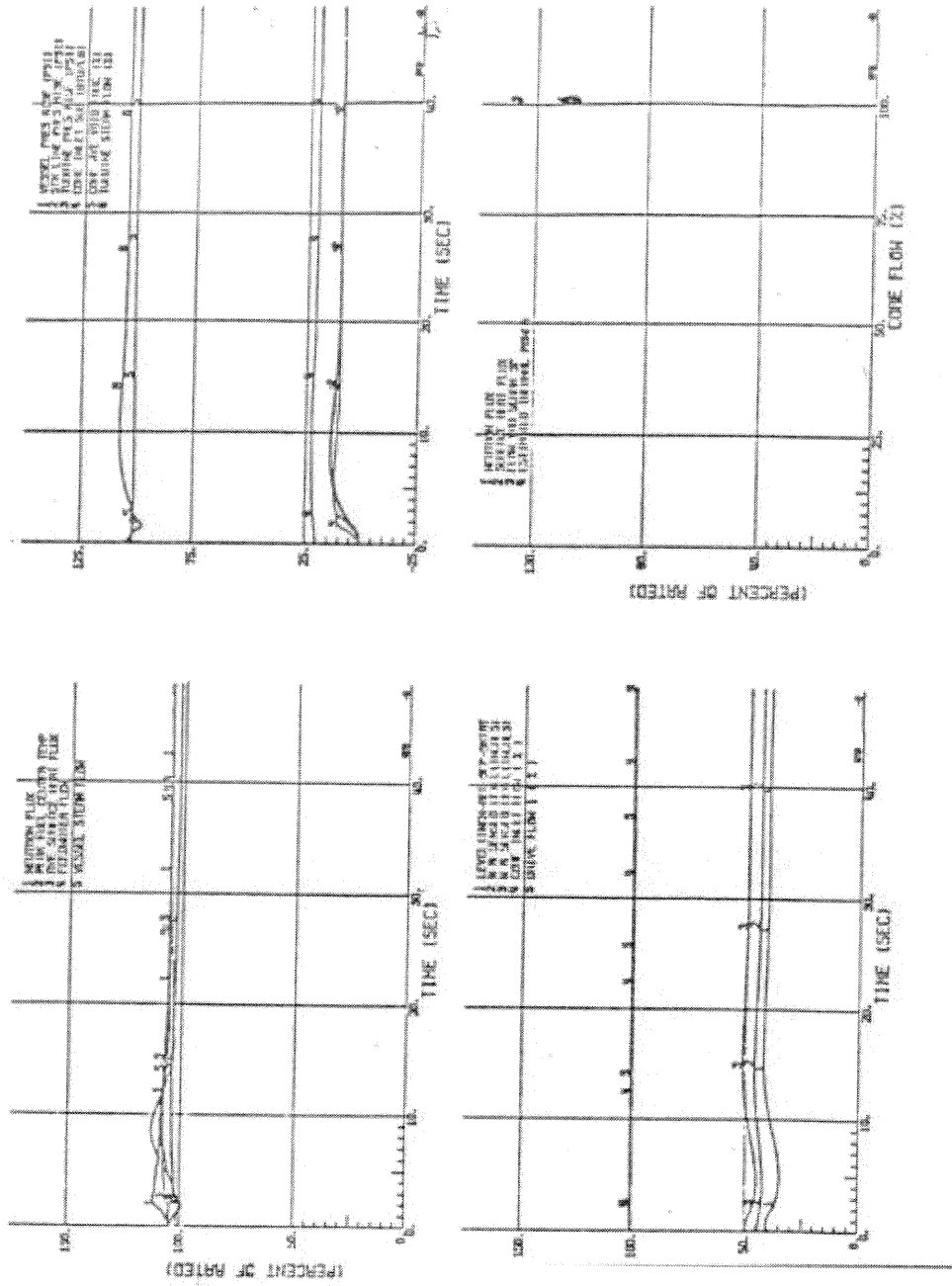
LASALLE COUNTY STATION
 UPDATED FINAL SAFETY ANALYSIS REPORT
 FIGURE 4.4-6
 INITIAL CORE
 10 PSI PRESSURE REGULATOR SETPOINT
 STEP AT 51.5% RATED POWER
 (NATURAL CIRCULATION)



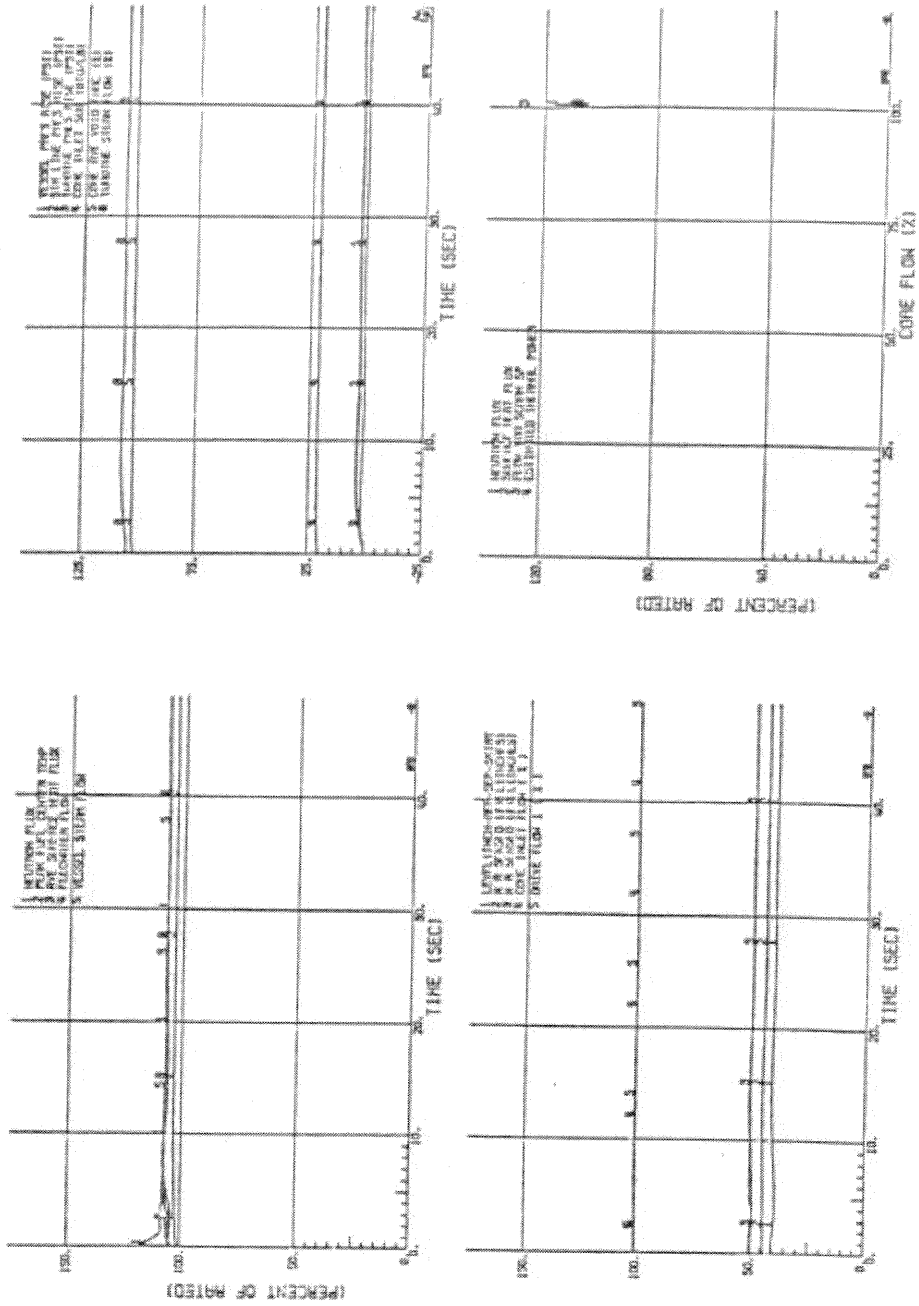
LASALLE COUNTY STATION
 UPDATED FINAL SAFETY ANALYSIS REPORT
 FIGURE 4.4-7
 INITIAL CORE
 10 CENT ROD REACTIVITY STEP AT 51.5%
 RATED POWER (NATURAL CIRCULATION)



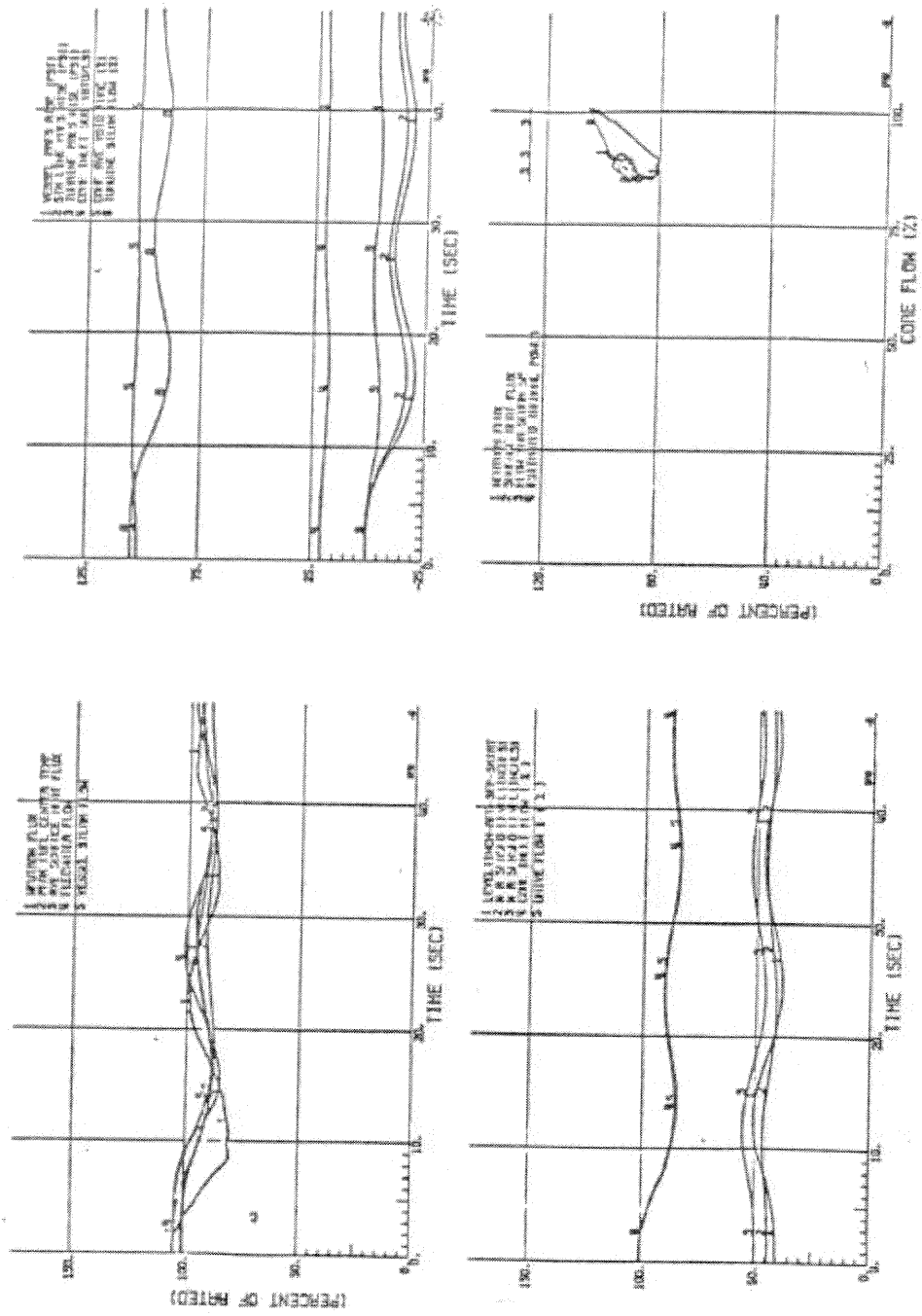
LASALLE COUNTY STATION
 UPDATED FINAL SAFETY ANALYSIS REPORT
 FIGURE 4.4-8
 INITIAL CORE
 6-INCH WATER LEVEL SETPOINT STEP
 AT 51.5% RATED POWER
 (NATURAL CIRCULATION)



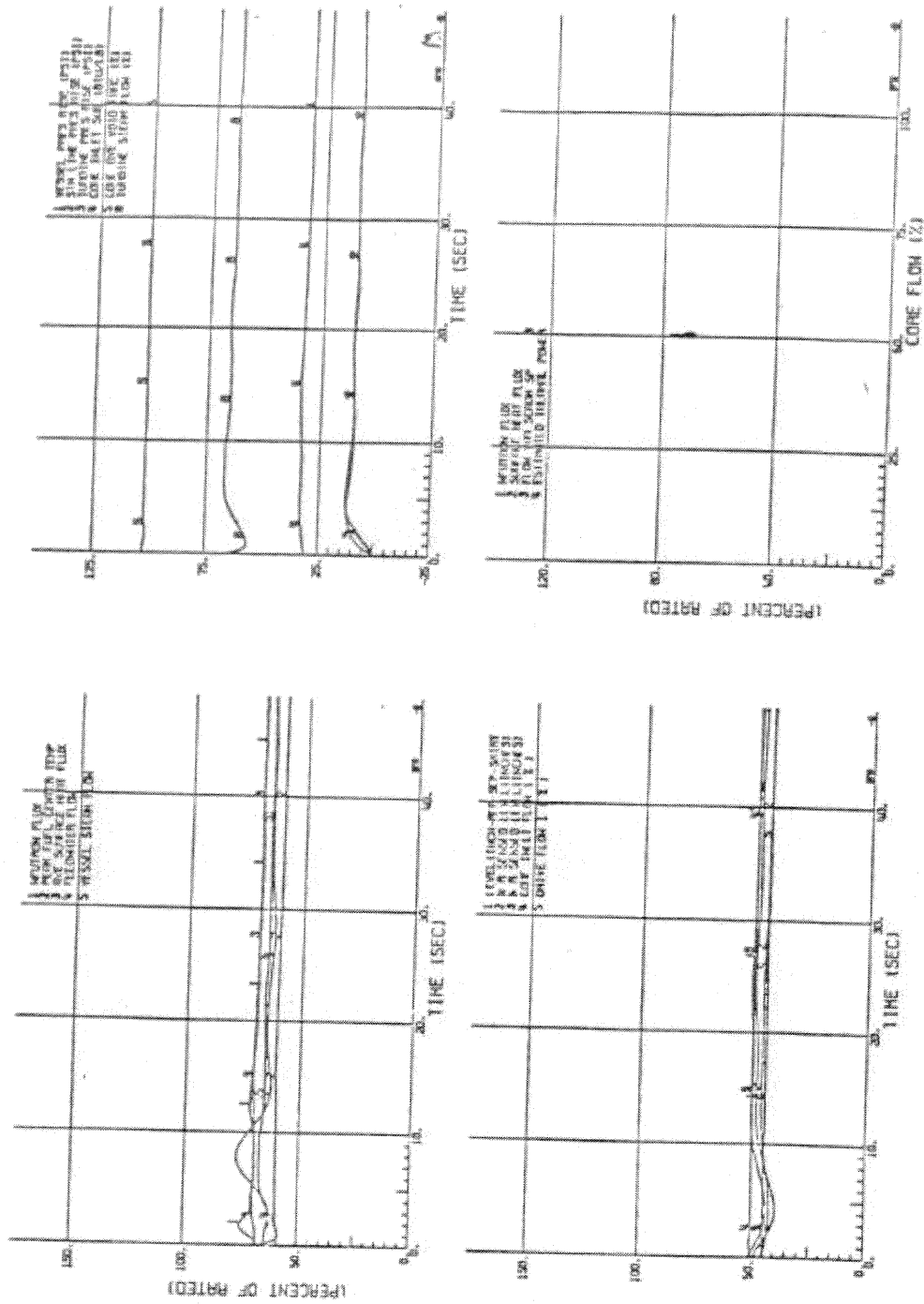
LASALLE COUNTY STATION
 UPDATED FINAL SAFETY ANALYSIS REPORT
 FIGURE 4.4.9
 INITIAL CORE
 10 PSI PRESSURE REGULATORY SETPOINT
 AT 105% RATED POWER AND 100% RATED FLOW



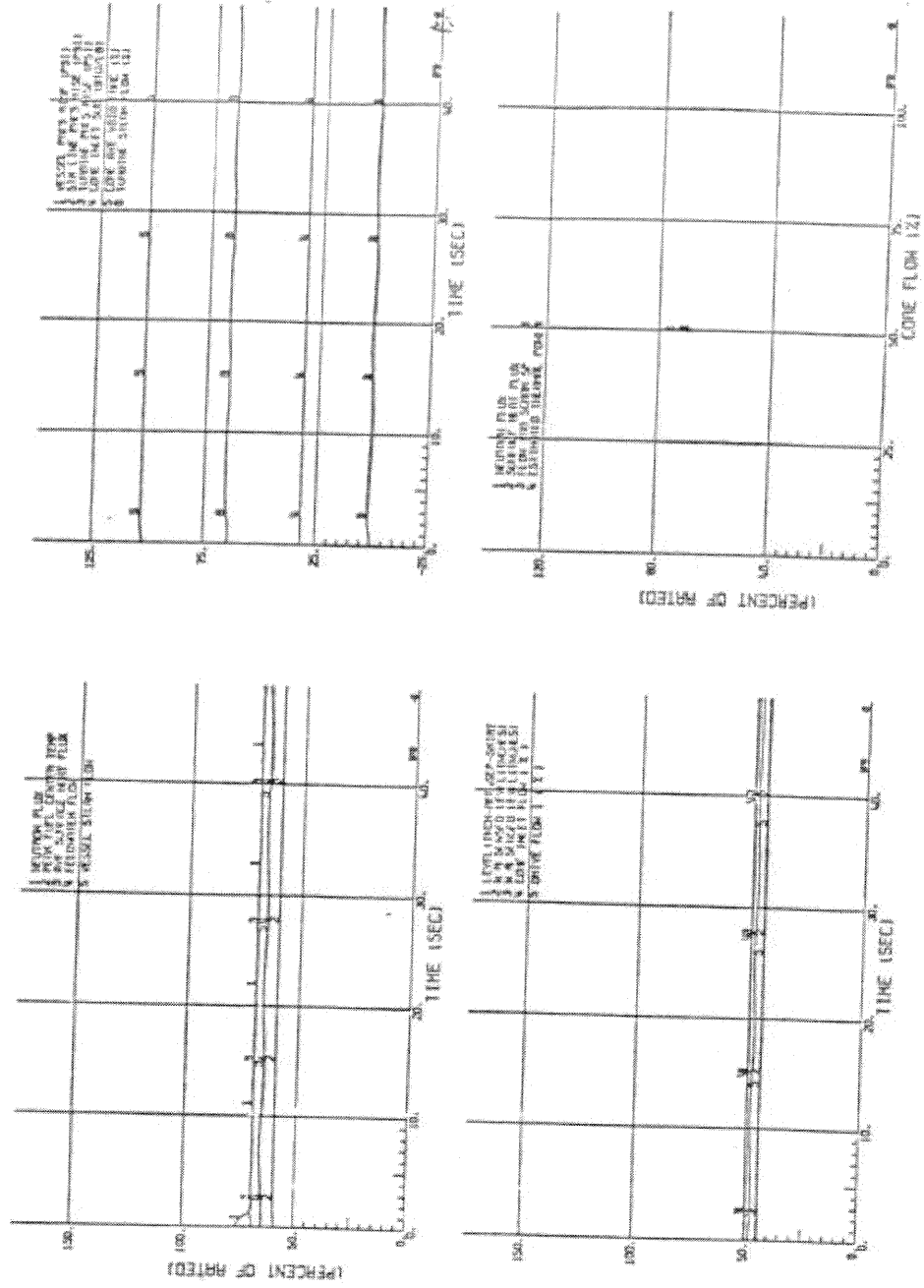
LASALLE COUNTY STATION
 UPDATED FINAL SAFETY ANALYSIS REPORT
 FIGURE 4.4-10
 INITIAL CORE
 10 CENT ROD REACTIVITY STEP
 AT 105% RATED POWER AND 100% RATED FLOW



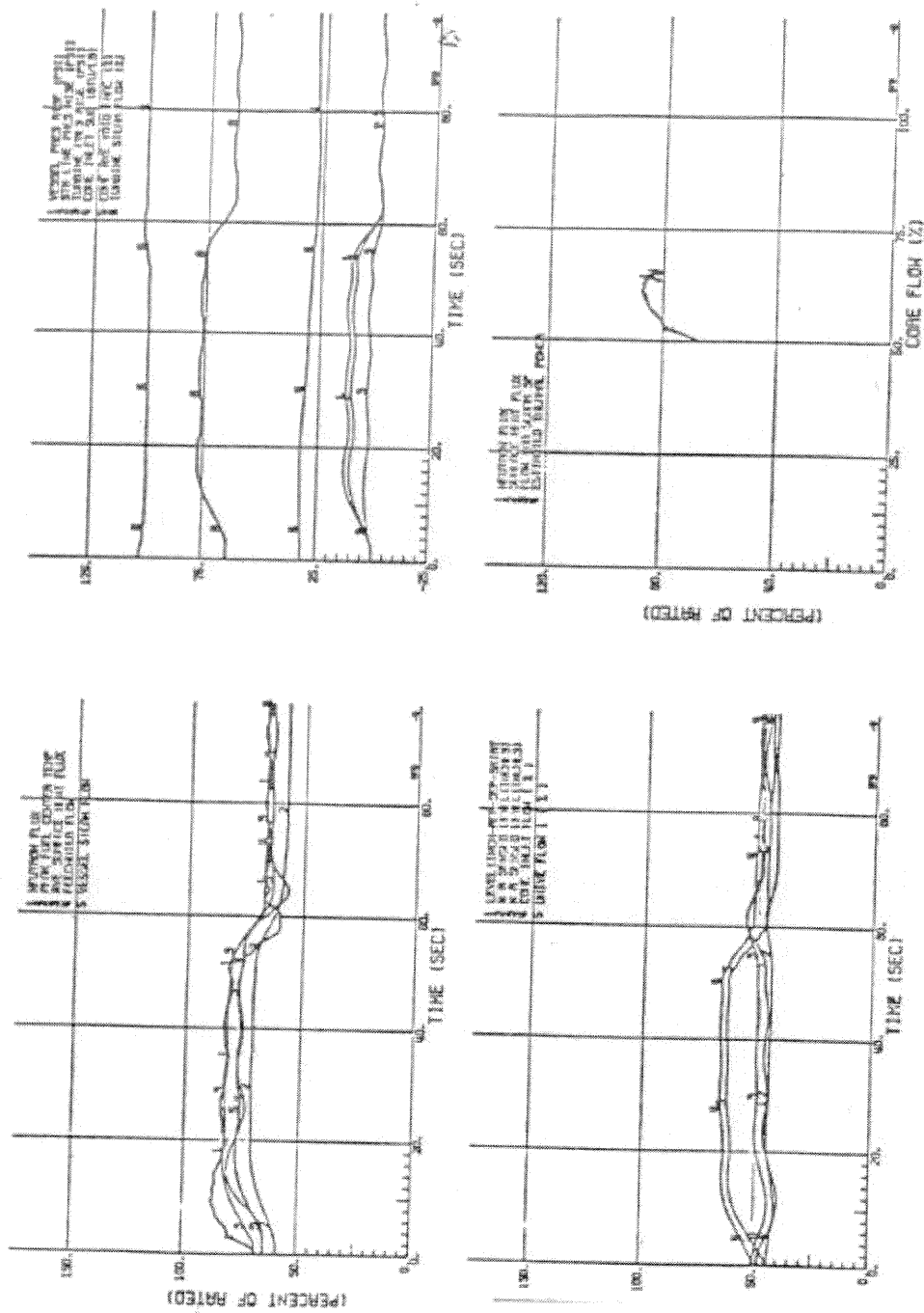
LASALLE COUNTY STATION
 UPDATED FINAL SAFETY ANALYSIS REPORT
 FIGURE 4.4-11
 INITIAL CORE
 10% LOAD DEMAND STEP
 AT 105% RATED POWER AND 100% RATED FLOW



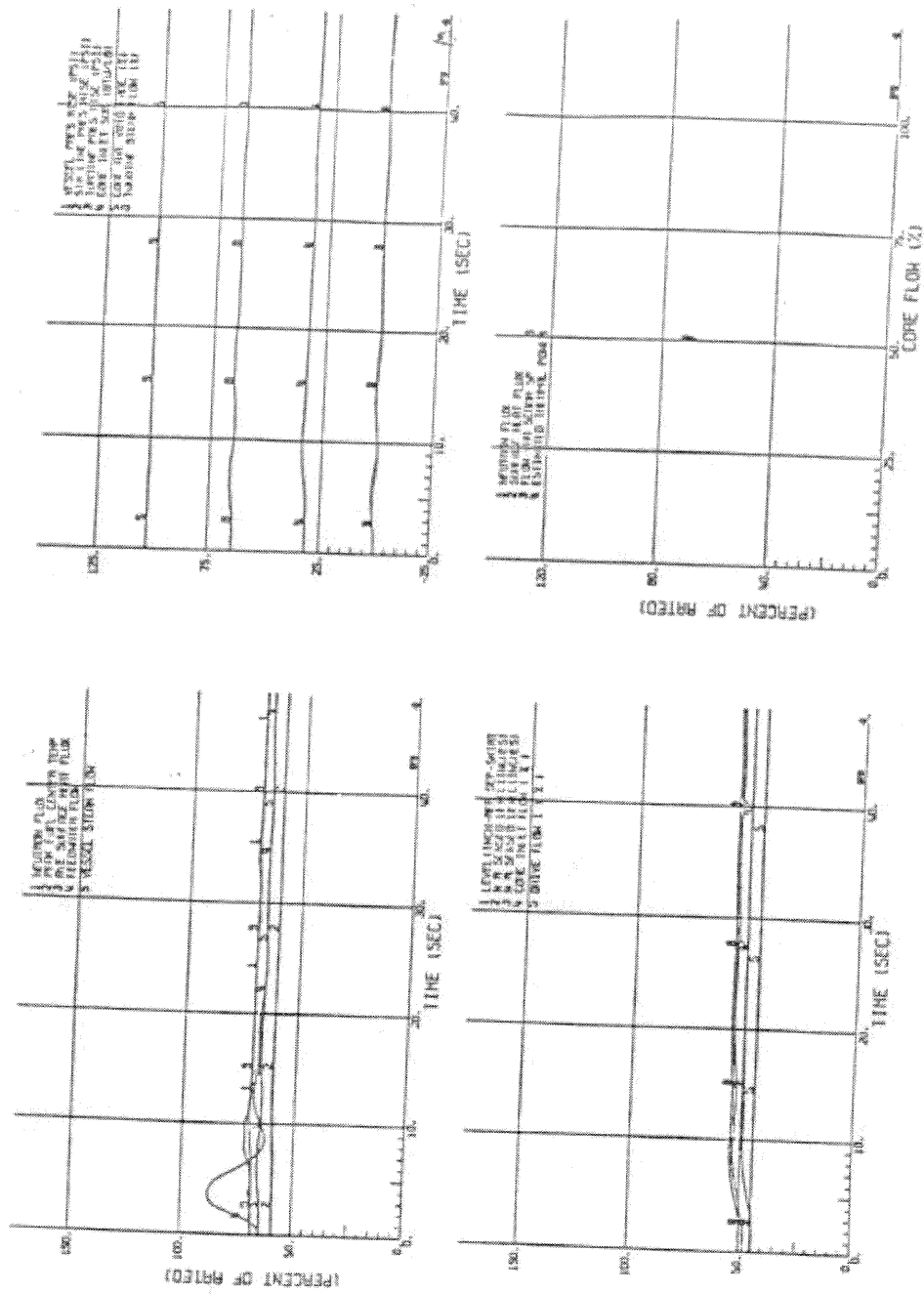
LASALLE COUNTY STATION
 UPDATED FINAL SAFETY ANALYSIS REPORT
 FIGURE 4.4-13
 INITIAL CORE
 10 PSI PRESSURE REGULATOR SETPOINT STEP
 AT 68% POWER AND 50% RATED FLOW



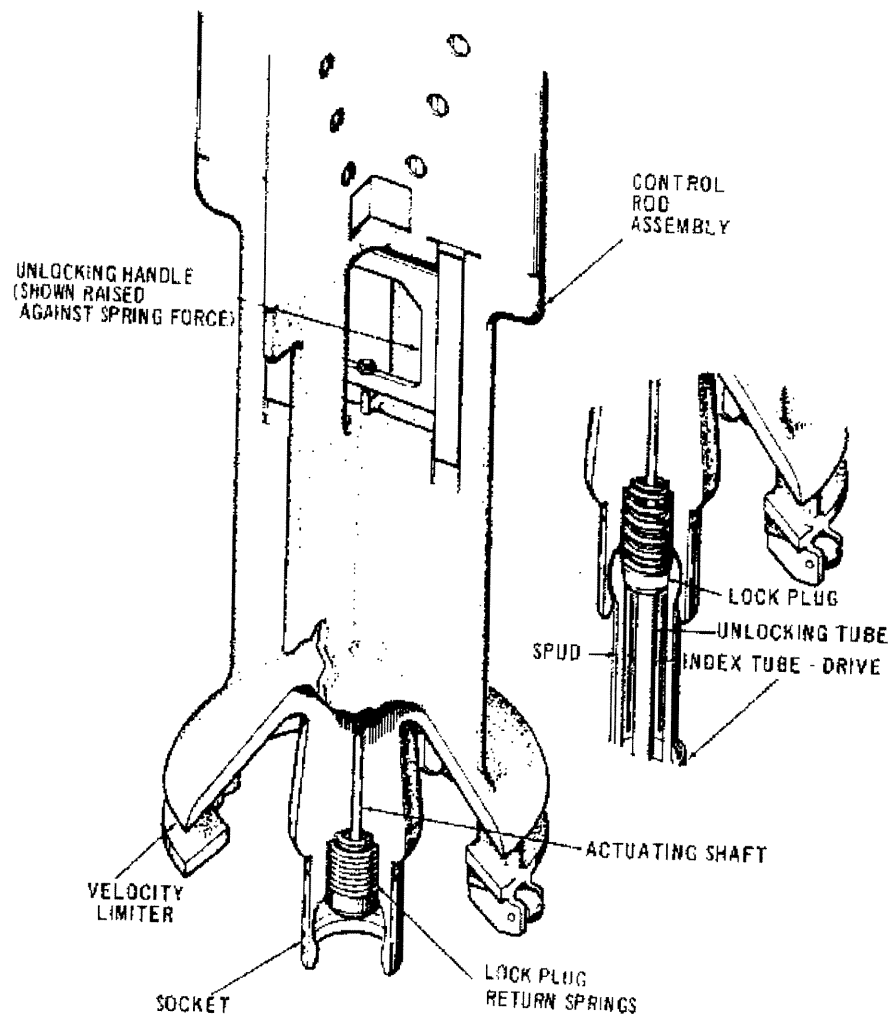
LASALLE COUNTY STATION
 UPDATED FINAL SAFETY ANALYSIS REPORT
 FIGURE 4.4-14
 INITIAL CORE
 10 CENT ROD REACTIVITY STEP
 AT 68% POWER AND 50% RATED FLOW



LASALLE COUNTY STATION
 UPDATED FINAL SAFETY ANALYSIS REPORT
 FIGURE 4.4-15
 INITIAL CORE
 10% LOAD DEMAND STEP
 AT 68% POWER AND 50% RATED FLOW



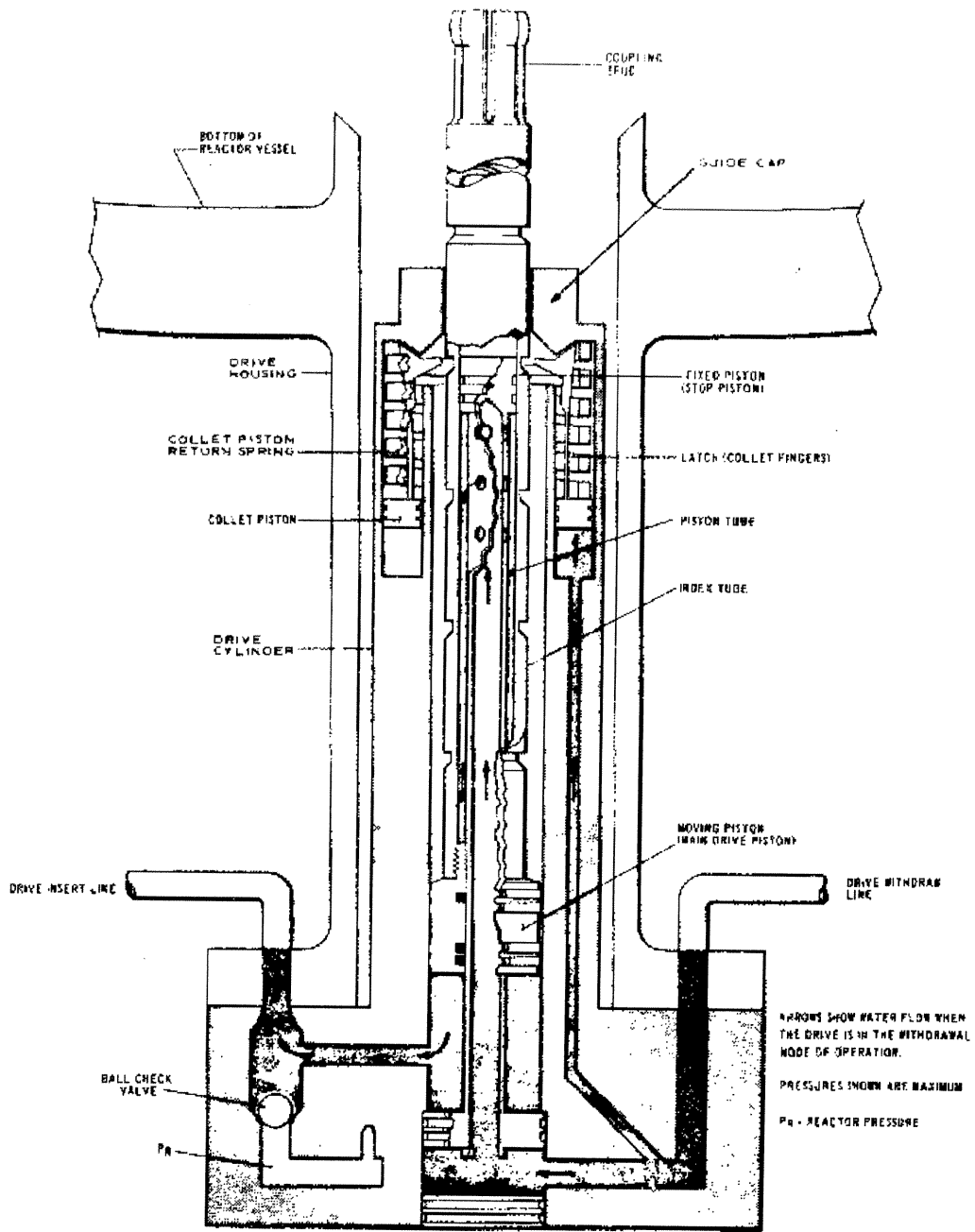
LASALLE COUNTY STATION
 UPDATED FINAL SAFETY ANALYSIS REPORT
 FIGURE 4.4-16
 INITIAL CORE
 6-INCH WATER LEVEL SETPOINT STEP
 AT 68% POWER AND 50% RATED FLOW



LA SALLE COUNTY STATION
UPDATED FINAL SAFETY ANALYSIS REPORT

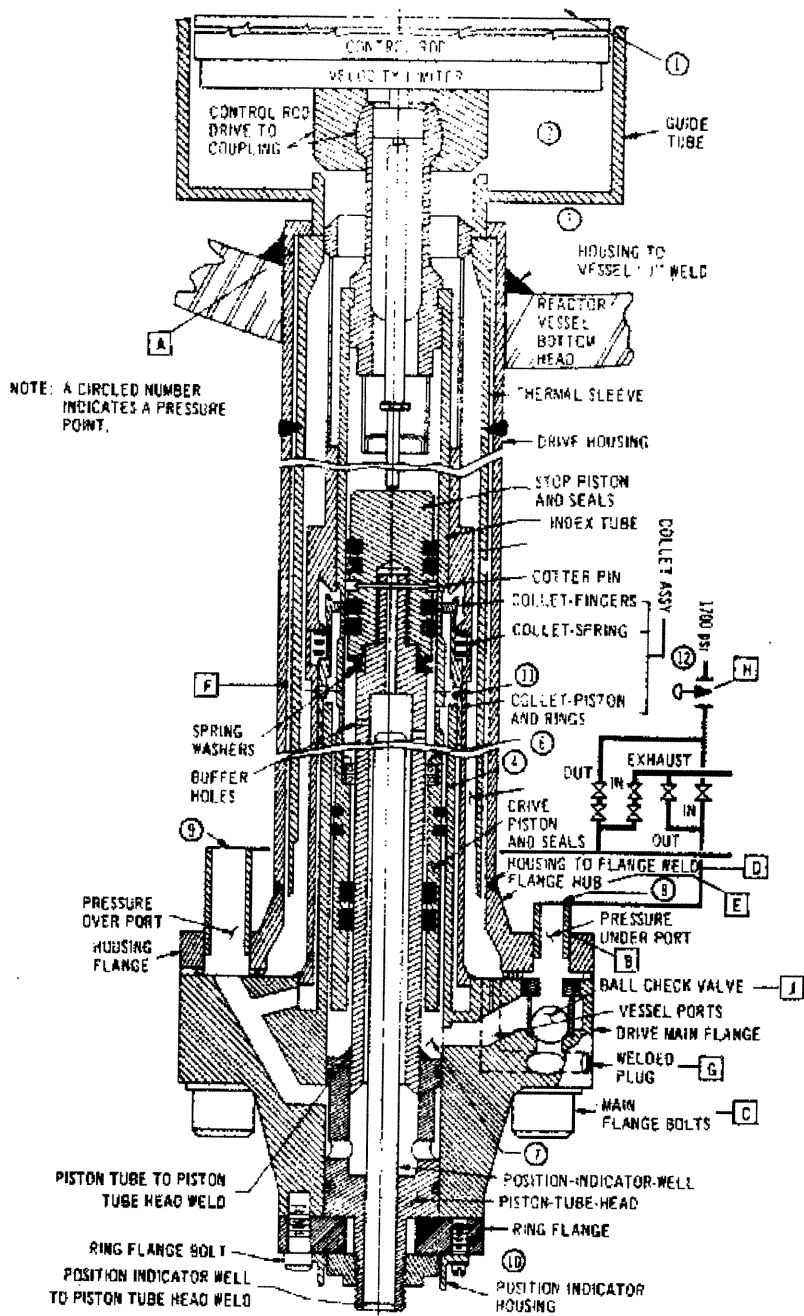
FIGURE 4.6-1
CONTROL ROD TO CONTROL ROD
DRIVE COUPLING

REV. 0 - APRIL 1984



LA SALLE COUNTY STATION
 UPDATED FINAL SAFETY ANALYSIS REPORT

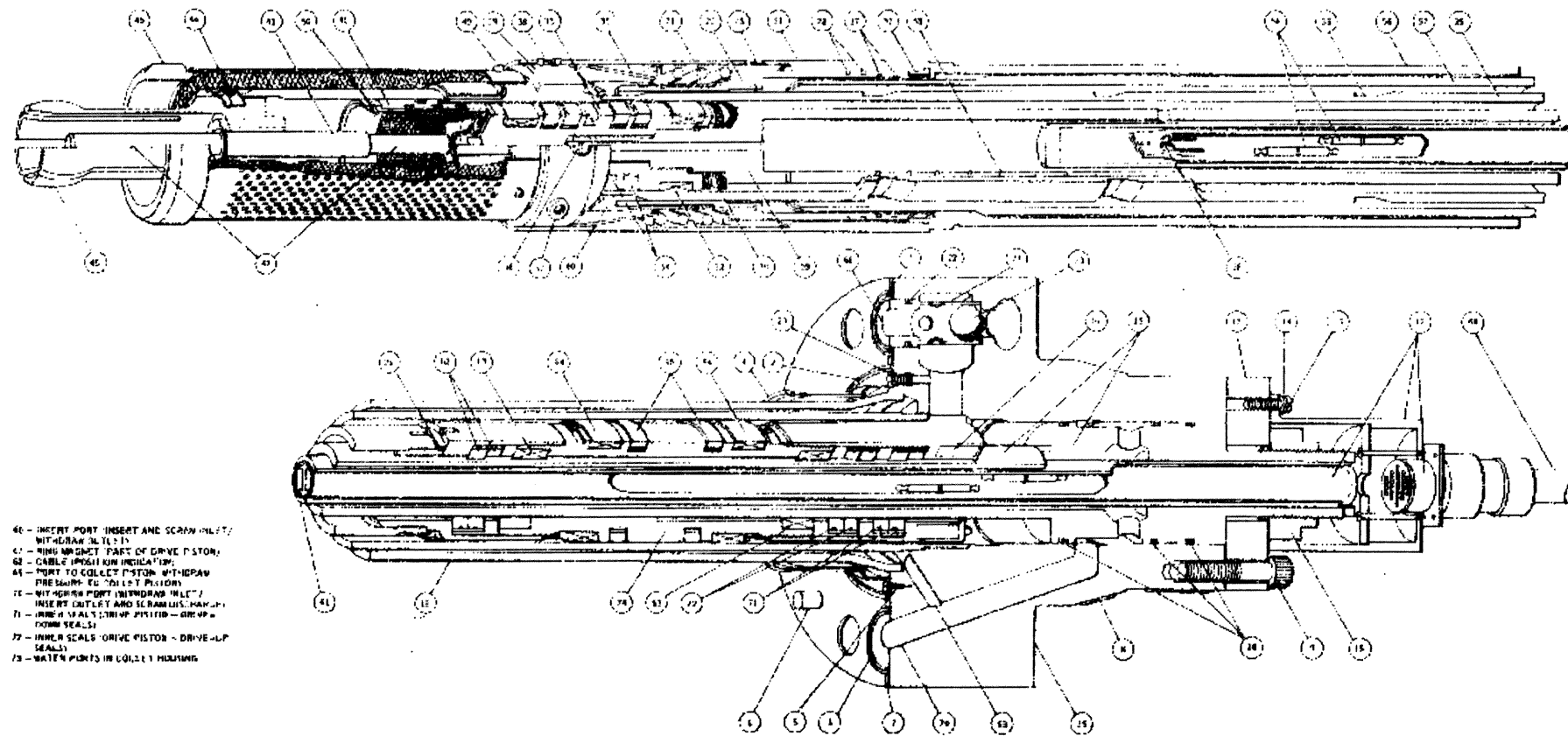
FIGURE 4.6-2
 CONTROL ROD DRIVE UNIT



LA SALLE COUNTY STATION
UPDATED FINAL SAFETY ANALYSIS REPORT

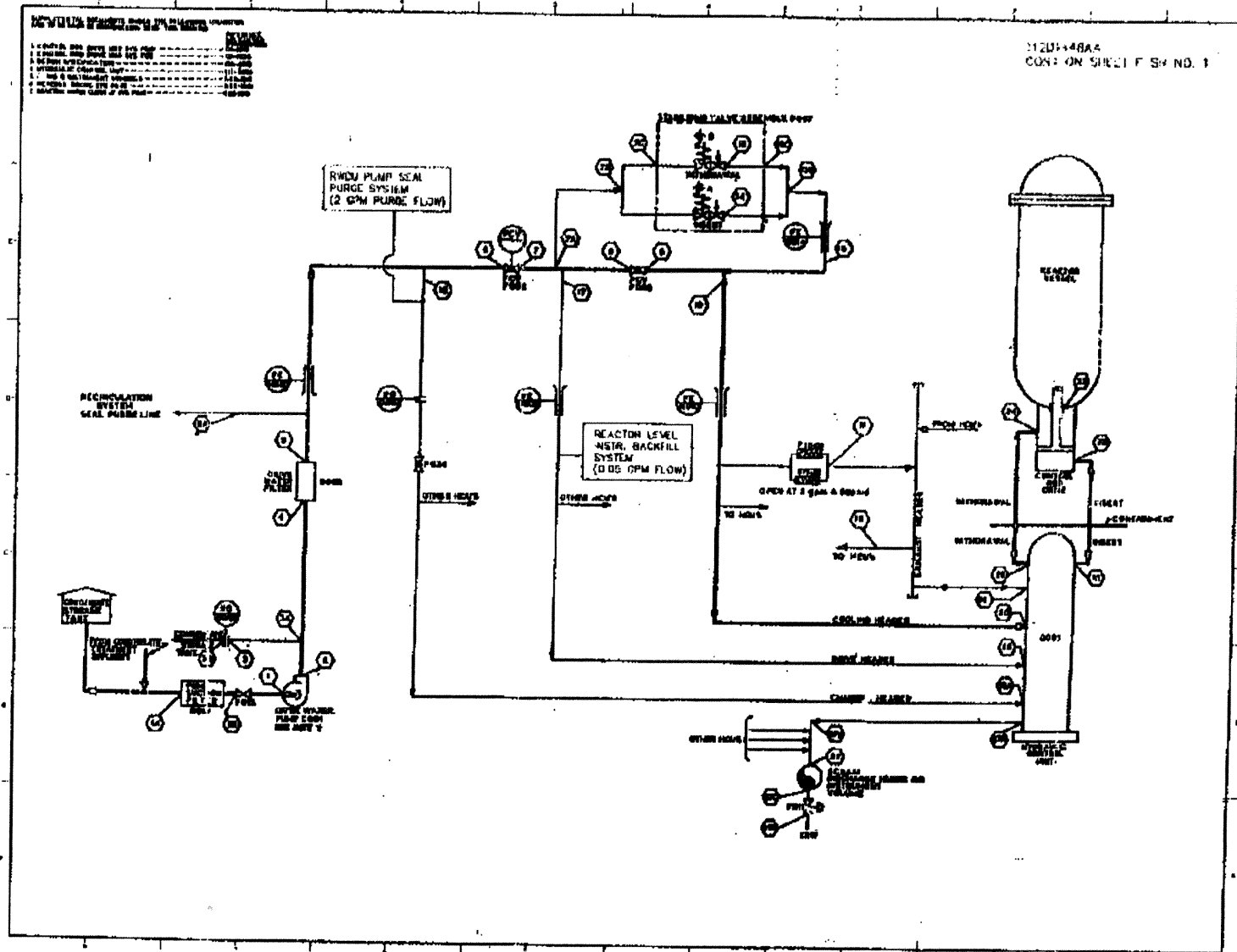
FIGURE 4.6-3
CONTROL ROD DRIVE UNIT (SCHEMATIC)

- 2 - O-RING (END FLANGE FACE)
- 3 - O-RING (INSERT AND WITHDRAW PORTS)
- 4 - STRAINER
- 5 - FLAT HEAD SCREW (STRAINER-MOUNTING)
- 6 - O-RING (MOUNTING PIN)
- 7 - O-RING (SPACER)
- 8 - NUT (FLANGE)
- 9 - SCREW (HEAD CAP SCREW - RING FLANGE MOUNTING)
- 10 - POSITION INDICATOR PROBE
- 11 - FILLISTER-HEAD SCREW (POSITION INDICATOR PROBE MOUNTING)
- 12 - LOCKWASHER (TOP "NUT")
- 13 - PISTON TUBE
- 14 - NUT (PISTON TUBE)
- 15 - O-RING (PISTON TUBE)
- 16 - O-RING (PISTON TUBE)
- 17 - O-RING (PISTON TUBE)
- 18 - O-RING (PISTON TUBE)
- 19 - O-RING (PISTON TUBE)
- 20 - O-RING (PISTON TUBE)
- 21 - BALL BEARING (NUT)
- 22 - BALL BEARING (NUT)
- 23 - BALL BEARING (NUT)
- 24 - BALL BEARING (NUT)
- 25 - BALL BEARING (NUT)
- 26 - BALL BEARING (NUT)
- 27 - BALL BEARING (NUT)
- 28 - BALL BEARING (NUT)
- 29 - BALL BEARING (NUT)
- 30 - BALL BEARING (NUT)
- 31 - BALL BEARING (NUT)
- 32 - BALL BEARING (NUT)
- 33 - BALL BEARING (NUT)
- 34 - BALL BEARING (NUT)
- 35 - BALL BEARING (NUT)
- 36 - BALL BEARING (NUT)
- 37 - BALL BEARING (NUT)
- 38 - BALL BEARING (NUT)
- 39 - BALL BEARING (NUT)
- 40 - BALL BEARING (NUT)
- 41 - BALL BEARING (NUT)
- 42 - BALL BEARING (NUT)
- 43 - BALL BEARING (NUT)
- 44 - BALL BEARING (NUT)
- 45 - BALL BEARING (NUT)
- 46 - BALL BEARING (NUT)
- 47 - BALL BEARING (NUT)
- 48 - BALL BEARING (NUT)
- 49 - BALL BEARING (NUT)
- 50 - BALL BEARING (NUT)
- 51 - BALL BEARING (NUT)
- 52 - BALL BEARING (NUT)
- 53 - BALL BEARING (NUT)
- 54 - BALL BEARING (NUT)
- 55 - BALL BEARING (NUT)
- 56 - BALL BEARING (NUT)
- 57 - BALL BEARING (NUT)
- 58 - BALL BEARING (NUT)
- 59 - BALL BEARING (NUT)
- 60 - BALL BEARING (NUT)
- 61 - BALL BEARING (NUT)
- 62 - BALL BEARING (NUT)
- 63 - BALL BEARING (NUT)
- 64 - BALL BEARING (NUT)
- 65 - BALL BEARING (NUT)
- 66 - BALL BEARING (NUT)
- 67 - BALL BEARING (NUT)
- 68 - BALL BEARING (NUT)
- 69 - BALL BEARING (NUT)
- 70 - BALL BEARING (NUT)
- 71 - BALL BEARING (NUT)
- 72 - BALL BEARING (NUT)
- 73 - BALL BEARING (NUT)
- 74 - BALL BEARING (NUT)
- 75 - BALL BEARING (NUT)
- 76 - BALL BEARING (NUT)
- 77 - BALL BEARING (NUT)
- 78 - BALL BEARING (NUT)
- 79 - BALL BEARING (NUT)
- 80 - BALL BEARING (NUT)
- 81 - BALL BEARING (NUT)
- 82 - BALL BEARING (NUT)
- 83 - BALL BEARING (NUT)
- 84 - BALL BEARING (NUT)
- 85 - BALL BEARING (NUT)
- 86 - BALL BEARING (NUT)
- 87 - BALL BEARING (NUT)
- 88 - BALL BEARING (NUT)
- 89 - BALL BEARING (NUT)
- 90 - BALL BEARING (NUT)
- 91 - BALL BEARING (NUT)
- 92 - BALL BEARING (NUT)
- 93 - BALL BEARING (NUT)
- 94 - BALL BEARING (NUT)
- 95 - BALL BEARING (NUT)
- 96 - BALL BEARING (NUT)
- 97 - BALL BEARING (NUT)
- 98 - BALL BEARING (NUT)
- 99 - BALL BEARING (NUT)
- 100 - BALL BEARING (NUT)



LA SALLE COUNTY STATION
 UPDATED FINAL SAFETY ANALYSIS REPORT

FIGURE 4.6-4
 CONTROL ROD DRIVE UNIT (CUTAWAY)



REVISIONS
1. REVISED FOR THE NEW DESIGN
2. REVISED FOR THE NEW DESIGN
3. REVISED FOR THE NEW DESIGN
4. REVISED FOR THE NEW DESIGN
5. REVISED FOR THE NEW DESIGN
6. REVISED FOR THE NEW DESIGN
7. REVISED FOR THE NEW DESIGN
8. REVISED FOR THE NEW DESIGN
9. REVISED FOR THE NEW DESIGN
10. REVISED FOR THE NEW DESIGN

11201-4804
CONT. ON SHEET F-54 NO. 1

LASALLE COUNTY STATION
UPDATED FINAL SAFETY ANALYSIS REPORT
FIGURE 4.6-6
CONTROL ROD DRIVE HYDRAULIC SYSTEM PROCESS
DIAGRAM

112D1448AA
CONT ON SHEET 2 SH NO. 1

MODE A NORMAL OPERATION

LOCATION	1A	1	2	3	4	5	5A	6	7	8	9	10	11	12	13
FLOW - GPM	95	93	95	20	75	75	103	63	63	57	57	63	0	0	20
PRESSURE - PSIG	21	15	1483	1483	1471	1456	1456	1448	PR+260	FR+260	PR+30 MAX	PR+30 MAX	FR	PR	PR+30 MAX

LOCATION	14	15	16	17	18	20	21	22	23	24	25	26	27
FLOW - GPM	4.0	6.4	0	0	0	3.4 MAX	3.4 MAX	3.4 MAX	3.4 MAX	0	0	0	0
PRESSURE - PSIG	PR+30 MAX	PR+30 MAX	1448			PR+15	PR+14	PR+14	PR	PR		PR	0

MODE B ROD INSERTION

LOCATION	1A	1	2	3	4	5	5A	6	7	8	9	10	11	12	13
FLOW - GPM	95	93	95	20	75	75	100	63	63	57	57	59	0	0.7	20
PRESSURE - PSIG	21	19	1483	1483	1471	1456	1456	1448	PR+260	FR+260	PR+30 MAX	PR+30 MAX	PR+8	PR+9	PR+30 MAX

LOCATION	14	15	16	17	18	20	21	22	23	24	25	26	27	
FLOW - GPM	0	2.0	0	4.0	4.0	0	4.0	4.0	1.3	7	7	7	0	
PRESSURE - PSIG		PR+10 MAX	1448	PR+260	PR+250		PR+15	PR+9	PR+90	PR	PR+20 MAX	PR+20 MAX	PR+8 MAX	0

MODE C SCRAM

LOCATION	1A	1	2	3	4	5	5A	6	7	8	9	10	11	12	13
FLOW - GPM	47	47	47	20	27	27	10	15	15	15	15	15	15	14.9	0
PRESSURE - PSIG	21	19	1526	1526									SEE NOTE 9	SEE NOTE 9	

LOCATION	14	15	16	17	18	20	21	22	23	24	25	26	27
FLOW - GPM	0	3	0	0	0	0	90	90	-3.6	30	30	0.1 SEE NOTE 9	APPROX 563
PRESSURE - PSIG							1187 MAX	731 MAX	PR	258 MAX	94		85 MAX

MODE D SCRAM COMPLETED

LOCATION	1A	1	2	3	4	5	5A	6	7	8	9	10	11	12	13
FLOW - GPM	200	200	200	20	100	100	10	15	15	15	15	15	15	14.9	0
PRESSURE - PSIG	25	19	1210					1005	>PR	>PR	>PR	>PR	>PR	>PR	>PR

LOCATION	14	15	16	17	18	20	21	22	23	24	25	26	27
FLOW - GPM	0	0	15.3	0	0	0	0.92	0.92	0.92	SEE NOTE 9	SEE NOTE 9	0.1	0
PRESSURE - PSIG			1005				76	78	PR	85 MAX	85 MAX		83 MAX

CONDITIONS:

- DRIVES LATCHED
- PRESSURE OF REACTOR (PR) AT 1000 PSIG
- MAXIMUM COOLING FLOW TO DRIVES MINIMUM REQUIRED
- PRESSURE AT POSITION 1A IS 10 FEET OF WATER AT 200 GPM.

(FOR NOTES SEE SHEET 2)

MODE A SIZES THE COOLING WATER HEADERS. PRESSURE AT LOCATION 16 SHALL NOT EXCEED 1510 PSIG
LINE LOSS FROM LOCATION 10 TO LOCATION 20 SHALL NOT EXCEED 3 PSIG

RWCU PUMP SEAL PURGE FLOW=2 GPM

CONDITIONS:

- DRIVES INSERTING
- PRESSURE OF REACTOR (PR) AT 1000 PSIG
- MAXIMUM DRIVING FLOW TO DRIVES

MODE B SIZES THE DRIVE WATER HEADERS.

RWCU PUMP SEAL PURGE FLOW=2 GPM

CONDITIONS:

- DRIVES SCRAMMING
- PRESSURE OF REACTOR (PR) AT 1000 PSIG
- FLWS BASED ON MAXIMUM ROD VELOCITY OF 85 INCHES PER SECOND

MODE C SIZES THE INSERT AND WITHDRAW LINES

RWCU PUMP SEAL PURGE FLOW=2 GPM

CONDITIONS:

- SCRAMMING OF DRIVES COMPLETED
- PRESSURE OF REACTOR (PR) AT 0 PSIG
- MAXIMUM CRD SUPPLY PUMP FLOW

MODE D SIZES THE PUMP SUCTION LINE

NOTE: MINIMUM ACCUMULATOR PRECHARGE PRESSURE IS 565 PSIG.

RWCU PUMP SEAL PURGE FLOW=2 GPM

LASALLE COUNTY STATION
UPDATED FINAL SAFETY ANALYSIS
REPORT

FIGURE 4.6-6
PROCESS DATA,
CONTROL ROD DRIVE
HYDRAULIC SYSTEM (SHEET 1 OF 2)

REVISION 13

TABLE 1

LOCATION	1A-1B	1B-11	2-11-6	3A-3B	6-1-9	7A-7B	7B-7C
DESIGN PRESS. (PSIG.)	150	250	1750	1750	1750	1750	1750
DESIGN TEMP. (DEG F)	150	150	150	150	150	150	150
ESTIMATED LINE SIZE (INCHES)	4.0	4.0	2.0	1.0	1.5	1.0	0.75

LOCATION	10-20	11-12	15B-15C	15-18B	16-18A	2-18	12-25
DESIGN PRESS. (PSIG.)	1750	1750	1750	1750	1750	1750	1750
DESIGN TEMP. (DEG F)	150	150	150	150	150	150	150
ESTIMATED LINE SIZE (INCHES)	2**	1.0	0.75	1.0	2.0	1.0	1.0

LOCATION	21-22	24-25	27A-27B	27D-27	27-27C	27C-27D
DESIGN PRESS. (PSIG.)	1750	1750	1250	1250	1250	1250
DESIGN TEMP. (DEG F)	150	150	200	200	200	200
ESTIMATED LINE SIZE (INCHES)	1.0	0.75	0.75	0	10.0	2.0

* SEE CRD SYSTEM DESIGN SPECIFICATION.

** 2 INCH HEADER TO EACH HALF OF THE TOTAL QUANTITY OF HCU'S.

NOTES:

1. DEFINITION OF SYMBOLS

PR - INDICATOR PRESSURE OF THE REACTOR

2. MAXIMUM OPERATING TEMPERATURES

THE MAXIMUM SYSTEM OPERATING TEMPERATURE WILL NOT EXCEED 150 DEG. F. FROM LOCATION 1 THROUGH 27 WITH THE FOLLOWING EXCEPTIONS.

	LOCATION	MAXIMUM TEMP. (DEG. F.)
MODE A -	23	200
MODE C -	23	546
	24	546
	25	280
	27	280
MODE D -	23	200
	24	280
	25	280
	27	280

3. MODE A -

A. DELETED

B. LOCATION 16 - THE MAXIMUM ACCUMULATOR CHARGING PRESSURE SHALL NOT EXCEED 1510 PSIG. ACCUMULATOR PRESSURE IN EXCESS OF 1510 PSIG. MAY CAUSE CRD DAMAGE DURING SCRAM.

C. LOCATION 20 - THE CRD COOLING WATER PRESSURE SHALL NOT BE LESS THAN PR + 15 PSIG. FOR THE CONDITIONS INDICATED.

D. LOCATION 23 - MAXIMUM DRIVE COOLING REQUIREMENTS WILL NOT EXCEED 0.24 GPM/DRIVE FOR THE CONDITIONS LISTED. MINIMUM DRIVE COOLING REQUIREMENTS WILL NOT BE LESS THAN 0.20 GPM/DRIVE.

4. MODE B -

A. LOCATION 13 AND 14 - INSERT VALVE F007-A CLOSING ON DRIVE INSERT SIGNAL. WITHDRAW VALVE F007-B CLOSING ON DRIVE WITHDRAW SIGNAL BUT DOES NOT STAY CLOSED DURING SETTLING.

B. LOCATION 18 - THE CRD DRIVE WATER PRESSURE SHALL NOT BE LESS THAN PR + 250 PSIG. FOR THE CONDITIONS INDICATED.

5. MODE C -

A. DELETED

B. THE 546 DEG. F. TEMPERATURE LISTED IN NOTE 2 FOR MODE C POSITIONS 23 AND 24 SHALL BE USED ONLY IN DETERMINING THE MINIMUM PIPE WALL THICKNESS IN VICINITY OF THE DRIVE HOUSING AND NOT IN DETERMINING STRESSES DUE TO THERMAL EXPANSION. IN DETERMINING MINIMUM WALL THICKNESS IT MAY BE ASSUMED THAT THIS TEMPERATURE OCCURS LESS THAN 1 PERCENT OF THE OPERATING LIFE OF THE SYSTEM. SEE THE CRD HYD. SYSTEM DESIGN SPECIFICATION TO DETERMINE CYCLIC STRESSES DUE TO THERMAL EXPANSION.

C. LOCATION 21 TO 22 - THE PRESSURE DROP FROM LOCATION 21 TO 22 SHALL NOT EXCEED 425 PSI AT 50 GPM FOR ANY CRD.

D. LOCATION 23 - A NEGATIVE FLOW RATE INDICATES FLOW FROM THE REACTOR THROUGH THE DRIVE SEAL INTO THE CRD. THE MAXIMUM LEAK RATE FROM THE REACTOR CAN REACH 10 GPM PER DRIVE.

E. LOCATION 24 TO 25 - THE PRESSURE DROP FROM LOCATION 24 TO 25 SHALL NOT EXCEED 162 PSI AT 30 GPM FOR ANY CRD.

F. RESPONSE TIME OF FCV-F008 IS SUCH THAT SCRAM IS COMPLETED BEFORE FCV-F008 STARTS TO CLOSE.

G. SCRAM DRAIN VALVE F01 AND VENT VALVE F012 CLOSE WITH A SCRAM SIGNAL.

6. MODE D -

A. DELETED

B. LOCATION 27 - THE SCRAM DISCHARGE VOLUME SHALL BE SIZED SO THAT THE RESULTING PRESSURE IMMEDIATELY AFTER 100 PERCENT STROKE IS LESS THAN 65 PSIG.

7. MAXIMUM ALLOWABLE PUMP SUCTION PRESSURE SHALL BE 50 PSIG.

8. DELETED

9. DURING SCRAM, FINE FLOW WILL BE DIRECTED INTO THE SCRAM DISCHARGE VOLUME. FOLLOWING SCRAM, THIS FLOW WILL DECLINE AS VALVE F002 CLOSING AND AS THE SCRAM DISCHARGE VOLUME PRESSURIZES TO EQUAL THE REACTOR PRESSURE. AFTER THE SCRAM DISCHARGE VOLUME AND THE REACTOR VESSEL PRESSURE HAVE EQUALIZED, FLOW WILL BE DIVERTED TO THE REACTOR VESSEL VIA THE CRD WITHDRAW LINES AT A FLOW RATE DEPENDENT ON THE REACTOR PRESSURE:

(I.E. 1A.) APPROX. 15 GPM AT 10" PSIG. REACTOR PRESSURE.

(I.E. 1B.) APPROX. 5 GPM AT 1000" PSIG. REACTOR PRESSURE.

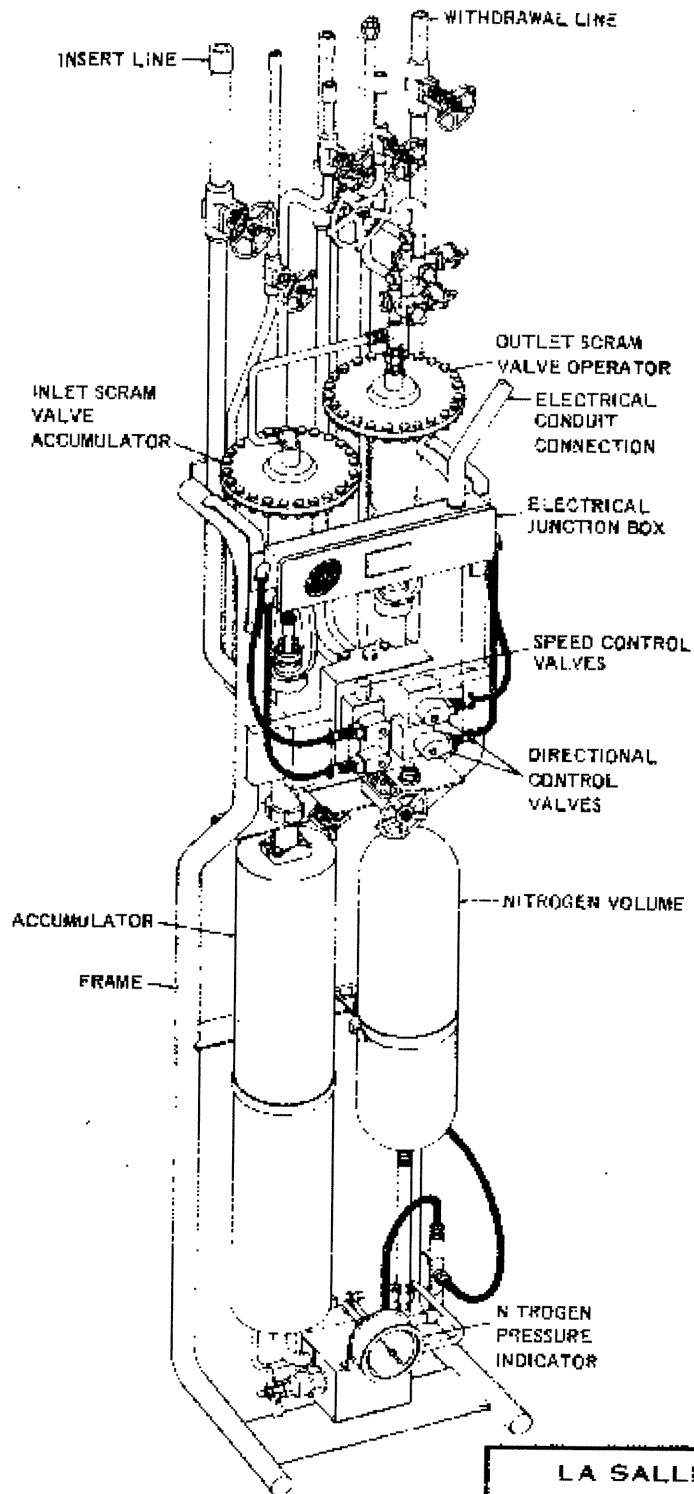
10. THIS VALUE APPLIES IMMEDIATELY FOLLOWING COMPLETION OF SCRAM. PRESSURE WILL SUBSEQUENTLY EQUALIZE WITH REACTOR PRESSURE.

11. DESIGN PRESSURE AND TEMPERATURE SHOWN IN "TABLE 1" IS FOR INFORMATION ONLY AND IS THE BASIS FOR DESIGN OF BARR SUPPLIED EQUIPMENT. ESTIMATED LINE SIZES ARE FOR INFORMATION ONLY. ACTUAL LINE SIZES AS DETERMINED BY THE PIPING DESIGNER SHALL MEET THE PROCESS DATA HYDRAULIC REQUIREMENTS.

12. ALL VALUES SHOWN IN MODES A, B, C, AND D ARE NOMINAL UNLESS OTHERWISE NOTED.

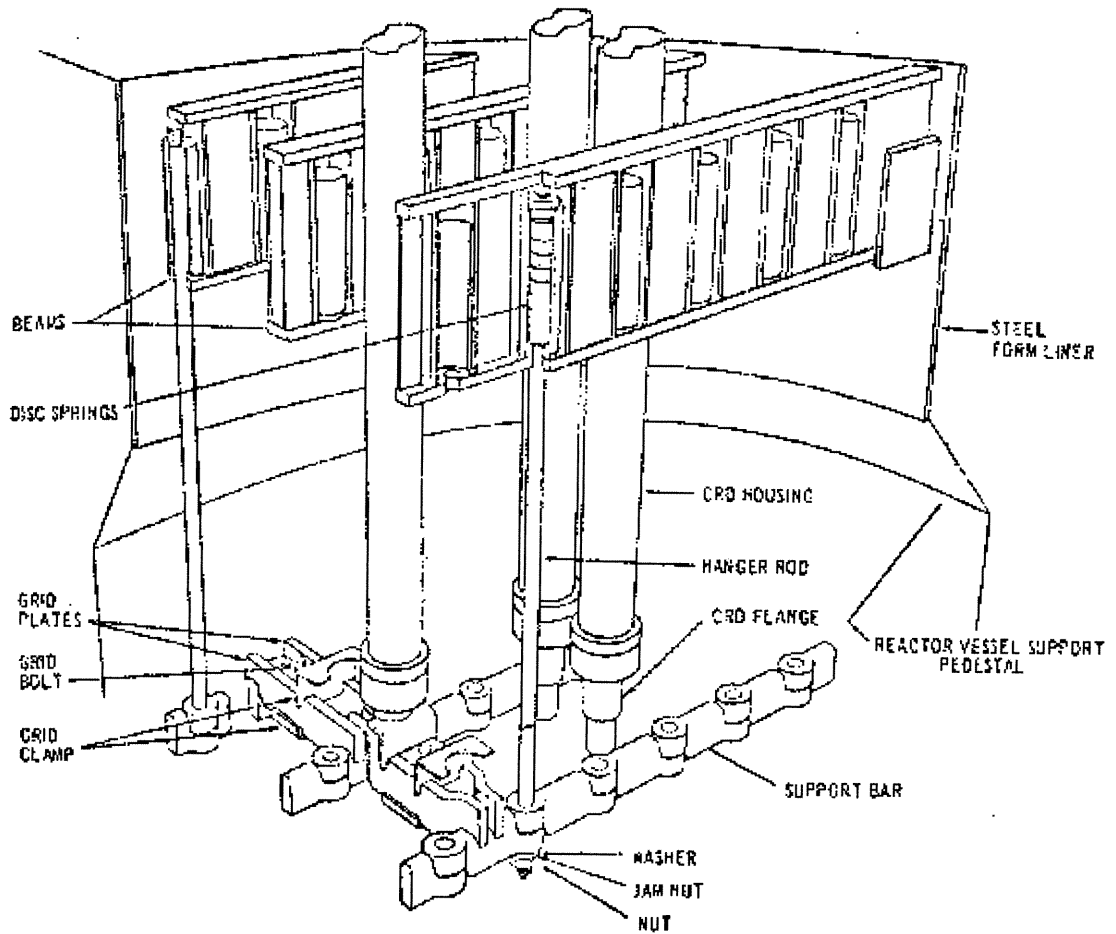
LA SALLE COUNTY STATION
UPDATED FINAL SAFETY ANALYSIS REPORT

FIGURE 4.6-6
PROCESS DATA, CONTROL ROD DRIVE
HYDRAULIC SYSTEM
(SHEET 2 OF 2)



LA SALLE COUNTY STATION
 UPDATED FINAL SAFETY ANALYSIS REPORT

FIGURE 4.6-7
 CONTROL ROD DRIVE HYDRAULIC
 CONTROL UNIT



LA SALLE COUNTY STATION
 UPDATED FINAL SAFETY ANALYSIS REPORT

FIGURE 4.6-3

CONTROL ROD DRIVE HOUSING SUPPORT

REV. 0 - APRIL 1984